Supplementary Information

Identification of γ-Butyrolactone Signalling Molecules in Diverse Actinomycetes Using Resin-Assisted Isolation and Chemoenzymatic Synthesis

Yuta Kudo[1,2]*, Keiichi Konoki[2] and Mari Yotsu-Yamashita[2]

[1]Frontier Research Institute for Interdisciplinary Sciences, Tohoku University, 6-3 Aramaki-Aza-Aoba, Aoba-ku, Sendai, Miyagi 980-8578, Japan

[2]Graduate School of Agricultural Science, Tohoku University 468-1 Aramaki-Aza-Aoba, Aoba-ku, Sendai, Miyagi 980-8572, Japan

*Correspondence: Yuta Kudo yuta.kudo.d5@tohoku.ac.jp

Table of contents

Methods

General experimental procedures

NMR spectra were recorded on a Bruker AVANCE III 600 MHz and Agilent 600 MHz NMR spectrometers with the 5 mm probe at 20 °C or 25 °C. CD (circular dichroism) spectra were recorded using a JASCO J-720WI CD spectrometer. The high-resolution MS spectra were recorded on a micrOTOF-QII mass spectrometer (Bruker Daltonics), equipped with an ESI source. LC was performed using two LC-30AD pumps (Shimadzu), a SIL-30AC autosampler (Shimadzu), a CTO-20AC column oven (Shimadzu), and a CBM-20A communications bus module (Shimadzu). The mass data acquisition was carried out using otofControl 3.2, and the data thus obtained were analyzed using Bruker Compass DataAnalysis 4.1. For the 6-keto GBLs detection in the negative ion mode, the source parameters of the mass spectrometer were as follows: Capillary, 2600 V; nebulizer, 1.6 Bar; dry heater, 180 °C; and dry gas, 8.0 L/min (nitrogen). Representative quadrupole parameters were as follows: Collision cell RF, 100–200 Vpp; transfer time, 20–35 μs; and pre-pulse storage time, 2.0 μs. For the SNACs and C-6 hydroxy-type GBLs detection in the positive ion mode, the source parameters of the mass spectrometer were as follows: Capillary, 4500 V; nebulizer, 1.6 Bar; dry heater, 180 °C; and dry gas, 8.0 L/min (nitrogen). Representative quadrupole parameters were as follows: Collision cell RF, 100 Vpp; transfer time, 60 μs; and pre-pulse storage time, 1.0 μs. Preparative LC was carried out using a JASCO PU-2089 Plus and a JASCO PU-4180 pump equipped with a photodiode array (PDA) detector MD-4010. PDA data were processed using a ChromNAV (JASCO, Ver. 2.04.00). FPLC was performed using BioLogic DuoFlow system (Bio-Rad) in the chromatography refrigerators set at 4 °C. LC-MS and HPLC grade CH_3CN, and HPLC grade CH_3OH, 2-propanol, and hexane were purchased from FUJIFILM Wako Pure Chemical Corporation and KANTO CHEMICAL. H_2O for LC was prepared using a Merck Millipore water purification system (Simplicity UV), using distilled water. The highest-grade NMR solvents were purchased from Sigma-Aldrich and KANTO CHEMICAL. Bioinformatics analysis was performed using Generous Prime 2019 (Biomatters).

Bacterial strains

The bacterial strains and media used in this study are summarized in Table S1. The bacterial strains were provided by the Riken BioResource Research Center, Japan Collection of

Microorganisms (JCM) and the National Institute of Technology and Evaluation (NITE), NITE Biological Resource Center (NBRC). In this study, bacterial strains were also isolated from soil collected in Okinawa, Japan. The rehydrated bacterial strains were cultured on agar plates. The starter liquid culture was inoculated from the colony into 40 to 50 mL of medium in 300 mL Erlenmeyer flasks with stainless steel springs, and the bacteria were allowed to grow for 2–3 days at 28 °C or 30 °C with shaking on an EYELA MMS-3020 device (180 rpm).

Isolation of GBLs from actinomycetes

For the isolation of **2**–**4**, *Rhodococcus rhodnii* JCM3203 was cultured in five 1 L Erlenmeyer flasks, each containing 500 mL of yeast extract-malt extract (ISP-2) medium, at 30 °C with shaking at 180 rpm using an EYELA MMS-3020 device. Forty hours after inoculation, sterile Amberlite XAD7HP resin (10 g, Sigma–Aldrich) was added to each flask, and fermentation was allowed to proceed for an additional 2 days. The cells and resin were collected from 2.5 L culture by filtration using a Buchner funnel *in vacuo*. The collected cells and resin were soaked in 300 mL of acetone for 1 hr with stirring, and the acetone extract was filtered *in vacuo*. The cells and resin were re-extracted with 300 mL of acetone and then filtered *in vacuo*. The collected filtrates of the acetone extracts were concentrated by rotary evaporation. The resulting residue was dissolved in a small amount of MeOH, and the solution was applied to a Cosmosil 140 C18-OPN (25 g, 20 mm i.d. × 170 mm) self-packed column with the following gradient conditions: mobile phase A, H_2O; mobile phase B, methanol (MeOH); and gradient, 0% B, hold for 30 min, 0–100% B in 70 min, 100% B, hold for 15 min, at a flow of 5.0 mL/min. The fractions containing GBLs were concentrated by rotary evaporation and subsequently purified using an InertSustain C18 column (10 mm i.d. × 250 mm, 5 μm, GL Sciences) with the following gradient conditions: mobile phase A, 0.1% formic acid in H_2O; mobile phase B, 0.1% formic acid in acetonitrile (MeCN); and gradient, 50% B, hold for 60 min, 50–60% B in 60 min, at a flow of 1.5 mL/min. Compound elution was monitored by diode array detection (DAD) and confirmed by LC–MS. Eventually, (3*R*)-*n*-C-9 GBL (**2**, 0.30 mg) was obtained and subjected to NMR spectroscopy analysis.

For the isolation of *n*-C-7 GBL (**4**), *R. rhodnii* JCM3203 was cultured in five 1 L Erlenmeyer flasks, each containing 500 mL of ISP-2 medium, at 30 °C with shaking at 180 rpm. Forty-eight hours after inoculation, sterile Amberlite XAD7HP resin (10 g) was added to each flask, and fermentation was allowed to proceed for an additional 5 days. The extraction and

purification scheme was essentially the same as that for **2** but modified as described below. The fractions obtained from the Cosmosil 140C18-OPN column containing **4** were purified using an InertSustain C18 column (10 mm i.d. × 250 mm, 5 μm) with the following gradient conditions: mobile phase A, 0.1% formic acid in H_2O; mobile phase B, 0.1% formic acid in MeCN; and gradient, 50% B, hold for 60 min, 50–60% B in 40 min, at a flow rate of 1.5 mL/min. The fraction containing **4** was purified using a Kinetex XB-C18 column (4.6 mm i.d. × 250 mm, 5 μm, Phenomenex) with the following gradient conditions: mobile phase A: 0.1% formic acid in H_2O; mobile phase B: 0.1% formic acid in MeCN; and gradient: 35% B, hold for 20 min; 35–40% B in 20 min, and 40% B, hold for 20 min, at a flow of 0.5 mL/min. Eventually, *n*-C-7 GBL (**4**, 0.11 mg) was obtained and subjected to NMR spectroscopy analysis.

n-C-8 GBL (**3**) was isolated from a total of 7.5 L culture of *R. rhodnii* JCM 3203. The fractions obtained from the purification using the InertSustain C18 column were further purified using a Kinetex XB-C18 column (4.6 mm i.d. × 250 mm, 5 μm) with isocratic conditions (H_2O:MeCN:HCOOH = 55:45:0.1) or gradient conditions: mobile phase A: 0.1% formic acid in H_2O; mobile phase B: 0.1% formic acid in MeCN; and gradient: 40% B, hold for 20 min, 40–45% B in 20 min at a flow rate of 0.5 mL/min. Eventually, *n*-C-8 GBL (**3**, 0.15 mg) was obtained and subjected to NMR spectroscopy analysis. The amounts of **2–4** were estimated on the basis of the area counts in the LC–MS EICs using enzymatically synthesized GBL (**10d**).

iso-C-6 GBL (**5**) was isolated from *Streptomyces* sp. YKOK-I1 with essentially the same method. *Streptomyces* sp. YKOK-I1 was cultured in five 1 L Erlenmeyer flasks, each containing 500 mL of ISP-2 media. GBL was extracted and purified using a Cosmosil 140 C18-OPN (25 g, 20 mm i.d. × 170 mm) self-packed column with the following gradient conditions: mobile phase A, H_2O; mobile phase B, methanol (MeOH); and gradient, 0% B, hold for 15 min, 0–100% B in 85 min, 100% B, hold for 10 min, at a flow rate of 5.0 mL/min. The fractions containing GBLs were concentrated by rotary evaporation and subsequently purified using an InertSustain C18 column (10 mm i.d. × 250 mm, 5 μm) with the following gradient conditions: mobile phase A, 0.1% formic acid in H_2O; mobile phase B, 0.1% formic acid in acetonitrile (MeCN); and gradient, 38% B, hold for 40 min, 38–50% B in 40 min, at a flow rate of 2.0 mL/min. Eventually, *iso*-C-6 GBL (**5**, 0.15 mg) was obtained and subjected to NMR spectroscopy analysis.

(3*R*)-*n*-C-9 GBL (**2**): clear waxy solid; 0.30 mg; HR-ESI-MS (*m/z*): $[M-H]^-$ calcd for $C_{15}H_{25}O_4$, 269.1758; found, 269.1761; ^1H NMR and ^{13}C NMR data, Table S2; CD (in MeOH), 284 nm, Δε + 0.446, 218 nm, Δε + 0.265.

(3*R*)-*n*-C-8 GBL (**3**): clear waxy solid; 0.15 mg; HR-ESI-MS (*m/z*): $[M-H]^-$ calcd for $C_{14}H_{23}O_4$, 255.1602; found, 255.1595; ^1H NMR and ^{13}C NMR data, Table S3; CD (in MeOH), 279 nm, Δε + 0.195, 221 nm, Δε + 0.133.

(3*R*)-*n*-C-7 GBL (**4**): clear waxy solid; 0.11 mg; HR-ESI-MS (*m/z*): $[M-H]^-$ calcd for $C_{13}H_{21}O_4$, 241.1445; found, 241.1445; ^1H NMR and ^{13}C NMR data, Table S4; CD (in MeOH), 280 nm, Δε + 0.242, 220 nm, Δε + 0.131.

(3*R*)-*iso*-C-6 GBL (**5**): clear waxy solid; 0.15 mg; HR-ESI-MS (*m/z*): $[M-H]^-$ calcd for $C_{12}H_{19}O_4$, 227.1289; found, 227.1291; ^1H NMR and ^{13}C NMR data, Table S5; CD (in MeOH), 281 nm, Δε + 0.607, 222 nm, Δε + 0.394.

Purification of (3*S*)-*n*-C-5 GBL (11) from *Streptomyces* sp. YKOK-J1

Streptomyces sp. YKOK-J1 was cultured in six 300 mL Erlenmeyer flasks, each containing 75 mL of yeast-starch medium, at 28 °C with shaking at 180 rpm using an EYELA MMS-320 device. Forty-eight hours after inoculation, sterile Amberlite XAD7HP resin (1.5 g) was added to each flask, and fermentation was allowed to proceed for an additional 4 days. The cells and resin were collected from each flask by centrifugation at 4000 × g for 10 min. The collected cells and resin were soaked in acetone for 30 min with shaking, and the acetone extract was filtered. The filtrates of acetone extracts were concentrated by rotary evaporation. The resulting residue was dissolved in 20 μL of MeOH, and the solution was applied to a Strata C18-E column (2 g). After washing with three volumes of H_2O, the compounds were eluted with three volumes of H_2O:MeOH (1:1), three volumes of H_2O:MeOH (1:4), and four volumes of H_2O:MeOH (1:1). The fractions were analysed using LCMS. The fractions containing a high concentration of (3*S*)-*n*-C-5 GBL (**11**) were selected and combined from three culture batches. The combined fractions were concentrated *in vacuo* and then purified using an InertSustain C18 column (10 mm i.d. × 250 mm, 5 μm) with the following gradient conditions: mobile phase A, 0.1% formic acid in H_2O; mobile phase B, 0.1% formic acid in acetonitrile (MeCN); and gradient, 40% B, hold for 10 min, 40–70% B in 60 min, at a flow rate of 2.0 mL/min. The fraction containing **11** was further purified using a Kinetex XB-C18 column (4.6 mm i.d. × 250

mm, 5 μm) with the following gradient conditions: mobile phase A: 0.1% formic acid in H_2O; mobile phase B: 0.1% formic acid in MeCN; and gradient: 30% B, hold for 20 min, 30–35% B in 20 min, 35% B, hold for 20 min, 35–40% B in 20 min at a flow rate of 0.5 mL/min. Compound elution was monitored by DAD and confirmed by ESI–MS. The obtained *n*-C-5 GBL (**11**, approximately 5 μg) was subjected to chiral column analysis.

(3*S*)-*n*-C-5 GBL (**11**): HR-ESI-MS (*m/z*): $[M-H]^-$ calcd for $C_{11}H_{17}O_4$, 213.1132; found, 213.1144.

Chiral column analysis

Chiral column analysis was performed using a JASCO PU-4180 pump equipped with an MD-4010 PDA detector with detection at 190–600 nm. Chiral column screening showed that CHIRALPAK AD-H enables the separation of enantiomers. The GBLs were dissolved in 10 μL of mobile phase and were analysed using a CHIRALPAK AD-H column (4.6 mm i.d. × 250 mm, 5 μm, DAICEL) with isocratic conditions (hexane:2-propanol = 92:8) at a flow rate of 0.5 mL/min. Chromatograms were obtained at a wavelength of 254 nm.

NMR measurements

NMR measurements of the purified compounds were performed in 0.4 mL of $CDCl_3$ in 5 mm i.d. tubes (PS-004, Shigemi). The signals of $CDCl_3$ at 7.26 ppm in the ^1H NMR spectra and those of $^{13}CDCl_3$ at 77.16 ppm in the ^{13}C NMR spectra were used as internal references. ^1H NMR, gradient COSY, TOCSY, gradient HSQC and gradient HMBC ($^3J_{CH}$ = 8 Hz) of isolated compounds (**2–5**) and synthesized GBLs (**10d**–**10f**, **10j**, **10l**) were performed (Figs. S66–S107). All the proton and carbon signals of **2**–**5** were assigned on the basis of the 1D and 2D NMR data (Tables S2–S5). The ^1H NMR and ^{13}C NMR data of the synthesized compounds (**6a–6l**) and the gradient COSY, TOCSY, gradient HSQC and gradient HMBC ($^3J_{CH}$ = 8 Hz) data of **6h** were collected (Figs. S108–S134). The data were processed using TopSpin 4.2.0 (Bruker), VnmrJ 4.2 (Agilent Technology) or MestReNova 14.2.0 (Mestrelab Research).

CD spectral measurements

The purified compounds were dissolved in MeOH. The CD spectra of **2** (2.78 mM), **3** (1.98 mM), **4** (1.58 mM), **5** (2.22 mM), synthesized and optically resolved (3*R*)-*n*-C-5 GBL (4.37 mM) and (3*S*)-*n*-C-5 GBL (4.71 mM) were measured using a 1 nm bandwidth in a 0.1 cm

quartz cell at room temperature (RT; approximately 25 °C) with 1 s/scan, an increment of 50 nm/min, and a range of 190 nm to 400 nm. The obtained data were processed using Excel (Microsoft 365 MSO).

Synthesis of β-ketoacyl-SNAC (6)

As a mimic of β-ketoacyl-ACP, β-ketoacyl *N*-acetylcysteamine thioesters (SNACs) were synthesized as described below.

SNAC synthesis (*n*-C-2 SNAC (6a), *n*-C-4 SNAC (6c))

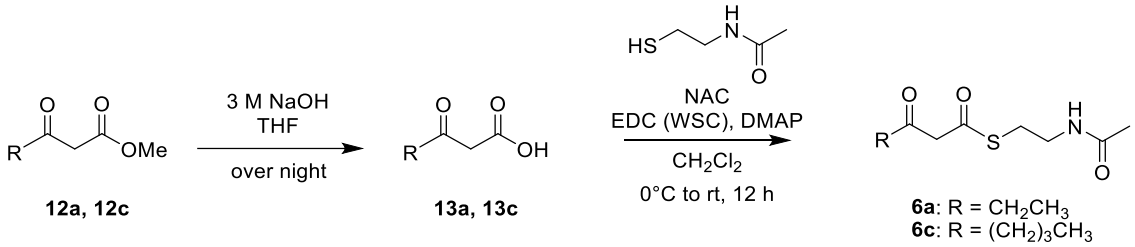

On the basis of a previous report[1], **6a** and **6c** were synthesized from methyl 3-oxopentanoate and methyl 3-oxoheptanoate (**12a**) and (**12c**), respectively. Compounds **12a** and **12c** were converted into carboxylic acids (**13a** and **13c**) via acid hydrolysis (~42.8%). β-Ketoacyl-carboxylic acids (**13a** and **13c**) were conjugated with NAC using 1-ethyl-3-(3-dimethylaminopropyl)carbodiimide (EDC) to yield β-ketoacyl-SNACs (**6a**, **6c**, white solid, ~41.8%). For *n*-C-2 GBL (**6a**), HPLC purification was conducted to increase the purity.

SNAC synthesis (6b, 6d–6l)

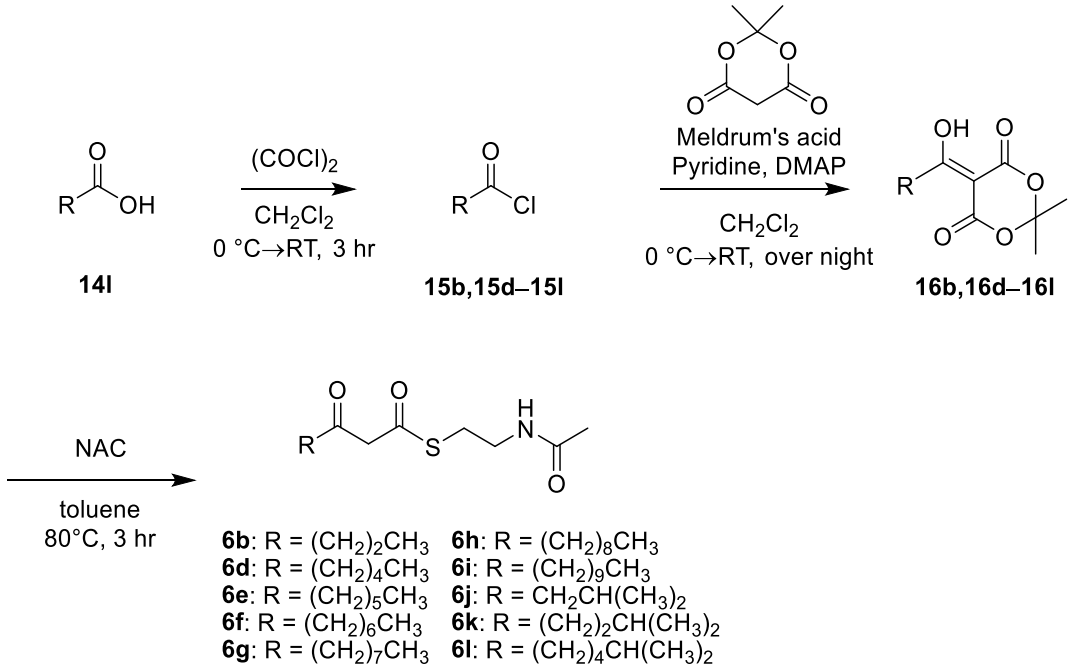

Compounds **6b** and **6d–6l** were synthesized from acyl halides (**15b**, **15d**–**15l**)[2]. As *iso*-C-7 acyl halide (**15l**) was unavailable commercially, it was synthesized from carboxylic acid (**14l**). 6-Methylheptanoic acid (**14l**, 1 eq) was placed in a two-necked round-bottomed flask and dissolved in CH_2Cl_2 (0.3 M), and two drops of DMF were added. The mixture was cooled on ice, and then oxalyl chloride (1.3 eq) was added slowly. The mixture was warmed to RT and then stirred for 3 hr. The resulting acyl chloride (**15l**) was subjected to the next reaction without purification to synthesize SNAC.

Meldrum's acid (1 eq) was dissolved in CH_2Cl_2 (500 mM) in a two-necked round-bottomed flask at RT. Pyridine (2 eq) and DMAP (20 mol%) were added, and the mixture was stirred for 10 min at RT. The mixture was cooled on ice for 5 min, then 1 eq of acyl chloride (**15b**, **15d**–**15l**, *n*-C-3, *n*-C-5, *n*-C-6, *n*-C-7, *n*-C-8, *n*-C-9, *n*-C-10, *iso*-C-4, *iso*-C-5, *iso*-C-7) was added dropwise, and the mixture was warmed to RT and stirred overnight. The mixture was subsequently washed with 0.1 M HCl aq and water. The organic layers were dried over Na_2SO_4, stirred, and then filtered. The solvent was removed from the filtrate under nitrogen gas. The product was applied to a Strata Silica column (Si-1, 5 g, Phenomenex) and eluted with a mixture of hexane and ethyl acetate, in which the solvent ratio was changed according to the product. The fractions containing acylated Meldrum's acid were identified via ESI–MS

(negative ion mode) and evaporated *in vacuo* to give the desired product (**16b**, **16d**–**16l**, yellow to orange–brown oily liquid, ~86.5%).

The acylated Meldrum's acid (**16b**, **16d**–**16l**) was placed in a two-necked round-bottomed flask and dissolved in toluene (0.5 M). The reaction solution was refluxed for three hours, and the solvent was evaporated *in vacuo* at 60 °C. The product was applied to a Strata Silica column (Si-1, 5 g) and eluted with a mixture of chloroform and ethyl acetate, in which the solvent ratio was changed according to the product. The fractions containing acylated Meldrum's acid were identified via ESI–MS (positive ion mode) and evaporated *in vacuo* to give the desired product (**6b**, **6d–6l**, white solid, ~87.4%).

6a: white solid, 4 mg (HPLC purified), HR-ESI-MS (*m/z*): $[M+H]^+$ calcd for $C_9H_{16}NO_3S$, 218.0845; found, 218.0845, $[M+Na]^+$ calcd for $C_9H_{15}NO_3SNa$, 240.0665; found, 240.0663; ^1H NMR ($CDCl_3$, 600 MHz) δ 5.87 (br s, NH), 5.47 (s, 1H), 3.70 (s, 2H), 3.47 (t, *J* = 6.2 Hz, 2H), 3.46 (t, *J* = 6.2 Hz, 2H), 3.09 (t, *J* = 6.2 Hz, 2H), 2.57 (q, *J* = 7.2 Hz, 2H), 2.23 (q, *J* = 7.5 Hz, 2H), 1.98 (s, 3H), 1.97 (s, 3H), 1.14 (t, *J* = 7.5 Hz, 3H), 1.09 (t, *J* = 7.3 Hz, 3H); ^{13}C NMR ($CDCl_3$, 150 MHz) δ 202.7, 192.6, 170.5, 98.5, 57.1, 39.4, 36.9, 29.4, 28.0, 23.3, 7.6. The signals derived from the enol form were observed (Figs. S108, S109).

6b: white solid, 129 mg, HR-ESI-MS (*m/z*): $[M+H]^+$ calcd for $C_{10}H_{18}NO_3S$, 232.1002; found, 232.1000, $[M+Na]^+$ calcd for $C_{10}H_{17}NO_3SNa$, 254.0821; found, 254.0829; ^1H NMR ($CDCl_3$, 600 MHz) δ 5.92 (br s, NH), 5.46 (s, 1H), 3.69 (s, 2H), 3.46 (t, *J* = 6.0 Hz, 2H), 3.45 (t, *J* = 6.1 Hz, 2H), 3.09 (t, *J* = 6.3 Hz, 2H), 3.08 (t, *J* = 6.1 Hz, 2H), 2.51 (t, *J* = 7.3 Hz, 2H), 2.15 (t, *J* = 7.4 Hz, 2H), 1.97 (s, 3H), 1.96 (s, 3H), 1.66–1.58 (m, 2H), 0.95 (t, *J* = 7.5 Hz, 3H), 0.92 (t, *J* = 7.5 Hz, 3H); ^{13}C NMR ($CDCl_3$, 151 MHz) δ 202.3, 194.5, 192.6, 177.6, 170.6, 170.4, 99.4, 57.4, 45.4, 40.1, 39.4, 36.9, 29.4, 28.0, 23.4, 23.3, 19.8, 17.1, 13.7, 13.7. The signals derived from the enol form were observed (Figs. S110, S111).

6c: white solid, 171 mg, HR-ESI-MS (*m/z*): $[M+H]^+$ calcd for $C_{11}H_{20}NO_3S$, 246.1158; found, 246.1154, $[M+Na]^+$ calcd for $C_{11}H_{19}NO_3SNa$, 268.0978; found, 268.0983; ^1H NMR ($CDCl_3$, 600 MHz) δ 5.91 (br s, NH), 5.46 (s, 1H), 3.69 (s, 2H), 3.46 (t, *J* = 6.4 Hz, 2H), 3.45 (t, *J* = 6.1 Hz, 2H), 3.09 (t, *J* = 6.4 Hz, 2H), 3.08 (t, *J* = 6.1 Hz, 2H), 2.53 (t, *J* = 7.3 Hz, 2H), 2.18 (t, *J* = 7.4 Hz, 2H), 1.97 (s, 3H), 1.96 (s, 3H), 1.60–1.53 (m, 2H), 1.40–1.28 (m, 2H), 0.92 (t, *J* = 7.5 Hz, 3H), 0.90 (t, *J* = 7.4 Hz, 3H); ^{13}C NMR ($CDCl_3$, 151 MHz) δ 202.4, 194.4, 192.6, 177.8,

170.6, 99.3, 57.3, 43.3, 40.1, 39.3, 34.7, 29.4, 28.5, 28.0, 25.6, 23.4, 23.3, 22.3, 22.2, 13.9, 13.9. The signals derived from the enol form were observed (Figs. S112, S113).

6d: white solid, 139 mg, HR-ESI-MS (*m/z*): $[M+H]^+$ calcd for $C_{12}H_{22}NO_3S$, 260.1315; found, 260.1308, $[M+Na]^+$ $C_{12}H_{21}NO_3SNa$, 282.1134, 310.1447; found, 282.1125; ^1H NMR ($CDCl_3$, 600 MHz) δ 5.91 (br s, 1H), 5.46 (s, 1H), 3.69 (s, 2H), 3.46 (t, *J* = 6.3 Hz, 2H), 3.45 (t, *J* = 6.4Hz, 2H), 3.09 (t, *J* = 6.5 Hz, 2H), 3.08(t, *J* = 6.4 Hz, 2H), 2.52 (t, *J* = 7.6 Hz, 2H), 2.17 (t, *J* = 7.6 Hz, 2H), 1.97 (s, 3H), 1.96 (s, 3H), 1.61–1.54 (m, 2H), 1.35–1.24 (m, 4H), 0.87 (t, *J* = 6.9 Hz, 3H); ^{13}C NMR ($CDCl_3$, 151 MHz) δ 202.4, 194.4, 192.6, 177.9, 170.6, 170.4, 99.3, 57.3, 43.6, 40.1, 39.4, 35.0, 31.4, 31.3, 29.4, 28.0, 26.1, 23.3, 23.2, 22.5, 22.5, 14.0, 14.0. The signals derived from the enol form were observed (Figs. S114, S115).

6e: white solid, 136 mg, HR-ESI-MS (*m/z*): $[M+H]^+$ calcd for $C_{13}H_{24}NO_3S$, 274.1471; found, 274.1465, $[M+Na]^+$ calcd for $C_{13}H_{23}NO_3SNa$, 296.1291; found, 296.1294; ^1H NMR ($CDCl_3$, 600 MHz) δ 5.91 (s, H), 5.46 (s, H), 3.69 (s, 2H), 3.46 (t, *J* = 6.3 Hz, 2H), 3.45 (t, *J* = 6.1 Hz, 2H), 3.09 (t, *J* = 6.2 Hz, 2H), 3.08 (t, *J* = 6.3 Hz, 2H), 2.52 (t, *J* = 7.3 Hz, 2H), 2.17 (t, *J* = 7.5 Hz, 2H), 1.97 (s, 3H), 1.96 (s, 3H), 1.61–1.54 (m, 2H), 1.35–1.22 (m, 6H), 0.88 (t, *J* = 6.9 Hz, 3H); ^{13}C NMR ($CDCl_3$, 151 MHz) δ 202.5, 192.6, 177.9, 170.6, 170.4, 99.3, 57.3, 43.6, 40.1, 39.4, 35.1, 31.6, 31.6, 29.4, 28.9, 28.8, 28.0, 26.3, 23.5, 23.4, 23.3, 22.6, 14.2, 14.1. The signals derived from the enol form were observed (Figs. S116, 117).

6f: white solid, 111 mg, HR-ESI-MS (*m/z*): $[M+H]^+$ calcd for $C_{14}H_{26}NO_3S$, 288.1628; found, 288.1622, $[M+Na]^+$ calcd for $C_{16}H_{29}NO_3SNa$, 310.1447; found, 310.1444; ^1H NMR ($CDCl_3$, 600 MHz) δ 5.90 (s, 1H), 5.46 (s, 1H), 3.69 (s, 2H), 3.46 (t, *J* = 6.3 Hz, 2H), 3.45 (t, *J* = 6.3 Hz, 2H), 3.09 (t, *J* = 6.2 Hz, 2H), 2.52 (t, *J* = 7.3 Hz, 2H), 1.97 (s, 3H), 1.61–1.55 (m, 2H), 1.33–1.20 (m, 8H), 0.87 (t, *J* = 6.3 Hz, 3H); ^{13}C NMR ($CDCl_3$, 151 MHz) δ 202.5, 192.6, 170.6, 57.3, 43.6, 39.4, 31.8, 29.4, 29.1, 29.1, 23.6, 23.3, 22.7, 14.2. The signals derived from the enol form were observed (Figs. S118, S119).

6g: white solid, 111 mg, HR-ESI-MS (*m/z*): $[M+H]^+$ calcd for $C_{15}H_{28}NO_3S$, 302.1784; found, 302.1778, $[M+Na]^+$ calcd for $C_{15}H_{27}NO_3SNa$, 324.1604; found, 324.1599; ^1H NMR ($CDCl_3$, 600 MHz) δ 5.90 (s, 1H), 5.46 (s, 1H), 3.69 (s, 2H), 3.46 (t, *J* = 6.0 Hz, 2H), 3.45 (t, *J* = 6.1 Hz, 2H), 3.09 (t, *J* = 6.2 Hz, 2H), 2.52 (t, *J* = 7.3 Hz, 2H), 1.97 (s, 3H), 1.61–1.53 (m, 2H), 1.32–1.20 (m, 10H), 0.87 (t, *J* = 6.3 Hz, 3H); ^{13}C NMR ($CDCl_3$, 151 MHz) δ 202.5, 192.6,

170.6, 57.3, 43.6, 42.6, 39.4, 31.9, 29.4, 29.4, 29.2, 29.1, 24.8, 23.6, 23.3, 22.8, 14.2. The signals derived from the enol form were observed (Figs. S120, S121).

6h: white solid, 206 mg, HR-ESI-MS (*m/z*): $[M+H]^+$ calcd for $C_{16}H_{30}NO_3S$, 316.1907; found, 316.1938, $[M+Na]^+$ calcd for $C_{16}H_{29}NO_3SNa$, 338.1727; found, 338.1754; ^1H NMR ($CDCl_3$, 600 MHz) δ 5.95 (s, 1H), 5.46 (s, 1H), 3.69 (s, 2H), 3.46 (t, *J* = 6.0 Hz, 2H), 3.45 (t, *J* = 6.1 Hz, 2H), 3.09 (t, *J* = 6.2 Hz, 2H), 2.52 (t, *J* = 7.3 Hz, 2H), 2.17 (t, *J* = 7.5 Hz, 2H), 1.98 (s, 3H), 1.97 (s, 3H), 1.61–1.53 (m, 2H), 1.33–1.20 (m, 12H), 0.87 (t, *J* = 6.3 Hz, 3H); ^{13}C NMR ($CDCl_3$, 151 MHz) δ 202.6, 194.5, 192.6, 177.9, 170.6, 170.5, 99.3, 57.3, 43.6, 40.1, 39.4, 35.1, 32.0, 29.6, 29.5, 29.5, 29.4, 29.4, 29.4, 29.2, 29.1, 28.0, 26.4, 23.6, 23.4, 23.3, 22.8, 14.3. The signals derived from the enol form were observed (Figs. S122–S126).

6i: white solid, 164 mg, HR-ESI-MS (*m/z*): $[M+H]^+$ calcd for $C_{17}H_{32}NO_3S$, 330.2097; found, 330.2089, $[M+Na]^+$ calcd for $C_{17}H_{31}NO_3SNa$, 352.1917; found, 352.1909; ^1H NMR ($CDCl_3$, 600 MHz) δ 5.90 (br s, 1H), 5.46 (s, 1H), 3.69 (s, 2H), 3.46 (t, *J* = 6.2 Hz, 2H), 3.45 (t, *J* = 6.1Hz, 2H), 3.09 (t, *J* = 6.2 Hz, 2H), 2.52 (t, *J* = 7.5 Hz, 2H), 2.17 (t, *J* = 7.6 Hz, 2H), 2.17 (t, *J* = 7.6 Hz, 2H), 1.97 (s, 3H), 1.96 (s, 3H), 1.60–1.54 (m, 2H), 1.34–1.20 (m, 14H), 0.87 (t, *J* = 6.8 Hz, 3H); ^{13}C NMR ($CDCl_3$, 151 MHz) δ 202.5, 194.4, 192.6, 170.6, 99.3, 57.3, 43.6, 40.1, 39.4, 35.1, 32.0, 29.7, 29.6, 29.6, 29.5, 29.4, 29.4, 29.2, 29.1, 28.0, 26.4, 23.6, 23.4, 23.3, 22.8, 14.3. The signals derived from the enol form were observed (Figs. S127, S128).

6j: white solid, 88 mg, HR-ESI-MS (*m/z*): $[M+H]^+$ calcd for $C_{11}H_{20}NO_3S$, 246.1158; found, 246.1172, $[M+Na]^+$ calcd for $C_{11}H_{19}NO_3SNa$, 268.0978; found, 268.0980; ^1H NMR ($CDCl_3$, 600 MHz) δ 5.93 (br s, 1H), 5.44 (s, 1H), 3.67 (s, 2H), 3.46 (t, *J* = 7.2 Hz, 2H), 3.45 (t, *J* = 6.1 Hz, 2H), 3.09 (t, *J* = 6.1 Hz, 2H), 3.08 (t, *J* = 6.0 Hz, 2H), 2.41 (d, *J* = 6.9 Hz, 2H), 2.19–2.10 (m, 1H), 2.03 (m), 1.97 (s, 3H), 1.96 (s, 3H), 0.93 (d, *J* = 6.7 Hz, 6H); ^{13}C NMR ($CDCl_3$, 151 MHz) δ 202.0, 194.4, 192.5, 176.9, 170.6, 170.4, 100.3, 57.7, 52.4, 44.2, 40.1, 39.4, 29.4, 28.0, 26.6, 24.5, 23.4, 23.3, 22.5, 22.5. The signals derived from enol form were observed (Figs. S129, S130).

6k: white solid, 92 mg, HR-ESI-MS (*m/z*): $[M+H]^+$ calcd for $C_{12}H_{22}NO_3S$, 260.1315; found, 260.1311, $[M+Na]^+$ calcd for $C_{12}H_{21}NO_3SNa$, 282.1134; found, 282.1131; ^1H NMR ($CDCl_3$, 600 MHz) δ 5.91 (s, 1H), 5.46 (s, 1H), 3.70 (s, 2H), 3.46 (t, *J* = 6.6 Hz, 2H), 3.45 (t, *J* = 6.3 Hz, 2H), 3.09 (t, *J* = 6.5 Hz, 2H), 3.08 (t, *J* = 7.3 Hz, 2H), 2.53 (t, *J* = 7.7 Hz, 2H), 2.18 (t, *J* = 7.9 Hz, 2H), 1.97 (s, 3H), 1.96 (s, 3H), 1.63–1.43 (m, 3H), 0.91 (d, *J* = 6.7 Hz, 3H), 0.89 (d, *J*

= 6.6 Hz, 3H); ^{13}C NMR ($CDCl_3$, 151 MHz) δ 202.6, 192.6, 170.6, 99.2, 57.3, 41.7, 40.1, 39.3, 35.3, 33.0, 32.3, 29.4, 28.0, 27.8, 27.7, 23.4, 23.3, 22.4. The signals derived from enol form were observed (Figs. S131, S132).

6l: white solid, 137 mg, HR-ESI-MS (*m/z*): $[M+H]^+$ calcd for $C_{16}H_{30}NO_3S$, 288.1628; found, 288.1630, $[M+Na]^+$ calcd for $C_{16}H_{29}NO_3SNa$, 310.1447; found, 310.1443; ^{1}H NMR ($CDCl_3$, 600 MHz) δ 5.90 (s, 1H), 5.46 (s, 1H), 3.70 (s, 2H), 3.47 (t, *J* = 6.6 Hz, 2H), 3.46 (t, *J* = 6.3 Hz, 2H), 3.09 (t, *J* = 6.5 Hz, 2H), 3.08 (t, *J* = 7.3 Hz, 2H), 2.53 (t, *J* = 7.4 Hz, 2H), 2.18 (t, *J* = 7.3 Hz, 2H), 1.98 (s, 3H), 1.97 (s, 3H), 1.66–1.45 (m, 3H), 1.37–1.25 (m, 2H), 1.21–1.13 (m, 2H), 0.87 (d, *J* = 6.5 Hz, 3H), 0.86 (d, *J* = 6.5 Hz, 3H); ^{13}C NMR ($CDCl_3$, 151 MHz) δ 202.5, 192.6, 99.3, 57.3, 43.7, 39.4, 38.8, 38.7, 29.4, 27.9, 26.9, 26.6, 23.8, 23.4, 22.7. The signals derived from enol form were observed (Figs. S133, S134).

16h: orange–brown oily liquid, 1157 mg, HR-ESI-MS (*m/z*): $[M-H]^-$ calcd for $C_{16}H_{25}O_5$, 297.1707; found, 297.1681.

DHAP synthesis (7)

DHAP was synthesized according to a previously reported method[3] and purified using a HILIC column[1], as previously reported. Commercial dihydroxyacetone phosphate hemimagnesium salt hydrate (Sigma–Aldrich) was also used as the substrate for the enzymatic reactions.

Docking study

The predicted structures of AfsA homologue proteins, including Rr-AfsA and SJ-AfsA, were generated using ColabFold (Figs. S10a, b).[4] Docking analysis between the AfsA homologues and the substrates was conducted using AutoDock Vina[5,6] implemented in UCSF Chimera.[7] The evaluation focused on the placement of the substrate within the binding pocket, particularly the accommodation of the acyl side chain within the binding pocket space. Docking analysis between BprA and the butenolide substrates was also performed (Fig. S10c).

Isolation of *Streptomyces* sp. strains and 16S rRNA sequence analysis

Mud samples were collected from Okinawa, Japan, and suspended in sterile water. The mud suspension was inoculated onto HV agar (humic acid 1 g, 0.2 M NaOH 10 mL, Na_2HPO_4 0.5 g, KCl 1.71 g, $MgSO_4$ 0.05 g, $FeSO_4$ 0.01 g, $CaCO_3$ 0.02 g, agar 18 g, thiamine-HCl 0.5 mg,

riboflavin 0.5 mg, niacin 0.5 mg, pyridoxin-HCl 0.5 mg, inositol 0.5 mg, Ca-pantothenate 0.5 mg, *p*-amino benzoic acid 0.5 mg, biotin 0.25 mg, cycloheximide 50 mg, 975 mL distilled H_2O pH 7.2). Colonies were subsequently cultured on ISP medium No. 4 (soluble starch 10 g, K_2HPO_4 1 g, $MgSO_4$-$7H_2O$ 1 g, NaCl, 1 g, NH_4SO_4 2 g, $CaCO_3$ 2 g, $FeSO_4$-$7H_2O$ 0.001 g, MnCl-$7H_2O$ 0.001 g, $ZnSO_4$-$7H_2O$ 0.001 g, agar 20 g, 1000 mL distilled H_2O, pH 7.2). Subculturing was performed until the pure strains were isolated (YKOK-D1, F1, G2b, I1 and J1). Genomic DNA from the isolated strains was prepared using a DNeasy Powersoil kit (QIAGEN). Using the extracted genomic DNA as a template, a partial 16S rRNA region was amplified with primers 9F and 1510R. The PCR products were purified using a FavorPrep GEL/PCR purification kit (FAVORGEN BIOTECH CORP) and sequenced via Sanger sequencing (Eurofins). A BLAST search of the obtained sequences revealed that all the collected strains belong to the genus *Streptomyces*. (Accession: LC855172–LC855174)

Whole-genome analysis of *Streptomyces* sp. YKOK-I1 and YKOK-J1

Streptomyces sp. YKOK-I1 and YKOK-J1 were cultured in 300 mL Erlenmeyer flasks containing 50 mL of ISP-2 medium at 28 °C with shaking at 180 rpm using an EYELA MMS-320 device. Forty hours after inoculation, the cells were collected from 2 mL of culture by centrifugation at 4000 × g for 10 min. The collected cells were washed with SET buffer (75 mM NaCl, 75 mM EDTA, 20 mM Tris, pH 7.2) and resuspended in 2 mL of SET buffer, followed by the addition of 40 µL of lysozyme solution (50 mg/mL). After 45 min of incubation at 37 °C, 56 µL of proteinase K solution (20 mg/mL) and 120 µL of 10% (m/v) SDS solution were added. The solution was incubated at 55 °C for 2 hr with occasional mixing by inversion, after which 280 µL of 5 M NaCl solution was added. After adding 2 mL of chloroform, the solution was gently mixed for 30 min. The solution was then centrifuged at 2200 × g for 15 min. The aqueous layer was transferred to a new tube using a bore tip, and then 60% volume of 2-propanol was added. The tube was inverted gently, and the precipitated gDNA was suspended and transferred to a new tube using a disposable loop cut in half. The gDNA was washed with 1 mL of cooled 70% ethanol two times and then dried at RT for 30 min. The obtained gDNA was dissolved in 100 µL of TE buffer (10 mM Tris-HCl, 1 mM EDTA, pH 8.0). The gDNA was analysed using a Sequel Ile system (PacBio) by Bioengineering Lab. Co., Ltd (accession: DRR623149, DRR623150). The *afsA* homologues were found via Local BLAST search (*sj-afsA*: LC855175, *si-afsA*: LC855177, *sj-afsA* pairwise identity: 17.6%,

pairwise positive (BLSM62): 26.2%, *si-afsA*, pairwise AA identity: 30.5%, pairwise positive (BLSM62): 40.4%, in the ClustalW alignment with *afsA*).

DNA synthesis

Local BLAST searches were performed on the genome sequences of *Rhodococcus rhodnii* JCM 3203 (accession: GCA_008011915.1), *Streptomyces* sp. YKOK-I1 (accession: DRR623149) and *Streptomyces* sp. YKOK-J1 (accession: DRR623150) with *afsA* (accession: BAG23718.1) and *bprA* (accession: B1VN94.1) in *Streptomyces griseus* NBRC 13350 as the query. The *afsA* homologue in *Rhodococcus rhodnii* JCM 3203 (*rr-afsA*, pairwise identity: 29.3%, pairwise positive (BLSM62): 42.4% in the ClustalW alignment with *afsA*), *bprA* in *Streptomyces griseus* and its homologue in *Streptomyces* sp. YKOK-J1 (*sj-bprA,* accession: LC855176, pairwise AA identity: 57.8%, pairwise positive (BLSM62): 67.0% in the ClustalW alignment with *bprA*) were codon-optimized for *E. coli*, synthesized, and cloned into the pET28a(+) vector using the BamHI and XhoI restriction sites by GenScript. Possible *bprA* homologues in *Rhodococcus rhodnii* JCM 3203 (*rr-bprA*, pairwise AA identity: 31.5%, pairwise positive (BLSM62): 45.4%) and *Streptomyces* sp. YKOK-I1 (*si-bprA*, accession: LC855178, pairwise AA identity: 34.6%, pairwise positive (BLSM62): 46.1%). On the basis of the protein alignment with BprA from *Streptomyces griseus* and the structure predicted by AlphaFold2, sequences on the N-terminal side appeared unnecessary in BprA in *Rhodococcus rhodnii* JCM 3203 and *Streptomyces* sp. YKOK-I1. Therefore, the truncated BprA sequences were codon optimized for *E. coli*, synthesized, and cloned into the pET28a(+) vector using the BamHI and XhoI restriction sites by GenScript.

Expression and purification of proteins

Rr-AfsA and BprA

Rr-AfsA and BprA were mainly expressed as insoluble proteins when pET28-*rr-afsA* and pET28-*bprA* were used for protein expression in *E. coli* BL21-Gold (DE3) (Agilent). Therefore, we attempted to express these proteins with maltose-binding protein (MBP) to enhance the protein solubility. pET28-MBP-TEV[8] (provided by Addgene # 69929) was cloned into *E. coli* NEB 10-beta (New England Biolabs), and pET28-MBP-TEV was extracted from the overnight culture using a plasmid extraction kit (FastGene). Next, *rr-afsA* and *bprA* were amplified by PCR with pET28-*rr-afsA* and pET28-*bprA* as the templates with the primers

pET28MBPTEV_F_afsA3203 TACTTCCAAGGATCC**ATGGATCATAGACGACTACA** (annealing sequence in bold) and pET28MBPTEV_R_afsA3203 GGTGGTGGTGCTCGAG**TTAGTCCAGTTGAACGCG** and the primers pET28MBPTEV_F_bprA ATACTTCCAAGGATCC**ATGATACTAGTAACTGGAGCAA** and pET28MBPTEV_R_bprA GGTGGTGGTGCTCGAG**TTATTCCGGTGCAAAGGCTT**, respectively, using Tks Gflex DNA polymerase (TaKaRa). The pET28-MBP-TEV plasmid was digested at the BamHI and XhoI sites. The purified PCR products and linear pET28-MBP-TEV were assembled using an In-Fusion HD Cloning Kit (TaKaRa), and *E. coli* NEB 10-beta were transformed with these In-Fusion products. Insertion of the complete nucleotide sequences into the vector was confirmed by Sanger sequencing (Eurofins Genomics). pET28-MBP-TEV-*rr-afsA* and pET28-MBP-TEV-*bprA* were transferred to *E. coli* BL21-Gold (DE3). *E. coli* BL21-Gold (DE3) cells harbouring pET28-MBP-TEV-*rr-afsA* or pET28-MBP-TEV-*bprA* were grown in terrific broth (TB) supplemented with 50 μg/mL kanamycin at 37 °C until the OD600 reached approximately 0.5, after which the culture flask was placed on ice for 20 min. After induction of the T7 promotor with 0.5 mM isopropyl β-D-1-thiogalactopyranoside (IPTG), the cells were grown overnight at 16 °C. The cells were centrifuged and washed with buffer (20 mM Tris-HCl, 500 mM NaCl, 10% (v/v) glycerol, pH 8.0) and then sonicated (15 sec on, 45 sec off, 10 times) in buffer containing 0.1 mM phenylmethylsulfonyl fluoride (PMSF) on ice. The sonicated cells were centrifuged at 20000 × *g* for 12 min at 4 °C, and the supernatant was centrifuged at 20000 × *g* for 20 min at 4 °C. The supernatant was purified using a His-trap Ni-NTA column (His-Trap FF, 5 mL, Cytiva) with the following gradient conditions: mobile phase A, 20 mM Tris-HCl, 500 mM NaCl, 10% (v/v) glycerol, pH 8.0; mobile phase B, 20 mM Tris-HCl, 500 mM NaCl, 10% (v/v) glycerol, 300 mM imidazole, pH 8.0; and gradient, 6% B, hold for 20 min, 6–100% B in 20 min, 100% B, hold for 10 min at a flow of 2.0 mL/min. The fractions were analysed by SDS–PAGE using e-PAGEL HR 5~20% (ATTO) precast gel. The eluent fraction was concentrated by ultrafiltration using a Vivaspin Turbo 15 (MWCO 30,000, RC, Sartorius). The concentrated eluent was desalted using a PD-10 desalting column (Cytiva) with buffer (20 mM Tris-HCl, 250 mM NaCl, 10% (v/v) glycerol, pH 8.0). The protein concentration was determined by using the Lowry assay (Bio-Rad, DC protein assay). MBP-Rr-AfsA and MBP-BprA were mainly used in this study since they showed high reaction rates, similar to the tag-free proteins prepared below.

For the cleavage of the MBP-tag with the His-tag, the proteins were treated with Tobacco Etch Virus (TEV) protease (glycerol-free, Nippon Gene) at 4 °C for 20 hr or 30 °C for 2 hr. The reaction mixture was subjected to a His-trap Ni-NTA column, and the flow-through was collected as the tag-free protein-containing fraction. Tag-free Rr-AfsA and BprA were desalted and concentrated as described above and then used for the reaction.

SJ-AfsA

To confirm the *afsA* homologue sequence in *Streptomyces* sp. YKOK-J1, the *afsA* homologue with approximately 60 bp flanking regions was amplified by PCR with the gDNA of *Streptomyces* sp. YKOK-J1 as a template and the primers sj-afsA-flanking-F, 5' - TCCCTCGGAAAGCGGACGGAT-3' and sj-afsA-flanking-R, 5' - AGGTGAGCTGCAGTGCGATGG-3' using Tks Gflex DNA polymerase (TaKaRa). The amplified PCR product was analysed using Sanger sequencing (Eurofins Genomics). The nucleotide sequence was completely identical to the sequence obtained from whole-genome analysis above. Next, *afsA* in *Streptomyces* sp. YKOK-J1 (*sj-afsA*) was amplified by PCR with the amplified PCR product as a template and the primers pET28MBPTEV_F_sj-afsA TATACTTCCAAGGATCC**ATGCCGGAGGCCGCTGCCGC** (annealing sequence in bold), and pET28MBPTEV_R_sj-afsA TGGTGGTGGTGGTGCTCGAG**TCATGCCGCCGTCCCGG** using Tks Gflex DNA polymerase. The pET28-MBP-TEV plasmid was digested at the BamHI and XhoI sites. With the amplified *sj-afsA* sequence, pET28-MBP-TEV-*sj-afsA* was constructed using the abovementioned method. pET28-MBP-TEV-*sj-afsA* was subsequently transferred to *E. coli* Rosetta2 (DE3). *E. coli* Rosetta2 cells harbouring pET28-MBP-TEV-*sj-afsA* were grown in TB containing 50 μg/mL kanamycin and 34 μg/mL chloramphenicol at 37 °C until the OD600 reached approximately 0.5, after which the culture flask was placed on ice for 20 min. After induction of the T7 promotor with 0.5 mM IPTG, the cells were grown overnight at 16 °C. The expressed protein was extracted and purified using the abovementioned method.

SJ-BprA

sj-bprA and its 200–300 bp flanking regions were amplified by PCR with the gDNA of *Streptomyces* sp. YKOK-J1 as a template and the primers sj_bprA_Flanking_F, 5' - CGTCGTACGGGGAGAAGTACTTCG-3' and sj_bprA_Flanking_R, 5' - TCGTTGGCGTGGTCATCCGTCTTC-3' using Tks Gflex DNA polymerase (TaKaRa).

Next, *sj-bprA* in *Streptomyces* sp. YKOK-J1 was amplified by PCR with the amplified PCR product as a template and the primers pET28MBPTEV_F_sj-bprA 5' - TATACTTCCAAGGATCC**ATGCCGCTGACCCCTGCCGG**-3' (annealing sequence in bold) and pET28MBPTEV_R_sj-bprA 5' - TGGTGGTGGTGGTGCTCGAG**CTAGACCCGCGCGGCCG**-3' using Tks Gflex DNA polymerase. The subsequent In-Fusion assembly, protein expression, and purification methods were the same as those described above. The obtained protein had a low reaction rate (~20%) with the substrate *n*-C-5 butenolide phosphate. The TEV protease could not cleave the MBP-tag with the His-tag from MBP-SJ-BprA with high efficiency, although the tag was completely cleaved from MBP-SJ-AfsA under the same reaction conditions (30 °C, 3 hr). Therefore, we attempted to express SJ-BprA without an MBP tag, although the protein yield and solubility were poor.

pET28-*sj-bprA* (see above, **DNA synthesis** section) was transferred to *E. coli* NiCo21 (DE3) (New England Biolabs). Protein expression was essentially the same as that of MBP-SJ-AfsA. SJ-BprA was purified using a His-trap Ni-NTA column (His-Trap FF, 5 mL) with the following gradient conditions: mobile phase A, 20 mM Tris-HCl, 500 mM NaCl, 10% (v/v) glycerol, pH 8.0; mobile phase B, 20 mM Tris-HCl, 500 mM NaCl, 10% (v/v) glycerol, 500 mM imidazole, pH 8.0; and gradient, 4% B, hold for 20 min, 4–100% B in 25 min, 100% B, hold for 15 min at a flow of 2.0 mL/min. The eluent fraction was concentrated by ultrafiltration using a Vivaspin Turbo 15 (MWCO 10,000, PES, Sartorius). The eluent was desalted using a PD-10 desalting column with buffer (20 mM Tris-HCl, 250 mM NaCl, 10% (v/v) glycerol, pH 8.0).

SI-BprA and Rr-BprA

pET28-*si-bprA* and pET28-*rr-bprA* (see above, **DNA synthesis** section) were transferred to *E. coli* NiCo21 (DE3). The proteins were expressed and purified using the same methods as those used for SJ-BprA.

Enzymatic reactions of AfsA and BprA

The purified MBP-Rr-AfsA and MBP-SJ-AfsA were used for the enzymatic reaction. The reaction mixture containing 25 μM AfsA, 2 mM β-ketoacyl-SNACs (**6**), and 2 mM DHAP (**7**) was incubated in 50 μL of 50 mM McIlvaine buffer (pH 7.0) at 25 °C for 10 min. To this AfsA reaction, a BprA reaction mixture containing 10 μM BprA, 2 mM $MgCl_2$, and 2 mM NADPH

in 50 µL of 100 mM HEPES buffer (pH 8.0) was added, and the mixture was then incubated at 25 °C for 60 min. One volume of EtOH was added to the reaction mixture and then centrifuged at 18,000 × g for 3 min. Two volumes of DEAE binding buffer (25 mM CH_3COONH_4, 20% MeOH, pH 7.1) were added to the supernatant. Half of the solution was applied to a MacroPrep DEAE (Bio-Rad) column packed in a Pasteur pipet (column volume: 500 µL). After washing with 3 volumes of DEAE binding buffer, the GBL phosphates were eluted with 6 volumes of DEAE elution buffer (*n*-C-2, *n*-C-3, *n*-C-4, *n*-C-5 GBL phosphate (**9a**–**9d**): 25 mM CH_3COONH_4, 20% MeOH, 1% NH_4OH; *n*-C-6, *n*-C-7, *n*-C-8, *iso*-C-4, *iso*-C-5, *iso*-C-7 GBL phosphate (**9e**–**9g**, **9j**–**9l**): 25 mM CH_3COONH_4, 50% MeOH, 1% NH_4OH; *n*-C-9, *n*-C-10 GBL phosphate (**9h**, **9i**): 25 mM CH_3COONH_4, 80% MeOH, 1% NH_4OH). The eluent was filtered and diluted with MeOH and then analysed using LCMS. Compounds **9a**–**9e**, **9j** and **9k** were analysed using a Mightysil RP18-GP column (4.6 × 100 mm, 3 µm) with the following conditions: negative ion mode; mobile phase A: 0.1% formic acid in H_2O (v/v); mobile phase B: 0.1% formic acid in MeCN (v/v); 0.3 mL/min; gradient conditions for **9a**–**9c**; 0−2.5 min (30% B), 2.5−10 min (30−100% B), and 10−17 min (100% B); gradient conditions for **9d**, **9e**, **9j** and **9k**: 0−2.5 min (50% B), 2.5−10 min (50−100% B), and 10−17 min (100% B). Compounds **9f**–**9i** and **9l** were analysed with an InertSustain C-8 column (4.6 × 100 mm, 3 µm) with the following conditions: negative ion mode; mobile phase A: 0.1% formic acid in H_2O (v/v); mobile phase B: 0.1% formic acid in MeCN (v/v); 0.3 mL/min; gradient conditions; 0−2.5 min (40% B), 2.5−10 min (40−100% B), and 10−17 min (100% B). The ions corresponding to the $[M-H]^-$ ion were analysed in the EICs.

9a: HR-ESI-MS (*m/z*): $[M-H]^-$ calcd for $C_8H_{12}O_7P$, 251.0326; found 251.0331.

9b: HR-ESI-MS (*m/z*): $[M-H]^-$ calcd for $C_9H_{14}O_7P$, 265.0483; found, 265.0476.

9c: HR-ESI-MS (*m/z*): $[M-H]^-$ calcd for $C_{10}H_{16}O_7P$, 279.0639; found, 279.0644.

9d: HR-ESI-MS (*m/z*): $[M-H]^-$ calcd for $C_{11}H_{18}O_7P$, 293.0796; found, 293.0784.

9e: HR-ESI-MS (*m/z*): $[M-H]^-$ calcd for $C_{12}H_{20}O_7P$, 307.0952; found, 307.0954.

9f: HR-ESI-MS (*m/z*): $[M-H]^-$ calcd for $C_{13}H_{22}O_7P$, 321.1109; found, 321.1110.

9g: HR-ESI-MS (*m/z*): $[M-H]^-$ calcd for $C_{14}H_{24}O_7P$, 335.1265; found, 335.1261.

9h: HR-ESI-MS (*m/z*): $[M-H]^-$ calcd for $C_{15}H_{26}O_7P$, 349.1422; found, 349.1424.

9i: HR-ESI-MS (*m/z*): $[M-H]^-$ calcd for $C_{16}H_{28}O_7P$, 363.1578; found, 363.1572.

9j: HR-ESI-MS (*m/z*): $[M-H]^-$ calcd for $C_{10}H_{16}O_7P$, 279.0639; found, 279.0640.

9k: HR-ESI-MS (*m/z*): $[M-H]^-$ calcd for $C_{11}H_{18}O_7P$, 293.0796; found, 293.0808.

9l: HR-ESI-MS (*m/z*): $[M-H]^-$ calcd for $C_{13}H_{22}O_7P$, 321.1109; found, 321.1102.

Enzymatic reaction of BAP

The GBL phosphates (**9a**–**9l**) prepared above were subjected to a phosphorylation reaction using BAP (*E. coli* C75, NIPPON GENE). GBL phosphate in DEAE eluent buffer was evaporated *in vacuo* or under N_2 gas and then resuspended in 99 μL of BAP buffer attached to the BAP enzyme. After the addition of 1 μL of BAP enzyme solution (0.5 unit), the mixtures were incubated at 37 °C for 1 hr. One volume of EtOH was added to the reaction mixture and then centrifuged at 18,000 × g for 3 min. The supernatant was evaporated *in vacuo* and then applied to a Strata C18-E SPE column (500 mg, Phenomenex). After washing with 3 volumes of H_2O, the GBL (**10a**–**10l**) was eluted with 4 volumes of MeOH. The eluent was diluted with MeOH and then subjected to HR-LCMS under the same conditions as those used for GBL screening.

10a: HR-ESI-MS (*m/z*): $[M-H]^-$ calcd for $C_8H_{11}O_4$, 171.0663; found, 171.0658.

10b: HR-ESI-MS (*m/z*): $[M-H]^-$ calcd for $C_9H_{13}O_4$, 185.0819; found, 185.0815.

10c: HR-ESI-MS (*m/z*): $[M-H]^-$ calcd for $C_{10}H_{15}O_4$, 199.0976; found, 199.0971.

10d: HR-ESI-MS (*m/z*): $[M-H]^-$ calcd for $C_{11}H_{17}O_4$, 213.1132; found, 213.1132; ^{1}H NMR ($CDCl_3$, 600 MHz) δ 4.44 (dd, *J* = 8.9, 8.2 Hz, 1H), 4.15 (dd, *J* = 8.9, 6.8 Hz, 1H), 3.74 (dt, *J* = 10.5, 5.2 Hz, 1H), 3.69 (ddd, *J* = 10.8, 5.1 Hz, 1H), 3.67 (d, *J* = 7.2 Hz, 1H), 3.26 (m, 1H), 2.99 (dt, *J* = 18.0, 7.5 Hz, 1H), 2.64 (dt, *J* = 18.0, 7.3 Hz, 1H), 1.62 (m, 2H), 1.57 (overlap, OH), 1.32–1.22 (m, 4H), 0.88 (t, *J* = 6.9 Hz, 3H); ^{13}C NMR ($CDCl_3$, 151 MHz, HSQC and HMBC) δ 201.6, 171.3, 68.8, 61.8, 54.8, 42.3, 38.9, 31.7, 31.1, 22.9, 22.4, 13.9.

10e: HR-ESI-MS (*m/z*): $[M-H]^-$ calcd for $C_{12}H_{19}O_4$, 227.1289; found, 227.1279; ^{1}H NMR ($CDCl_3$, 600 MHz) δ 4.44 (t, *J* = 8.7 Hz, 1H), 4.15 (dd, *J* = 8.9, 6.8 Hz, 1H), 3.74 (ddd, *J* = 9.7, 4.9 Hz, 1H), 3.69 (ddd, *J* = 9.7, 4.9 Hz, 1H), 3.67 (d, *J* = 7.2 Hz, 1H), 3.26 (m, 1H), 2.99 (dt, *J* = 18.0, 7.4 Hz, 1H), 2.64 (dt, *J* = 18.0, 7.3 Hz, 1H), 1.62 (m, 2H), 1.60 (overlap, OH), 1.37–

1.25 (m, 6H), 0.88 (t, J = 6.9 Hz, 3H); ^{13}C NMR ($CDCl_3$, 151 MHz, HSQC and HMBC) δ 203.0, 172.3, 68.8, 61.9, 54.9, 42.6, 39.1, 31.8, 29.9, 28.6, 23.3, 22.5, 14.1.

10f: HR-ESI-MS (*m/z*): $[M-H]^-$ calcd for $C_{13}H_{21}O_4$, 241.1445; found, 241.1438; ^{1}H NMR ($CDCl_3$, 600 MHz) δ 4.44 (dd, J = 8.9, 8.2 Hz, 1H), 4.15 (dd, J = 9.0, 6.8 Hz, 1H), 3.74 (ddd, J = 10.4, 5.1 Hz, 1H), 3.69 (ddd, J = 9.7, 5.2 Hz, 1H), 3.67 (d, J = 7.2 Hz, 1H), 3.26 (m, 1H), 2.99 (dt, J = 18.0, 7.5 Hz, 1H), 2.64 (dt, J = 18.0, 7.2 Hz, 1H), 1.32–1.22 (m, 6H), 0.88 (t, J = 6.9 Hz, 3H).

10g: HR-ESI-MS (*m/z*): $[M-H]^-$ calcd for $C_{14}H_{23}O_4$, 255.1602; found, 255.1598.

10h: HR-ESI-MS (*m/z*): $[M-H]^-$ calcd for $C_{15}H_{25}O_4$, 269.1758; found, 269.1758.

10i: HR-ESI-MS (*m/z*): $[M-H]^-$ calcd for $C_{16}H_{27}O_4$, 283.1915; found, 283.1918.

10j: HR-ESI-MS (*m/z*): $[M-H]^-$ calcd for $C_{10}H_{16}O_7P$, 199.0976; found, 199.0979.

10k: HR-ESI-MS (*m/z*): $[M-H]^-$ calcd for $C_{11}H_{18}O_7P$, 213.1132; found, 213.1128; ^{1}H NMR ($CDCl_3$, 600 MHz) δ 4.44 (t, J = 8.6 Hz, 1H), 4.15 (dd, J = 8.9, 6.8 Hz, 1H), 3.74 (ddd, J = 10.5, 5.2 Hz, 1H), 3.69 (m, 1H), 3.68 (d, J = 7.2 Hz, 1H), 3.26 (m, 1H), 3.00 (ddd, J = 17.8, 8.9, 6.5 Hz, 1H), 2.65 (ddd, J = 17.8, 8.7, 6.4 Hz, 1H), 0.90 (d, J = 6.6 Hz, 6H).

10l: HR-ESI-MS (*m/z*): $[M-H]^-$ calcd for $C_{13}H_{21}O_4$, 241.1445; found, 241.1449; ^{1}H NMR ($CDCl_3$, 600 MHz) δ 4.44 (t, J = 8.6 Hz, 1H), 4.15 (dd, J = 8.9, 6.8 Hz, 1H), 3.74 (dd, J = 10.5, 5.5 Hz, 1H), 3.69 (dd, J = 10.5, 5.6 Hz, 1H), 3.68 (d, J = 7.2 Hz, 1H), 3.26 (m, 1H), 2.99 (ddd, J = 17.8, 8.9, 6.5 Hz, 1H), 2.65 (ddd, J = 17.8, 8.7, 6.4 Hz, 1H), 1.38–1.26 (m, 2H), 1.22–1.15 (m, 2H), 0.90 (d, J = 6.6 Hz, 6H); ^{13}C NMR ($CDCl_3$, 151 MHz, HSQC and HMBC) δ 202.6, 172.1, 68.9, 61.8, 54.9, 42.5, 38.9, 38.6, 27.9, 27.4, 26.8, 23.6, 22.7.

Reduction of C-6 ketone in GBLs (10d–10g, 10k, 10l)

6-keto GBLs (**10d**–**10g**, **10k**, **10l**) were resuspended in EtOH, and $NaBH_4$ (1 mg/mL EtOH) was added. After incubation at RT for 30 min, 0.5 M AcOH was added to acidify the reaction mixture. The solution was dried under nitrogen gas and then applied to a Strata C18-E column (500 mg). After washing with three volumes of H_2O, the eluate fractions were obtained using three volumes of H_2O/MeOH (1:1, v/v) and four volumes of pure MeOH. Aliquots of the fractions were subjected to HR-LCMS analysis. HR-LCMS was performed using a Kinetex

XB-C_{18} column (2.6 μm, 4.6 mm i.d. × 100 mm, 100 Å) with the following conditions: positive mode, mobile phase A: 0.1% formic acid in H_2O (v/v), mobile phase B: 0.1% formic acid in MeCN (v/v), 0.3 mL/min, 0–20 min (20–40% B), 20–25 min (40–100% B), 25–35 min (100% B), and 30 °C.

6-hydroxy *n*-C-7 GBL (18.6 min): HR-ESI-MS (*m/z*): $[M+H]^+$ calcd for $C_{13}H_{25}O_4$, 245.1747; found, 245.1724.

6-hydroxy *n*-C-7 GBL (19.4 min): HR-ESI-MS (*m/z*): $[M+H]^+$ calcd for $C_{13}H_{25}O_4$, 245.1747; found, 245.1731.

6-hydroxy *iso*-C-7 GBL (18.0 min): HR-ESI-MS (*m/z*): $[M+H]^+$ calcd for $C_{13}H_{25}O_4$, 245.1747; found, 245.1725.

6-hydroxy *iso*-C-7 GBL (18.8 min): HR-ESI-MS (*m/z*): $[M+H]^+$ calcd for $C_{13}H_{25}O_4$, 245.1747; found, 245.1727.

References

1 Y. Kudo, T. Awakawa, Y. L. Du, P. A. Jordan, K. E. Creamer, P. R. Jensen, R. G. Linington, K. S. Ryan and B. S. Moore, *ACS Chem. Biol.*, 2020, **15**, 3253–3261.

2 J. B. Davis, J. D. Bailey and J. K. Sello, *Org. Lett.*, 2009, **11**, 2984–2987.

3 S. H. Jung, J. H. Jeong, P. Miller and C. H. Wong, *J. Org. Chem.*, 1994, **59**, 7182–7184.

4 M. Mirdita, K. Schütze, Y. Moriwaki, L. Heo, S. Ovchinnikov and M. Steinegger, *Nat. Methods*, 2022, **19**, 679–682.

5 O. Trott and A. J. Olson, *J. Comput. Chem.*, 2010, **31**, 455–461.

6 J. Eberhardt, D. Santos-Martins, A. F. Tillack and S. Forli, *J. Chem. Inf. Model.*, 2021, **61**, 3891–3898.

7 E. F. Pettersen, T. D. Goddard, C. C. Huang, G. S. Couch, D. M. Greenblatt, E. C. Meng and T. E. Ferrin, *J. Comput. Chem.*, 2004, **25**, 1605–1612.

8 H. Currinn, B. Guscott, Z. Balklava, A. Rothnie and T. Wassmer, *Cell. Mol. Life Sci.*, 2016, **73**, 393–408.

DNA and Protein Sequences

Rr-AfsA from *Rhodococcus rhodnii* JCM 3203

Protein (Accession: TXG89839.1)

MDHRRLHPYRHRVAMRRVAHDPRRRGLTGGLSCPPPTSRRGPGVQMRRRFLCATV
MRNWRRGGHMVVETVDSSTPVGRAPEWLSWERTVERSLVHRAAVAEVLLTDSGPT
DDTDTHWVAAQLPRLHGFYRPVAGVHDPMLLVEAFRQSASMLGHRVHDVPSGHAF
VISALRFTCEAAALRMRDVPARLAMRATFSDVAQRGGTVAGFALAADLFLDDRPAG
SAGGYCAVMNPEAYSRMRGGRTSTPRIAIRIDPAPAADVGVARPADVVVGPRRGDE
WPIRVDITHPVLFDHPSDHLPGMVTLEAIRQACRMHEGRPHALIQSFDISFHRFVELD
AAAFVSVRPTGEPGVLRARVEQDGAVCASGRVQLD

DNA (codon optimized by GenScript)

ATGGATCATAGACGACTACACCCCTATAGGCACCGCGTTGCGATGCGTCGTGTGG
CCCATGACCCACGTCGTCGTGGGTTAACTGGTGGCTTGTCTTGCCCGCCTCCGAC
GAGCCGTCGCGGTCCGGGTGTGCAGATGCGTAGGAGATTCCTGTGCGCGACCGT
CATGCGCAACTGGCGTCGCGGAGGCCACATGGTGGTTGAGACCGTTGATTCGTCC
ACCCCGGTGGGCAGAGCCCCAGAATGGCTGAGCTGGGAACGTACCGTCGAGCGT
AGCCTCGTGCACCGTGCAGCGGTCGCGGAAGTTCTGCTGACTGACAGCGGCCCG
ACGGACGACACCGATACCCATTGGGTTGCTGCTCAGCTGCCGAGATTGCACGGCT
TCTATCGTCCGGTGGCGGGCGTCCACGACCCGATGCTGCTGGTTGAGGCCTTTCG
TCAGTCTGCAAGCATGCTGGGTCATCGTGTGCATGACGTTCCGTCCGGTCACGCG
TTCGTGATTAGTGCCCTGCGTTTTACCTGTGAAGCTGCGGCCTTACGCATGCGGG
ATGTGCCGGCTCGCTTGGCAATGCGTGCTACCTTTAGCGATGTGGCGCAACGTGG
CGGTACAGTTGCTGGCTTTGCTTTGGCGGCGGATCTGTTCCTGGACGATCGCCCG
GCTGGCTCTGCAGGTGGCTACTGCGCTGTGATGAATCCGGAGGCGTACAGCAGA
ATGAGAGGTGGCCGTACCAGCACGCCGCGTATTGCAATCCGCATTGATCCAGCA
CCGGCGGCGGACGTTGGCGTTGCGCGTCCTGCCGACGTGGTGGTAGGTCCGCGC
CGTGGTGATGAATGGCCCATCCGCGTAGATATCACCCATCCGGTATTGTTTGATC
ACCCGTCGGACCACCTGCCGGGTATGGTTACCCTGGAGGCGATCCGCCAAGCAT
GTCGTATGCATGAAGGTCGTCCGCATGCTCTTATCCAGTCCTTTGATATTAGCTTC
CACCGTTTCGTCGAGCTGGACGCAGCGGCGTTCGTCAGCGTTCGTCCGACGGGTG

AACCGGGTGTTCTGAGAGCGCGCGTGGAGCAGGATGGTGCAGTGTGCGCGTCCG
GCCGCGTTCAACTGGACTAA

SJ-AfsA from *Streptomyces* sp. YKOK-J1

Protein

MPEAAAAGRGQRHVRRLVKTAADTGPTTARTDAAGHRARRRGRAPRGGPGAGRR
AATASAGTDAAGRPGPSDSTVRNRGRRMTTPTTRAQTRVQQSGHGPAGAPRPAAG
GYDADPWLTDLTVDQSNPFFYDHPLDHVPGMLLVCAMADAVSDRVDVPAGSRVK
WVVNFRVMPELTPRLVLYAAPPENGRHTLRVTQGPVVVSDSWFTLTADPEADRPAA
ASLPPAPAAEPARAFLVHRTRPENVMLGEPLAEDGVFTAAVLLPEAGHTLASRRPDR
RSVKSVVEAGRQFATWLSHRVGGWPDEVQMLWLRLTADLPADLPAGLPLALRWR
QARMSDDKARLTFELIASDGPGTRIGSLVYVSKGLTPEAYRAFRAGAGTAA

DNA

ATGCCGGAGGCCGCTGCCGCCGGCAGGGGTCAGCGGCATGTCAGGCGGCTCGTC
AAGACTGCCGCGGACACCGGGCCGACGACGGCCCGCACCGATGCGGCCGGCCAC
CGGGCCCGGCGCCGCGGACGCGCCCCACGTGGTGGACCGGGGGCCGGGCGGCGC
GCCGCCACCGCGAGCGCGGGAACAGACGCCGCGGGCCGGCCCGGGCCGAGCGA
CAGCACAGTCAGGAATCGAGGAAGACGGATGACCACGCCAACGACCCGAGCCC
AGACACGCGTTCAGCAGAGCGGCCACGGCCCGGCCGGGGCCCCGCGCCCCGCGG
CCGGGGGCTACGACGCCGACCCCTGGCTCACCGACCTCACCGTCGACCAGAGCA
ACCCGTTCTTCTACGACCACCCGCTGGACCACGTCCCCGGCATGCTCCTGGTGTG
CGCCATGGCCGACGCCGTCAGCGACCGCGTCGACGTCCCGGCGGGCTCCCGGGT
GAAATGGGTCGTCAACTTCCGGGTGATGCCCGAGCTGACCCCGCGCCTGGTGCTC
TACGCCGCGCCGCCCGAGAACGGCCGCCACACCCTGCGCGTCACCCAGGGCCCC
GTCGTCGTGTCGGACAGCTGGTTCACCCTCACCGCCGACCCGGAGGCCGACCGG
CCCGCCGCCGCGTCCTTACCGCCCGCCCCGGCCGCCGAGCCCGCCCGCGCCTTCC
TGGTGCACCGCACCCGCCCGGAGAACGTCATGCTCGGCGAACCCCTCGCCGAGG
ACGGCGTGTTCACCGCCGCGGTCCTGCTGCCGGAGGCCGGGCACACCCTGGCGA
GCCGGCGCCCGGACCGGCGCTCGGTGAAGTCGGTCGTCGAGGCCGGCCGCCAGT
TCGCCACCTGGCTCTCGCACCGGGTCGGCGGCTGGCCGGACGAGGTGCAGATGC

TGTGGCTGCGGCTCACCGCCGACCTGCCGGCCGACCTGCCCGCCGGGCTCCCGCT
GGCGCTGCGCTGGCGGCAGGCCCGCATGTCCGACGACAAGGCCCGGCTCACCTT
CGAGCTGATCGCGAGCGACGGACCGGGCACCCGCATCGGCAGCCTCGTCTACGT
CAGCAAGGGCCTGACACCCGAGGCCTACCGGGCCTTCCGAGCCGGTGCCGGGAC
GGCGGCATGA

BprA from *Streptomyces griseus*

Protein (Accession:WP_012382293.1)

MILVTGATGAVGREVAGRLADAGPVRILARRPERLTVRGTGVEVVQGAYGDRAAL
DRALRGVDAVFLVTNDPTEPDDERVAAAAAAAGVRHLVKLSMMAVEEPDAEDFIT
RRQRENEQAVRDSGVPWTFVRPRTFMSNTLSWAPGIRSAGVVRALYGDAPVACVDP
RDVAAVAVAALTGTGHEGRAYAVSGPEAITAREQTAQLSRVLGRPLRFEELGVDAA
RTALMAKYPPPVAEAFLQSAERQRTGAKASVVPTVQELTGRPARPFRDWSAEHAEA
FAPE

DNA (codon optimized by GenScript)

ATGGGCAGCAGCCATCATCATCATCATCACAGCAGCGGCCTGGTGCCGCGCGGC
AGCCATATGGCTAGCATGACTGGTGGACAGCAAATGGGTCGCGGATCCATGATA
CTAGTAACTGGAGCAACAGGGGCTGTTGGTCGCGAAGTTGCGGGTCGTTTAGCT
GATGCGGGTCCGGTGCGTATCCTGGCGCGTCGTCCGGAGCGCTTGACTGTACGCG
GCACCGGTGTTGAAGTTGTTCAAGGCGCGTACGGCGACCGCGCCGCTCTGGATC
GTGCGCTCAGGGGGGTGGATGCGGTGTTCCTGGTTACGAACGATCCGACCGAGC
CGGATGATGAACGTGTTGCGGCTGCTGCTGCGGCTGCCGGTGTTCGCCACTTGGT
TAAACTGTCCATGATGGCAGTCGAGGAACCGGATGCAGAGGACTTCATCACCCG
TCGTCAACGTGAGAACGAACAGGCAGTGCGTGACAGCGGCGTGCCGTGGACCTT
CGTGCGTCCTCGTACCTTTATGAGCAATACCCTGTCGTGGGCACCGGGTATTCGT
TCTGCGGGCGTCGTGCGCGCGCTTTATGGCGACGCTCCCGTTGCCTGCGTCGACC
CGCGTGACGTCGCGGCCGTGGCGGTGGCGGCTTTGACCGGTACCGGTCATGAAG
GTAGAGCGTACGCGGTCAGCGGTCCAGAGGCGATTACCGCCCGCGAGCAGACCG
CACAGCTGAGCCGTGTGCTGGGTCGTCCGCTGCGTTTTGAAGAGCTGGGCGTGGA

CGCAGCGCGCACTGCGTTGATGGCGAAGTATCCGCCGCCGGTTGCGGAGGCATT
CCTGCAGAGCGCTGAGCGTCAGCGTACGGGCGCGAAAGCCTCCGTGGTTCCGAC
GGTACAAGAACTGACCGGCCGCCCGGCACGCCCATTTAGAGACTGGTCAGCGGA
GCACGCTGAAGCCTTTGCACCGGAATAA

SJ-BprA from *Streptomyces* sp. YKOK-J1

Protein

MPLTPAGGSGLRHDSVVRMSAAGQRPGPRSVIRPLSEGPDAVAGRVRSPWSHWGGL
RMILVTGATGVVGGEVARTLAAAGPVRVFCRDPARLPVLAPGCEVAVGSYQDHGSL
LRALAGVDRAFLVTRDPGGDSDARFLRAAEAAGVRHVVKLSAYAAGEDGADDLIT
RWQRDCEDLVRSCGLEWTLLRPRAFMSNTLAWAGSIRSEGVVHALHPEAPSACVDP
RDIAEVAVAALTSPGHAGRVHALTGPEAISAVGQTRELSRVLGRPLVCRALTAEQAA
VRWSRRHPPHVVEALLRGAERQSRGGKATVDPSVTRLTGRAARSYARWAADHREA
FGPVPATAVLSAAARV

DNA

ATGCCGCTGACCCCTGCCGGCGGCAGCGGCCTCCGGCATGACAGCGTTGTCCGC
ATGTCAGCGGCGGGTCAGCGGCCCGGACCACGATCGGTCATCCGTCCGCTTTCCG
AGGGACCGGACGCGGTCGCCGGCCGGGTCCGGTCCCCGTGGTCCCACTGGGGAG
GTCTCCGCATGATTCTGGTGACGGGCGCGACCGGTGTGGTGGGCGGCGAGGTGG
CGCGGACGCTGGCGGCGGCCGGTCCGGTGCGGGTGTTCTGCCGTGACCCGGCCC
GGCTGCCGGTGCTCGCTCCGGGCTGCGAGGTGGCCGTCGGCTCCTACCAGGACC
ACGGGTCCCTGCTGCGCGCGCTCGCGGGGGTGGACCGGGCGTTCCTGGTCACCC
GTGATCCCGGCGGCGACAGCGACGCGCGCTTCCTGCGGGCCGCGGAGGCGGCCG
GGGTGCGGCACGTGGTGAAGCTGTCCGCGTACGCGGCCGGTGAGGACGGCGCCG
ACGACCTGATCACGCGGTGGCAGCGGGACTGCGAGGACCTGGTGCGCTCCTGCG
GCCTGGAGTGGACGCTGCTGCGGCCGCGCGCGTTCATGTCGAACACGCTGGCGT
GGGCGGGCTCGATCCGCTCCGAGGGCGTGGTGCACGCCCTGCACCCCGAGGCGC
CGAGCGCCTGCGTCGATCCCCGTGACATCGCCGAGGTCGCGGTGGCCGCGCTGA
CCTCACCCGGCCACGCGGGCCGGGTGCACGCGCTCACCGGCCCGGAGGCGATCT

CCGCCGTGGGGCAGACCCGGGAGCTGTCCCGGGTGCTGGGACGCCCGCTGGTGT
GCCGCGCGCTGACGGCGGAGCAGGCCGCGGTCCGCTGGTCGCGCCGTCATCCGC
CGCATGTGGTCGAGGCGCTGCTGCGCGGCGCCGAACGGCAGTCGAGGGGCGGCA
AGGCCACGGTGGATCCGTCCGTCACCCGCCTCACCGGCCGCGCGGCCCGGTCGT
ACGCCCGCTGGGCGGCGGATCACCGGGAGGCGTTCGGACCGGTGCCCGCGACCG
CGGTGCTCTCCGCGGCCGCGCGGGTC

DNA (codon optimized by GenScript)

ATGCCCCTAACACCAGCTGGGGGATCAGGTCTCCGCCACGATAGCGTTGTGCGTA
TGTCTGCTGCGGGCCAACGTCCGGGCCCGCGTAGCGTAATTCGTCCTCTGAGCGA
AGGTCCGGATGCAGTCGCGGGTCGTGTACGCTCCCCGTGGTCCCATTGGGGTGGC
CTCCGTATGATTCTGGTCACGGGTGCCACCGGCGTGGTGGGCGGCGAGGTGGCG
CGTACCCTTGCTGCGGCTGGTCCGGTTCGTGTATTTTGCCGTGACCCGGCACGTCT
GCCGGTTTTGGCGCCGGGGTGCGAGGTGGCCGTTGGTAGTTACCAGGATCACGG
CAGCCTGCTGCGTGCGTTGGCGGGGGTGGACCGTGCCTTCCTGGTTACCCGTGAC
CCGGGTGGTGACAGCGATGCCCGTTTTCTGCGTGCGGCCGAAGCGGCGGGCGTG
CGCCACGTTGTTAAGCTGTCCGCGTATGCGGCTGGCGAGGACGGCGCAGATGAT
CTGATCACCCGCTGGCAGCGTGATTGTGAAGACCTGGTGCGCTCCTGCGGTCTGG
AATGGACCCTGCTGCGCCCGCGTGCGTTCATGAGCAACACGCTGGCGTGGGCTG
GCTCGATCCGCTCGGAGGGTGTGGTTCACGCACTGCATCCGGAGGCACCGTCTGC
CTGCGTTGACCCGAGAGACATCGCCGAGGTTGCGGTCGCGGCGTTAACCAGCCC
GGGTCATGCGGGTCGTGTGCACGCATTGACCGGCCCAGAAGCTATTAGCGCAGT
GGGTCAAACCCGTGAGCTGTCACGTGTGCTGGGTCGACCATTGGTCTGTCGCGCG
TTGACTGCTGAGCAGGCAGCTGTGCGTTGGTCTCGTCGTCACCCACCGCATGTTG
TTGAAGCGTTGTTGCGCGGTGCAGAGCGCCAAAGCCGCGGTGGTAAAGCAACGG
TGGACCCGAGCGTTACCCGGCTGACCGGTCGCGCGGCGCGTTCTTACGCAAGAT
GGGCTGCTGATCATCGTGAAGCGTTCGGCCCCGTGCCGGCGACGGCGGTTTTAAG
CGCTGCCGCCAGAGTC

Rr-BprA from *Rhodococcus rhodnii* JCM 3203

Protein (Accession: WP_010840455.1)

MTIAVTGATGVIGGGVFARLAERQEVRLVGRDGSRLSALAGTFPDASVAVAHYGDA
AAMESALAGVNTMLLVSAHESPTRRDDHATAVAAAVRAGVGRIVYLSFLGAGPEC
TFTFGRDHWYTEQEIRESGVAHTFLRDSWYQSMIPAMVDDEGVIRGPAGDGRVSAV
APADVVDSAAEVVEAGAERDPSPYDGETYELTGPAAFTLAEAATQLSDVTGTTIRYA
EETIEEAYLSREVYDAPKWEVDGWVTSYAAVATGELSTVTDDVSMLTGRPATSFAQ
YLHDHPESWARLR

DNA (codon optimized by GenScript)

ATGACAATAGCTGTAACTGGAGCAACGGGGGTGATCGGCGGCGGCGTGTTTGCG
CGTTTGGCGGAGCGCCAAGAGGTGCGTCTGGTAGGTCGCGACGGTAGCAGACTT
TCAGCGCTGGCGGGTACATTCCCGGATGCGAGCGTGGCCGTCGCCCACTACGGC
GATGCAGCGGCTATGGAATCGGCACTGGCGGGTGTCAACACCATGCTGCTGGTG
TCCGCGCACGAATCTCCGACCCGTCGTGACGATCACGCGACCGCAGTTGCTGCGG
CAGTTCGTGCAGGTGTCGGTCGCATTGTTTACTTGAGCTTTCTCGGCGCGGGTCC
GGAGTGCACCTTTACCTTCGGTAGAGACCATTGGTACACCGAACAAGAAATTCGT
GAAAGCGGTGTGGCGCACACCTTCTTGCGTGACAGCTGGTACCAGAGCATGATC
CCGGCTATGGTTGACGACGAAGGAGTTATCCGTGGTCCAGCTGGCGACGGCCGT
GTTAGCGCTGTGGCACCGGCGGATGTGGTGGACAGTGCCGCAGAGGTCGTGGAA
GCGGGCGCGGAACGCGATCCGAGCCCGTATGATGGTGAAACGTACGAGCTGACT
GGTCCGGCGGCCTTTACCCTGGCGGAGGCTGCTACCCAGCTGAGCGACGTGACC
GGCACTACGATCCGCTATGCGGAGGAGACCATTGAAGAGGCGTATTTATCCCGC
GAGGTTTATGACGCCCCTAAATGGGAAGTCGATGGTTGGGTTACGTCTTACGCGG
CTGTTGCTACCGGCGAGCTGTCGACCGTTACCGATGACGTTTCCATGTTGACGGG
CCGTCCGGCTACCAGCTTCGCCCAGTATCTGCATGATCATCCGGAGTCTTGGGCA
CGTCTGCGTTAA

SI-BprA from *Streptomyces* sp. YKOK-I1

Protein

MYLITGANGVVGRRVTDLLLRENGGGGGNGENGEKAAVAAVTRGPGAATLPDGVR
AVAGDLFHPGWIEPALAGVRALQISPRATGPGLGELLRLAAGQGVRRVVLLSATTVE

HPAGEARFADRFRHAEELVRDSGLDWTVLRLADFAANALAWAPQTGSGDVVRGAY
GRAATSPVHEDDIAEIAVHALRGTLPPGSVHTLTGPQSLDQAEKVRLIGAALGRDLSF
QELPPERIRQAMLAQGLPEEVPDRLLGSLADYARRPGPTTATVADLLGRPARTFADW
ARENAPAFGRGVS

DNA (codon optimized by GenScript)

ATGTATCTAATAACAGGAGCTAATGGGGTAGTTGGTCGCCGTGTTACCGATTTGC
TGCTGCGCGAAAACGGCGGCGGCGGCGGAAACGGTGAGAACGGTGAGAAAGCC
GCGGTCGCAGCTGTGACCCGTGGCCCAGGTGCTGCGACCCTGCCGGATGGTGTCC
GCGCGGTGGCCGGCGATCTCTTTCATCCGGGTTGGATTGAACCGGCGCTGGCAGG
CGTACGTGCGCTCCAGATCAGCCCGCGTGCGACCGGTCCGGGTCTGGGCGAATT
GCTGAGATTGGCGGCGGGCCAGGGCGTTCGTCGCGTGGTGCTGCTGAGCGCGAC
CACGGTCGAGCACCCGGCGGGCGAGGCACGCTTCGCGGATCGTTTCCGCCATGC
CGAGGAATTGGTTCGTGACTCTGGTCTGGATTGGACCGTGTTGCGCCTAGCGGAC
TTCGCGGCGAATGCCCTGGCTTGGGCACCGCAGACCGGCTCCGGTGATGTTGTTC
GCGGTGCGTACGGCCGTGCGGCAACGAGCCCGGTTCATGAAGATGACATTGCGG
AAATCGCCGTGCACGCCCTGCGTGGTACTCTGCCGCCTGGCTCTGTCCACACCCT
GACCGGTCCGCAAAGCCTGGACCAAGCTGAGAAGGTGCGTCTTATCGGTGCTGC
GCTTGGGCGTGACTTGTCGTTCCAAGAGCTGCCACCGGAACGTATTCGTCAGGCA
ATGCTGGCGCAGGGTTTACCAGAGGAAGTTCCGGACCGCCTGCTGGGTTCCCTGG
CCGACTATGCACGTCGTCCGGGTCCGACCACGGCTACTGTTGCTGACTTGTTAGG
CCGTCCGGCGCGTACCTTTGCCGACTGGGCGAGAGAGAATGCACCGGCTTTTGGT
AGGGGTGTGAGCTAA

Table S1. The list of bacteria strains used in this study. Bacteria origin, medium, number of days of pre-culture and culture, and timing of XAD addition from inoculation are listed.

Actinomycete species	Strain	Temperature (°C)	Medium	Preculture term (days)	Culture term (days)	XAD-7HP addition from inoculation (days)
Dietzia timorensis	NBRC 104184	28	ISP-2	2	7	2
Gordonia polyisoprenivorans	JCM 10675	28	ISP-2	3	6	2
Kitasatospora cheerisanensis	JCM 21757	28	ISP-2	2	7	2
Kutzneria albida	JCM 3240	28	Yeast-Starch (A)	3	4	2
Mycobacterium cookii	JCM 12404	28	Middlebrook 7H10 OADC	9	16	9
Mycolicibacterium austroafricanum	JCM 13017	28	Soybean-Casein Digest	4	9	3
Mycolicibacterium chlorophenolicum	JCM 7439	28	ISP-2	2	7	2
Nocardia anaemiae	JCM 12396	28	ISP-2	4	5	2
Nocardia carnea	JCM 30727	28	ISP-2	3	12	7
Nocardia harenae	JCM 14548	28	ISP-2	3	6	2
Nocardia lijiangensis	JCM 13592	28	Yeast-Krainsky's medium	7	6	3
Nocardia pseudovaccinii	JCM 11883	28	ISP-2	2	5	2
Nocardia tenerifensis	JCM 12693	28	ISP-2	3	2	2
Nocardia xishanensis	JCM 12160	28	Yeast-Krainsky's medium	3	6	2
Rhodococcus erythropolis	NBRC 15567	28	ISP-2	2	7	2
Rhodococcus jostii RHA-1	NBRC 108803	28	ISP-2	2	7	2
Rhodococcus rhodnii	JCM 3203	28	ISP-2	3	4	2
Rhodococcus rhodochrous	NBRC 16069	28	ISP-2	2	7	2
Salinispora tropica	JCM 13857	28	A1	2	7	2
Streptomyces capuensis	JCM 4460	28	Yeast-Starch (A)	3	4	2
Streptomyces durhamensis	JCM 4291	28	V8 juice medium	4	6	3
Streptomyces ghanaensis	JCM 4963	28	Yeast-Starch (A)	2	12	2
Streptomyces griseoaurantiacus	JCM 4763	28	Yeast-Starch (A)	2	12	2
Streptomyces griseus	NBRC 12875	28	ISP-2	2	7	2
Streptomyces rimosus subsp. *rimosus*	JCM 4073	28	Yeast-Starch (A)	3	6	2
Streptomyces coelicolor A3(2) (*S. violaceoruber*)	NBRC 15146	28	ISP-2	2	7	2
Streptomyces sp.[a)]	YKOK-D1	28	ISP-2	4	8	3
Streptomyces sp.[b)]	YKOK-F1	28	ISP-2	2	7	2
Streptomyces sp.[c)]	YKOK-G2b	28	ISP-2	3	6	2
Streptomyces sp.[d)]	YKOK-I1	28	ISP-2	3	7	2
Streptomyces sp.[e)]	YKOK-J1	28	ISP-2	3	6	2

[a)] Partial 16s rRNA sequence shows 100 % identity with *Streptomyces wuyuanensis.*

[b)] Partial 16s rRNA sequence shows 100 % identity with *Streptomyces sporoverrucosus* and some *Streptomyces* spp.

[c)] Partial 16s rRNA sequence shows 99.8 % identity with *Streptomyces cinereoruber* subsp. fructofermentans.

[d)] Whole 16s rRNA sequence shows 98.8 % identity with *Streptomyces acidiscabies.*

[e)] Whole 16s rRNA sequence shows 98.6 % identity with *Streptomyces cyaneochromogenes*.

Table S2. NMR spectroscopic data for (3*R*)-*n*-C-9 GBL (**2**) isolated from *Rhodococcus rhodnii* JCM 3203[a]

	(3*R*)-*n*-C-9 GBL (**2**)		
position	δ_C, type	δ_H (*J* in Hz)	gHMBC
1	172.2, C		
2	54.8, CH	3.67, d (7.2)	1, 3, 4, 5, 6
3	39.0, CH	3.26, m	2, 4, 6
4	68.8, CH_2	4.44, dd (9.0, 8.2)	1, 5
		4.15, dd (9.0, 6.8)	1, 5
5	61.8, CH_2	3.74, ddd (10.5, 5.4, 4.0)	2, 3, 4
		3.69, ddd (10.5, 5.7, 4.2)	2, 3, 4
6	202.8, C		
7	42.5, CH_2	2.99, dt (17.9, 7.5)	6, 8, 9–12
		2.64, dt (17.9, 7.2)	6, 8, 9–12
8	23.2, CH_2	1.60, m	6, 7, 9–12
9–12	28.9–29.7, CH_2	1.21–1.38, m	
13	22.7, CH_2	1.21–1.38, m	9–12, 13, 14, 15
14	31.8, CH_2	1.21–1.38, m	
15	14.1, CH_3	0.88, t (7.0)	13, 14
5-OH	-	1.59, overlap	3, 5

[a]The ^1H (600 MHz) and ^{13}C (151 MHz) NMR spectra were recorded using $CDCl_3$ as the solvent. The signal of residual $CDCl_3$ (7.26 ppm) in the ^1H NMR spectrum and that of $^{13}CDCl_3$ (77.16 ppm) in the ^{13}C NMR spectrum were used as the internal references.

Table S3. NMR spectroscopic data for (3*R*)-*n*-C-8 GBL (**3**) isolated from *Rhodococcus rhodnii* JCM3203[a]

	(3*R*)-*n*-C-8 GBL (**3**)		
position	$\delta_{C,}$ type	δ_H (*J* in Hz)	gHMBC
1	172.1, C		
2	54.4, CH	3.67, d (7.2)	1, 3, 5, 6
3	39.3, CH	3.26, m	2, 4, 6
4	69.0, CH_2	4.44, t (8.5)	
		4.15, dd (8.9, 6.9)	5
5	61.8, CH_2	3.74, ddd (10.5, 5.4, 4.0)	2, 4
		3.69, ddd (10.5, 5.7, 4.2)	2, 4
6	202.6, C		
7	43.0, CH_2	2.99, dt (18.0, 7.6)	6, 8, 9
		2.64, dt (18.0, 7.3)	6, 8, 9
8	23.3, CH_2	1.60, m	9–11
9–11	28.9–29.7, CH_2	1.22–1.32, m	
12	22.6, CH_2	1.22–1.32, m	9–11, 13
13	31.5, CH_2	1.22–1.32, m	
14	14.0, CH_3	0.88, t (6.9)	12, 13
5-OH	-	1.59, overlap	3

[a]The ^1H (600 MHz) and ^{13}C (151 MHz) NMR spectra were recorded using $CDCl_3$ as the solvent. The signal of residual $CDCl_3$ (7.26 ppm) in the ^1H NMR spectrum and that of $^{13}CDCl_3$ (77.16 ppm) in the ^{13}C NMR spectrum were used as the internal references.

Table S4. NMR spectroscopic data for (3*R*)-*n*-C-7 GBL (**4**) isolated from *Rhodococcus rhodnii* JCM3203[a]

	(3*R*)-*n*-C-7 GBL (**4**)		
position	$\delta_{C,}$ type	δ_H (*J* in Hz)	gHMBC
1	172.0, C		
2	54.8, CH	3.67, d (7.2)	1, 3, 5, 6
3	38.9, CH	3.26, m	2, 4, 6
4	68.8, CH_2	4.44, dd (8.9, 8.2)	
		4.15, dd (8.9, 6.8)	5
5	61.9, CH_2	3.74, dt (10.5, 5.2)	2, 4
		3.69, ddd (10.8, 5.1)	2, 4
6	202.6, C		
7	42.3, CH_2	2.99, dt (18.0, 7.5)	6, 8
		2.64, dt (18.0, 7.3)	6, 8
8	23.2, CH_2	1.59, m	9–10
9–10	28.9–29.7, CH_2	1.22–1.32, m	
11	22.5, CH_2	1.22–1.32, m	9–10, 12, 13
12	31.5, CH_2	1.22–1.32, m	
13	14.0, CH_3	0.88, t (6.9)	11, 12
5-OH	-	1.58, overlap	

[a]The ^1H (600 MHz) and ^{13}C (151 MHz) NMR spectra were recorded using $CDCl_3$ as the solvent. The signal of residual $CDCl_3$ (7.26 ppm) in the ^1H NMR spectrum and that of $^{13}CDCl_3$ (77.16 ppm) in the ^{13}C NMR spectrum were used as the internal references.

Table S5. NMR spectroscopic data for (3*R*)-*iso*-C-6 GBL (**5**) isolated from *Streptomyces* sp. YKOK-I1[a]

	(3*R*)-*iso*-C-6 GBL (**5**)		
position	δ_C, type	δ_H (*J* in Hz)	gHMBC
1	172.2, C		
2	55.1, CH	3.67, d (7.2)	1, 3, 5, 6
3	39.0, CH	3.26, m	6
4	69.1, CH_2	4.44, dd (9.0, 8.2)	1
		4.15, dd (9.0, 6.9)	1, 5
5	61.9, CH_2	3.73, m	
		3.69, m	
6	202.6, C		
7	42.9, CH_2	2.98, dt (18.0, 7.3)	6, 8, 9
		2.64, dt (18.1, 7.2)	6, 8, 9
8	21.3, CH_2	1.61, overlap	6, 7, 9
9	38.3, CH_2	1.19, br dd (16.6, 6.9)	7, 10, 11–12
10	28.1, CH	1.56, overlap	9, 11–12
11–12	22.7, CH_3	0.88, d (6.7)	9, 10, 11–12
5-OH	-	1.59, overlap	

[a]The ^1H (600 MHz) and ^{13}C (151 MHz) NMR spectra were recorded using $CDCl_3$ as the solvent. The signal of residual $CDCl_3$ (7.26 ppm) in the ^1H NMR spectrum and that of $^{13}CDCl_3$ (77.16 ppm) in the ^{13}C NMR spectrum were used as the internal references.

Table S6. The estimated reaction rate of AfsA and BprA combined *in vitro* reactions.

	Enzymes	
Substrate	Rr-AfsA + BprA	SJ-AfsA + BprA
n-C-2 (**6a**)	13.4	0.2
n-C-3 (**6b**)	73.4	7.2
n-C-4 (**6c**)	100.0	80.9
n-C-5 (**6d**)	80.2	100.0
n-C-6 (**6e**)	75.9	56.4
n-C-7 (**6f**)	27.2	3.8
n-C-8 (**6g**)	21.3	0.7
n-C-9 (**6h**)	26.3	No product
n-C-10 (**6i**)	10.1	No product
iso-C-4 (**6j**)	6.3	1.6
iso-C-5 (**6k**)	21.2	40.7
iso-C-7 (**6l**)	68.3	Not tested

The enzyme reactions were conducted under the same conditions, and the results were normalized with the most efficiently converted substrates (**6c** or **6d**) set as 100%. By adjusting the reaction temperature or time, other major substrates can also be converted to 100%.

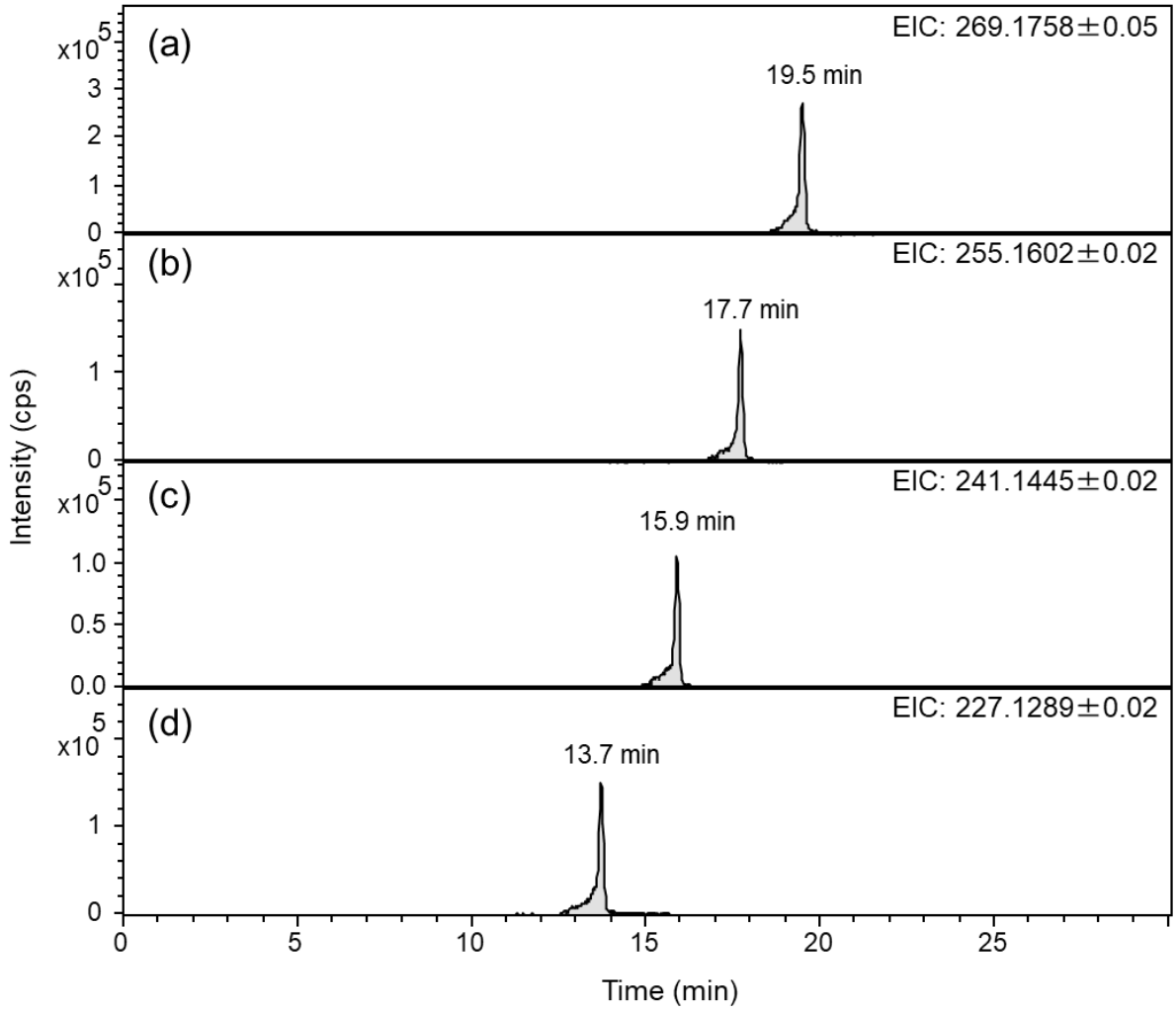

Figure S1. LCMS extracted ion chromatograms of purified natural (**a**) (3*R*)-*n*-C-9 GBL (**2**), (**b**) (3*R*)-*n*-C-8 GBL (**3**), (**c**) (3*R*)-*n*-C-7 GBL (**4**), and (**d**) (3*R*)-*iso*-C-6 GBL (**5**). EIC values were denoted on the chromatogram panels (negative ion mode).

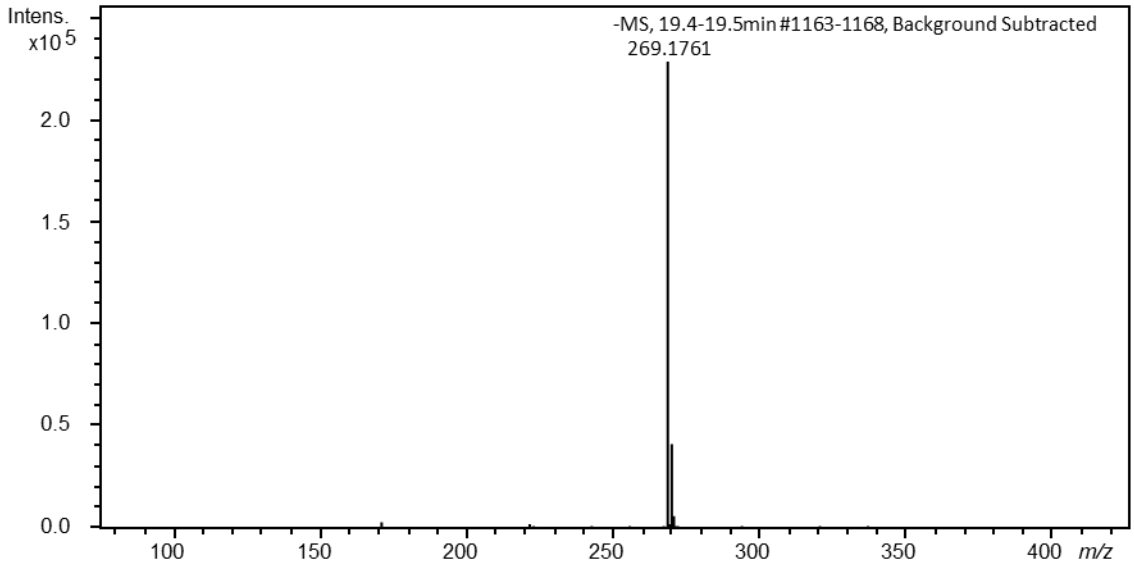

Figure S2. HR-ESI-TOF mass spectrum of purified natural (3*R*)-*n*-C-9 GBL (**2**).

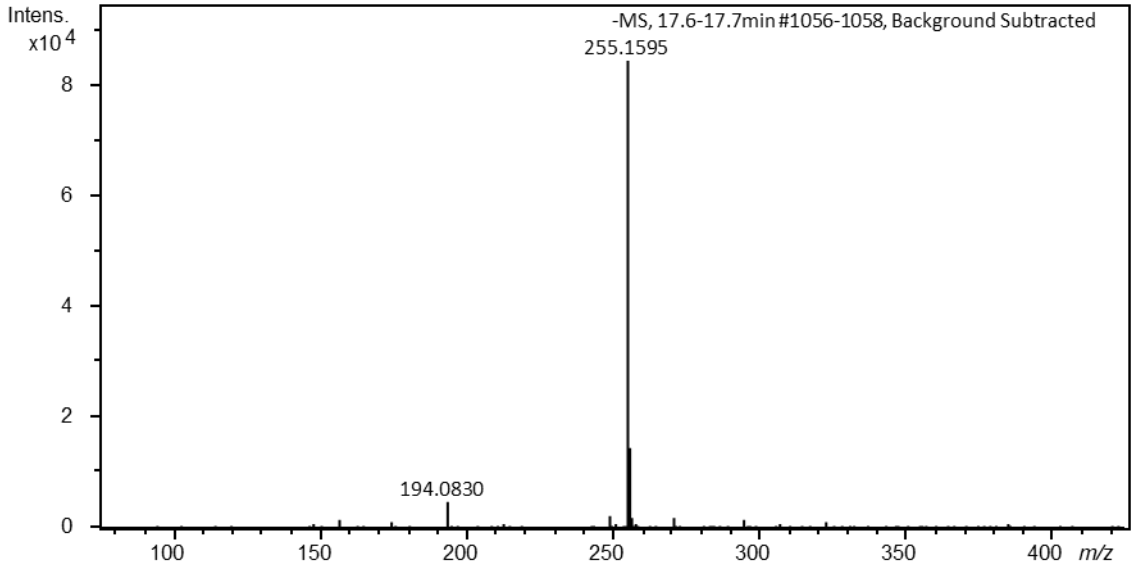

Figure S3. HR-ESI-TOF mass spectrum of purified natural (3*R*)-*n*-C-8 GBL (**3**).

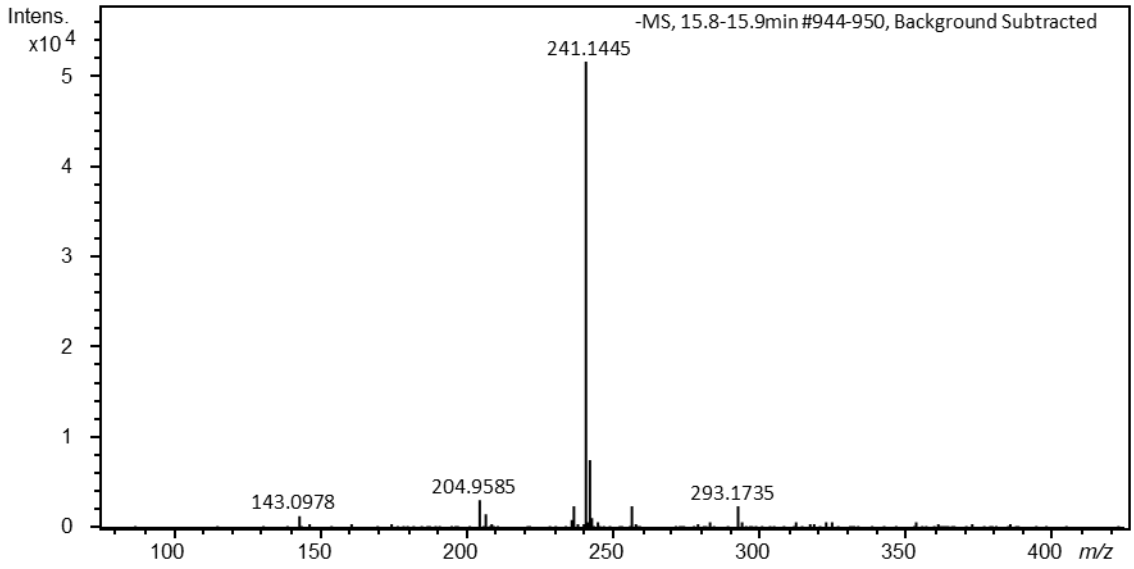

Figure S4. HR-ESI-TOF mass spectrum of purified natural (3*R*)-*n*-C-7 GBL (**4**).

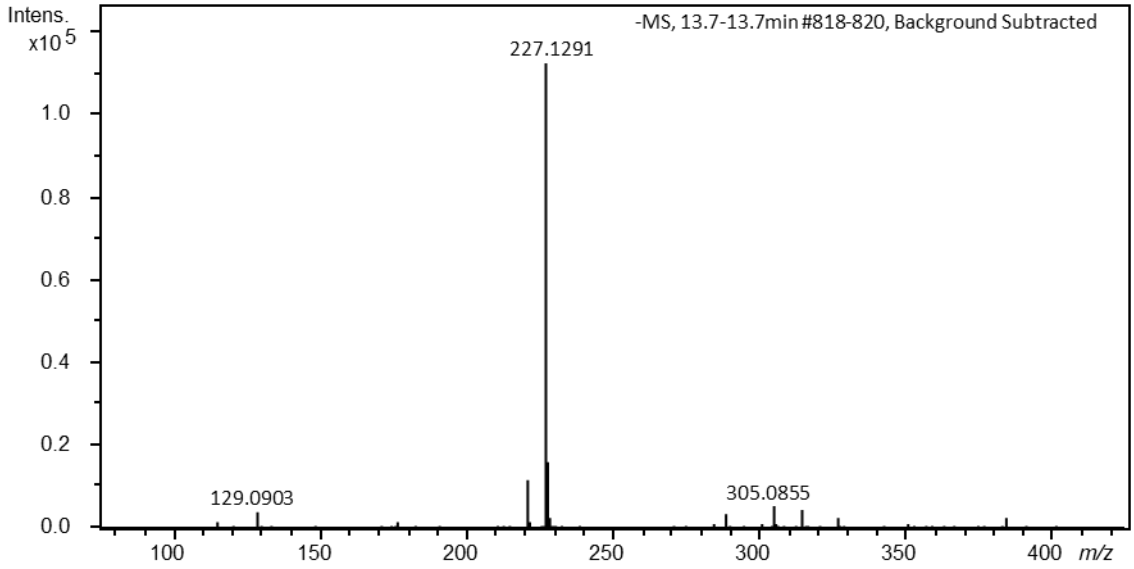

Figure S5. HR-ESI-TOF mass spectrum of purified natural (3*R*)-*iso*-C-6 GBL (**5**).

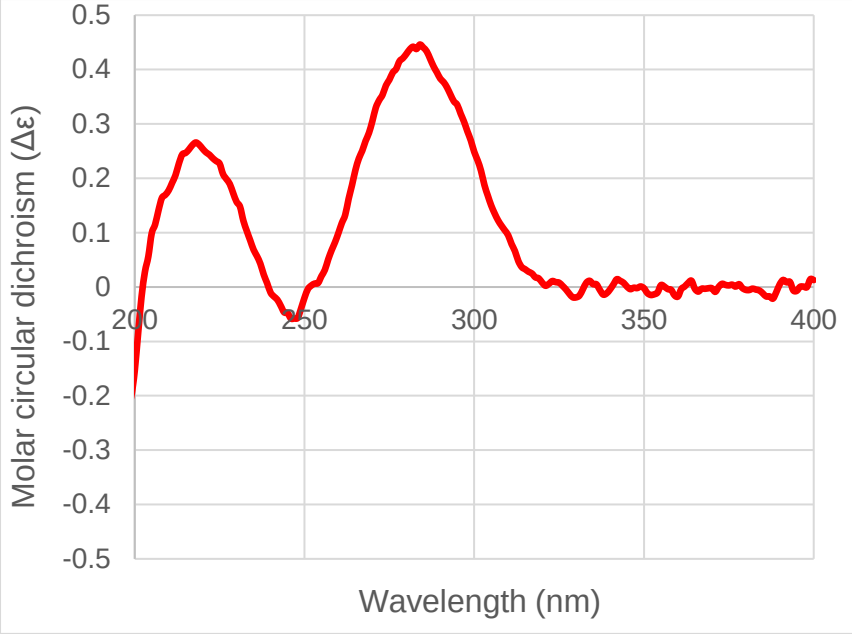

Figure S6. CD spectrum of purified natural (3*R*)-*n*-C-9 GBL (**2**).

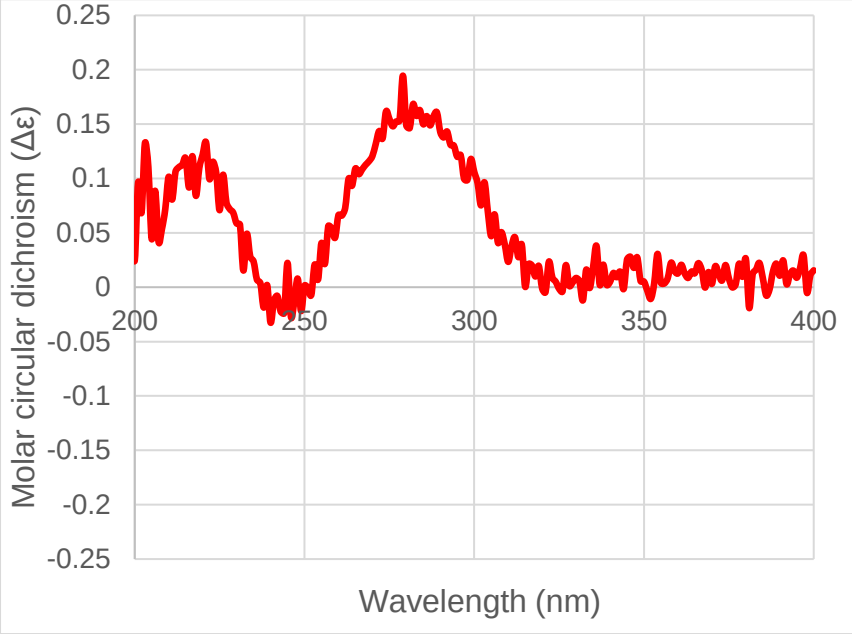

Figure S7. CD spectrum of purified natural (3*R*)-*n*-C-8 GBL (**3**).

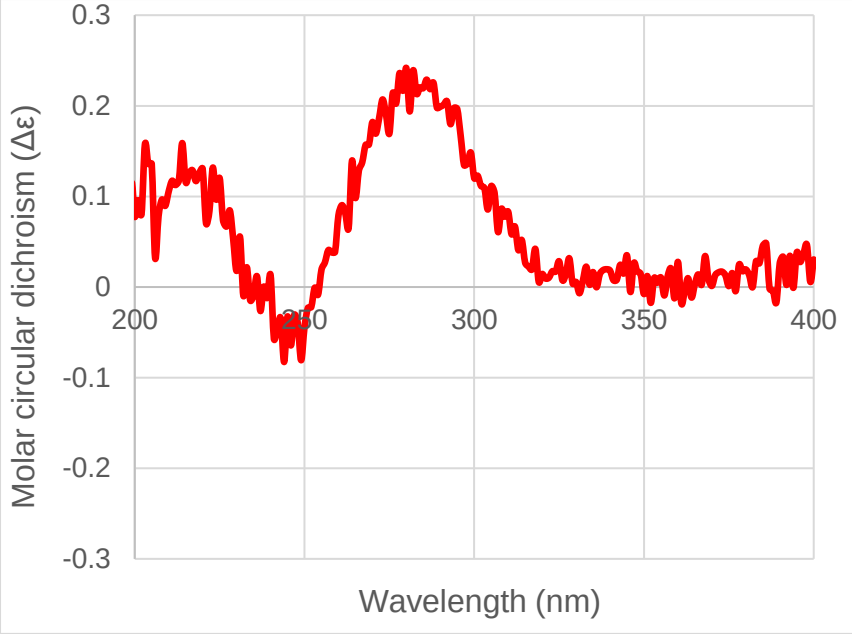

Figure S8. CD spectrum of purified natural (3*R*)-*n*-C-7 GBL (**4**).

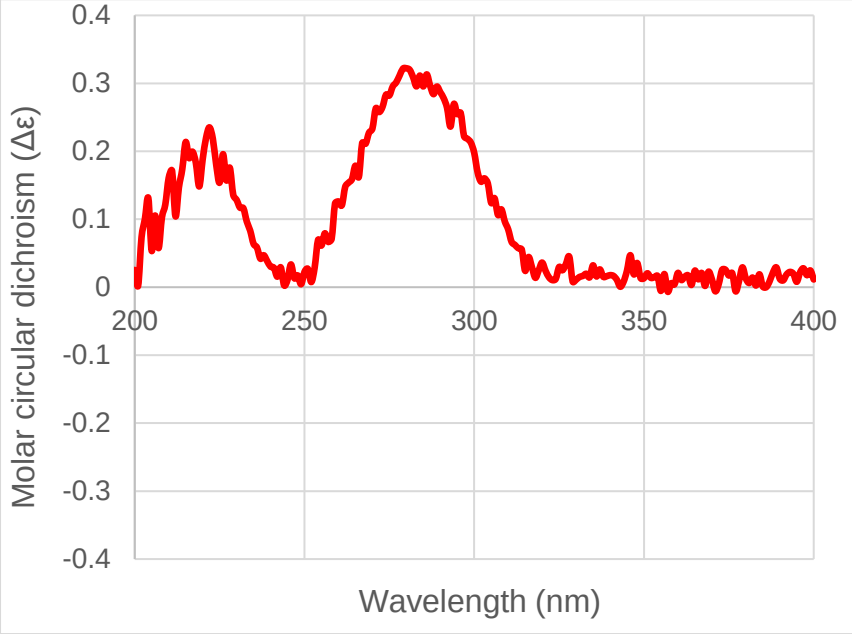

Figure S9. CD spectrum of purified natural (3*R*)-*iso*-C-6 GBL (**5**).

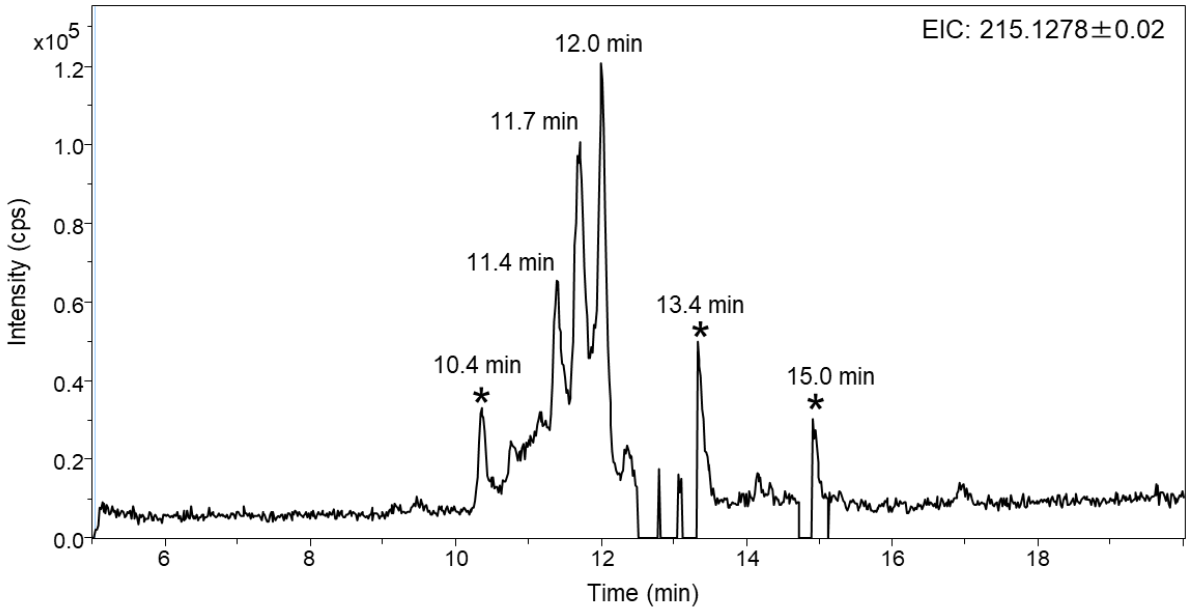

Figure S10. HR-LCMS chromatograms of extract of *Streptomyces* sp. YKOK-J1. EIC values were denoted on the chromatogram (positive ion mode). Peaks marked with an asterisk correspond to compounds whose exact masses differ from C-5 GBLs such as **10d** and **10j**.

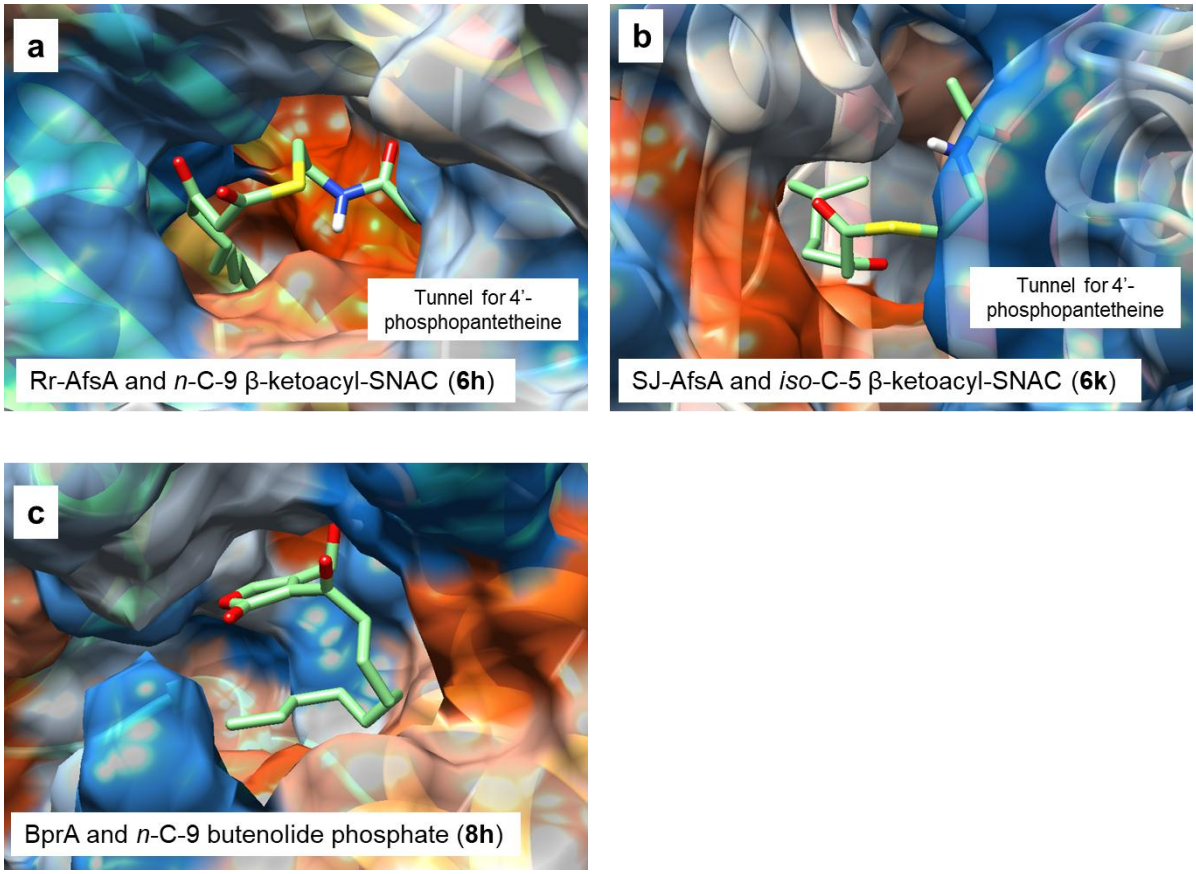

Figure S11. Docking models of AfsA homologues and BprA with substrates. (**a**) Predicted structure of Rr-AfsA and *n*-C-9 β-ketoacyl-SNAC (**6h**). (**b**) Predicted structure of SJ-AfsA and *n*-C-5 β-ketoacyl-SNAC (**6k**). (**c**) Predicted structure of BprA and *n*-C-9 butenolide phosphate (**8h**).

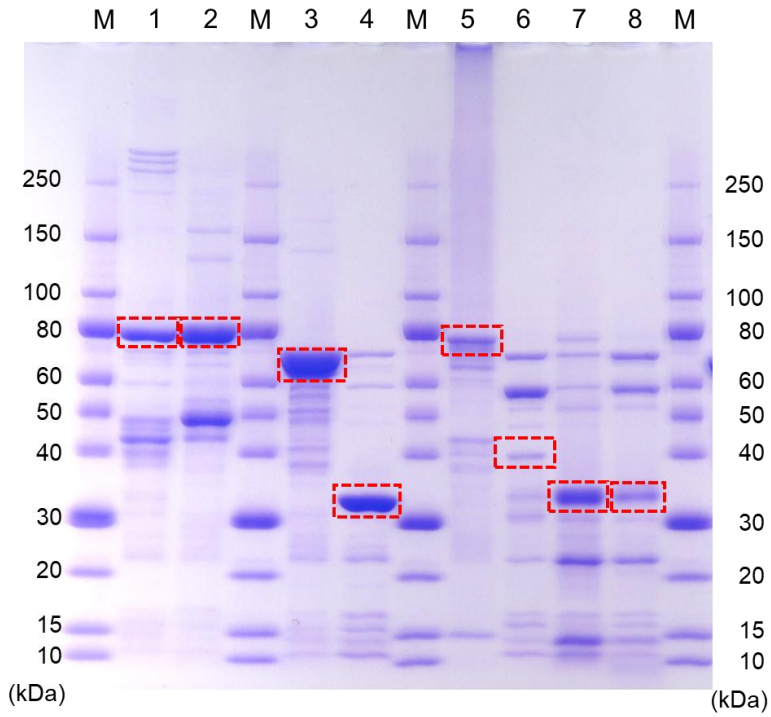

Lane	Protein	size (kDa)
1	MBP-Rr-AfsA	84.9
2	MBP-SJ-AfsA	84.8
3	MBP-BprA	74.3
4	BprA (tag-free)	32.4
5	MBP-SJ-BprA	81.1
6	His-SJ-BprA	40.5
7	His-Rr-BprA	34.7
8	His-Sl-BprA	34.3
M	Marker	as displayed

Figure S12. SDS-PAGE gel (5–20% gradient) of proteins used in this study. Target proteins were outlined in red dot boxes, and their predicted sizes were listed in the right table.

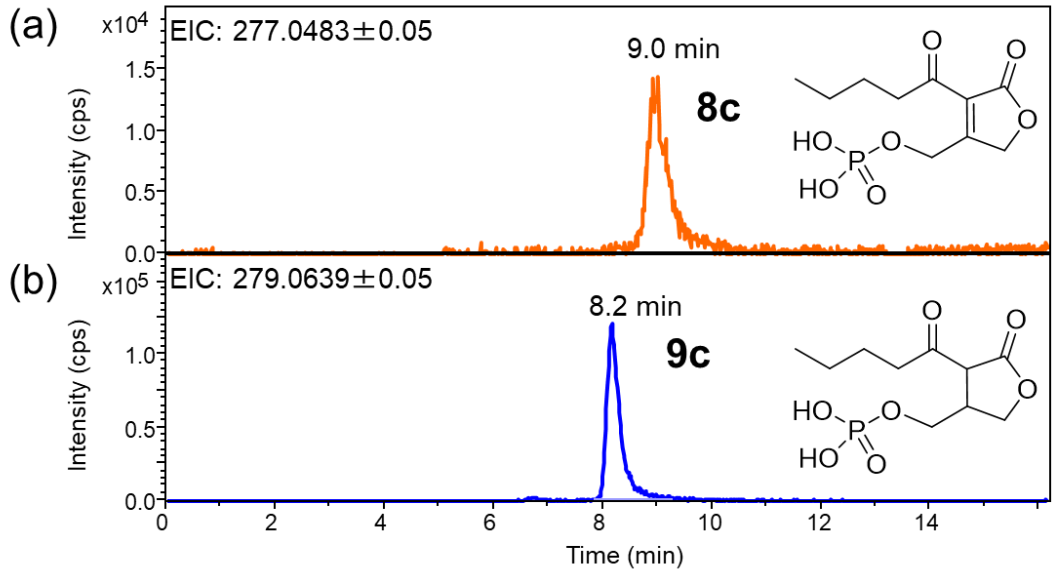

Figure S13. LCMS chromatograms of AfsA enzymatic reaction product using substrate **6c**. (**a**) The enzymatic products measured immediately after the reaction. (**b**) The enzymatic products treated with $NaBH_3CN$. EIC values were denoted on the chromatogram panels (negative ion mode).

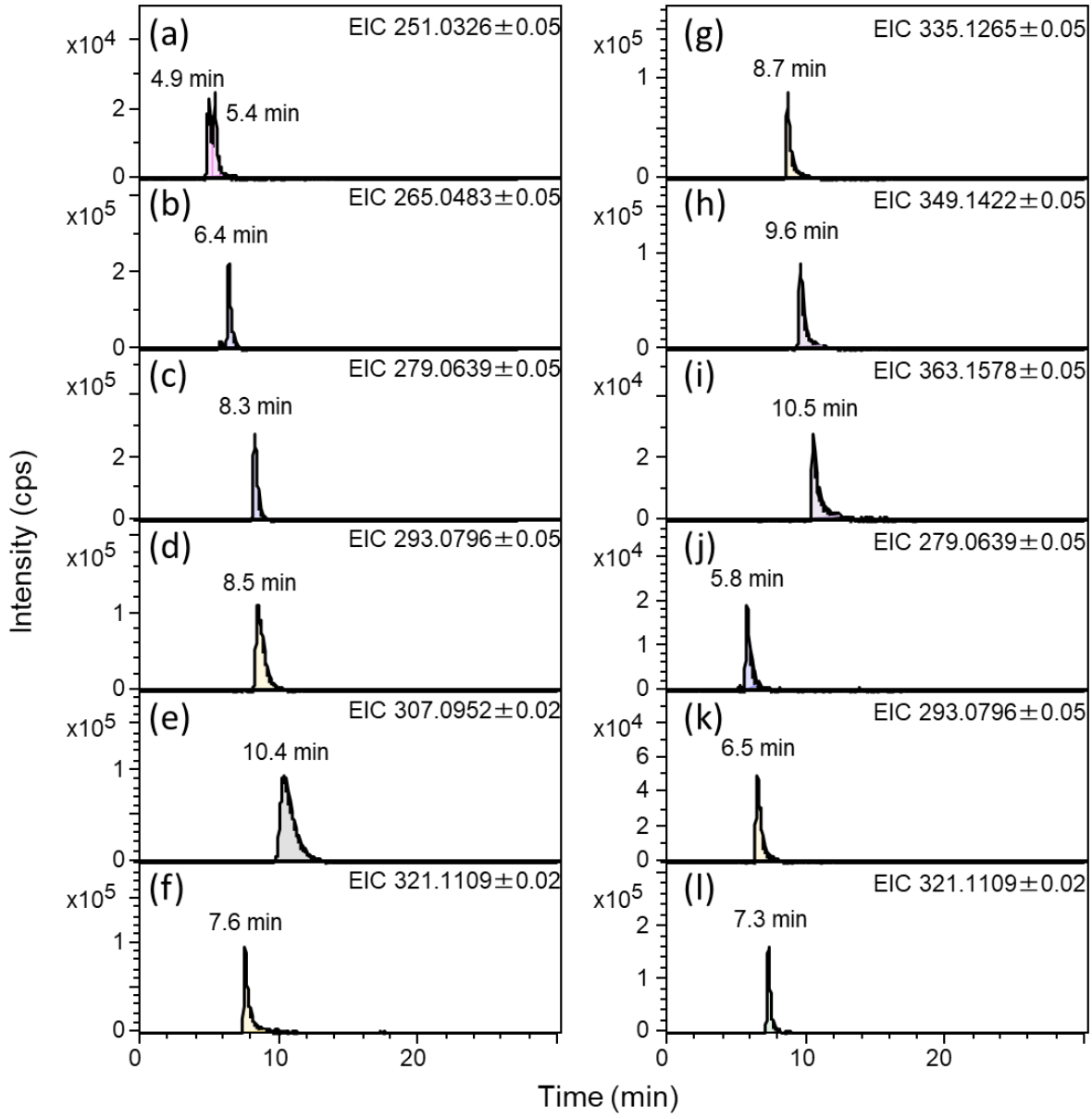

Figure S14. LCMS extracted ion chromatograms of synthesized butenolide phosphate. (**a**) *n*-C-2 butenolide phosphate (**9a**), (**b**) *n*-C-3 butenolide phosphate (**9b**), (**c**) *n*-C-4 butenolide phosphate (**9c**), (**d**) *n*-C-5 butenolide phosphate (**9d**), (**e**) *n*-C-6 butenolide phosphate (**9e**), (**f**) *n*-C-7 butenolide phosphate (**9f**), (**g**) *n*-C-8 butenolide phosphate (**9g**), (**h**) *n*-C-9 butenolide phosphate (**9h**), (**i**) *n*-C-10 butenolide phosphate (**9i**), (**j**) *iso*-C-4 butenolide phosphate (**9j**), (**k**) *iso*-C-5 butenolide phosphate (**9k**), (**l**) *iso*-C-7 butenolide phosphate (**9l**). EIC values were denoted on the chromatogram panels (negative ion mode).

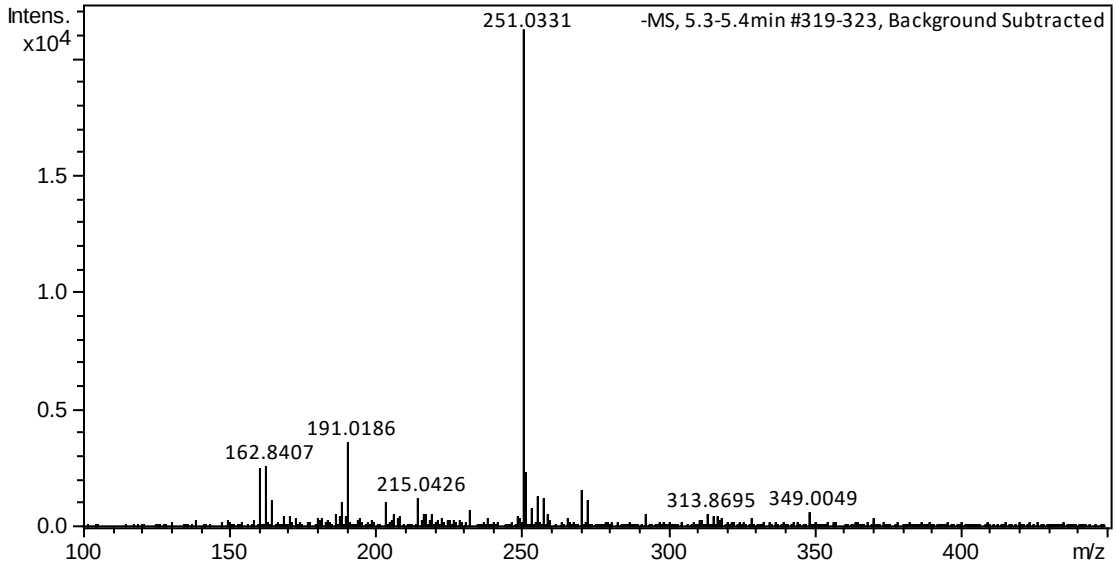

Figure S15. HR-ESI-TOF mass spectrum of *n*-C-2 butenolide phosphate (**9a**).

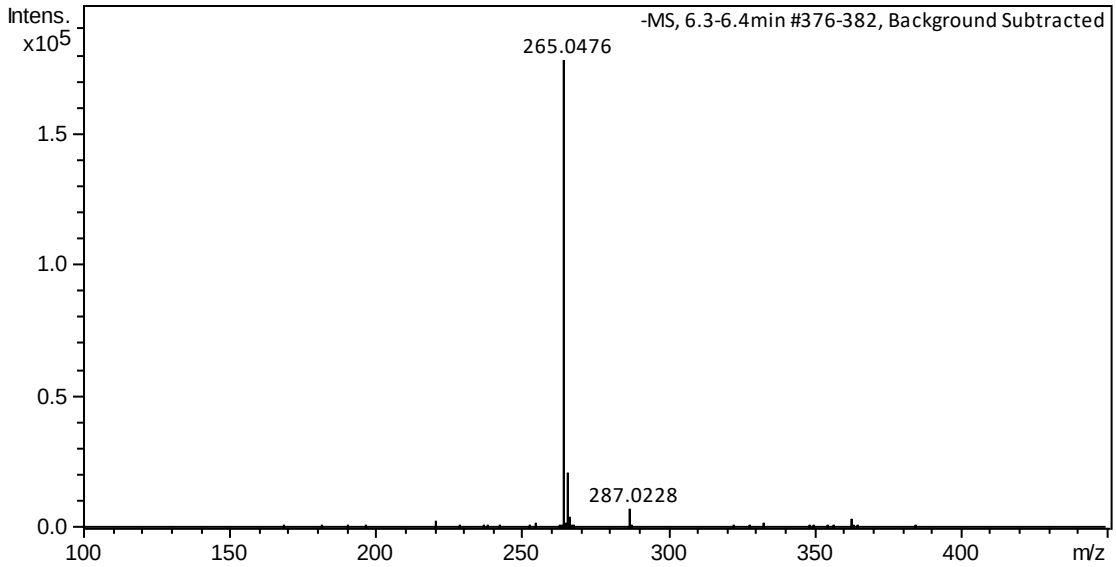

Figure S16. HR-ESI-TOF mass spectrum of *n*-C-3 butenolide phosphate (**9b**).

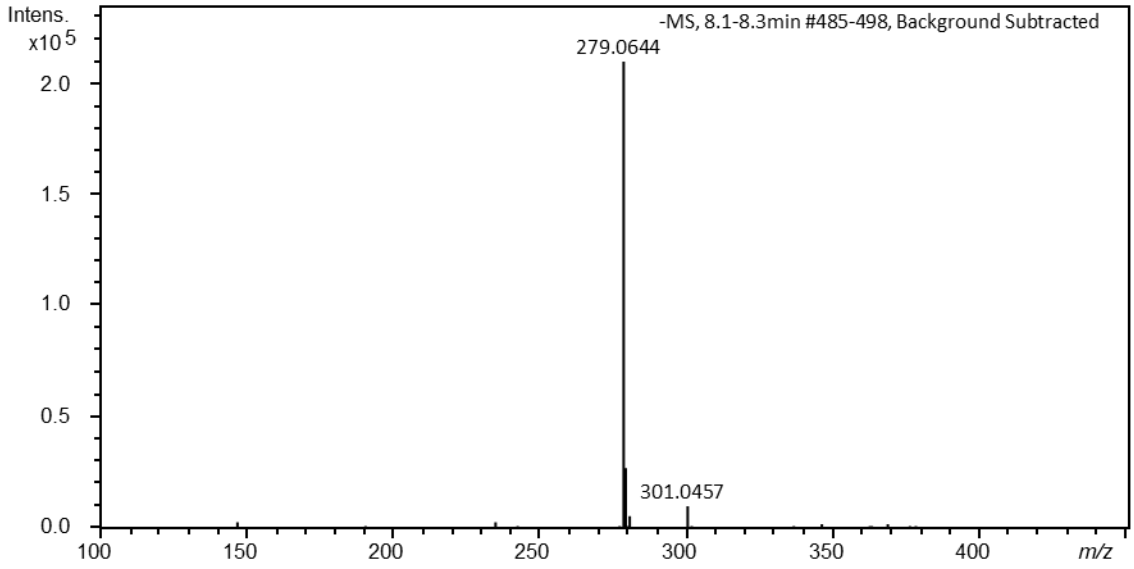

Figure S17. HR-ESI-TOF mass spectrum of *n*-C-4 butenolide phosphate (**9c**).

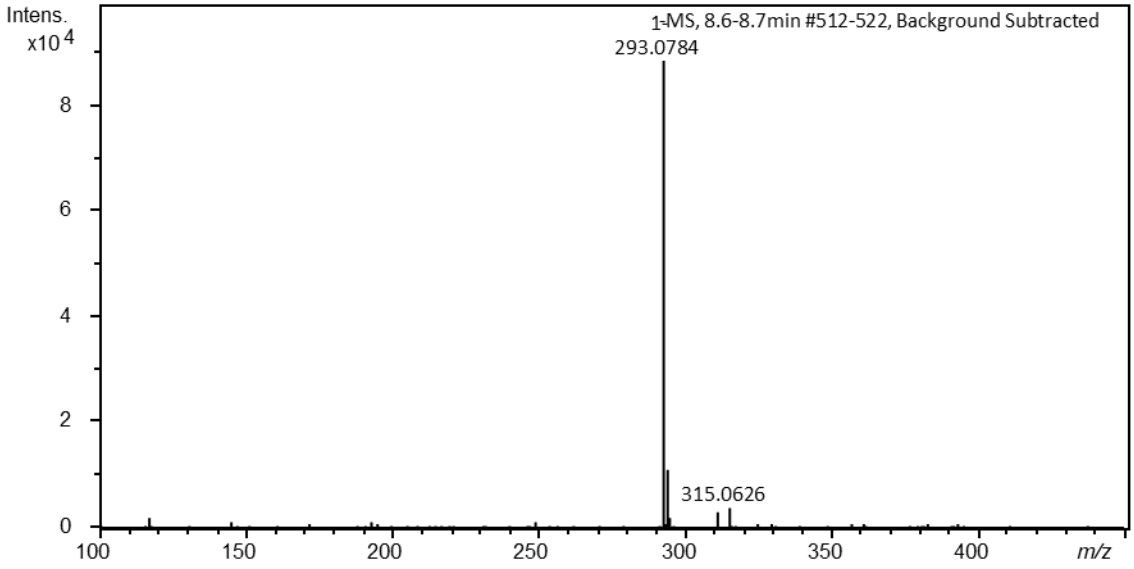

Figure S18. HR-ESI-TOF mass spectrum of *n*-C-5 butenolide phosphate (**9d**)

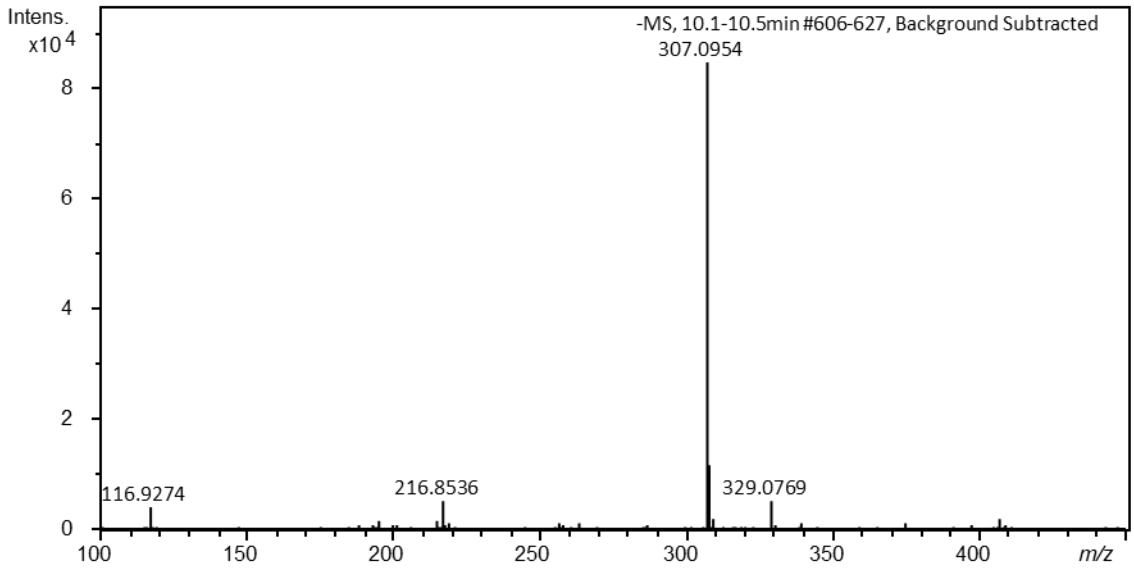

Figure S19. HR-ESI-TOF mass spectrum of *n*-C-6 butenolide phosphate (**9e**)

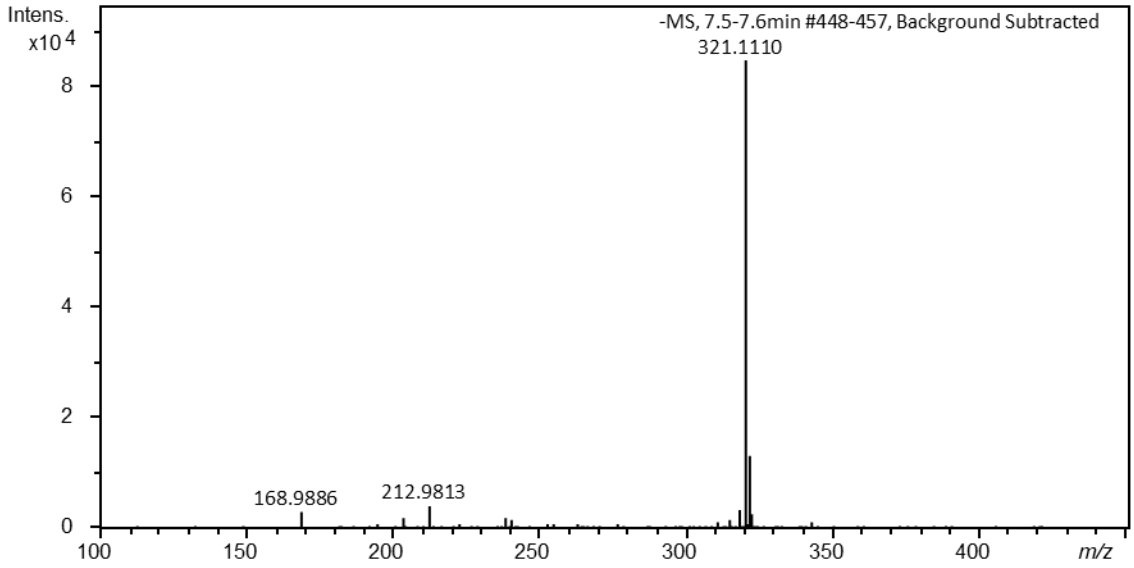

Figure S20. HR-ESI-TOF mass spectrum of *n*-C-7 butenolide phosphate (**9f**)

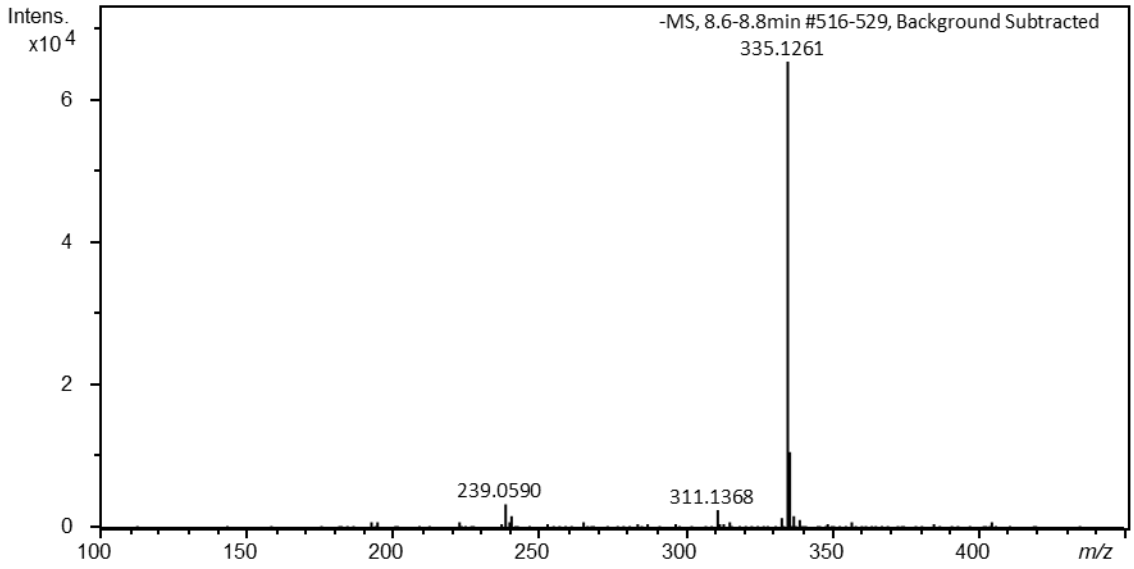

Figure S21. HR-ESI-TOF mass spectrum of *n*-C-8 butenolide phosphate (**9g**)

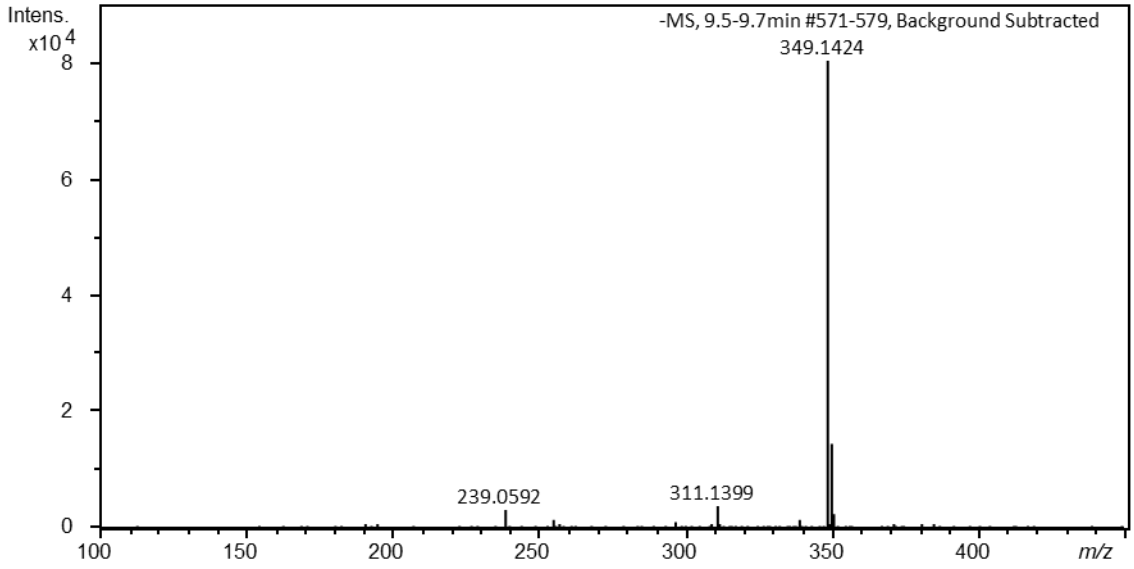

Figure S22. HR-ESI-TOF mass spectrum of *n*-C-9 butenolide phosphate (**9h**)

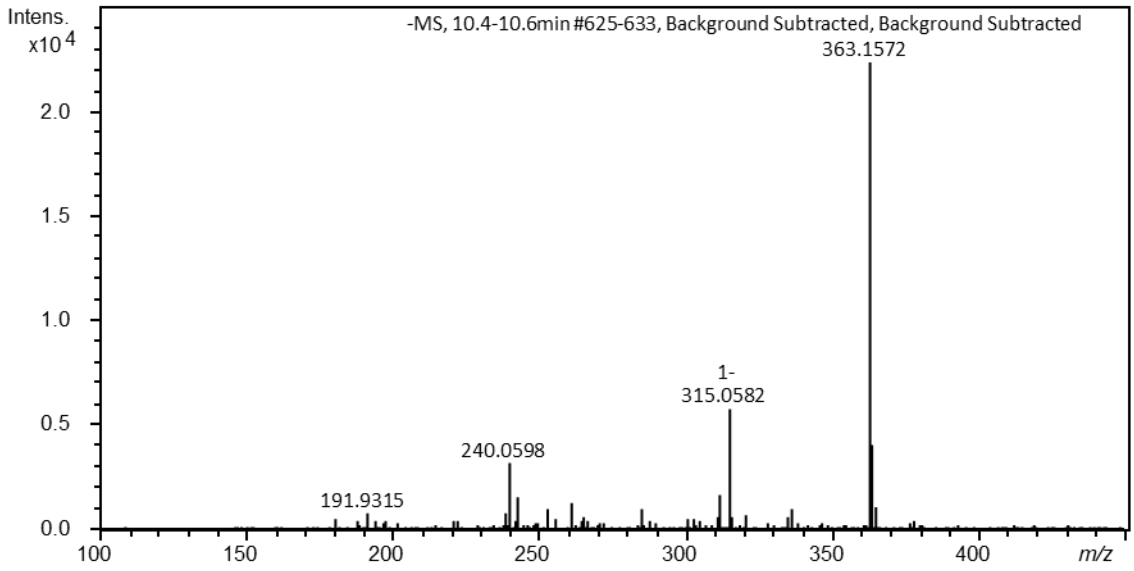

Figure S23. HR-ESI-TOF mass spectrum of *n*-C-10 butenolide phosphate (**9i**).

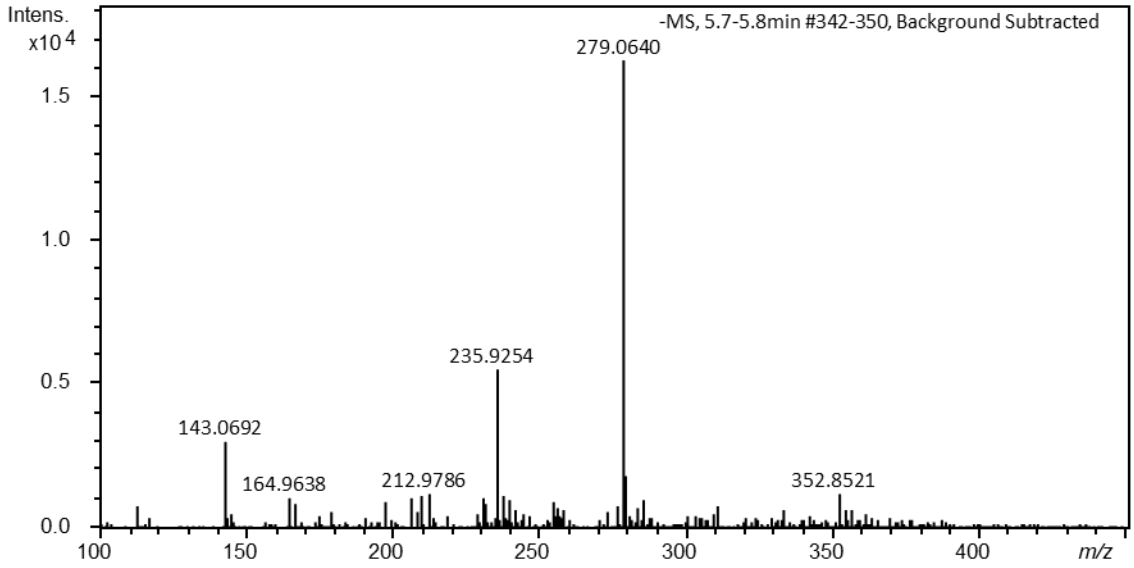

Figure S24. HR-ESI-TOF mass spectrum of *iso*-C-4 butenolide phosphate (**9j**).

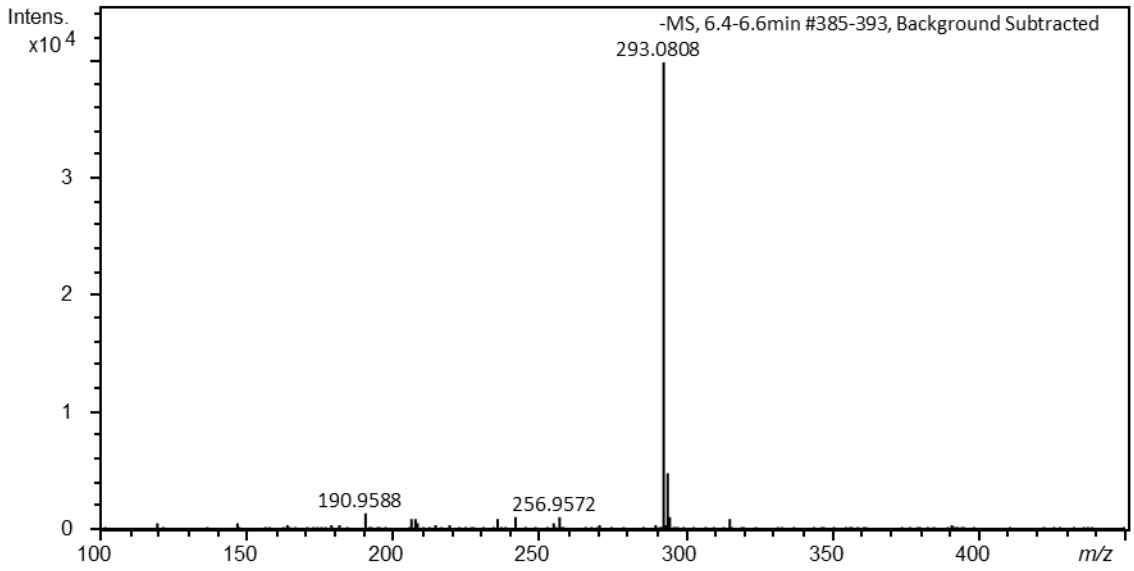

Figure S25. HR-ESI-TOF mass spectrum of *iso*-C-5 butenolide phosphate (**9k**).

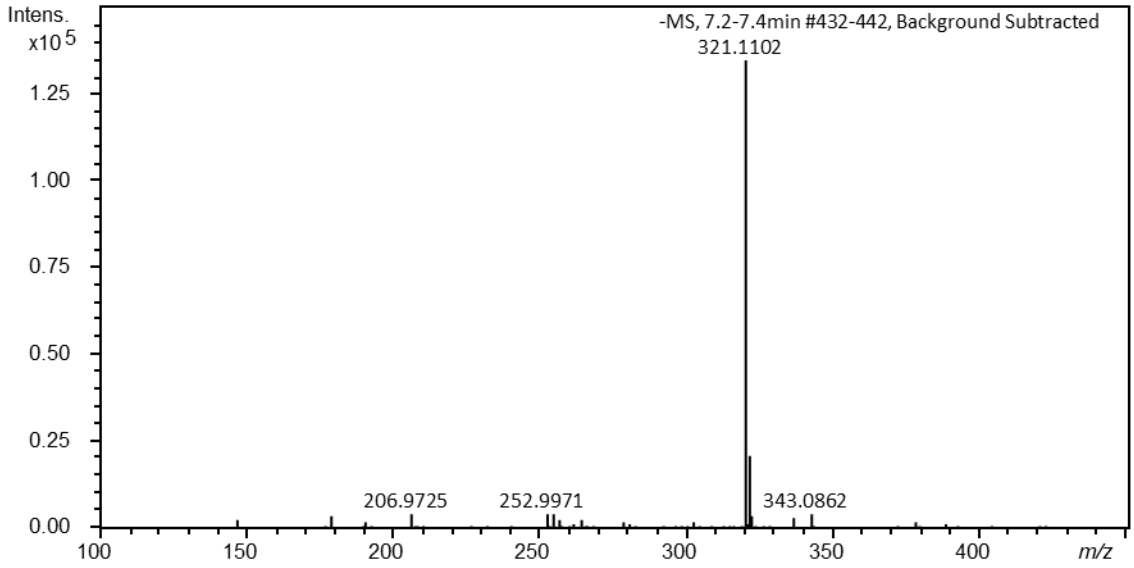

Figure S26. HR-ESI-TOF mass spectrum of *iso*-C-7 butenolide phosphate (**9l**).

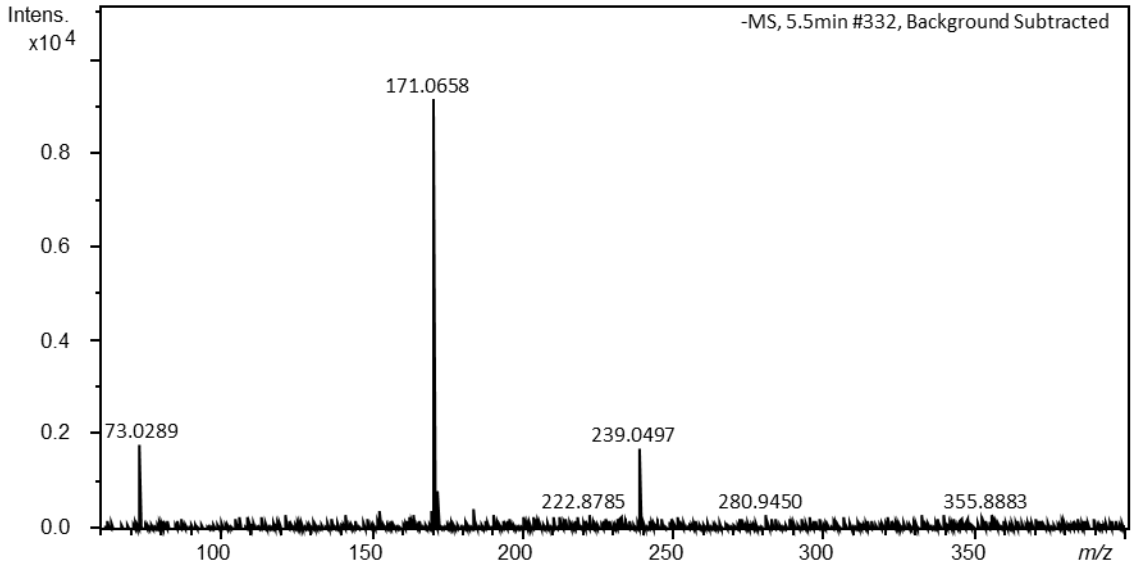

Figure S27. HR-ESI-TOF mass spectrum of *n*-C-2 GBL (**10a**).

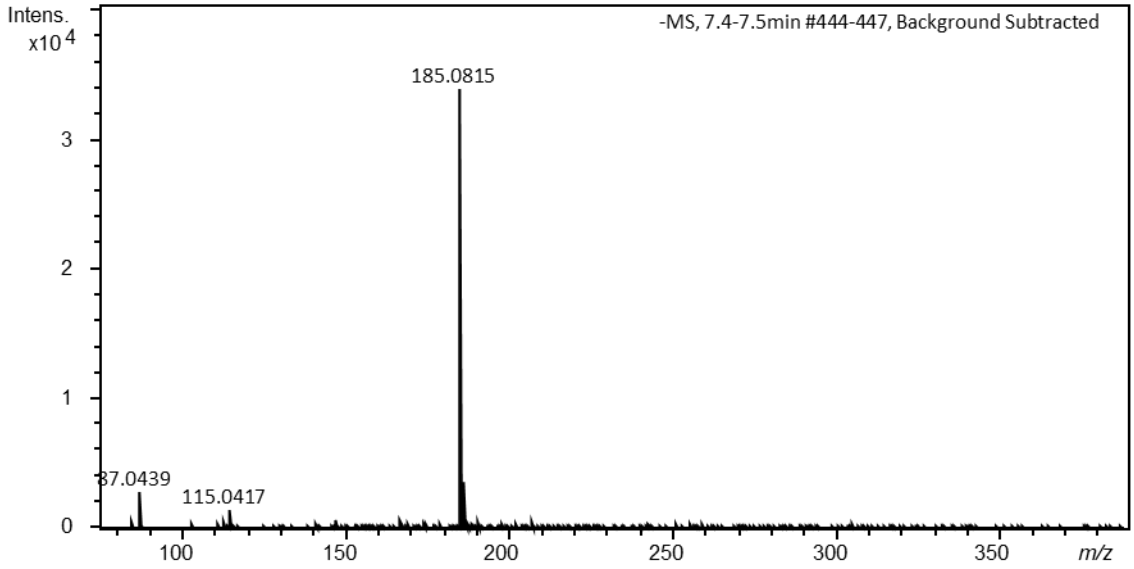

Figure S28. HR-ESI-TOF mass spectrum of *n*-C-3 GBL (**10b**).

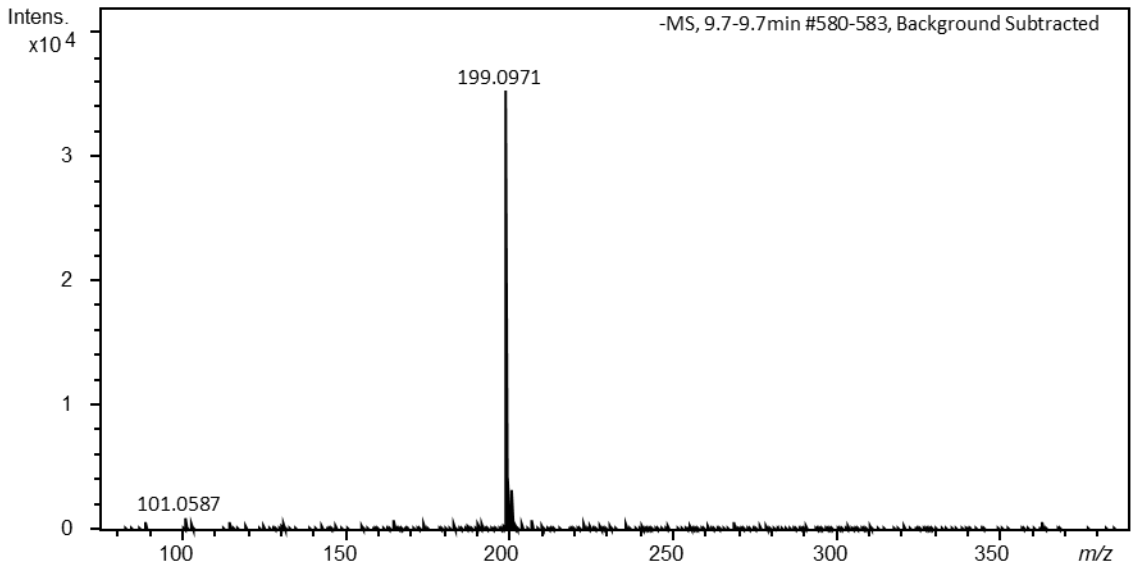

Figure S29. HR-ESI-TOF mass spectrum of *n*-C-4 GBL (**10c**).

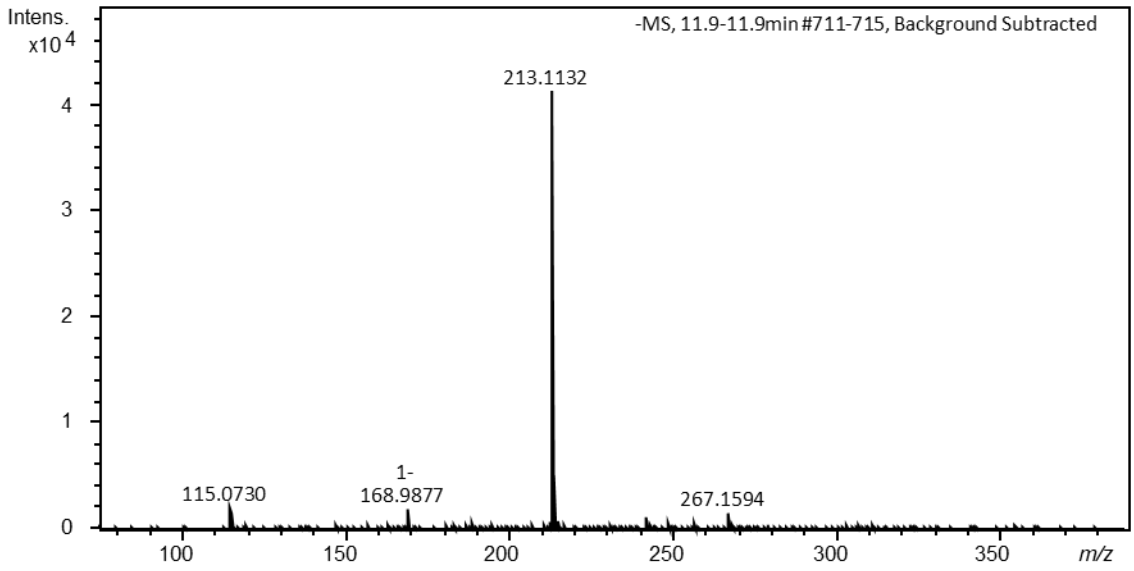

Figure S30. HR-ESI-TOF mass spectrum of *n*-C-5 GBL (**10d**)

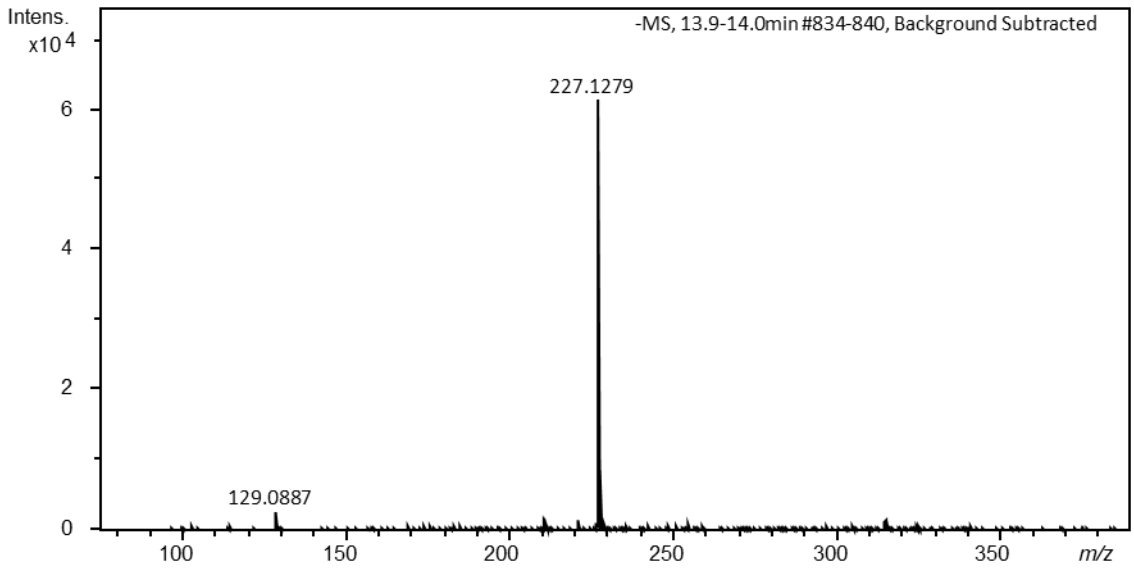

Figure S31. HR-ESI-TOF mass spectrum of *n*-C-6 GBL (**10e**)

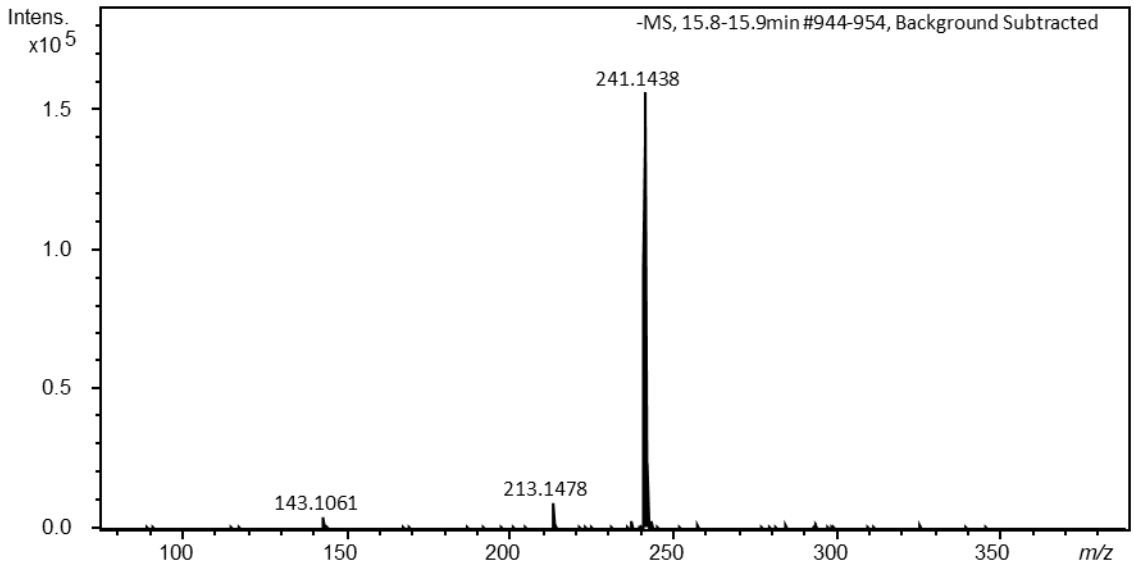

Figure S32. HR-ESI-TOF mass spectrum of *n*-C-7 GBL (**10f**)

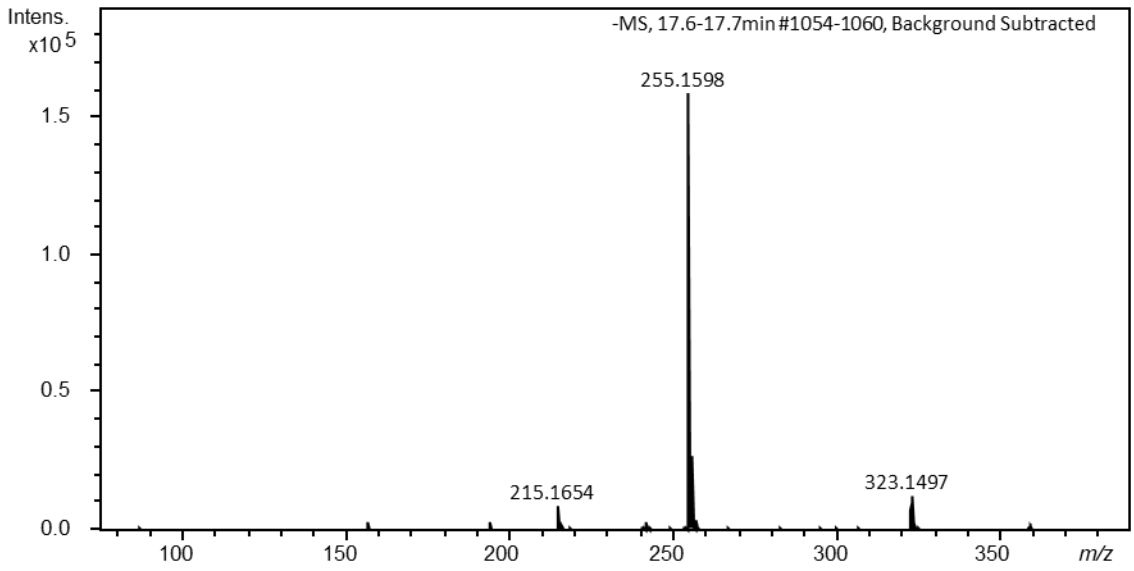

Figure S33. HR-ESI-TOF mass spectrum of *n*-C-8 GBL (**10g**)

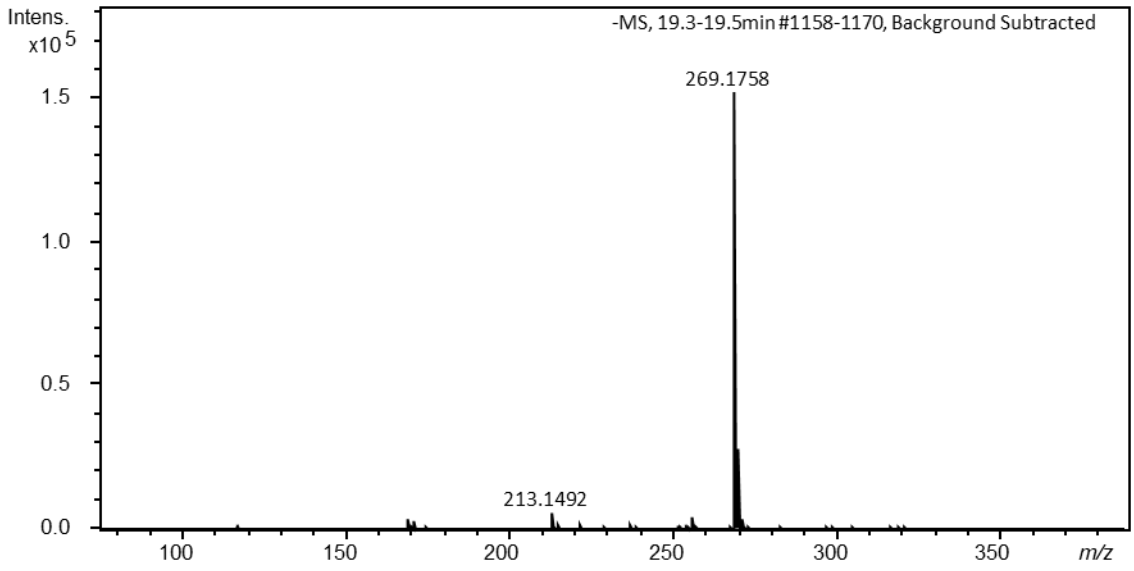

Figure S34. HR-ESI-TOF mass spectrum of *n*-C-9 GBL (**10h**)

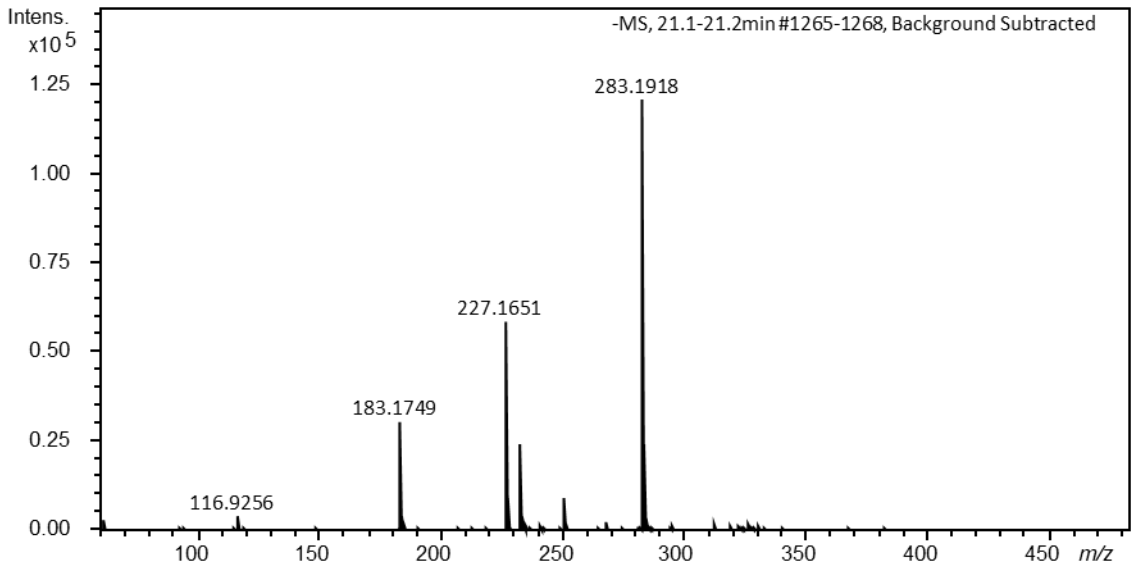

Figure S35. HR-ESI-TOF mass spectrum of *n*-C-10 GBL (**10i**).

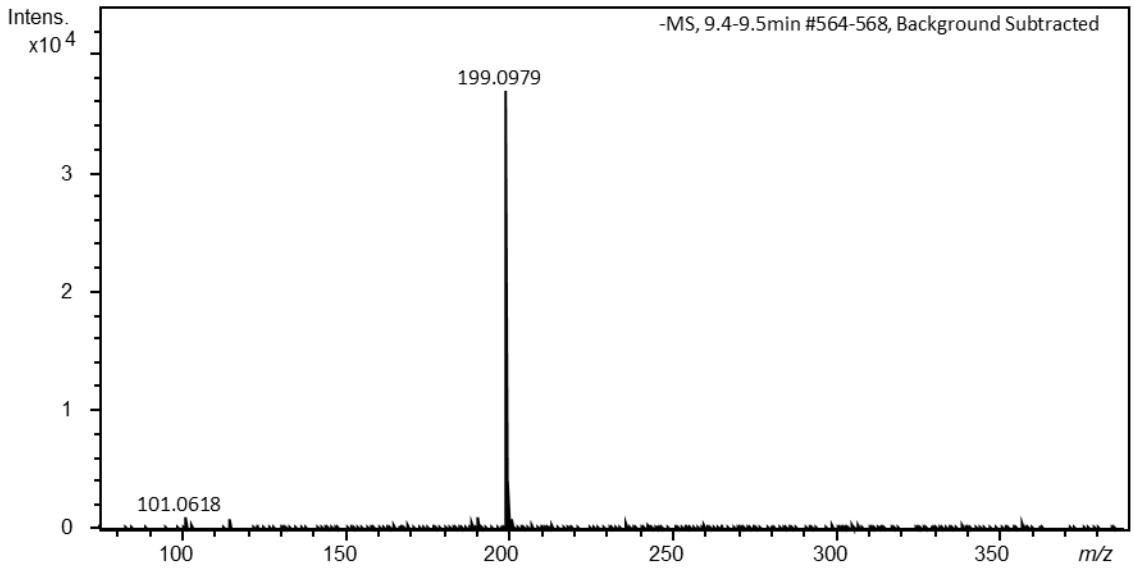

Figure S36. HR-ESI-TOF mass spectrum of *iso*-C-4 GBL (**10j**).

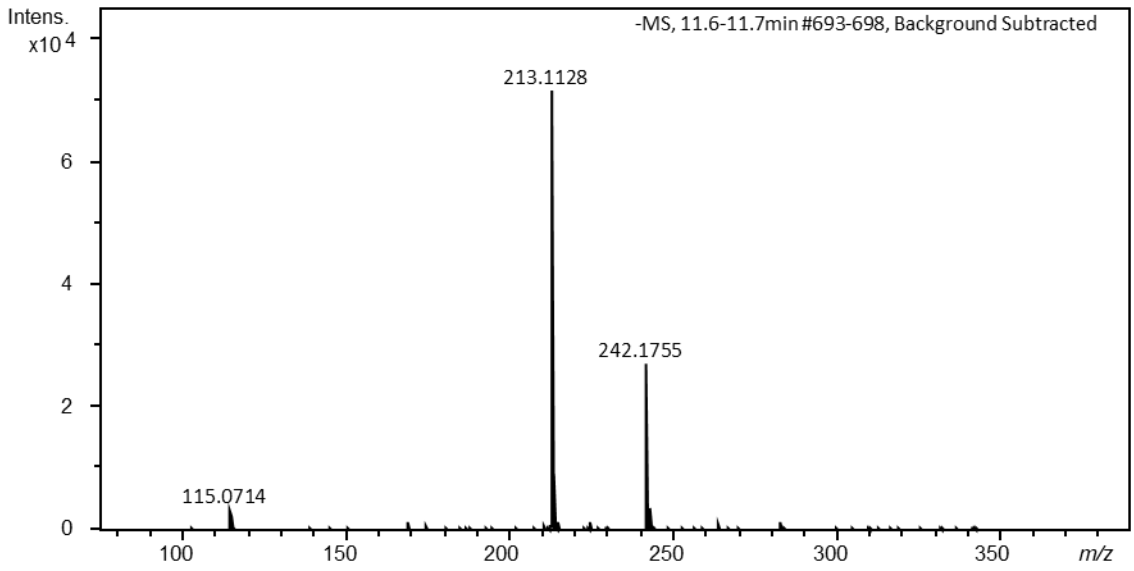

Figure S37. HR-ESI-TOF mass spectrum of *iso*-C-5 GBL (**10k**).

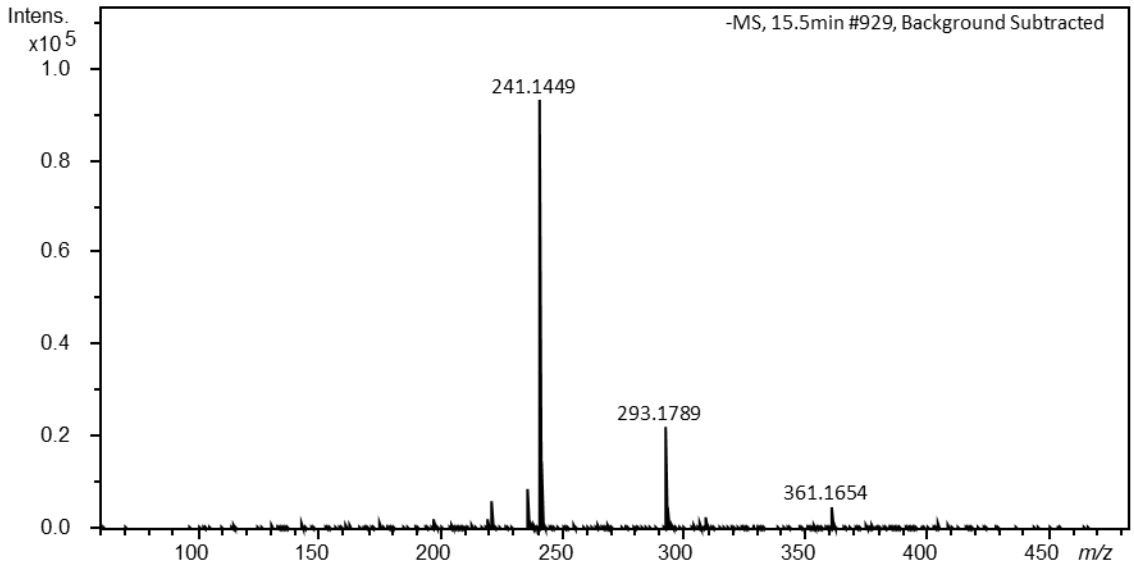

Figure S38. HR-ESI-TOF mass spectrum of *iso*-C-7 GBL (**10l**).

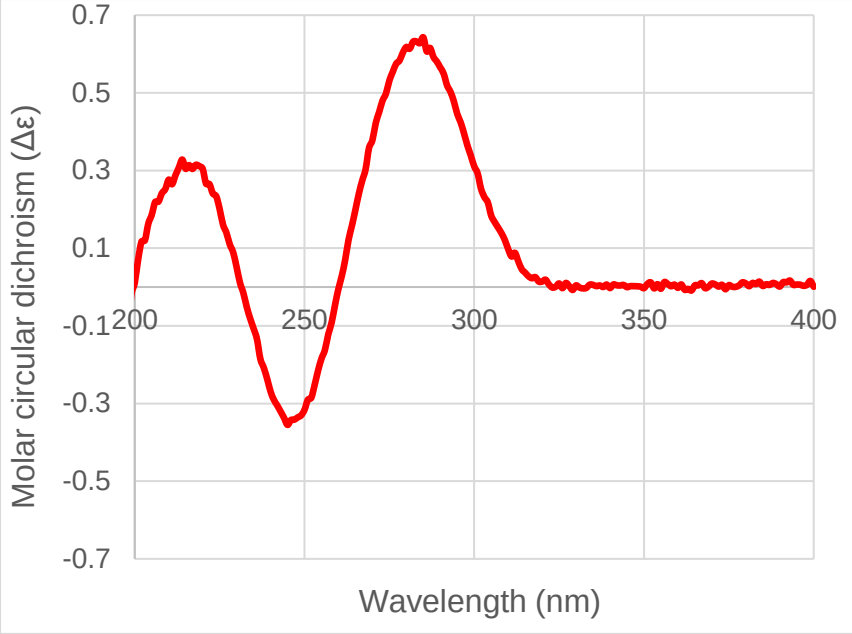

Figure S39. CD spectrum of synthesized and enantio-purified (3*R*)-form major *n*-C-5 GBL.

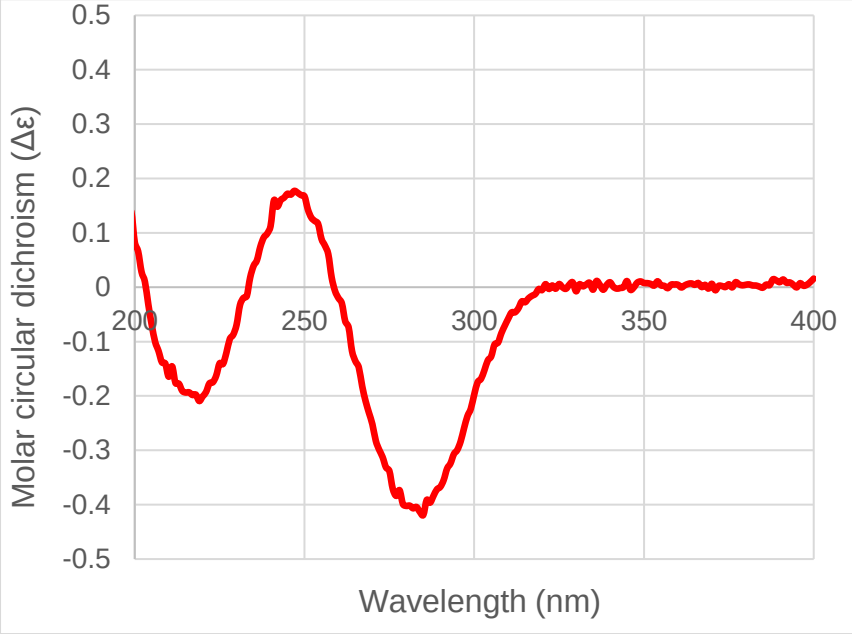

Figure S40. CD spectrum of synthesized and enantio-purified (3*S*)-form major *n*-C-5 GBL.

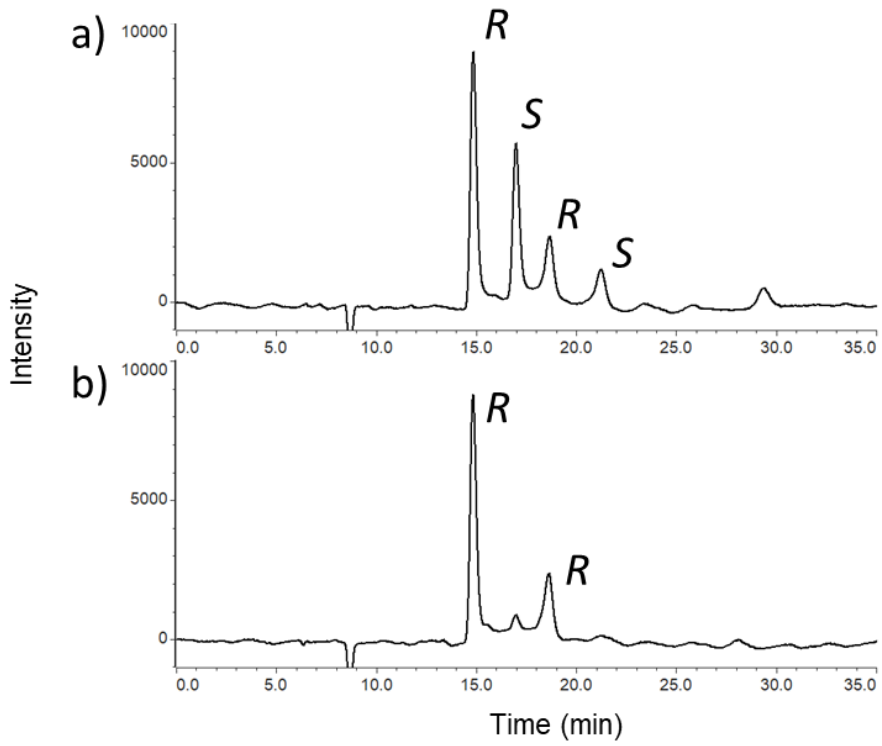

Figure S41. Chiral HPLC chromatograms of (a) enzymatically synthesized *n*-C-7 GBL (**10f**). (b) isolated (3*R*)-*n*-C-7 GBL (**4**) from *Rhodococcus rhodnii*.

Condition: CHIRALPAK AD-H column (4.6 x 250 mm, 5 µm), isopropanol: hexane = 8: 92, 0.5 mL/min, detection at 254 nm.

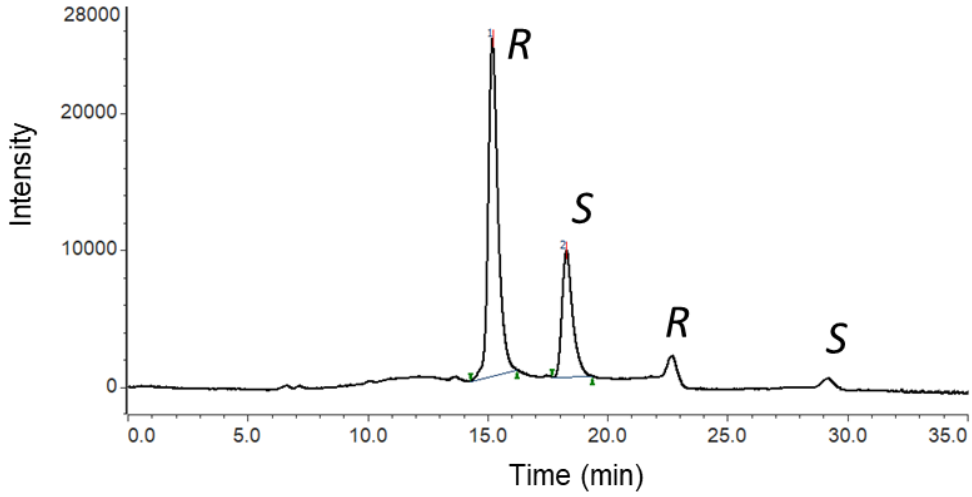

Figure S42. Chiral HPLC chromatograms of enzymatically synthesized *iso*-C-7 GBL (**10l**).

Condition: CHIRALPAK AD-H column (4.6 x 250 mm, 5 µm), isopropanol: hexane = 8: 92, 0.5 mL/min, detection at 254 nm.

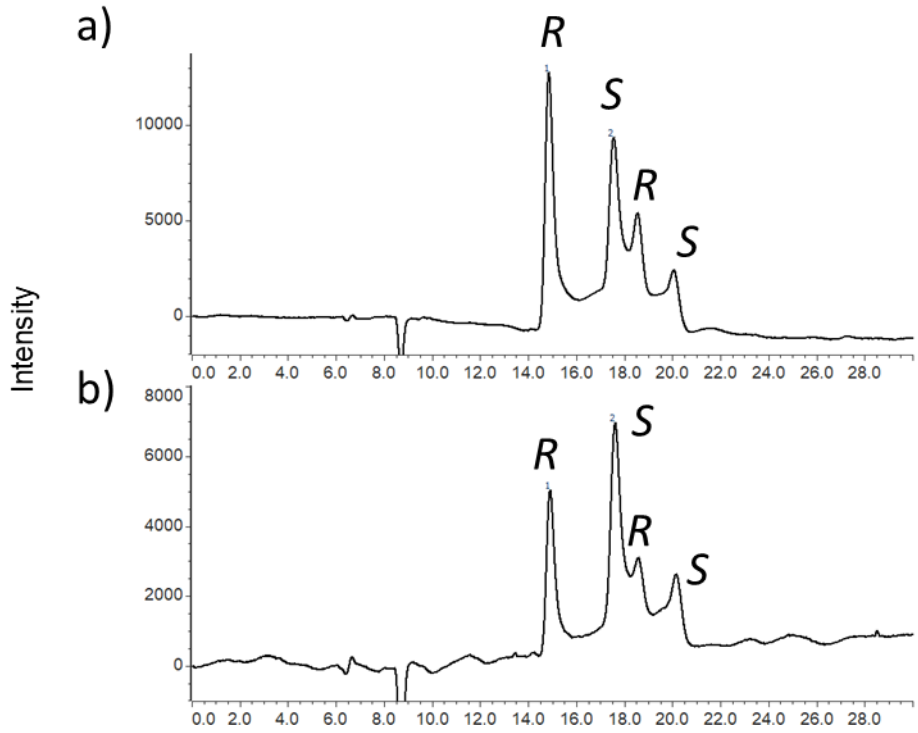

Figure S43. Chiral HPLC chromatograms (a) enzymatically synthesized *n*-C-5 GBL (**10d**) using BprA (b) enzymatically synthesized *n*-C-5 GBL (**10d**) using SJ-BprA.

Condition: CHIRALPAK AD-H column (4.6 x 250 mm, 5 µm), isopropanol: hexane = 8: 92, 0.5 mL/min, detection at 254 nm.

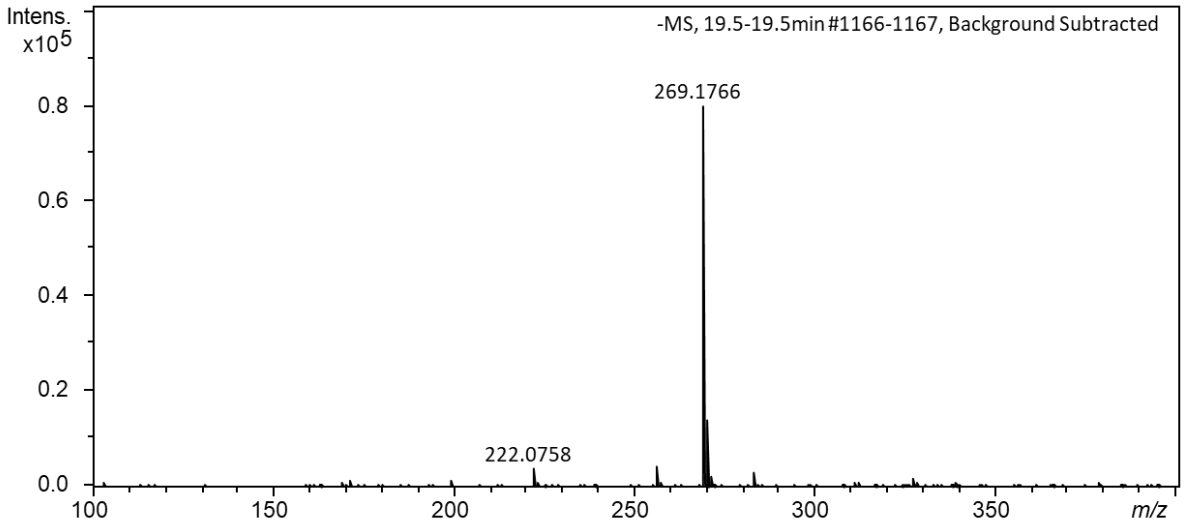

Figure S44. HR-ESI-TOF mass spectrum of *n*-C-9 GBL (**10h**) in the extract of *Rhodococcus rhodochrous*.

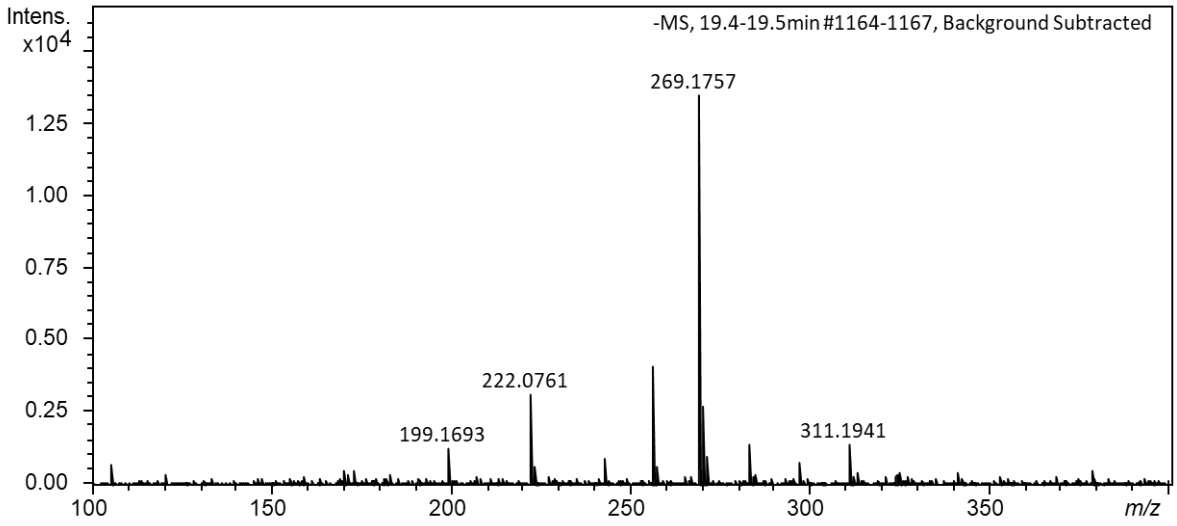

Figure S45. HR-ESI-TOF mass spectrum of *n*-C-9 GBL (**10h**) in the extract of *Nocardia harenae*.

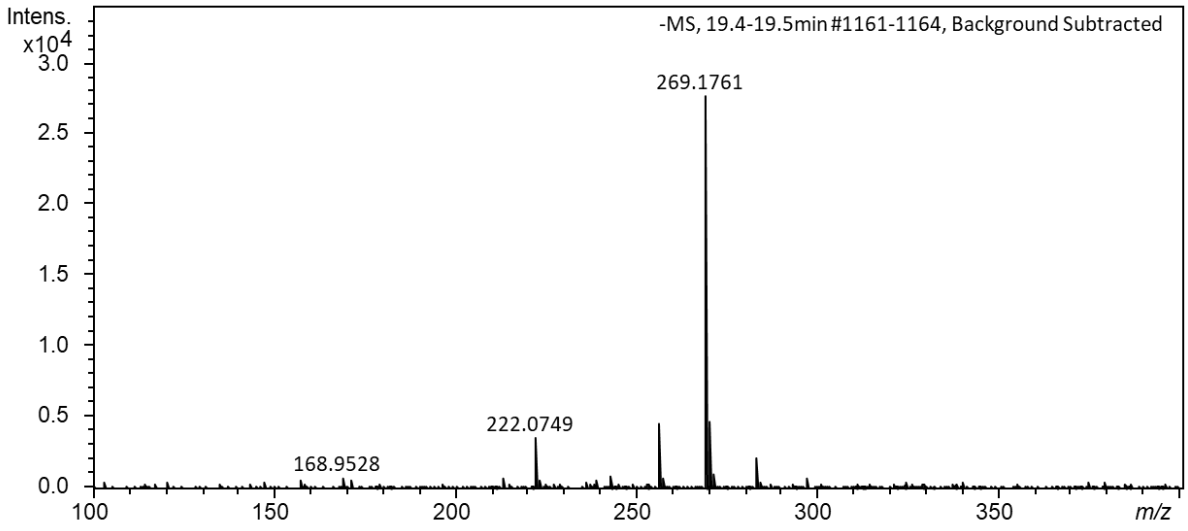

Figure S46. HR-ESI-TOF mass spectrum of *n*-C-9 GBL (**10h**) in the extract of *Gordonia polyisoprenivorans*.

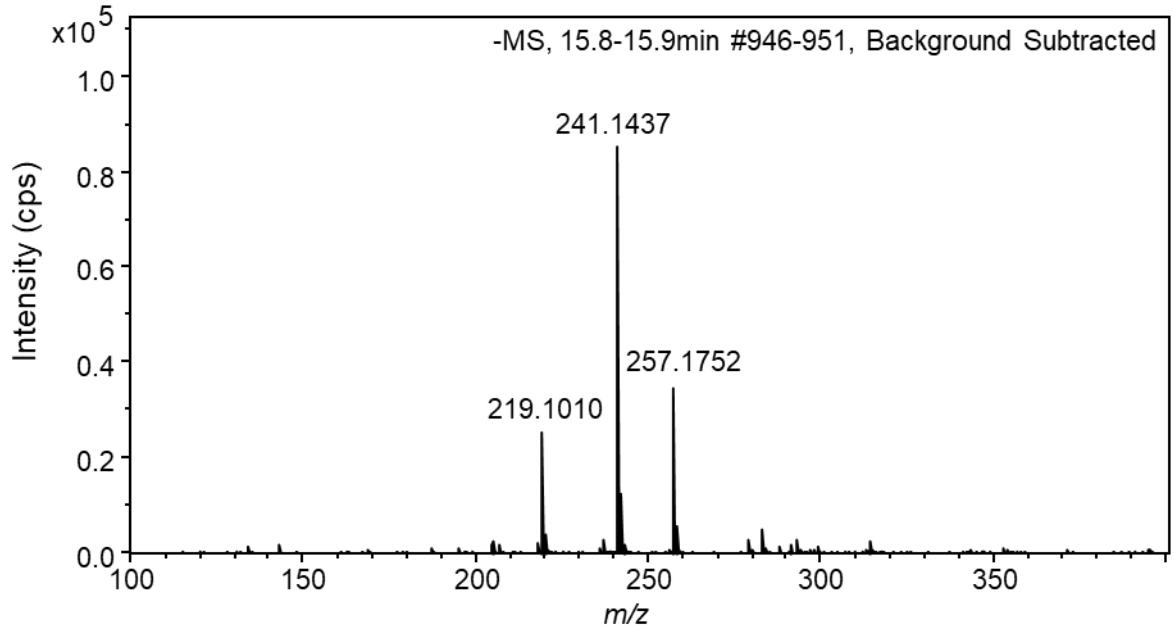

Figure S47. HR-ESI-TOF mass spectrum of *n*-C-7 GBL (**10f**) in the extract of *Dietzia timorensis*.

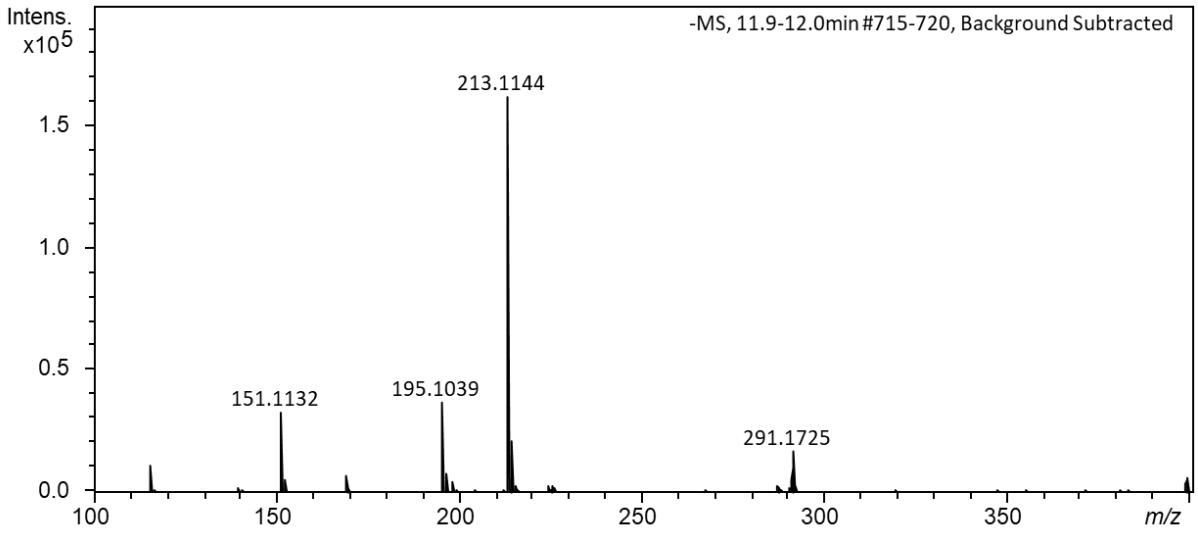

Figure S48. HR-ESI-TOF mass spectrum of (3*S*)-*n*-C-5 GBL (**11**) in the extract of *Streptomyces* sp. YKOK-J1.

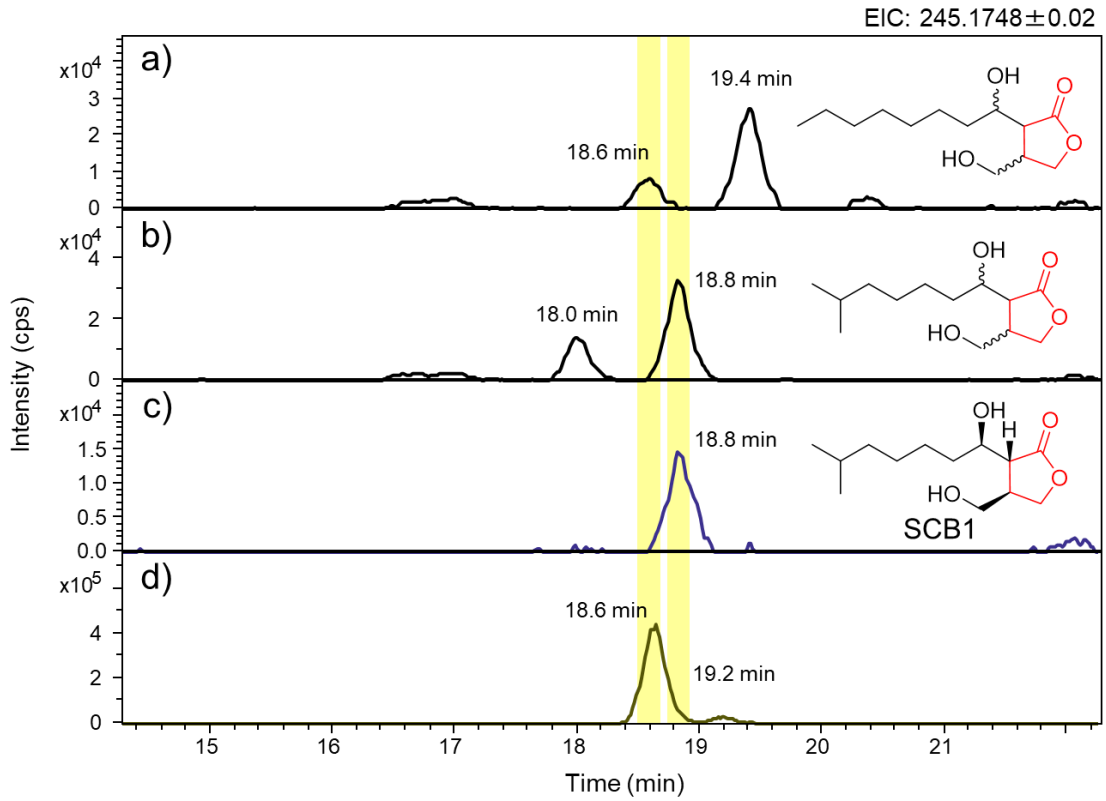

Figure S49. HR-LCMS chromatograms of (**a**) synthesized 6-hydroxy *n*-C-7 GBLs, (**b**) synthesized 6-hydroxy *iso*-C-7 GBLs, (**c**) extract of *Streptomyces coelicolor* A3(2) (*S. violaceoruber*), and (**d**) extract of *Streptomyces* sp. YKOK-D1. EIC values were denoted on the chromatogram (positive ion mode).

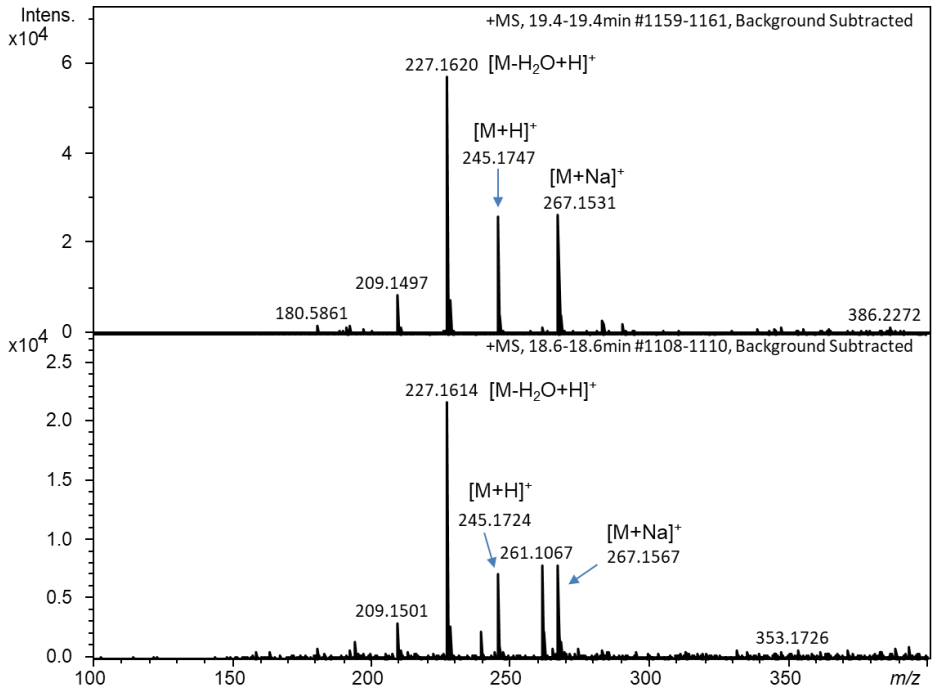

Figure S50. HR-ESI-TOF mass spectrum of synthesized 6-hydroxy *n*-C-7 GBLs.

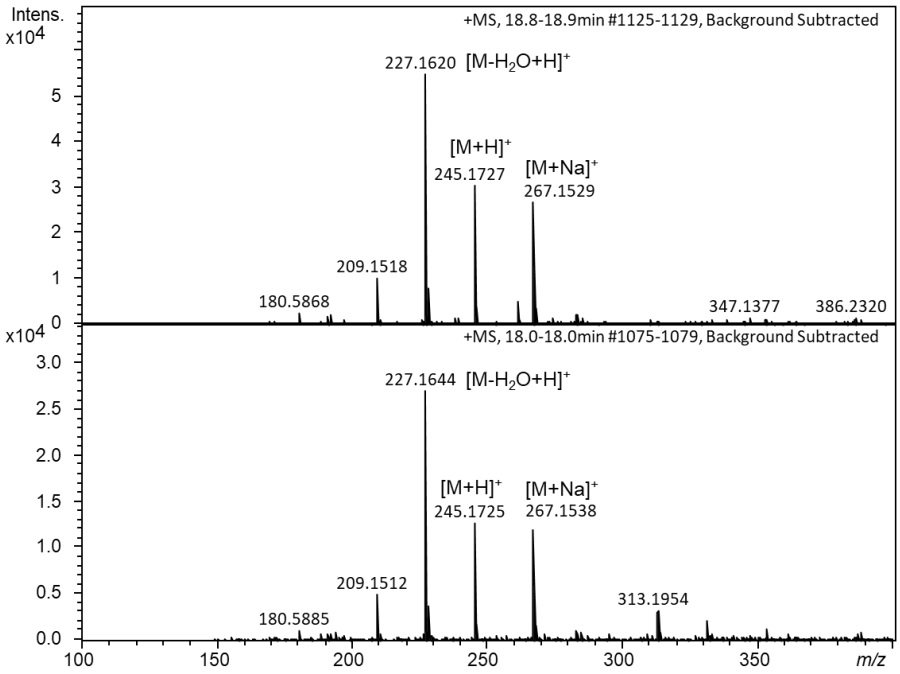

Figure S51. HR-ESI-TOF mass spectrum of synthesized 6-hydroxy *iso*-C-7 GBLs.

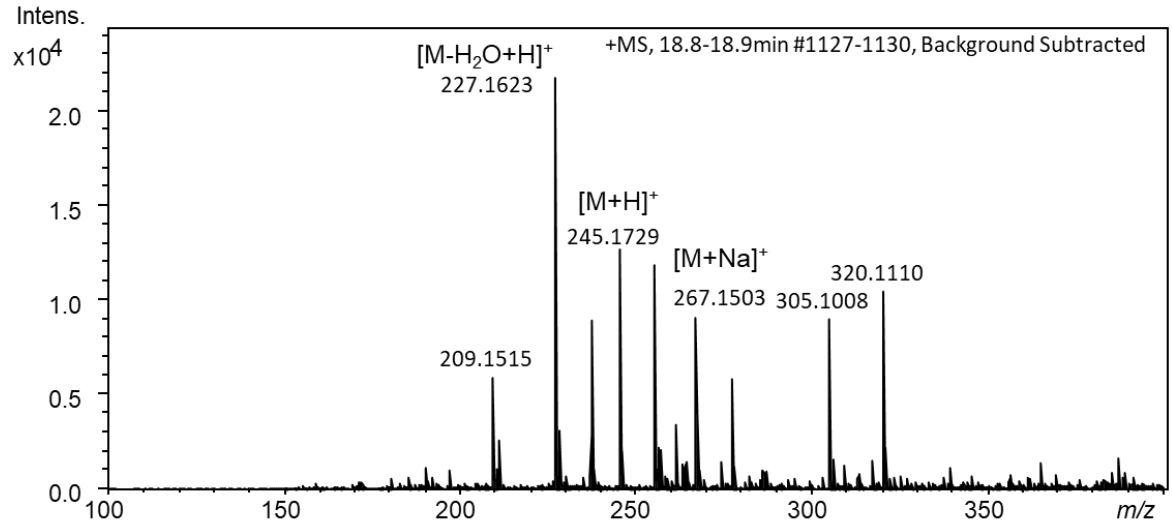

Figure S52. HR-ESI-TOF mass spectrum of 6-hydroxy *iso*-C-7 GBL (SCB1) in the extract of *Streptomyces coelicolor* A3(2) (*S. violaceoruber*).

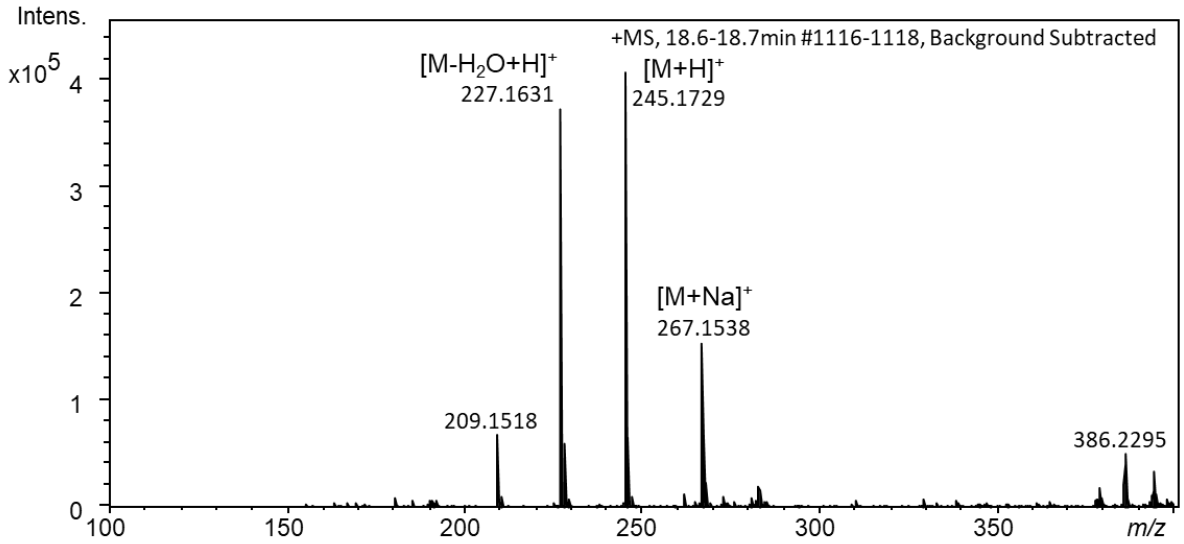

Figure S53. HR-ESI-TOF mass spectrum of 6-hydroxy *n*-C-7 GBL in the extract of *Streptomyces* sp. YKOK-D1.

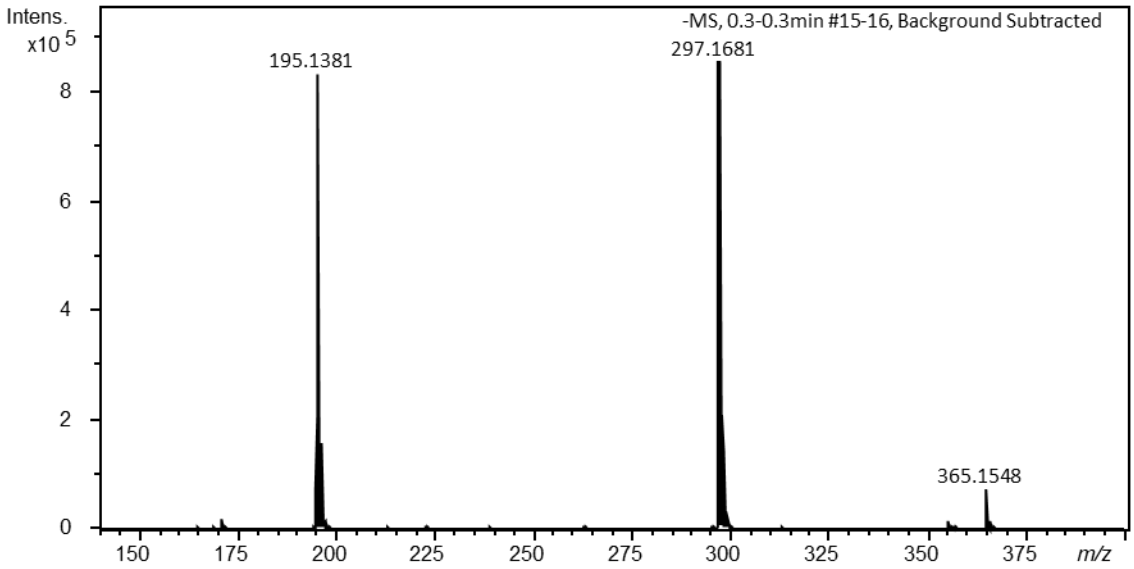

Figure S54. HR-ESI-TOF mass spectrum of *n*-C-9 acylated Meldrum 's acid (**16h**).

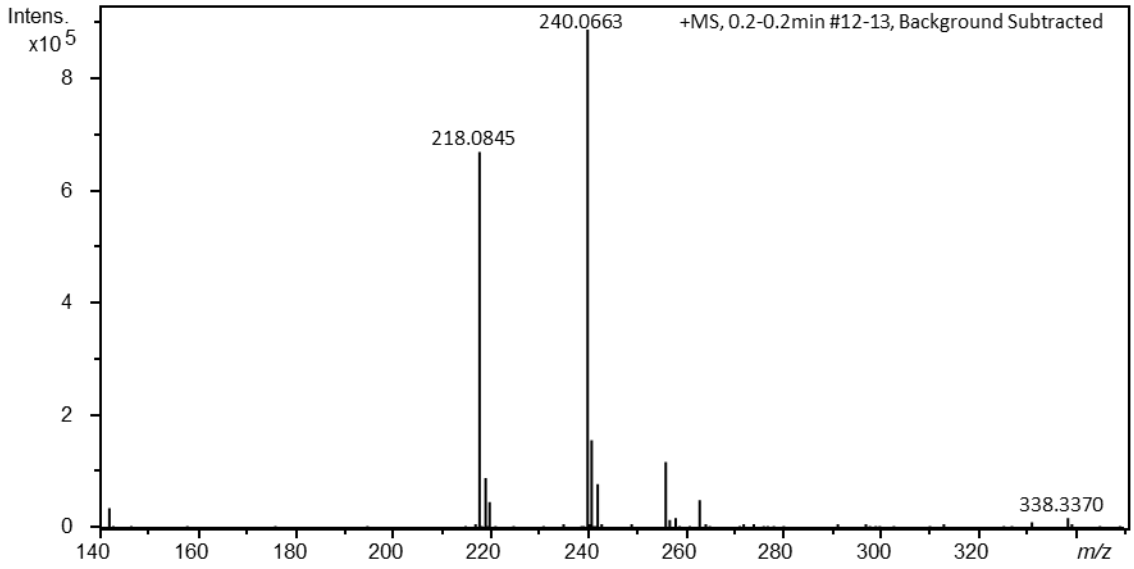

Figure S55. HR-ESI-TOF mass spectrum of β-keto pentanoyl SNAC (*n*-C-2 β-ketoacyl SNAC, **6a**).

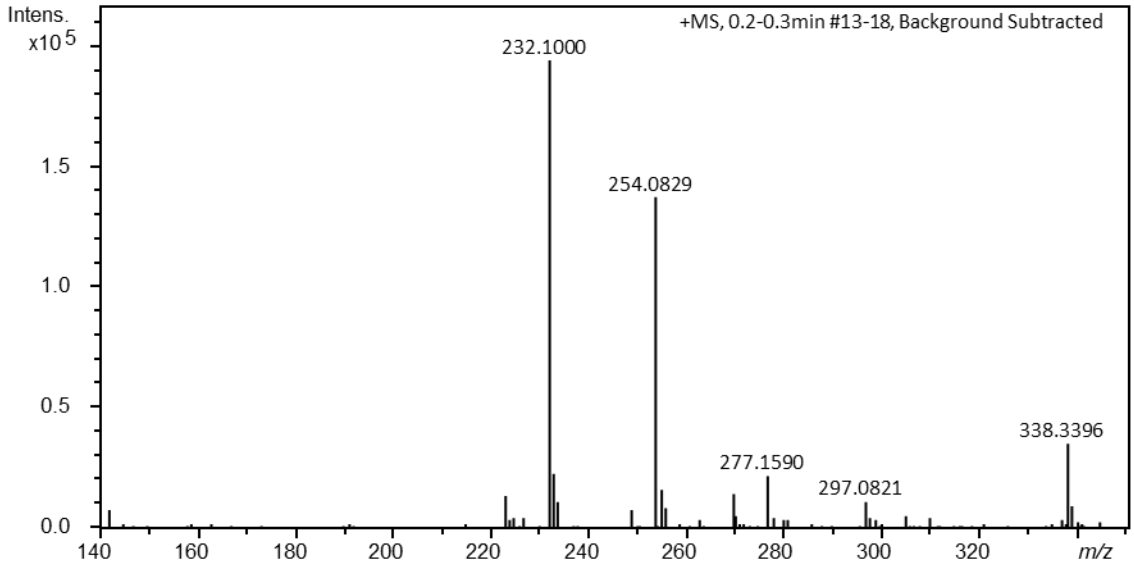

Figure S56. HR-ESI-TOF mass spectrum of β-keto hexanoyl SNAC (*n*-C-3 β-ketoacyl SNAC, **6b**).

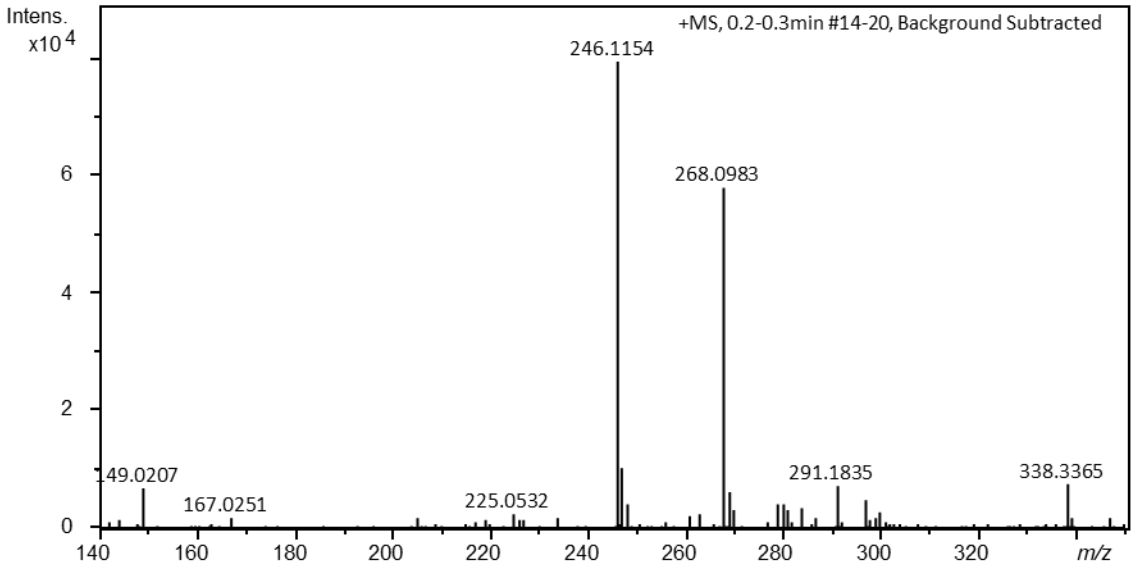

Figure S57. HR-ESI-TOF mass spectrum of β-keto heptanoyl SNAC (*n*-C-4 β-ketoacyl SNAC, **6c**).

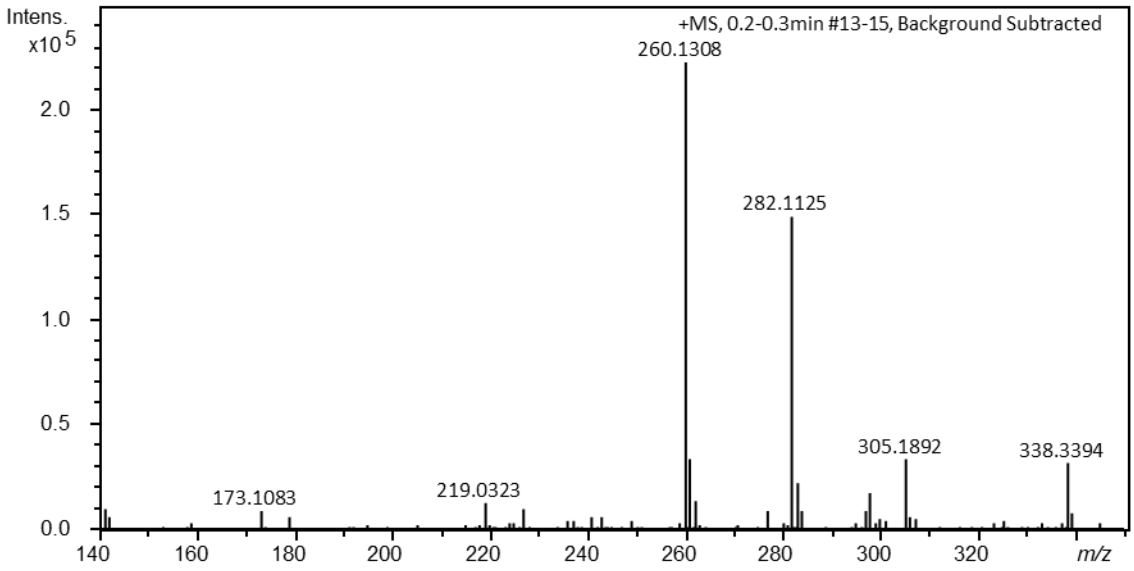

Figure S58. HR-ESI-TOF mass spectrum of β-keto octanoyl SNAC (*n*-C-5 β-ketoacyl SNAC, **6d**).

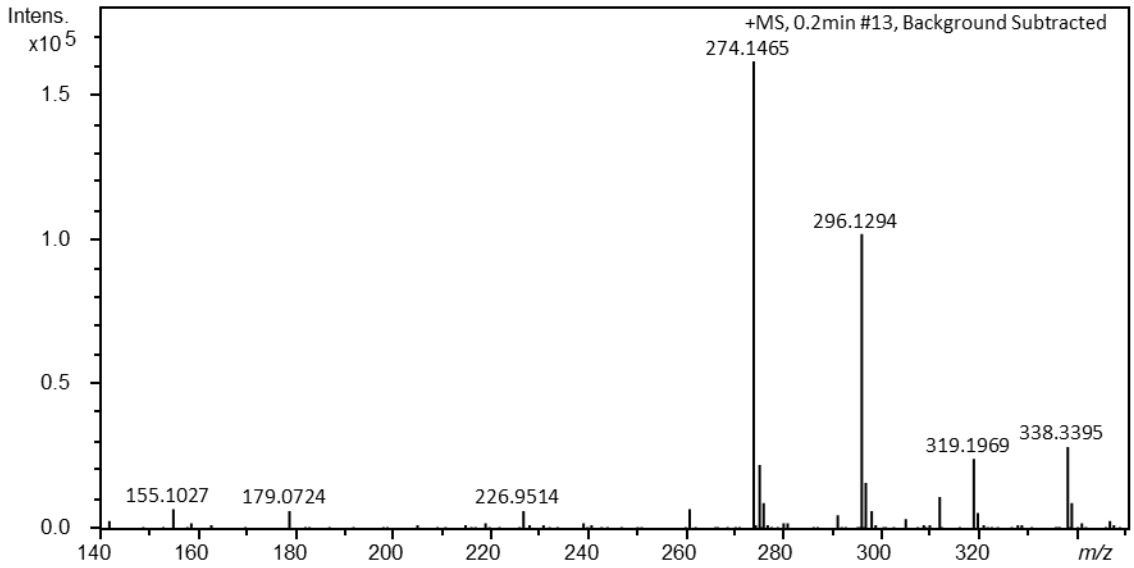

Figure S59. HR-ESI-TOF mass spectrum of β-keto nonanoyl SNAC (*n*-C-6 β-ketoacyl SNAC, **6e**).

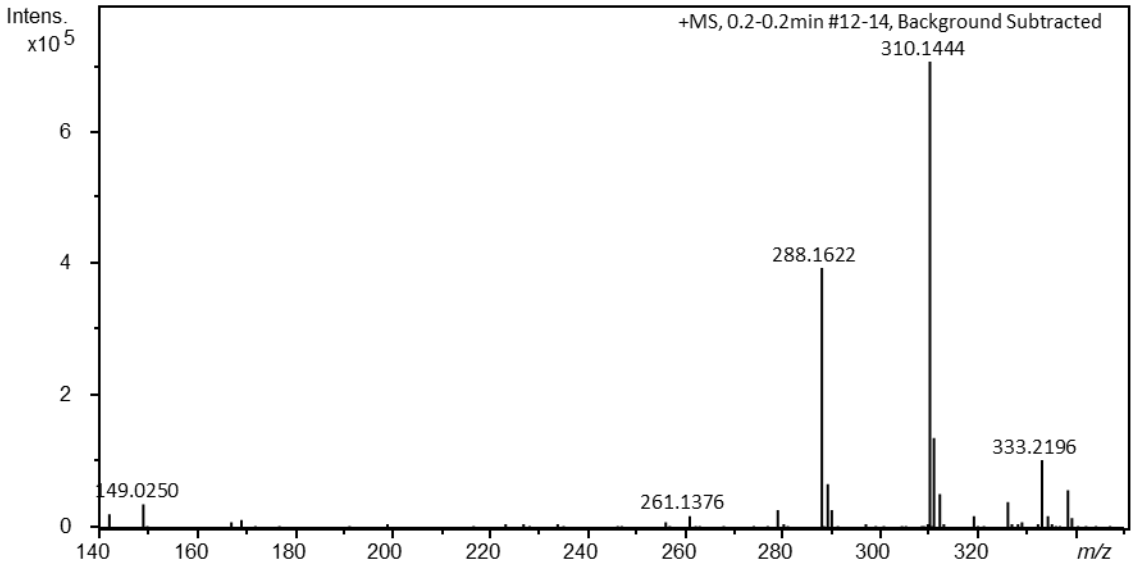

Figure S60. HR-ESI-TOF mass spectrum of β-keto decanoyl SNAC (*n*-C-7 β-ketoacyl SNAC, **6f**).

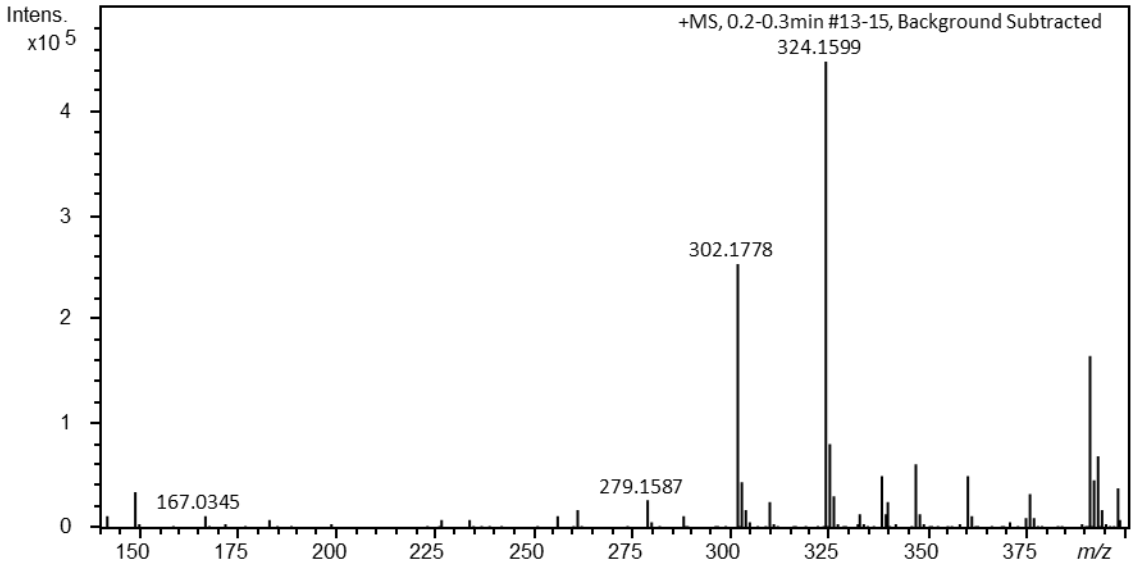

Figure S61. HR-ESI-TOF mass spectrum of β-keto undecanoyl SNAC (*n*-C-8 β-ketoacyl SNAC, **6g**).

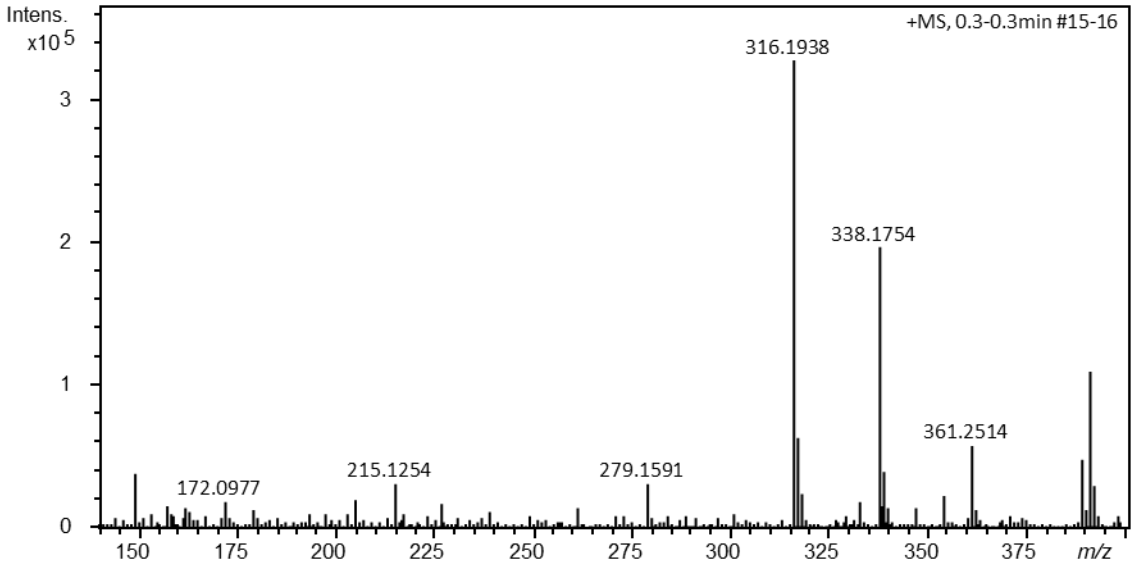

Figure S62. HR-ESI-TOF mass spectrum of β-keto dodecanoyl SNAC (*n*-C-9 β-ketoacyl SNAC, **6h**).

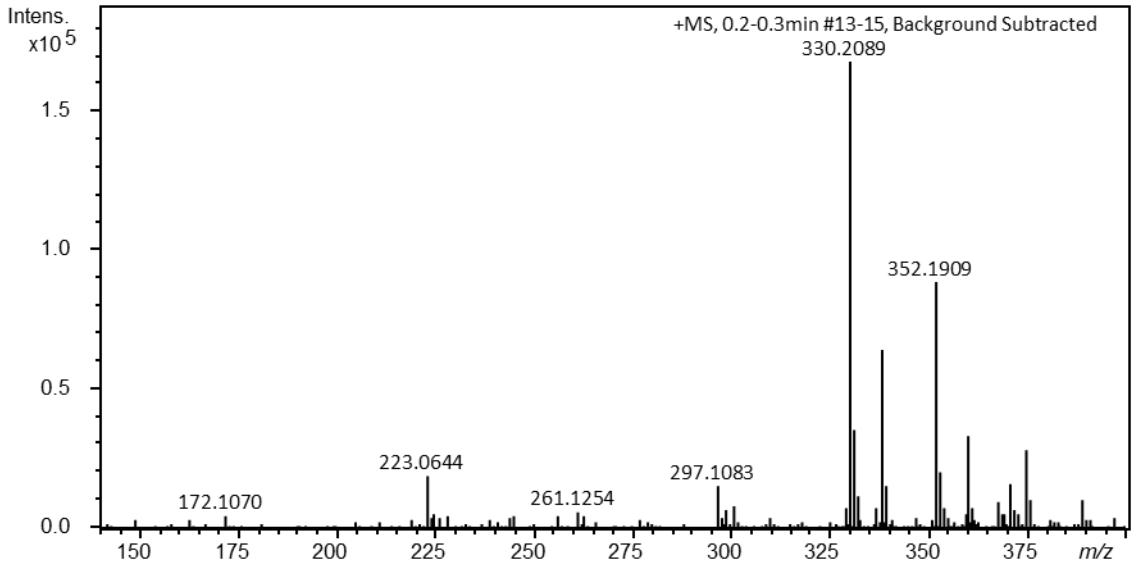

Figure S63. HR-ESI-TOF mass spectrum of β-keto tridecanoyl SNAC (*n*-C-10 β-ketoacyl SNAC, **6i**).

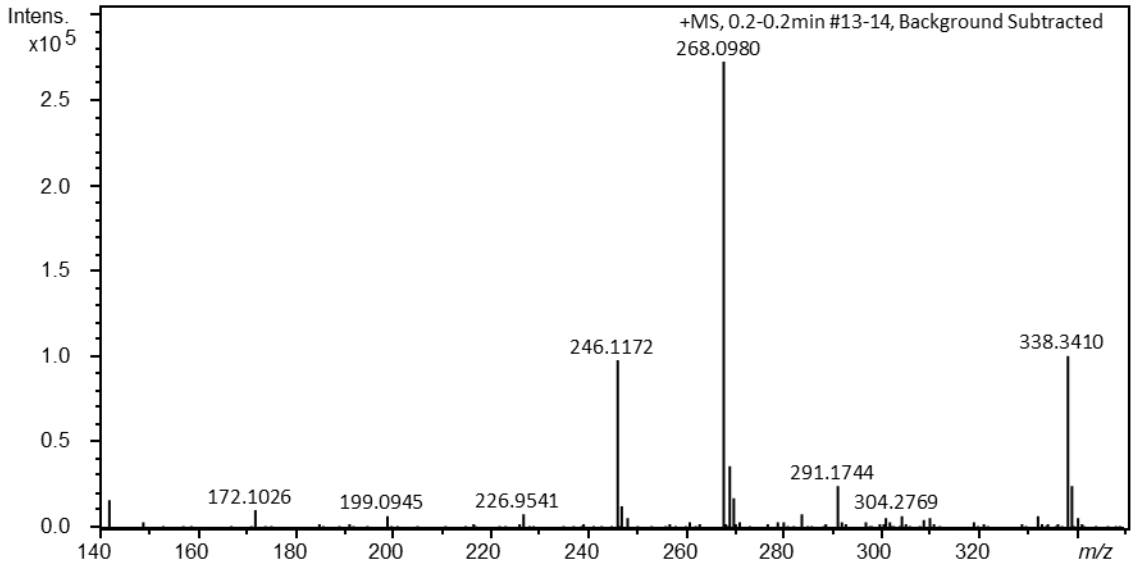

Figure S64. HR-ESI-TOF mass spectrum of β-keto *iso*-heptanoyl SNAC (*iso*-C-4 β-ketoacyl SNAC, **6j**).

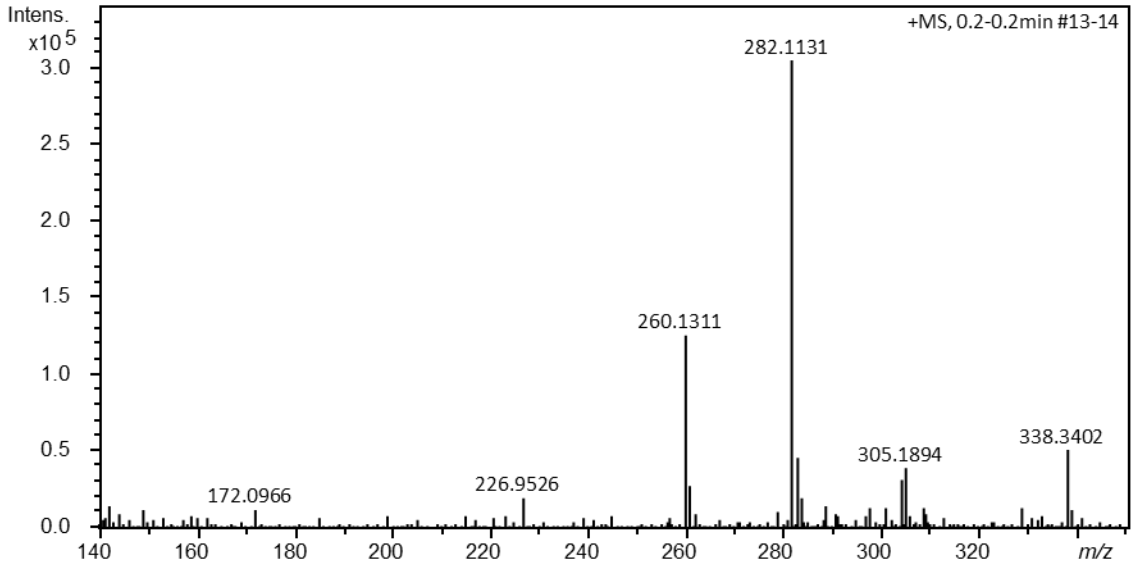

Figure S65. HR-ESI-TOF mass spectrum of β-keto *iso*-octanoyl SNAC (*iso*-C-5 β-ketoacyl SNAC, **6k**).

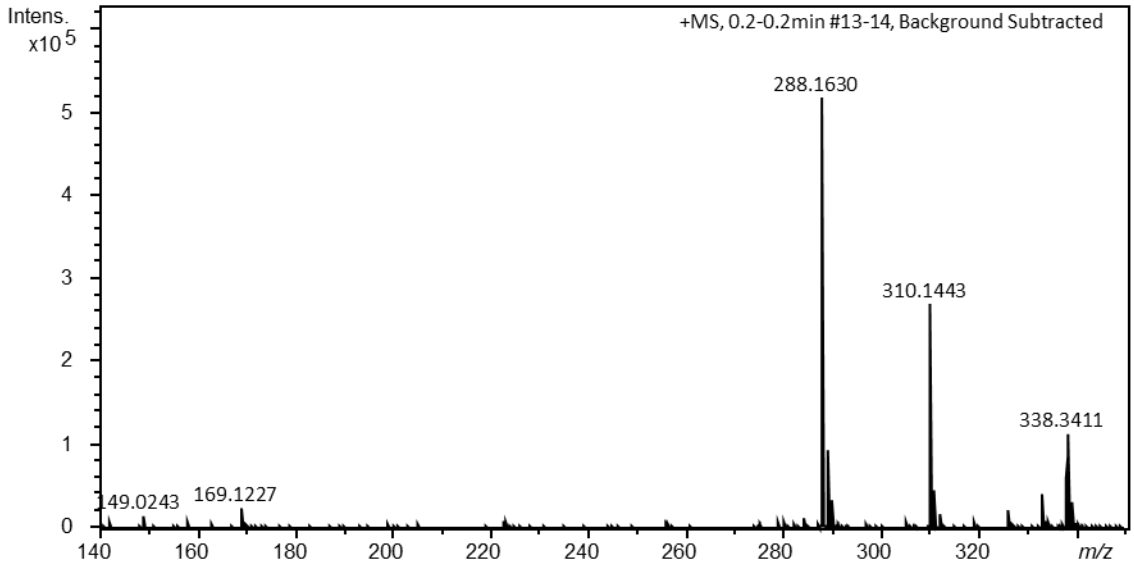

Figure S66. HR-ESI-TOF mass spectrum of β-keto *iso*-decanoyl SNAC (*iso*-C-7 β-ketoacyl SNAC, **6l**).

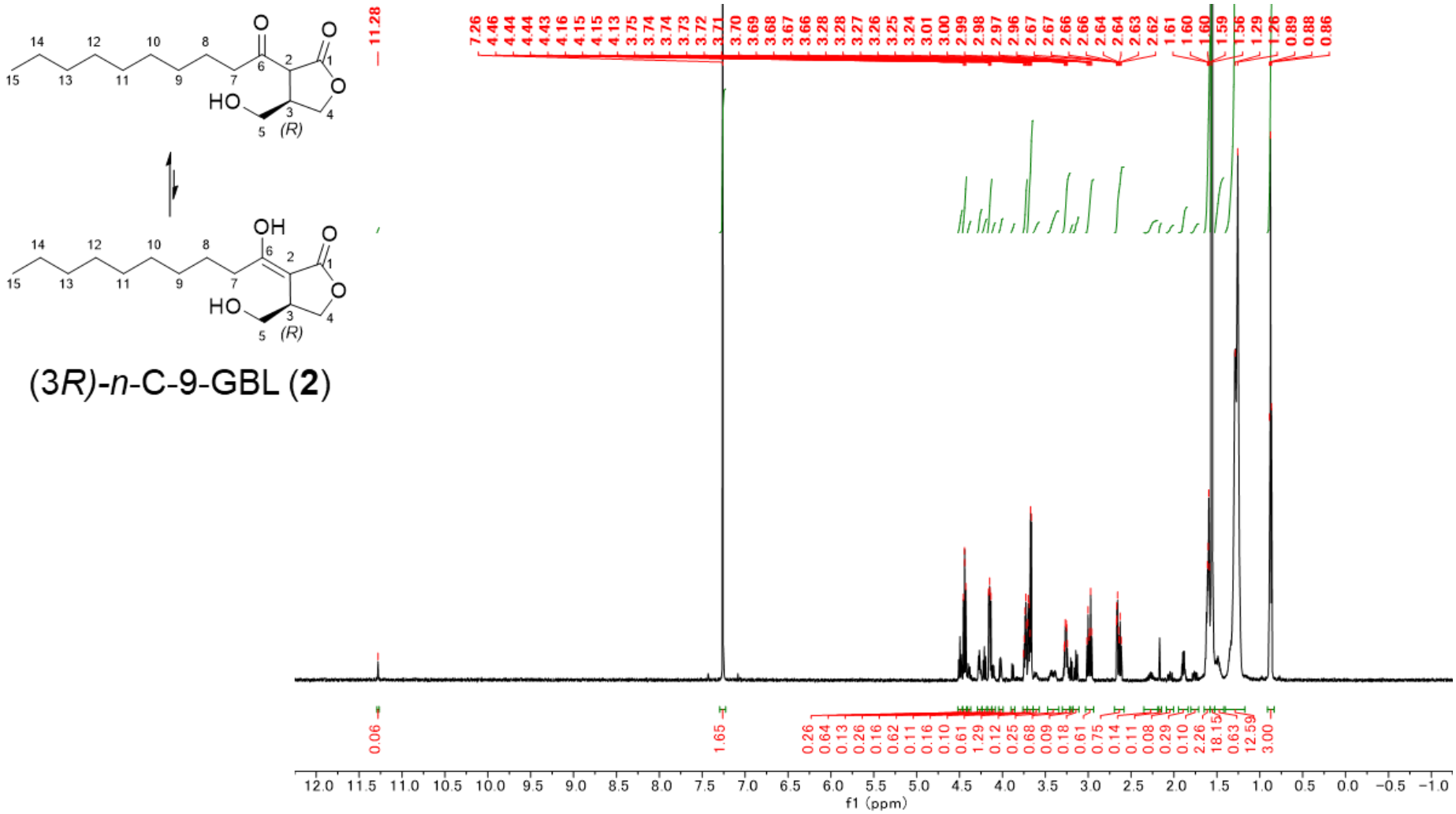

Figure S67. ^{1}H NMR (600 MHz, $CDCl_3$) spectrum of isolated *n*-C-9 GBL from *Rhodococcus rhodnii* JCM3203 (**2**).

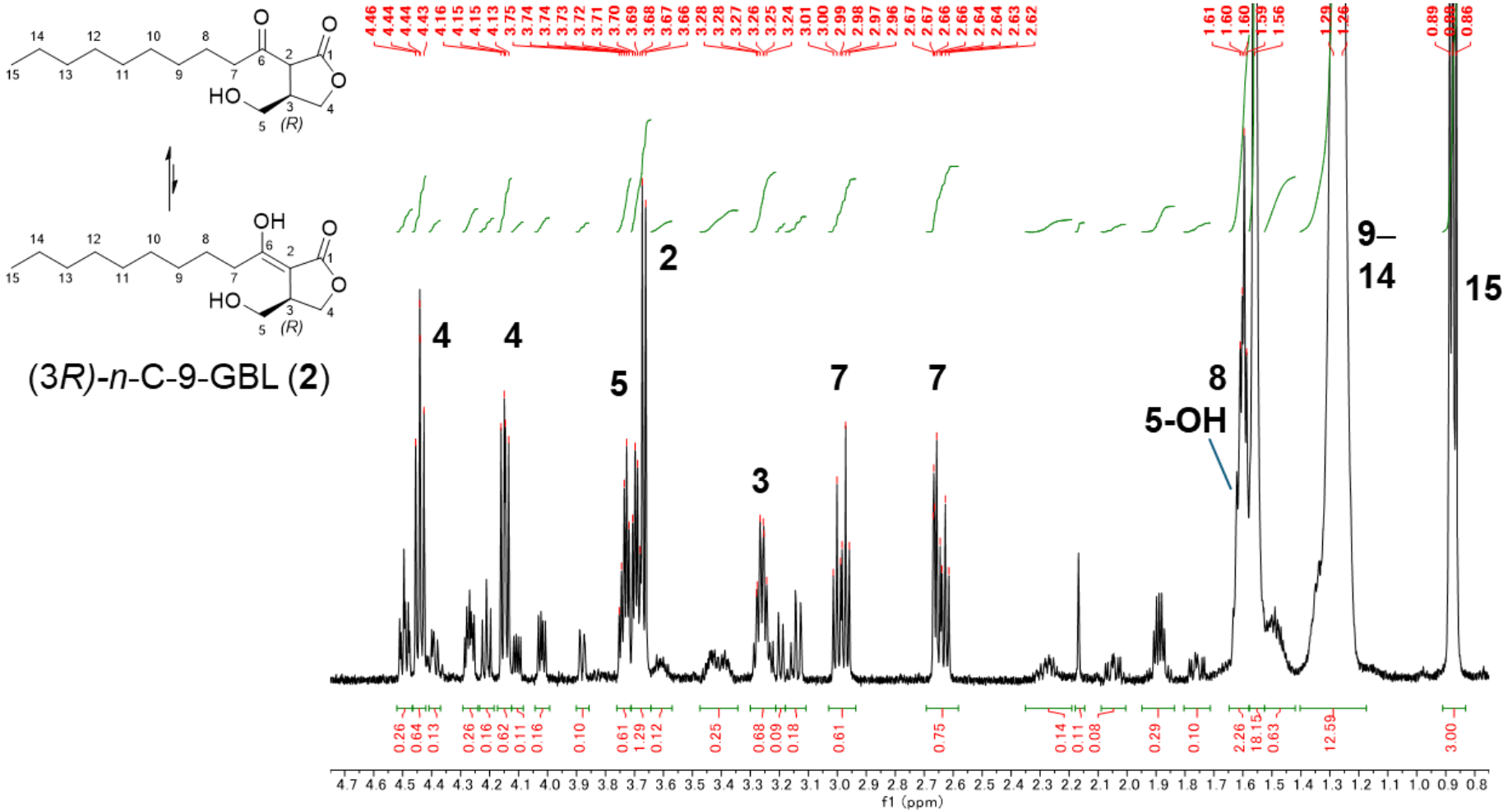

Figure S68. Expanded ^{1}H NMR (600 MHz, $CDCl_3$) spectrum of isolated *n*-C-9 GBL from *Rhodococcus rhodnii* JCM3203 (**2**).

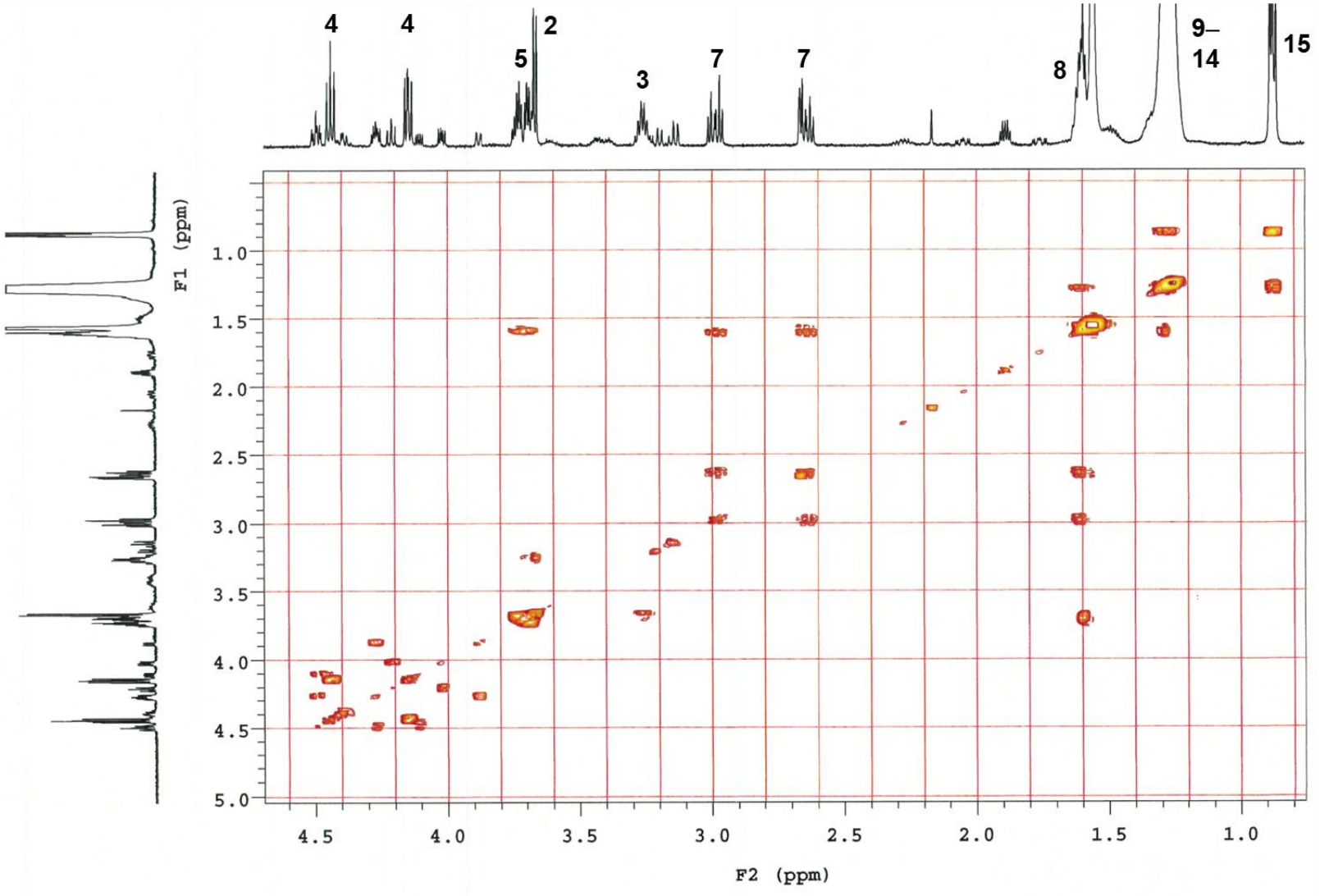

Figure S69. The gradient COSY (600 MHz, $CDCl_3$) spectrum of isolated *n*-C-9 GBL from *Rhodococcus rhodnii* JCM3203 (**2**).

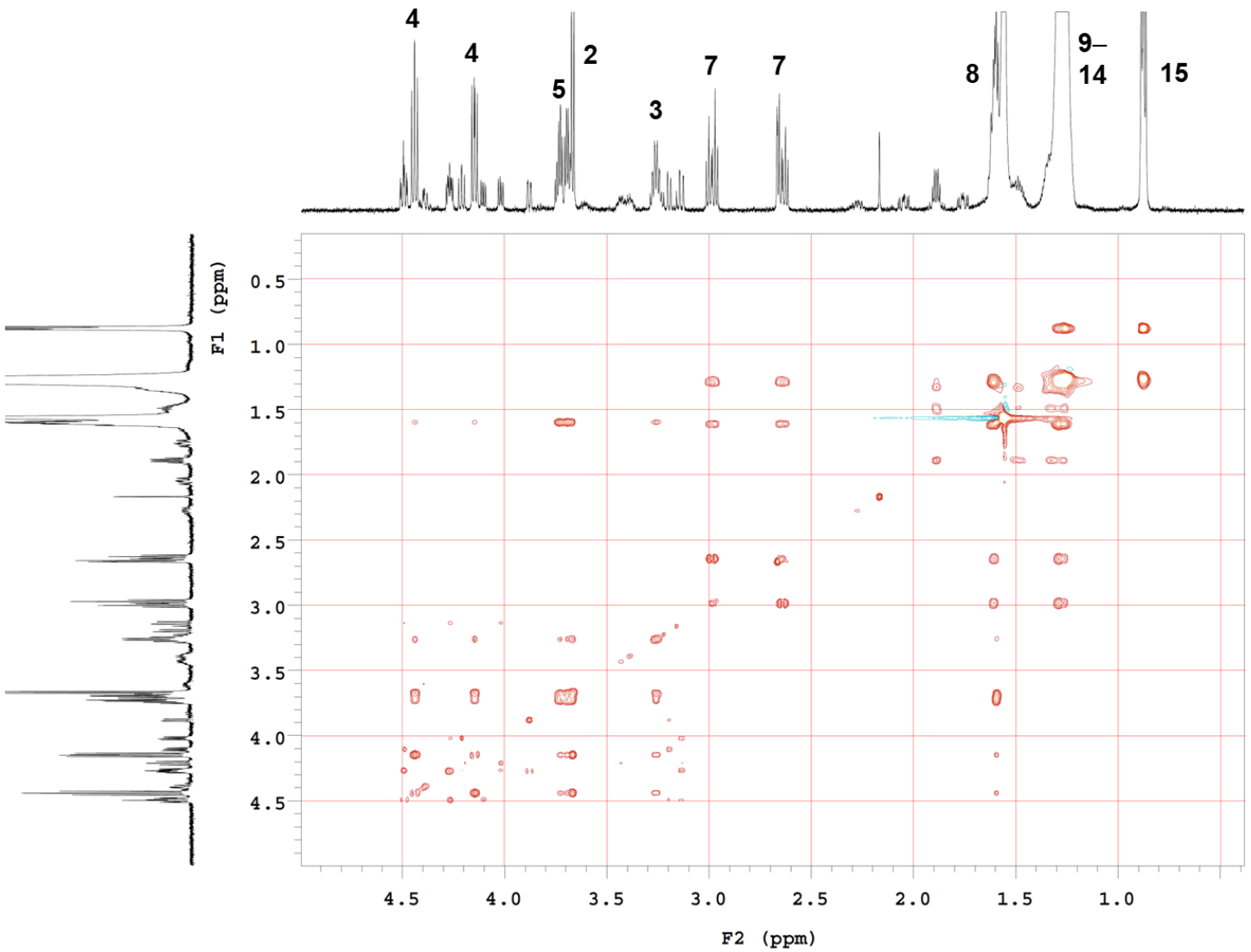

Figure S70. The TOCSY (600 MHz, $CDCl_3$) spectrum of isolated *n*-C-9 GBL from *Rhodococcus rhodnii* JCM3203 (**2**).

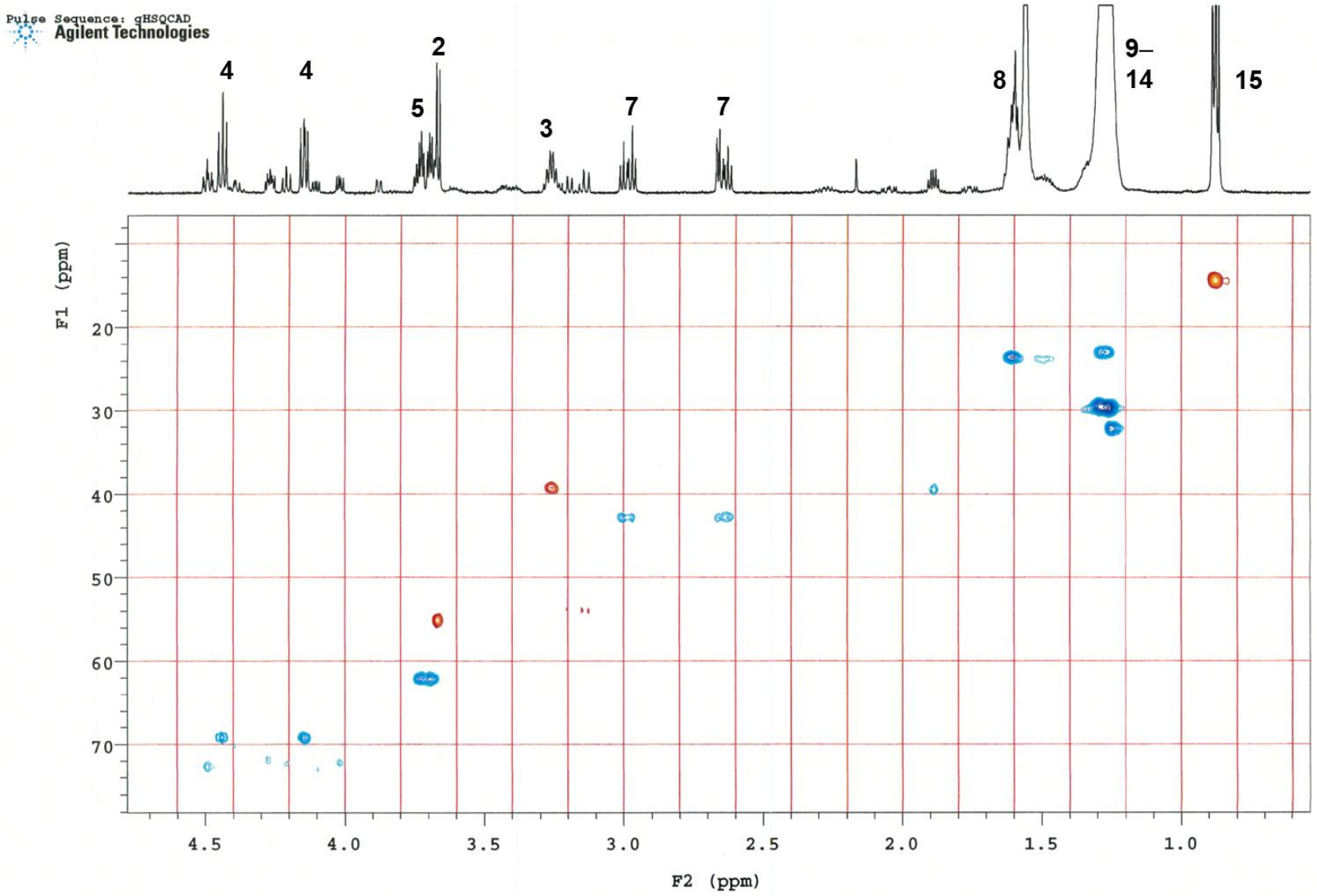

Figure S71. The gradient HSQC (600 MHz, $CDCl_3$) spectrum of isolated *n*-C-9 GBL from *Rhodococcus rhodnii* JCM3203 (**2**).

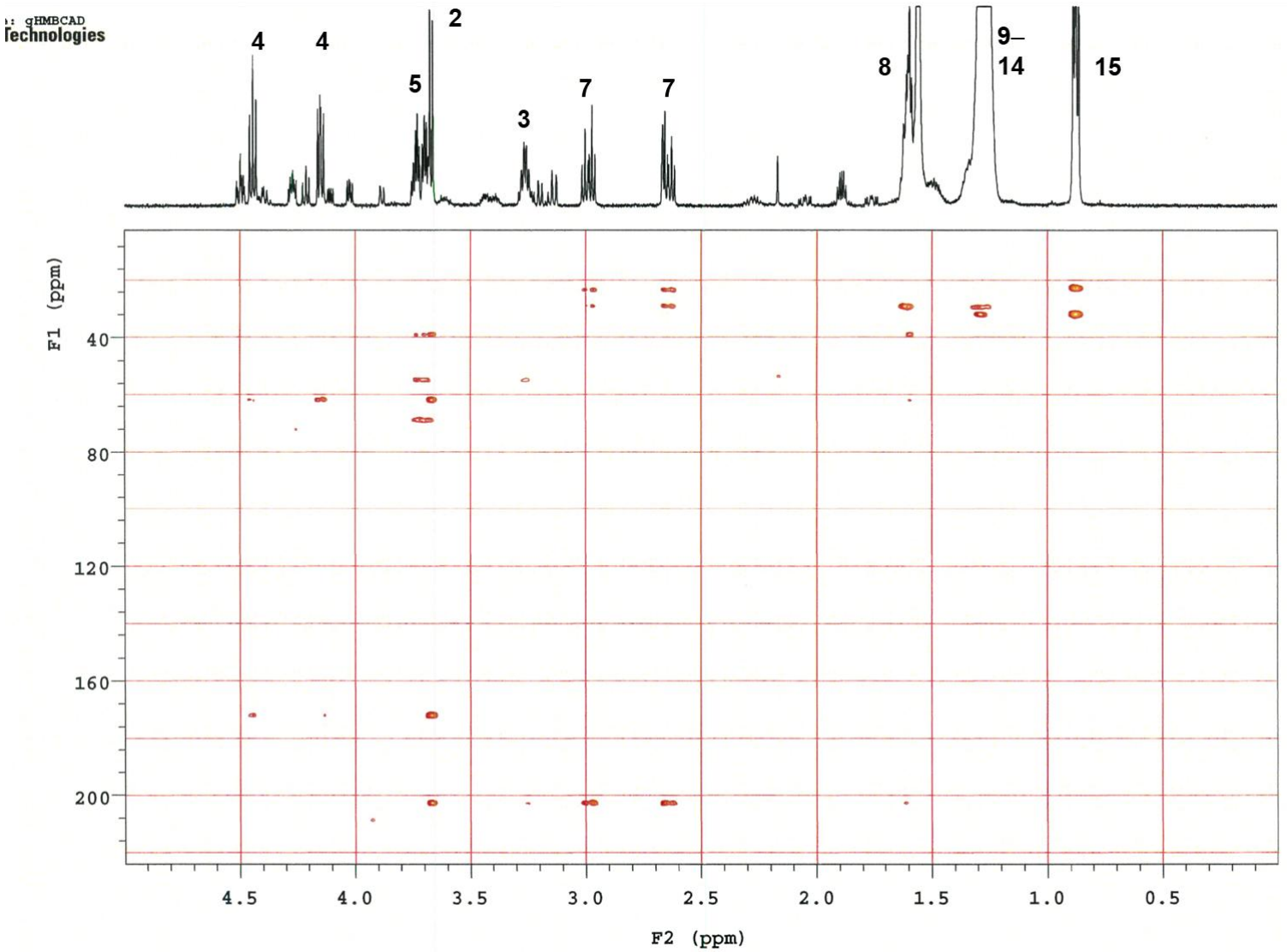

Figure S72. The gradient HMBC (600 MHz, $CDCl_3$) spectrum of isolated *n*-C-9 GBL from *Rhodococcus rhodnii* JCM3203 (**2**).

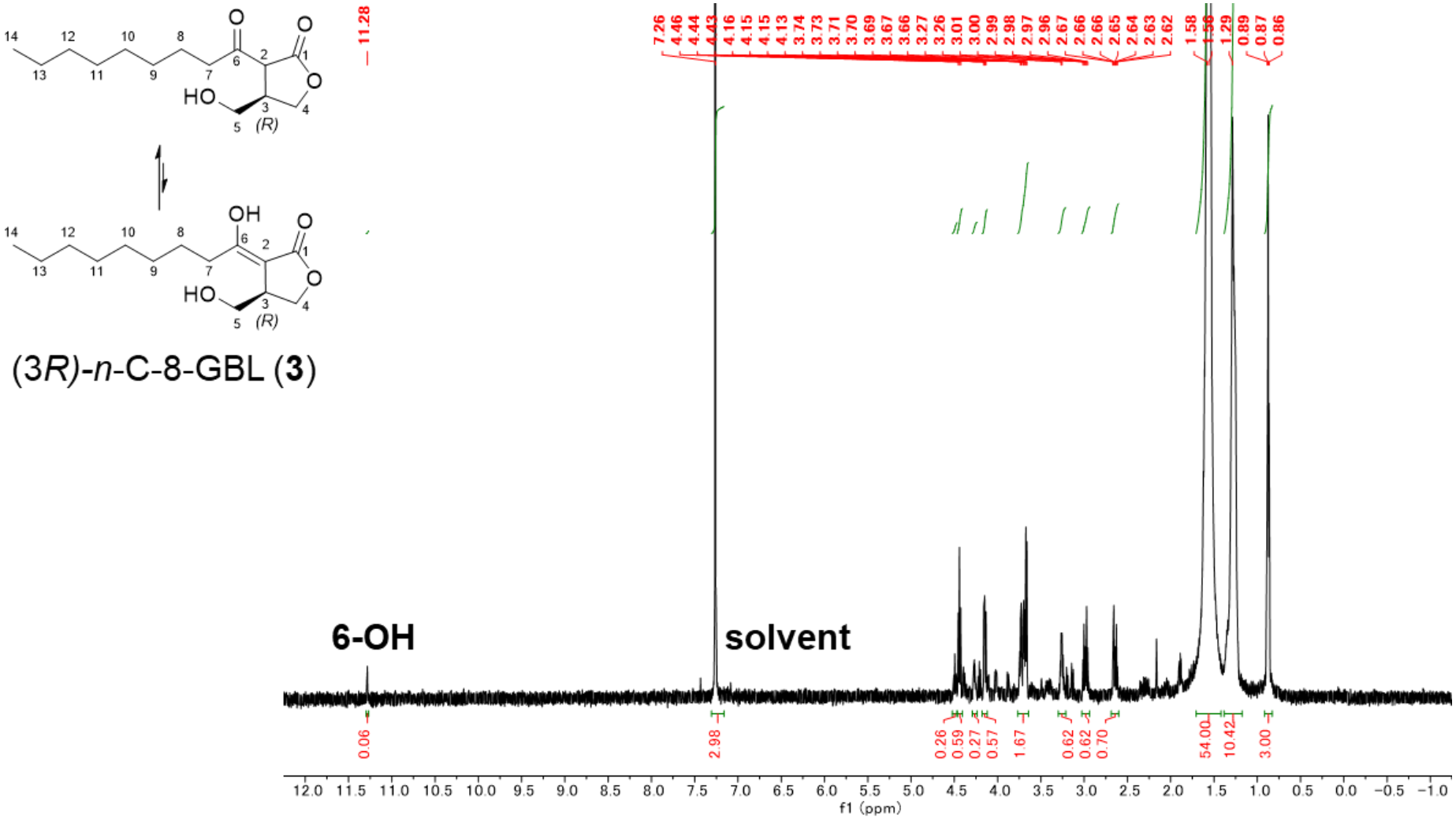

Figure S73. ^{1}H NMR (600 MHz, $CDCl_3$) spectrum of isolated *n*-C-8 GBL from *Rhodococcus rhodnii* JCM3203 (**3**).

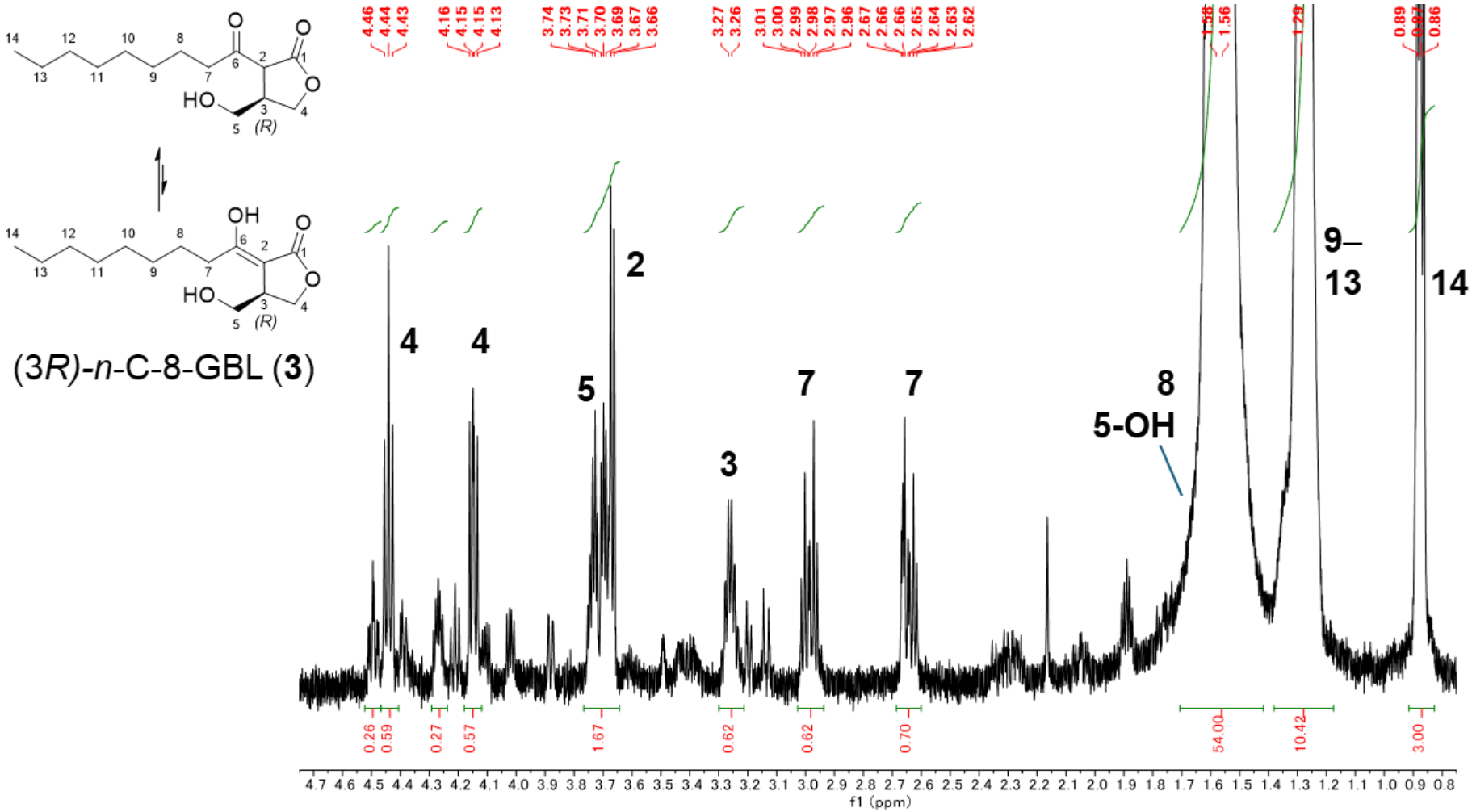

Figure S74. Expanded ^{1}H NMR (600 MHz, $CDCl_3$) spectrum of isolated *n*-C-8 GBL from *Rhodococcus rhodnii* JCM3203 (**3**).

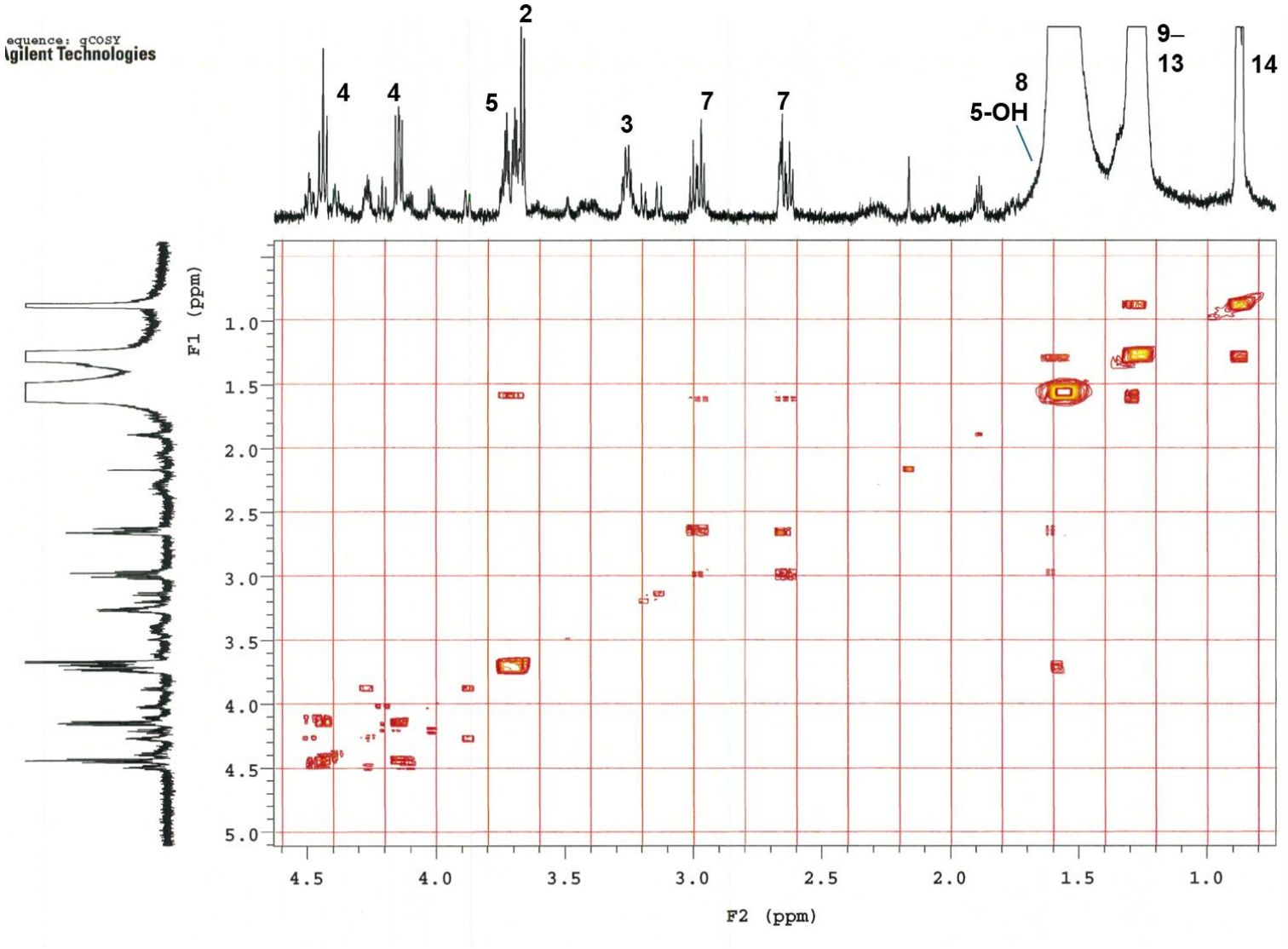

Figure S75. The gradient COSY (600 MHz, $CDCl_3$) spectrum of isolated *n*-C-8 GBL from *Rhodococcus rhodnii* JCM3203 (**3**).

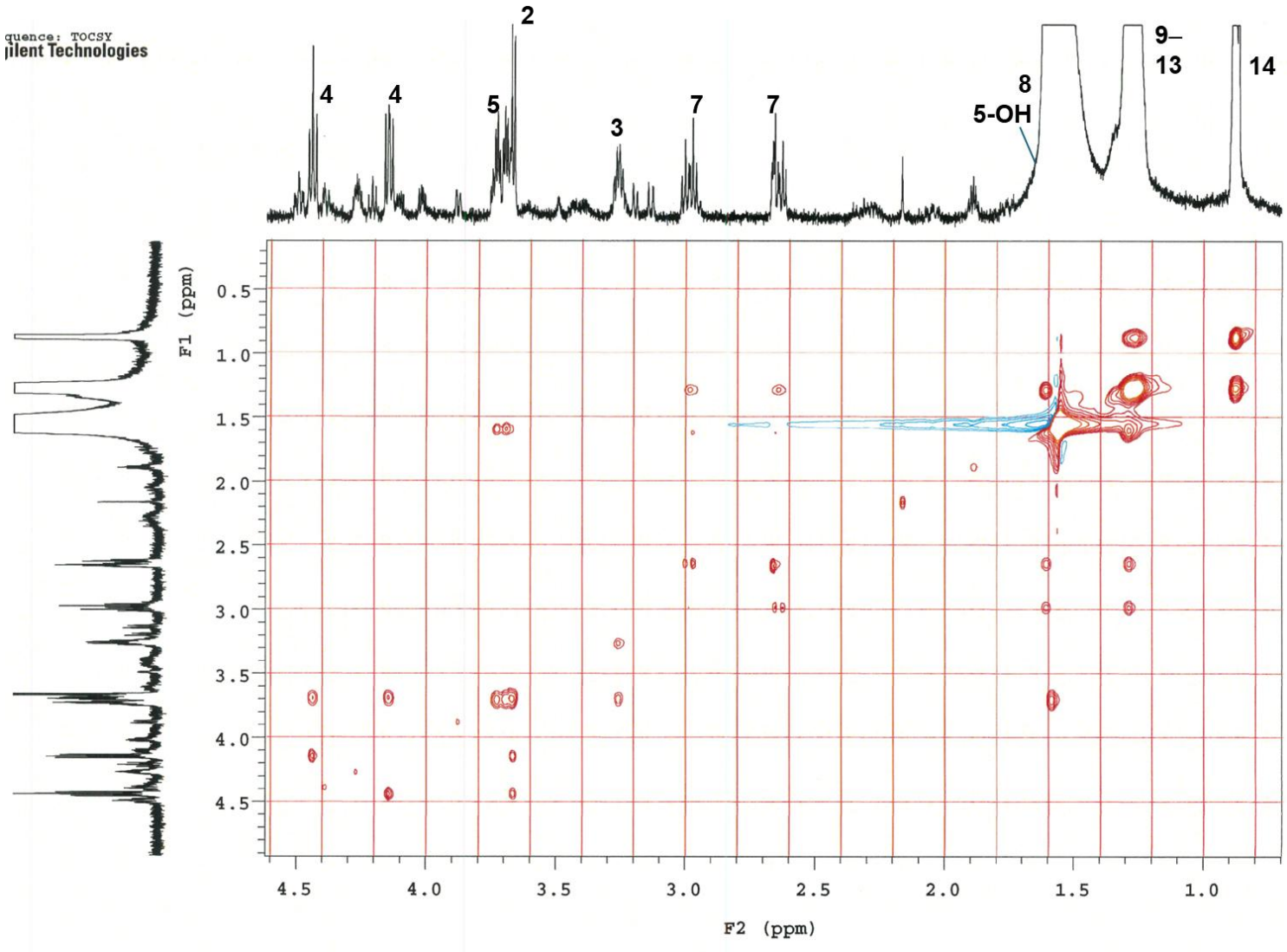

Figure S76. The TOCSY (600 MHz, $CDCl_3$) spectrum of isolated *n*-C-8 GBL from *Rhodococcus rhodnii* JCM3203 (**3**).

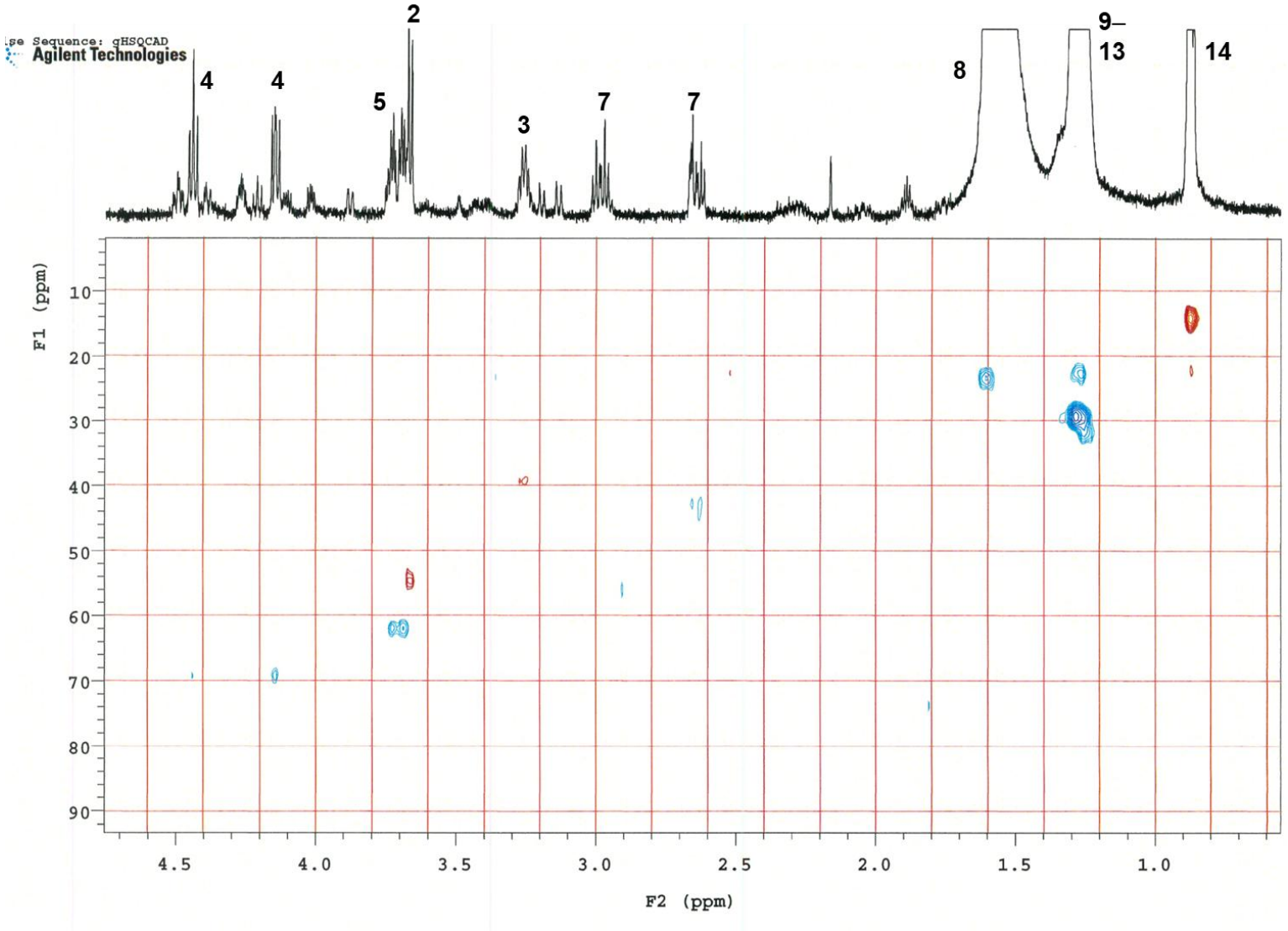

Figure S77. The gradient HSQC (600 MHz, $CDCl_3$) spectrum of isolated *n*-C-8 GBL from *Rhodococcus rhodnii* JCM3203 (**3**).

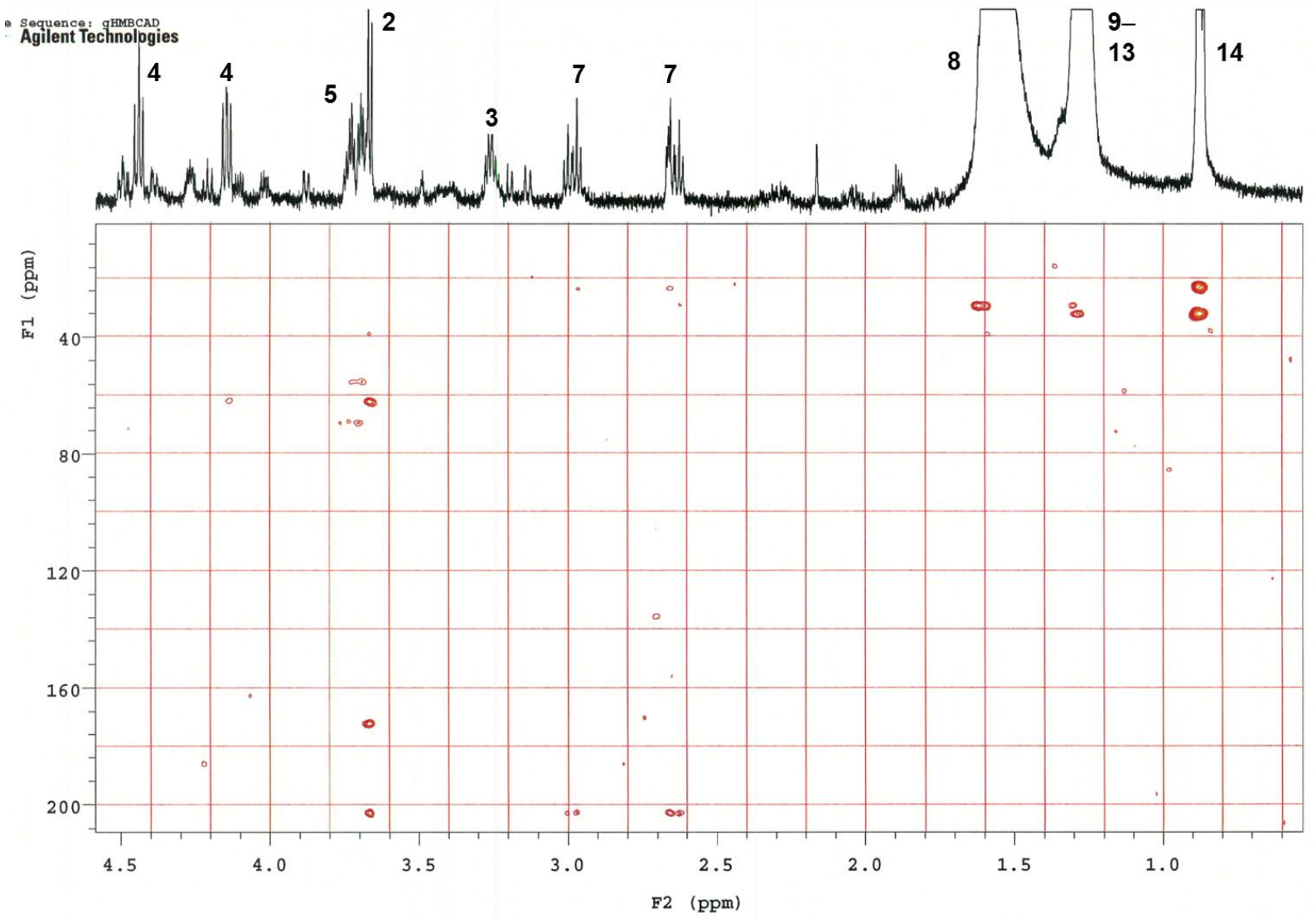

Figure S78. The gradient HMBC (600 MHz, $CDCl_3$) spectrum of isolated *n*-C-8 GBL from *Rhodococcus rhodnii* JCM3203 (**3**).

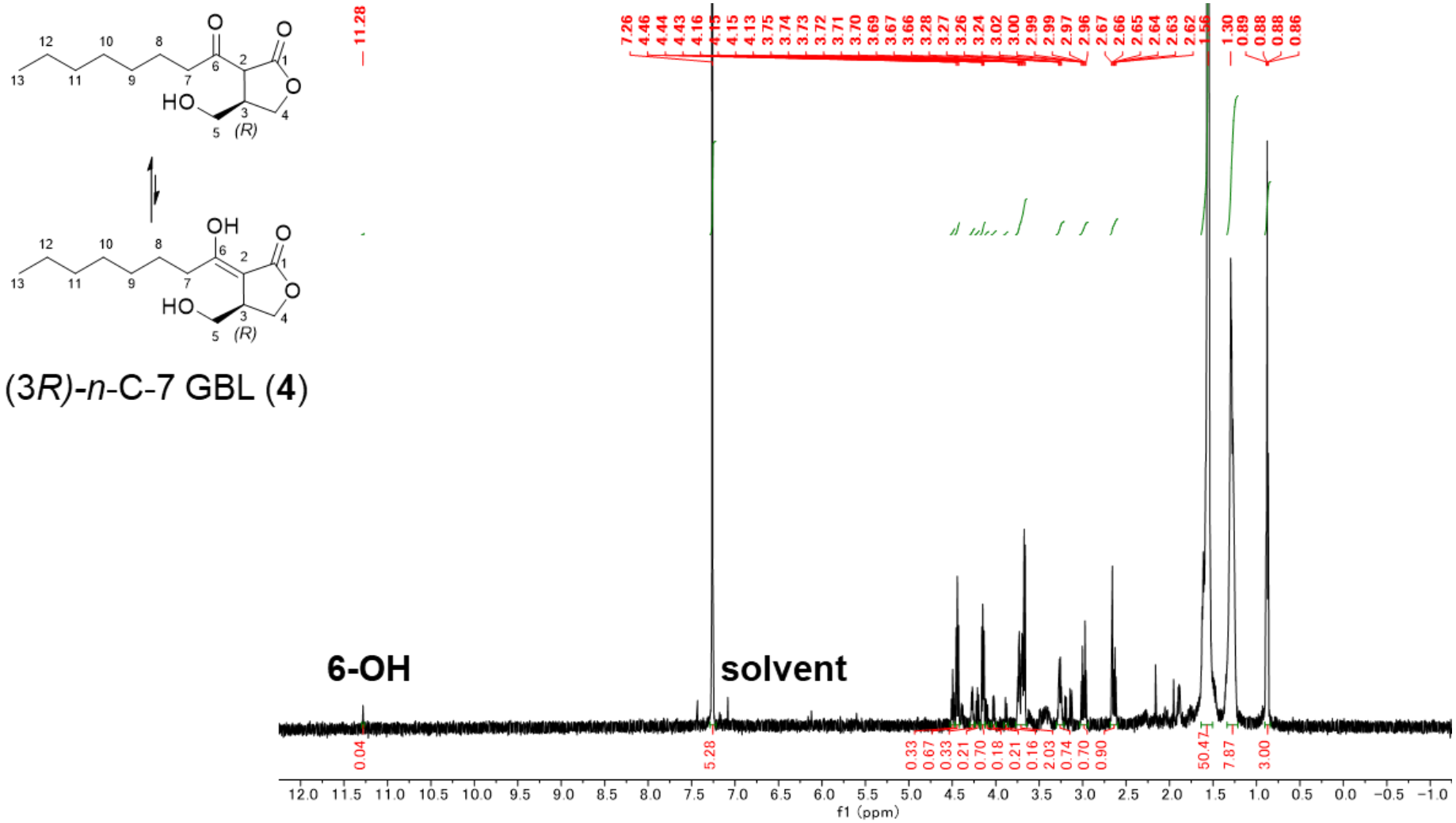

Figure S79. ^{1}H NMR (600 MHz, $CDCl_3$) spectrum of isolated *n*-C-7 GBL from *Rhodococcus rhodnii* JCM3203 (**4**).

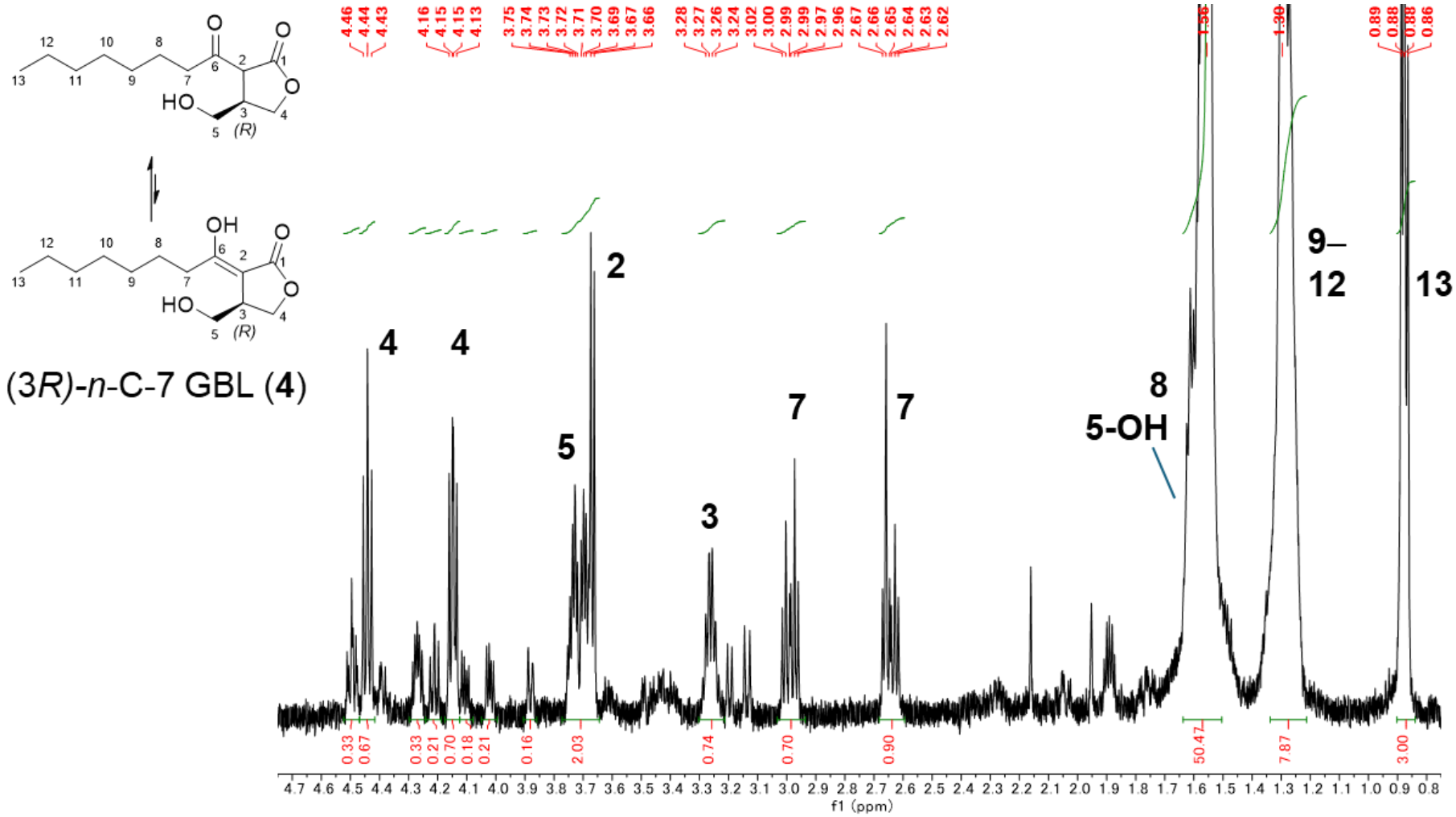

Figure S80. Expanded ^{1}H NMR (600 MHz, $CDCl_3$) spectrum of isolated *n*-C-7 GBL from *Rhodococcus rhodnii* JCM3203 (**4**).

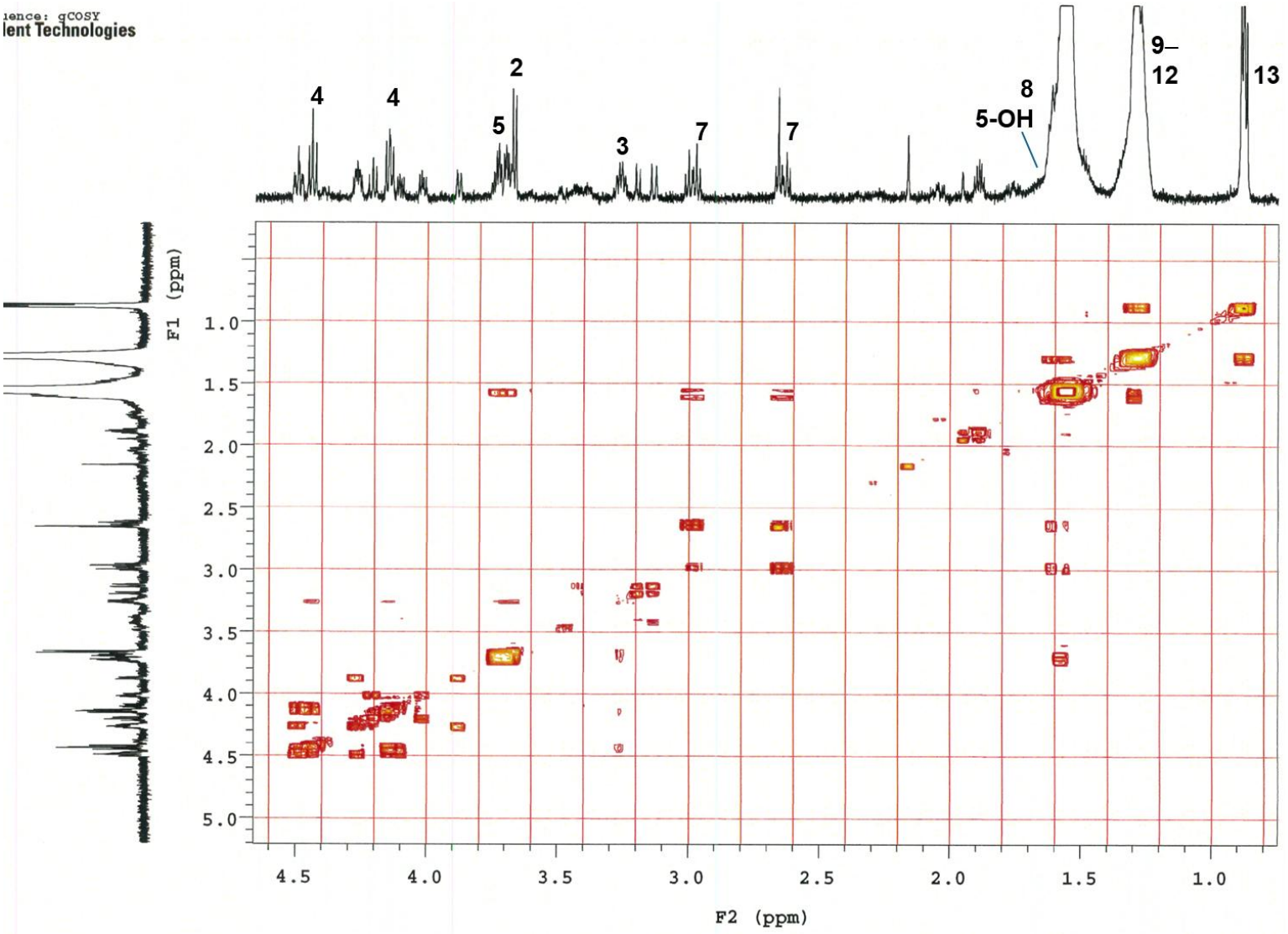

Figure S81. The gradient COSY (600 MHz, $CDCl_3$) spectrum of isolated *n*-C-7 GBL from *Rhodococcus rhodnii* JCM3203 (**4**).

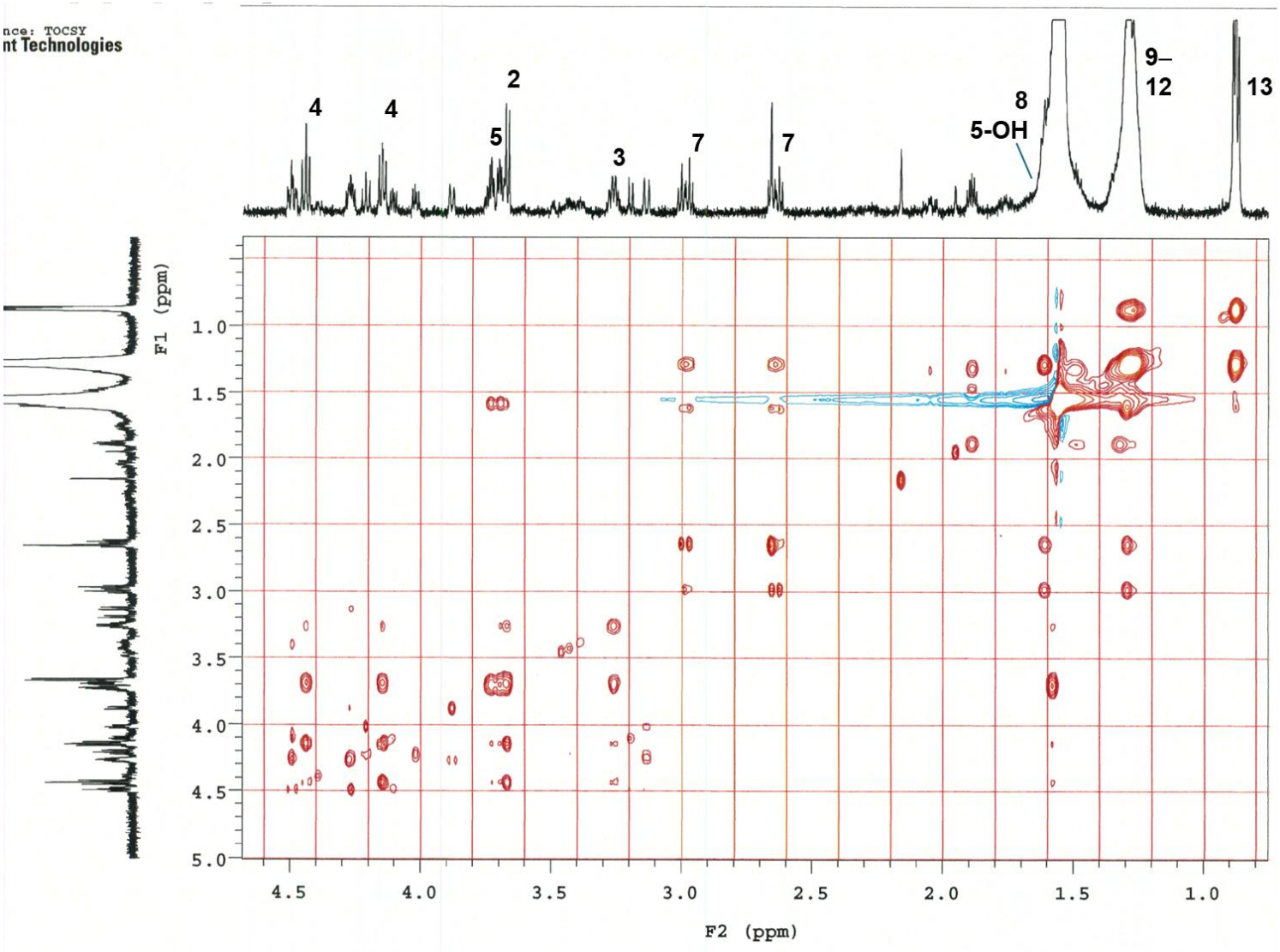

Figure S82. The TOCSY (600 MHz, $CDCl_3$) spectrum of isolated *n*-C-7 GBL from *Rhodococcus rhodnii* JCM3203 (**4**).

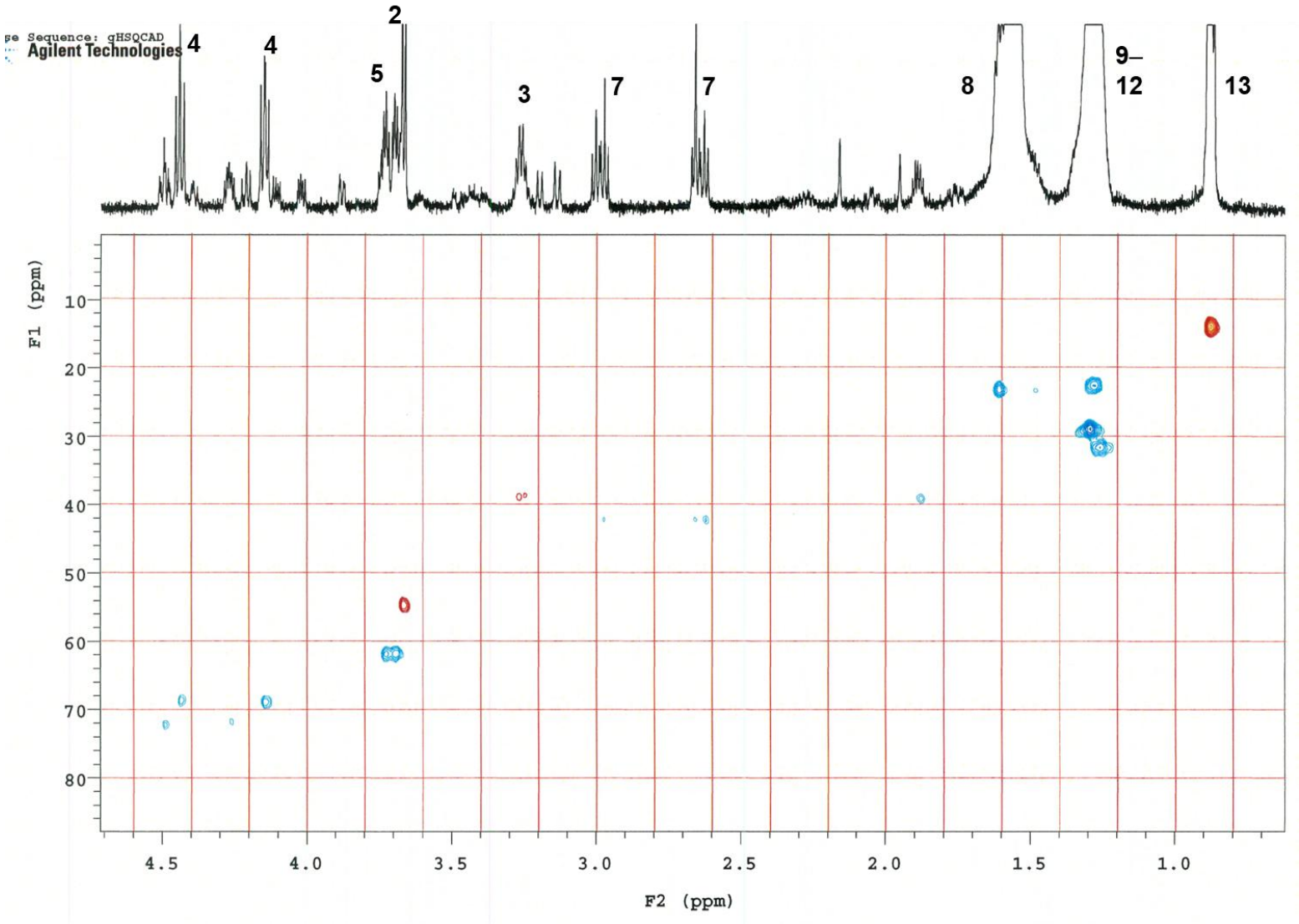

Figure S83. The gradient HSQC (600 MHz, $CDCl_3$) spectrum of isolated *n*-C-7 GBL from *Rhodococcus rhodnii* JCM3203 (**4**).

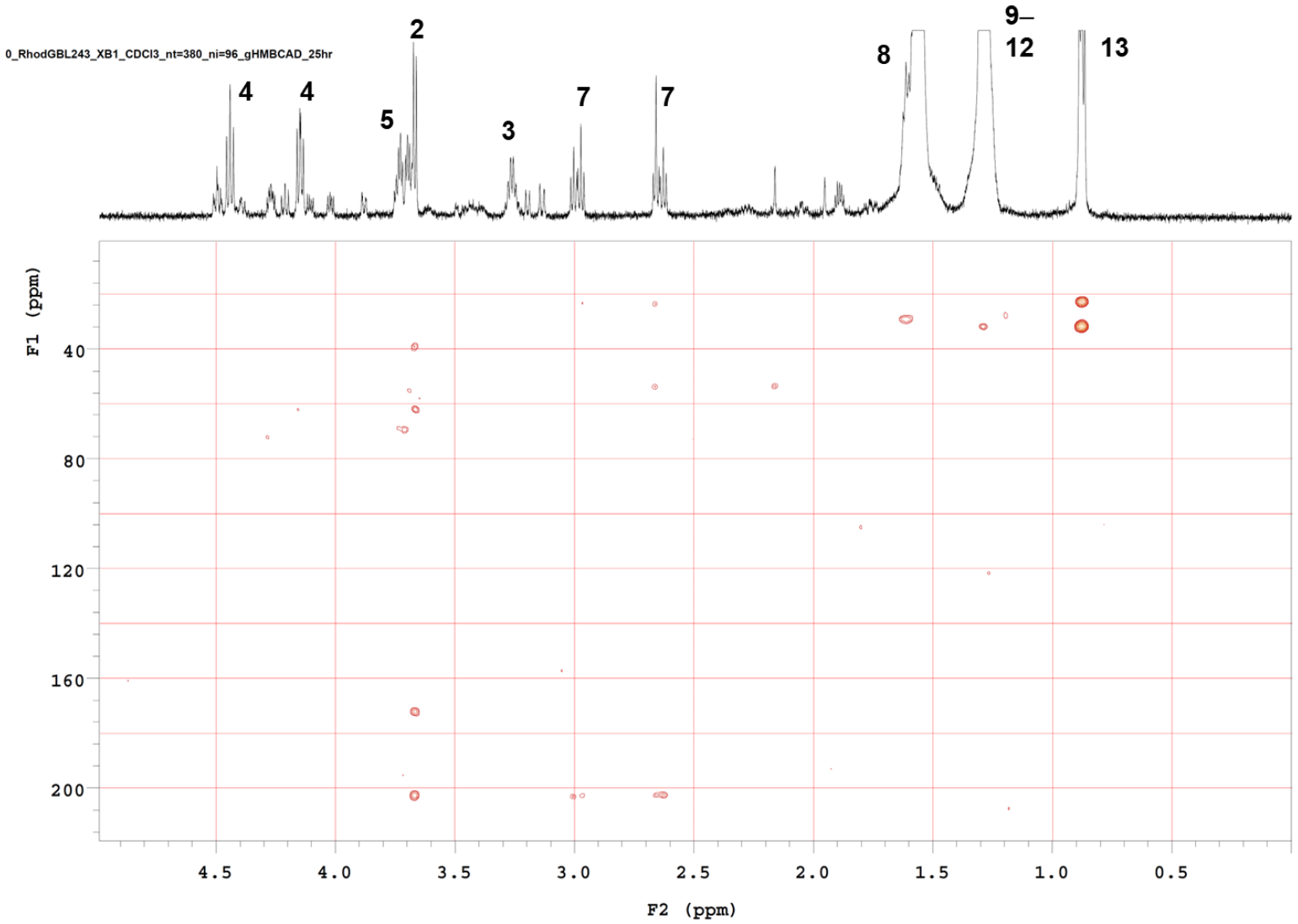

Figure S84. The gradient HMBC (600 MHz, $CDCl_3$) spectrum of isolated *n*-C-7 GBL from *Rhodococcus rhodnii* JCM3203 (**4**).

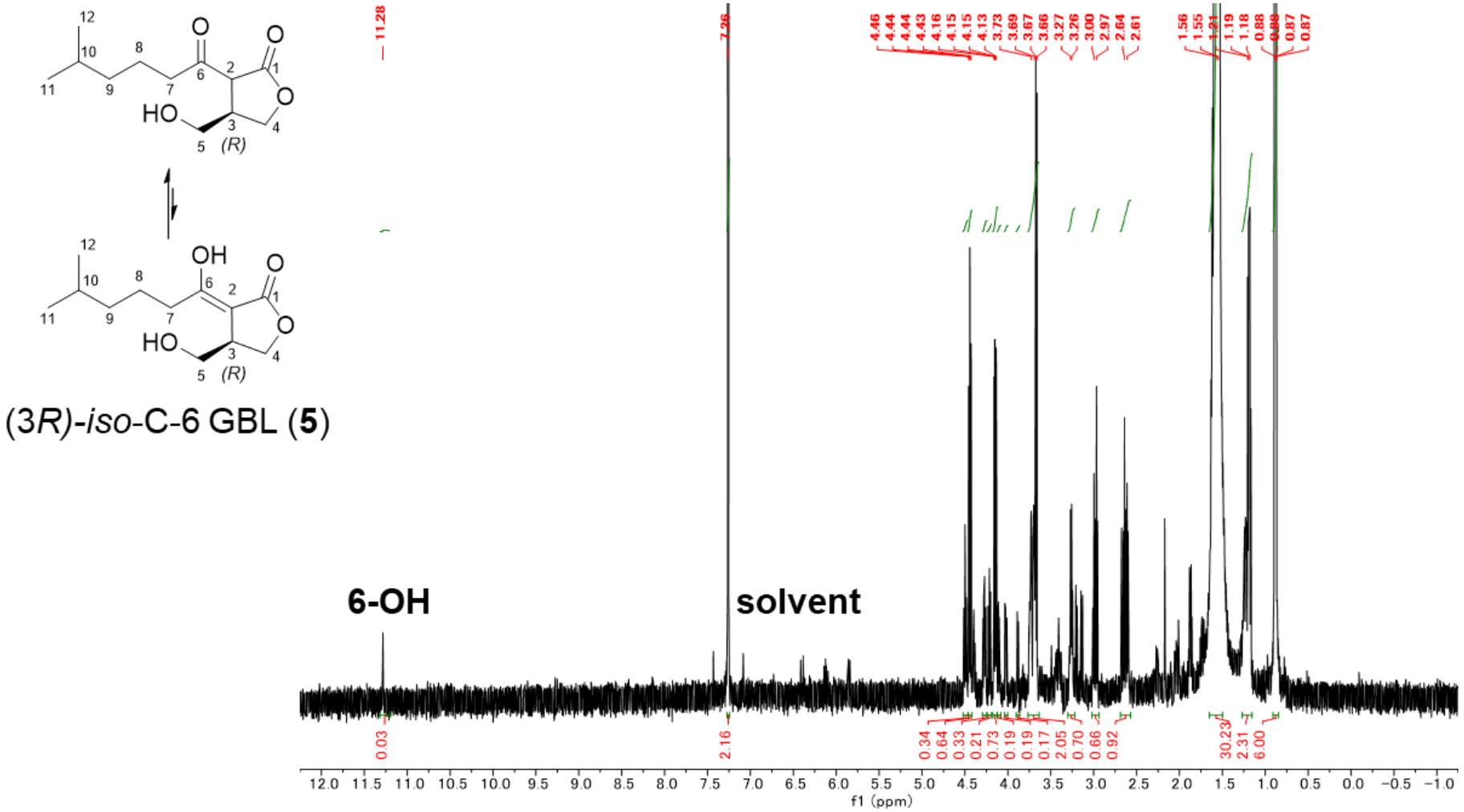

Figure S85. ^{1}H NMR (600 MHz, $CDCl_3$) spectrum of isolated *iso*-C-6 GBL from *Streptomyces* sp. YKOK-I1 (**5**).

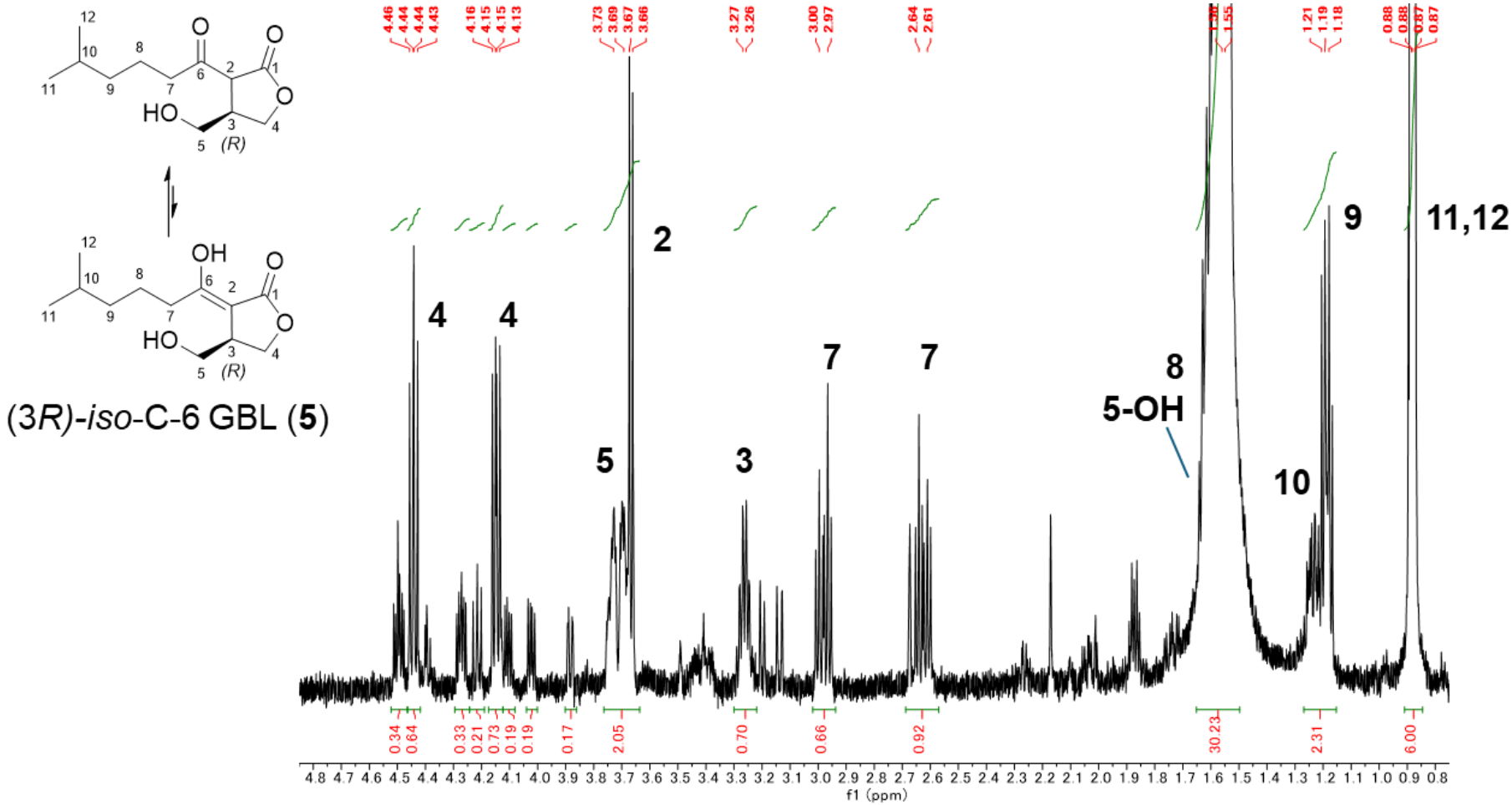

Figure S86. Expanded ^{1}H NMR (600 MHz, $CDCl_3$) spectrum of isolated *iso*-C-6 GBL from *Streptomyces* sp. YKOK-I1 (**5**).

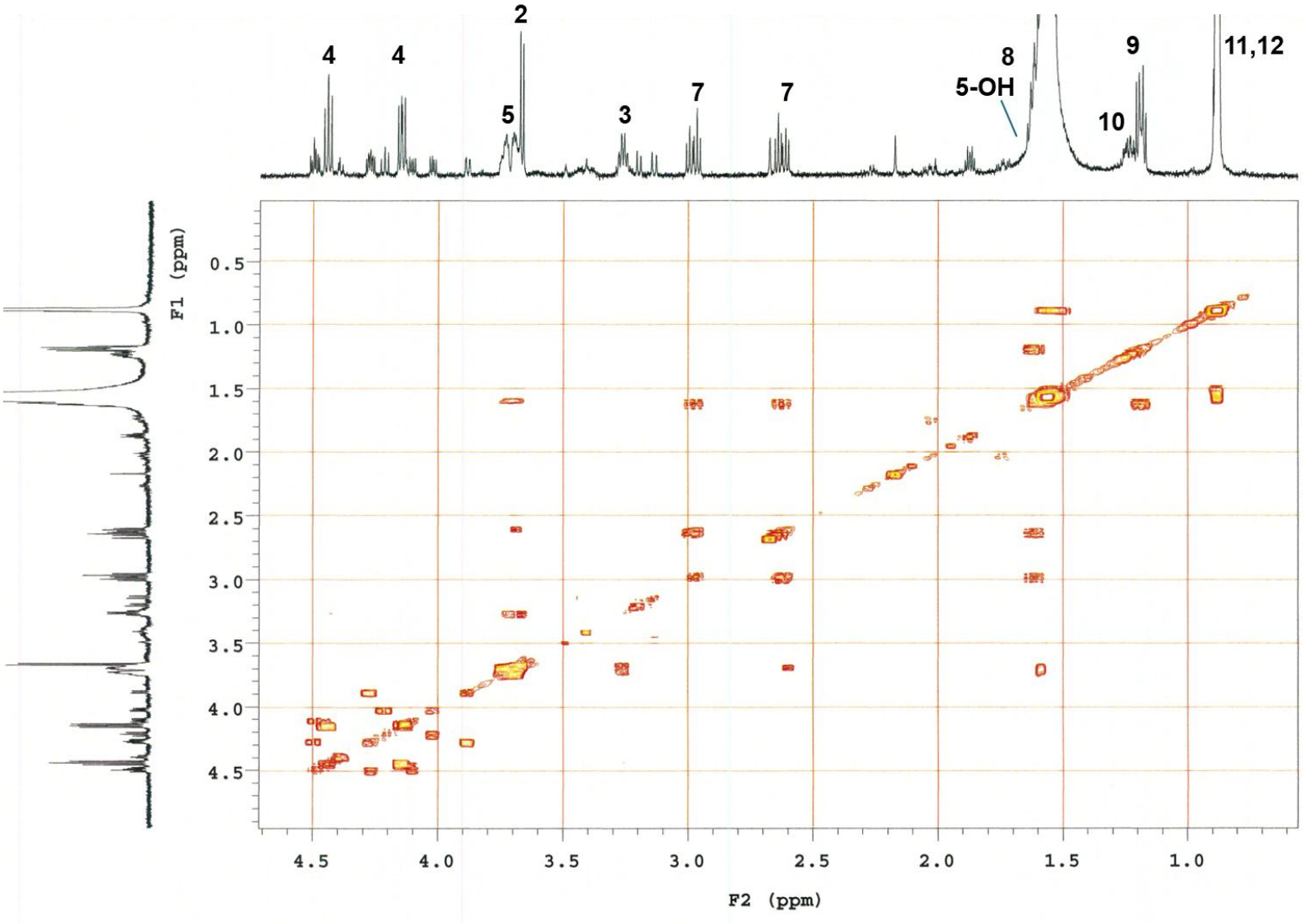

Figure S87. The gradient COSY (600 MHz, $CDCl_3$) spectrum of isolated *iso*-C-6 GBL from *Streptomyces* sp. YKOK-I1 (**5**).

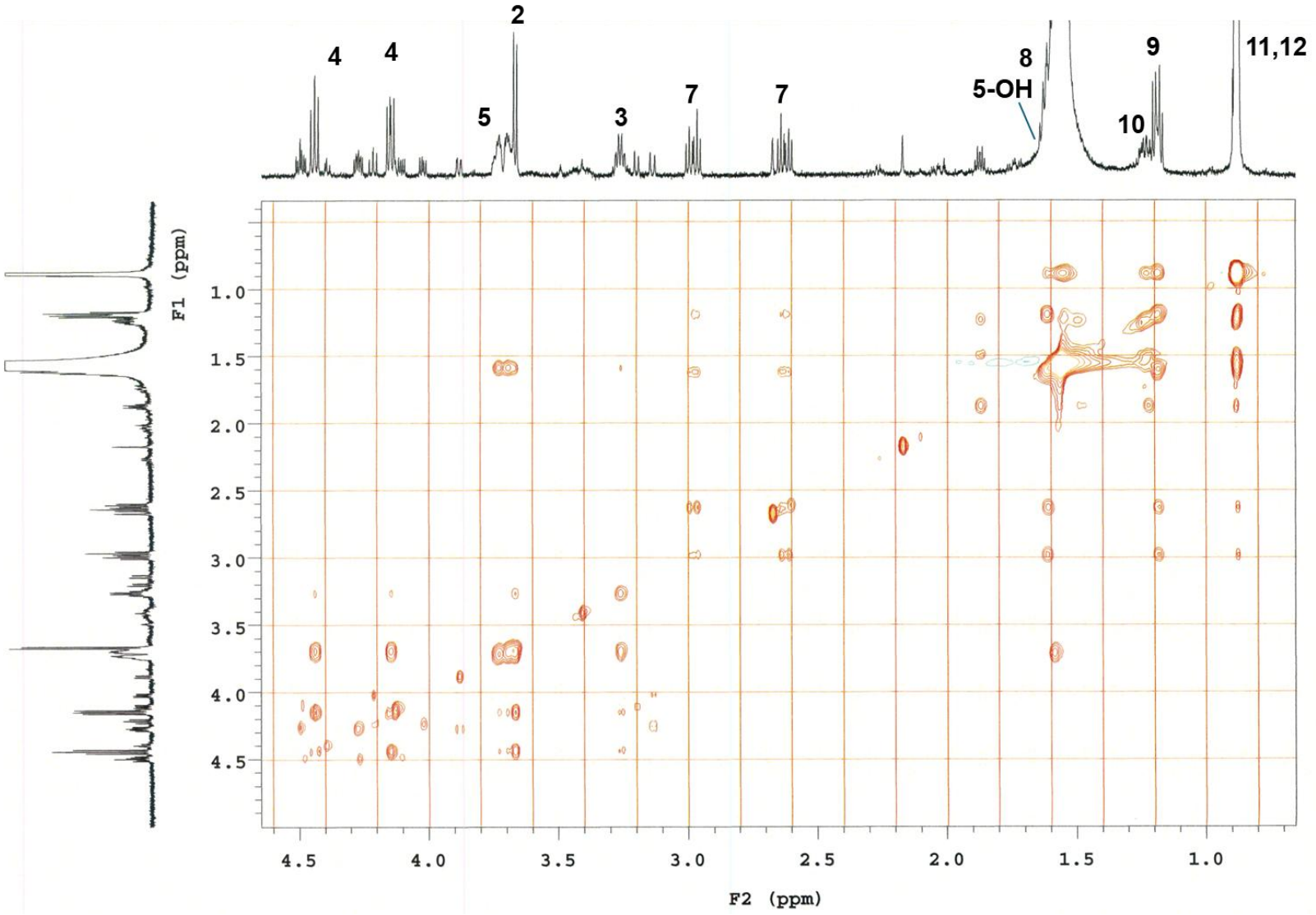

Figure S88. The TOCSY (600 MHz, $CDCl_3$) spectrum of isolated *iso*-C-6 GBL from *Streptomyces* sp. YKOK-I1 (**5**).

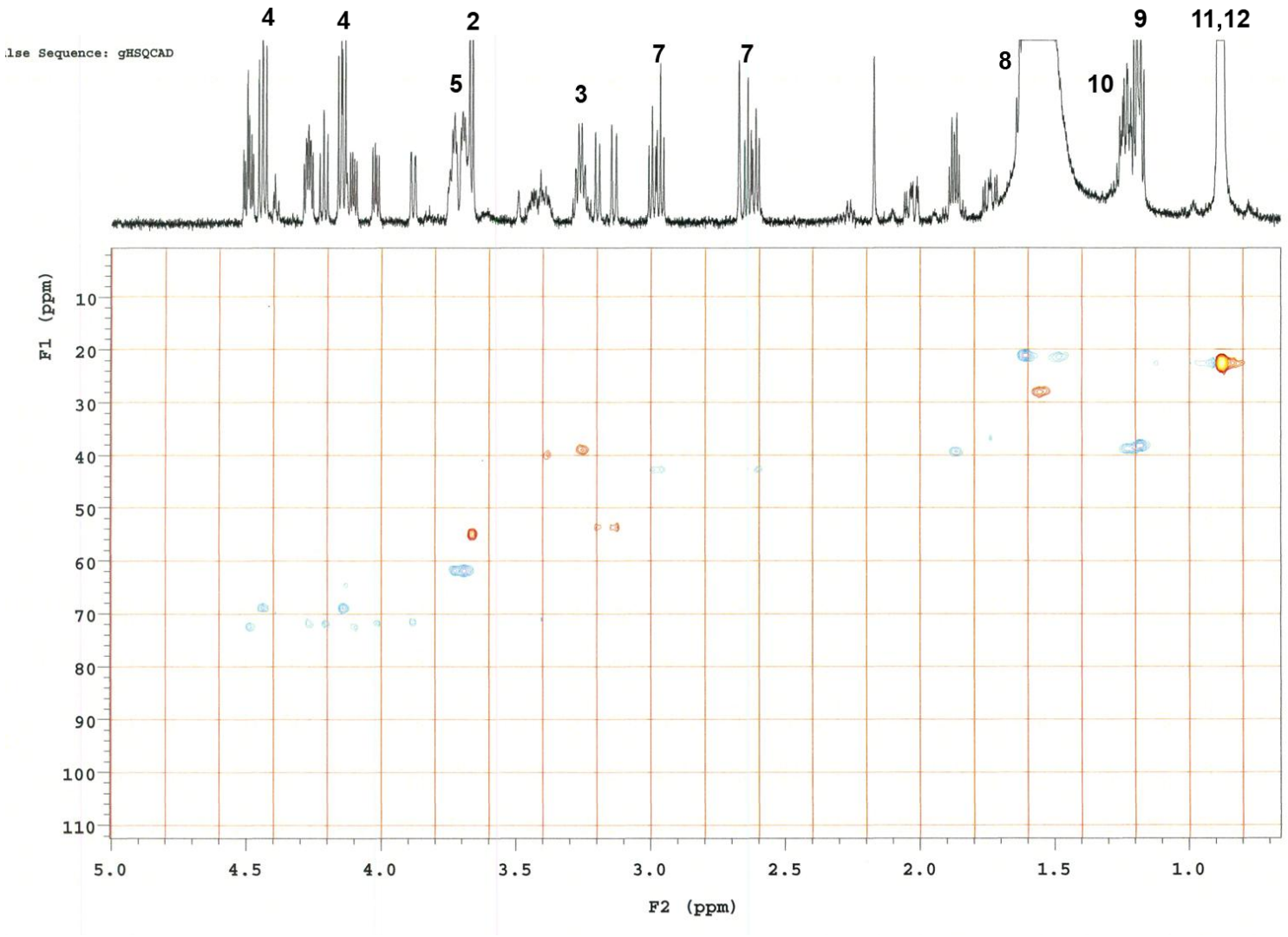

Figure S89. The gradient HSQC (600 MHz, $CDCl_3$) spectrum of isolated *iso*-C-6 GBL from *Streptomyces* sp. YKOK-I1 (**5**).

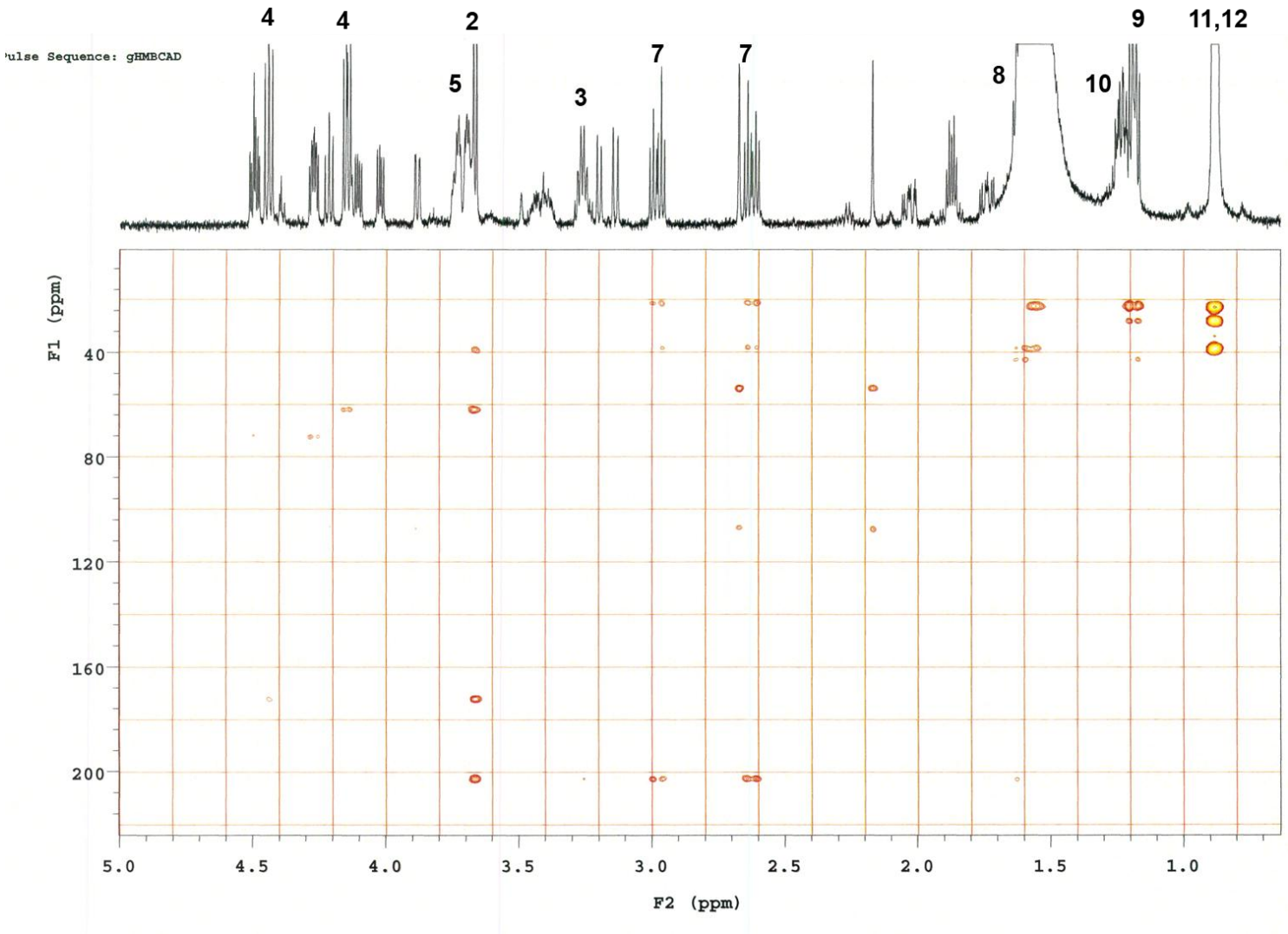

Figure S90. The gradient HMBC (600 MHz, $CDCl_3$) spectrum of isolated *iso*-C-6 GBL from *Streptomyces* sp. YKOK-I1 (**5**).

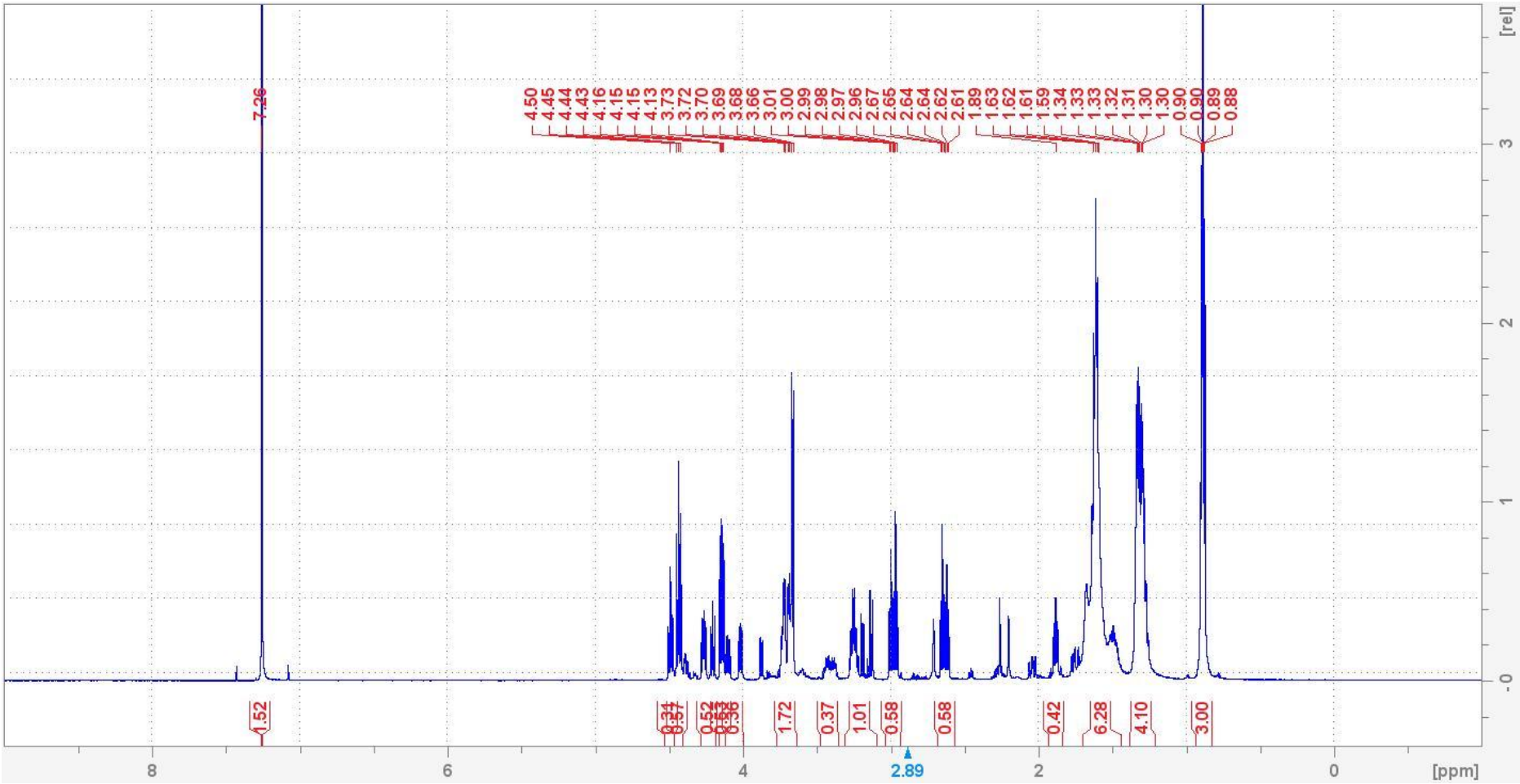

Figure S91. ^{1}H NMR (600 MHz, $CDCl_3$) spectrum of synthesized *n*-C-5 GBL (**10d**).

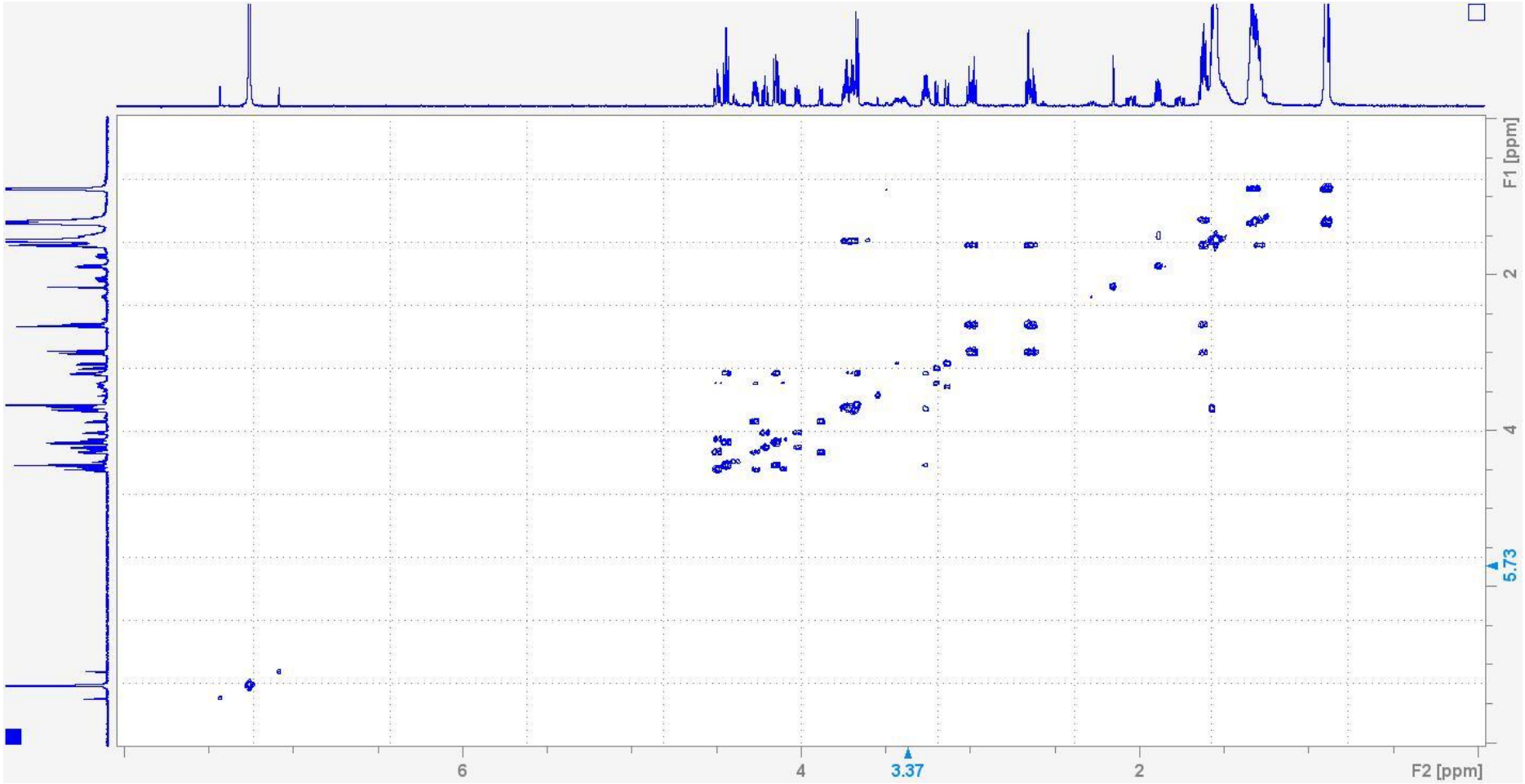

Figure S92. The gradient COSY (600 MHz, $CDCl_3$) spectrum of synthesized *n*-C-5 GBL (**10d**).

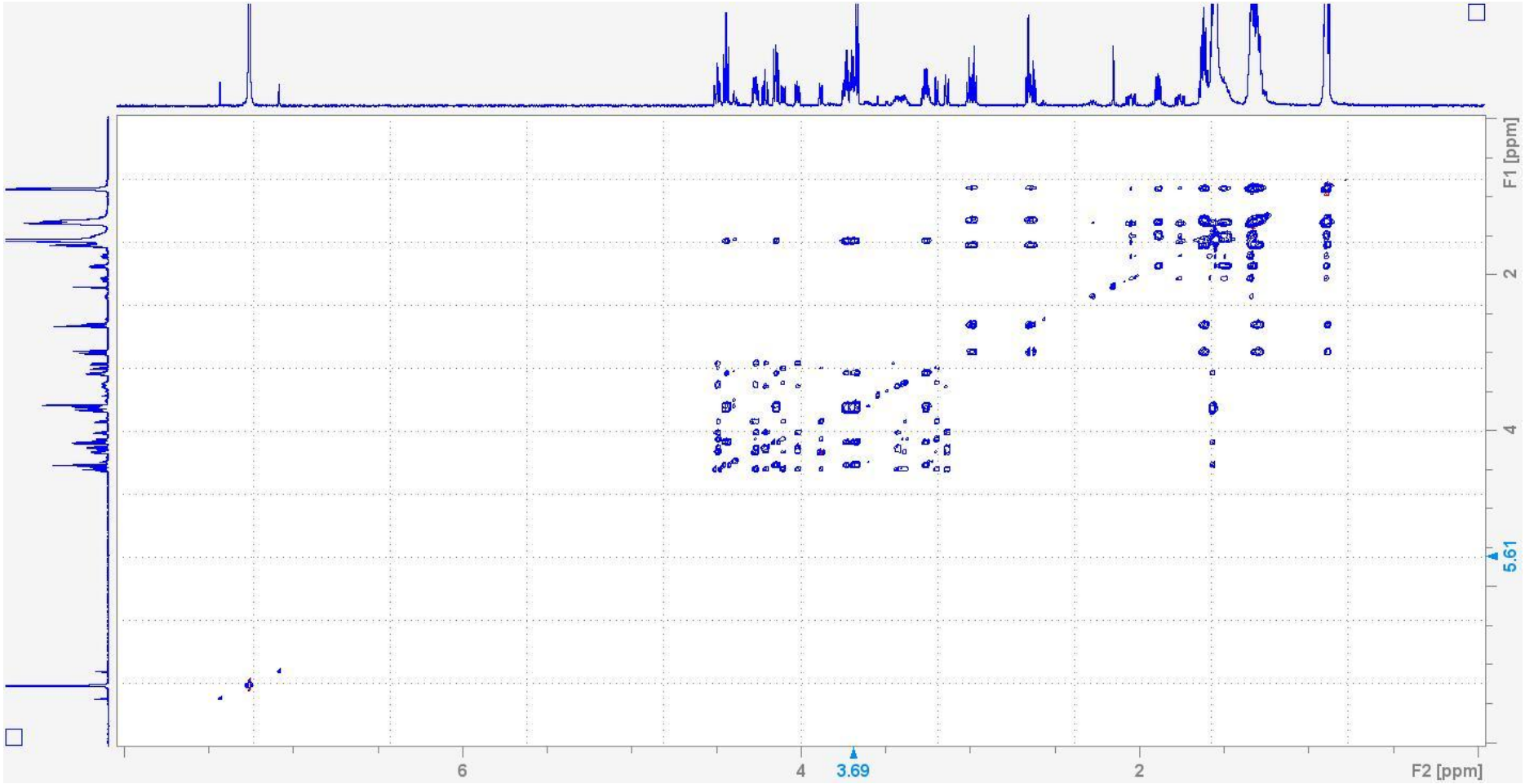

Figure S93. The TOCSY (600 MHz, $CDCl_3$) spectrum of synthesized *n*-C-5 GBL (**10d**).

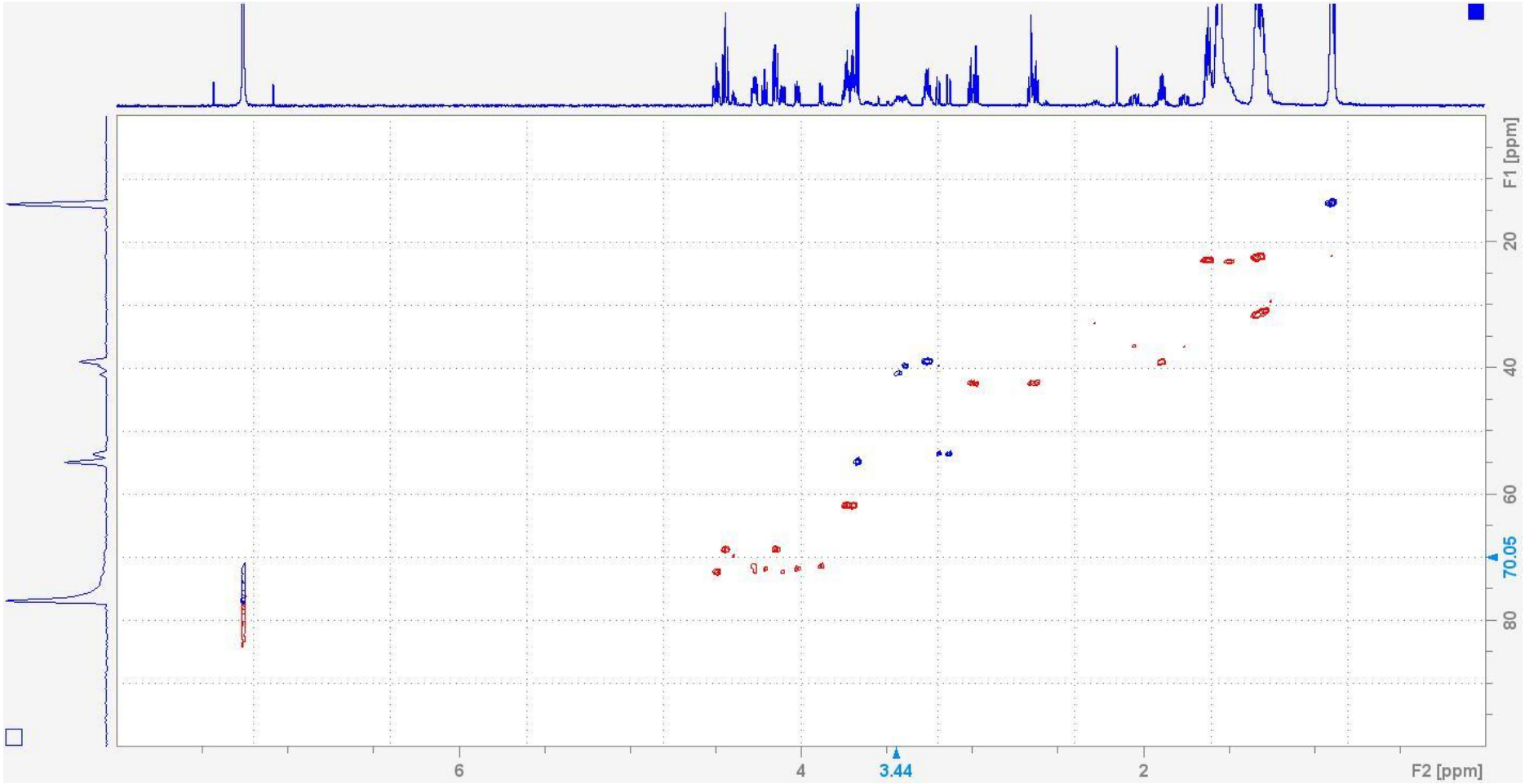

Figure S94. The gradient HSQC (600 MHz, $CDCl_3$) spectrum of synthesized *n*-C-5 GBL (**10d**).

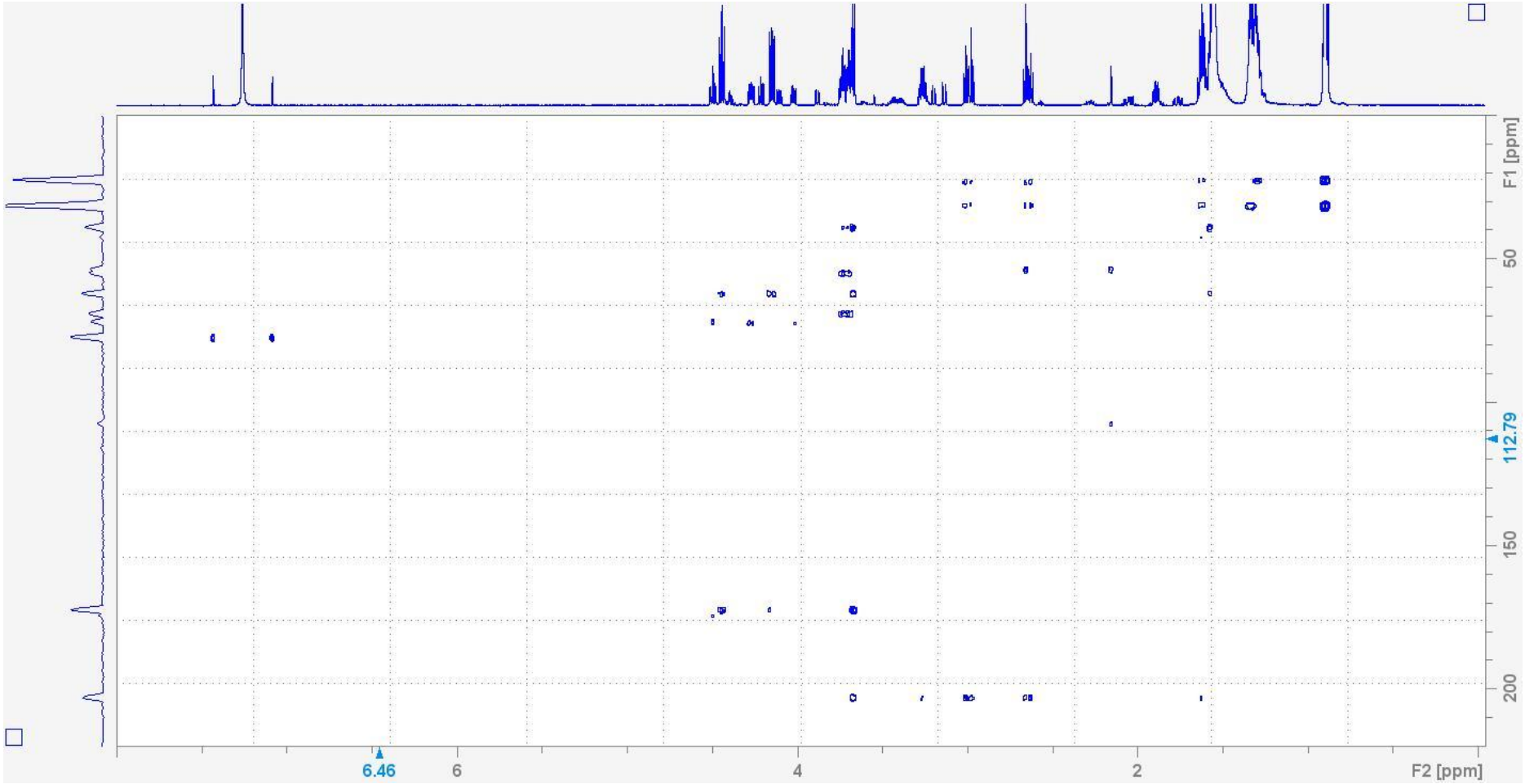

Figure S95. The gradient HMBC (600 MHz, $CDCl_3$) spectrum of synthesized *n*-C-5 GBL (**10d**).

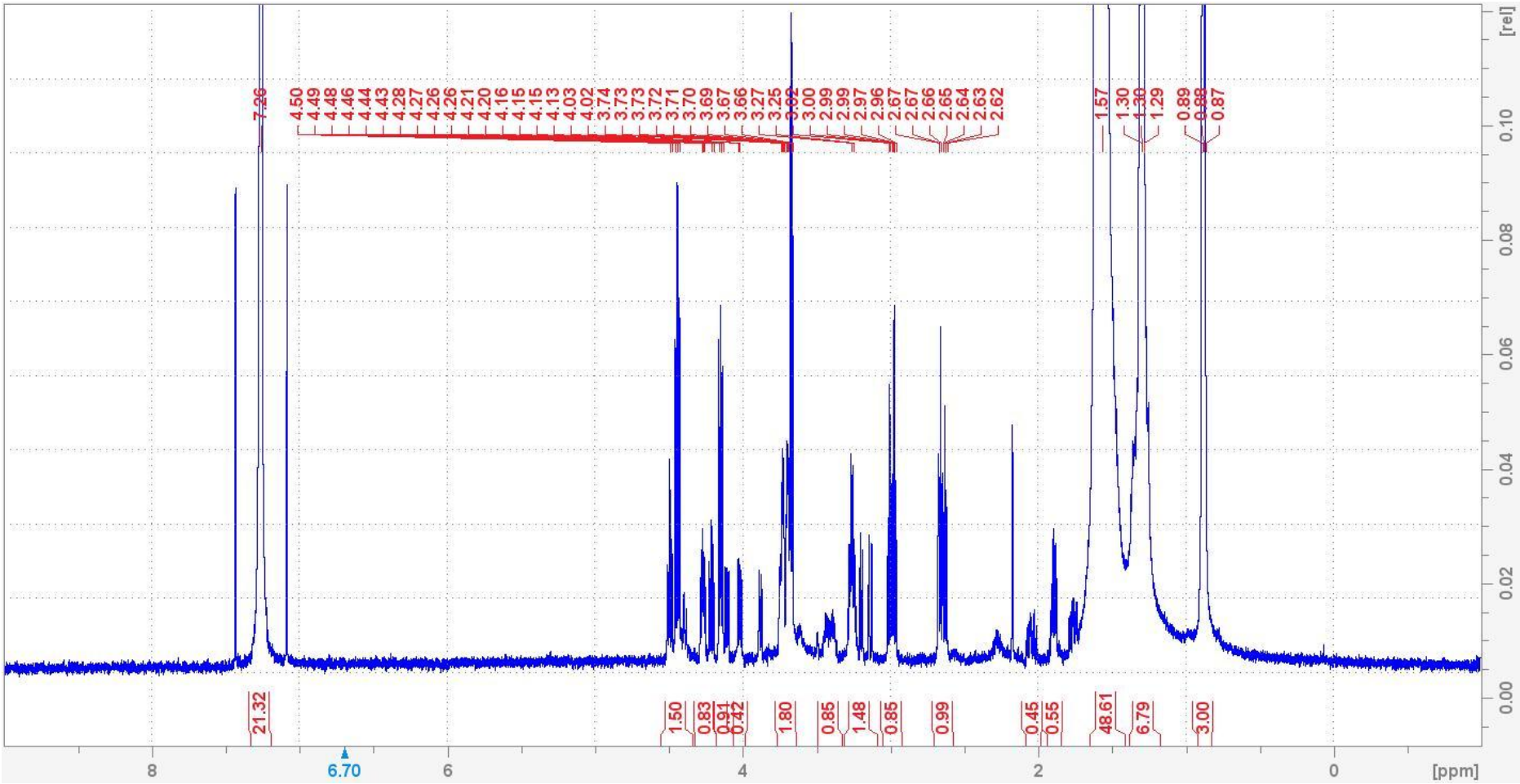

Figure S96. ^{1}H NMR (600 MHz, $CDCl_3$) spectrum of synthesized *n*-C-6 GBL (**10e**).

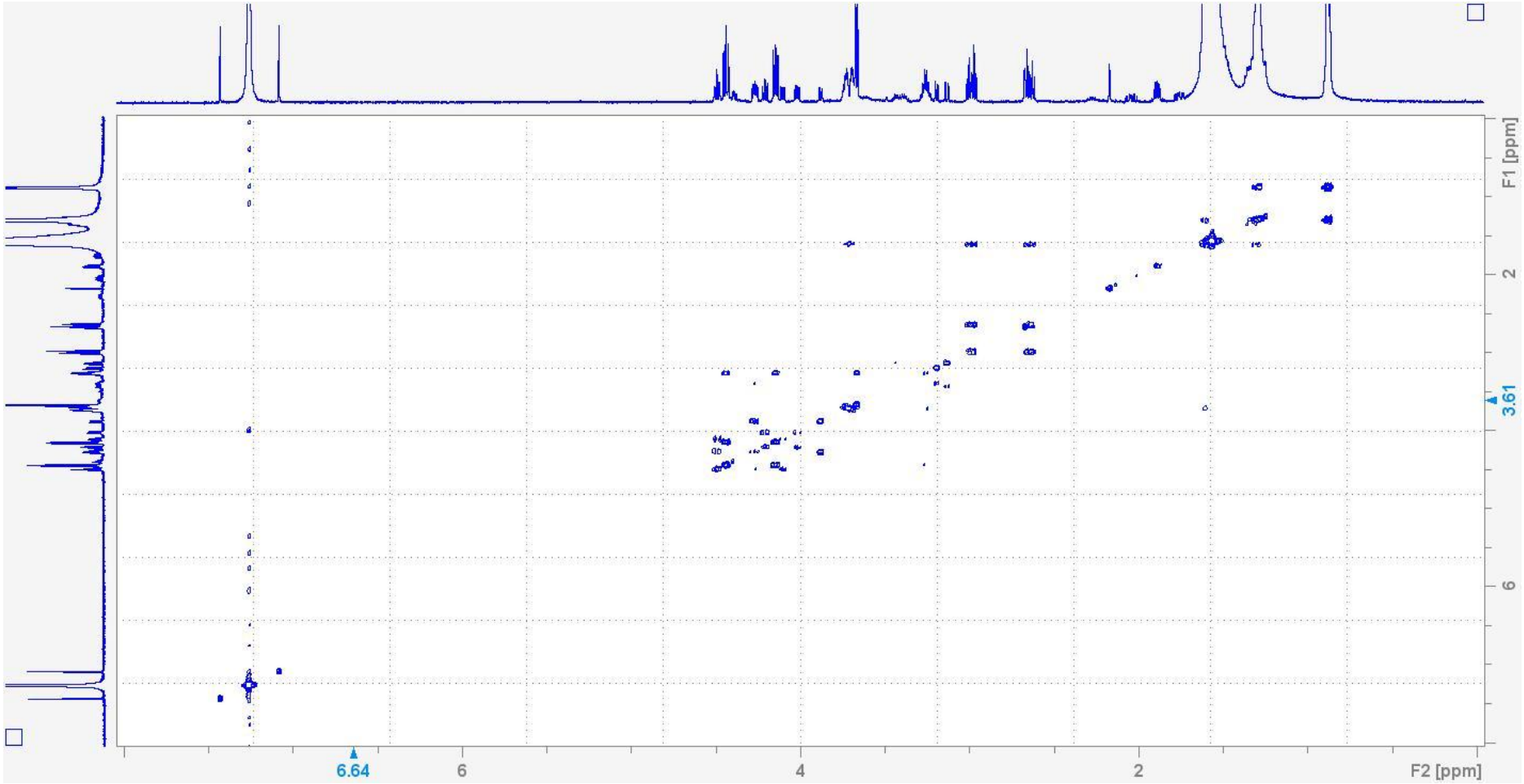

Figure S97. The gradient COSY (600 MHz, $CDCl_3$) spectrum of synthesized *n*-C-6 GBL (**10e**).

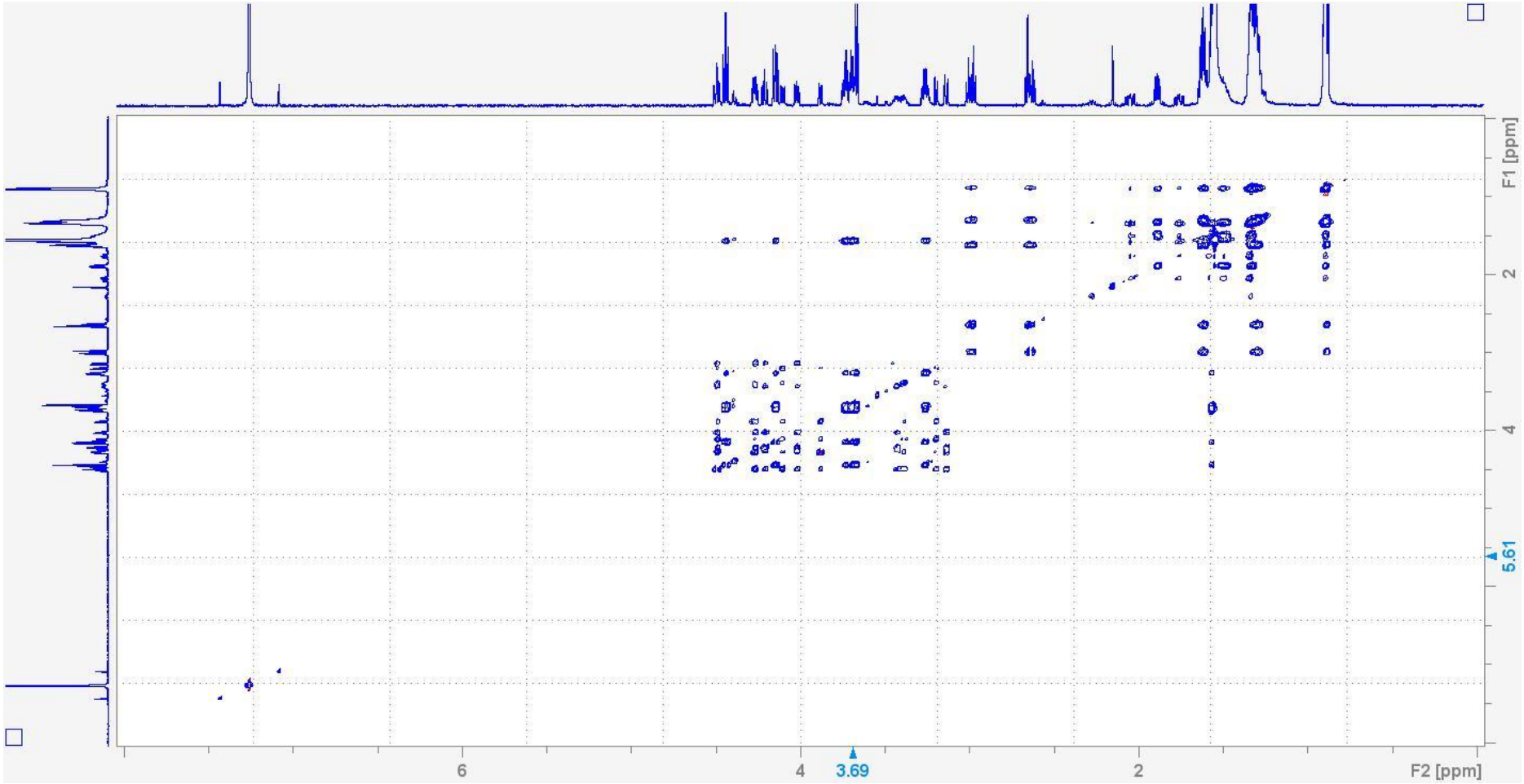

Figure S98. The TOCSY (600 MHz, $CDCl_3$) spectrum of synthesized *n*-C-6 GBL (**10e**).

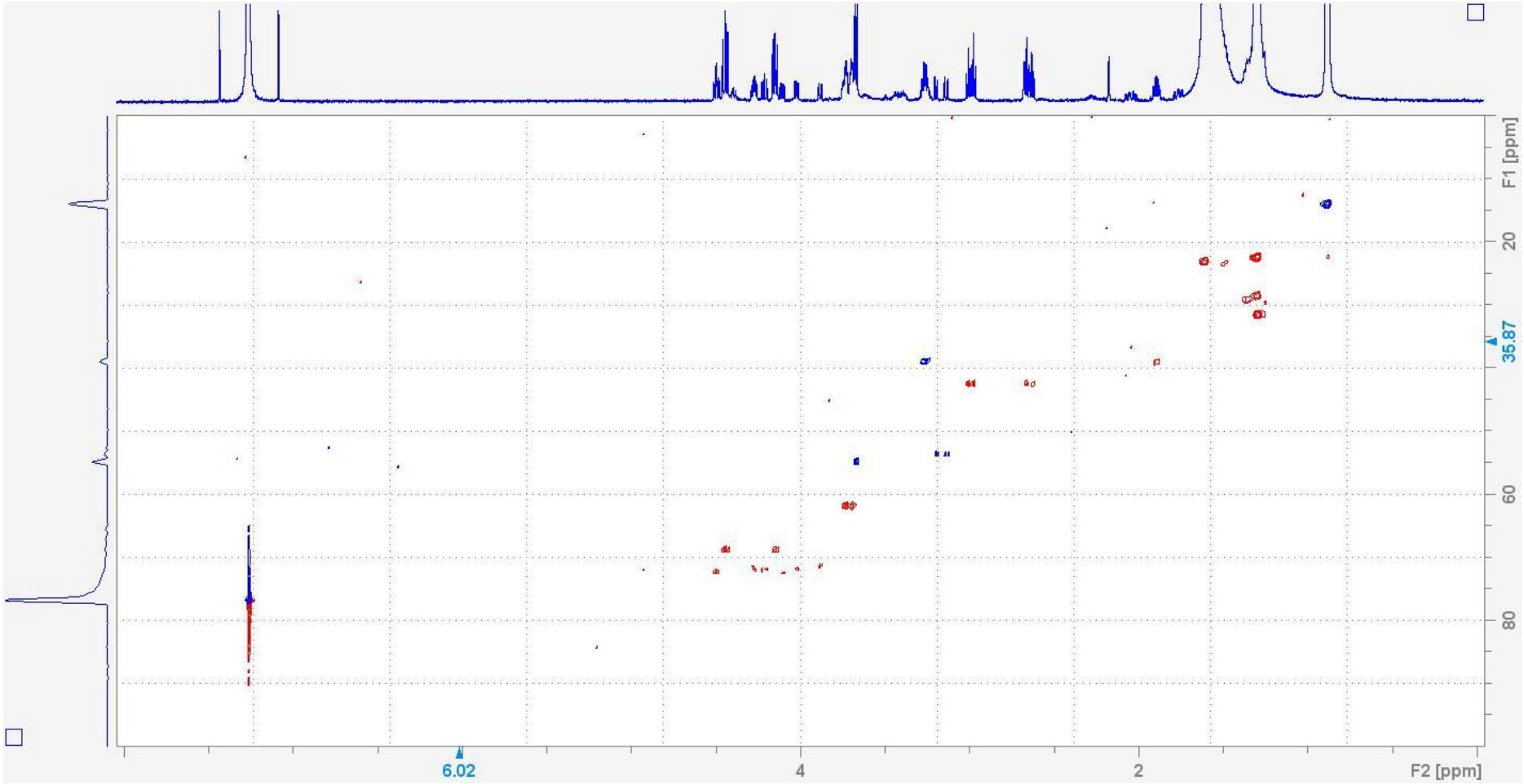

Figure S99. The gradient HSQC (600 MHz, $CDCl_3$) spectrum of synthesized *n*-C-6 GBL (**10e**).

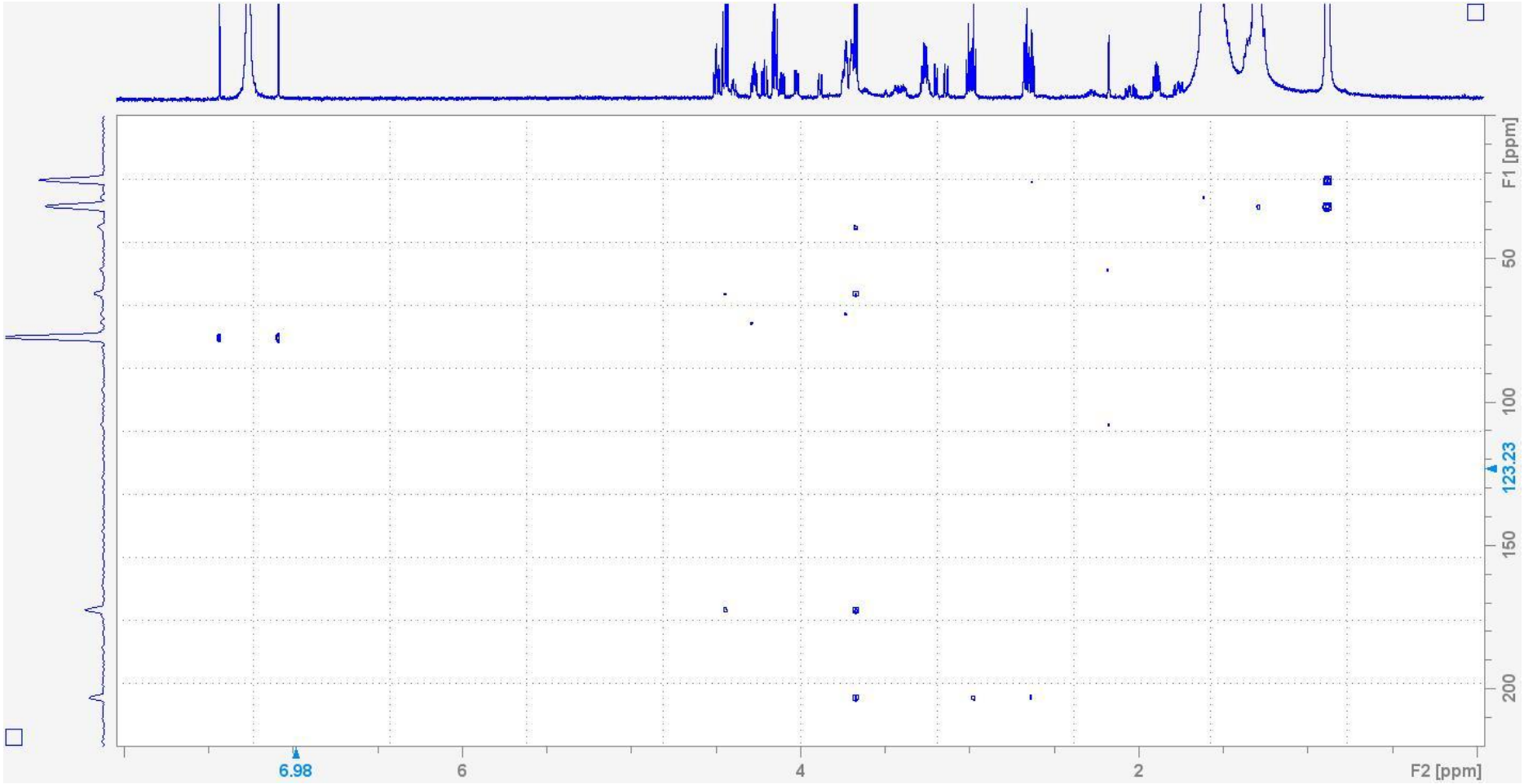

Figure S100. The gradient HMBC (600 MHz, $CDCl_3$) spectrum of synthesized *n*-C-6 GBL (**10e**).

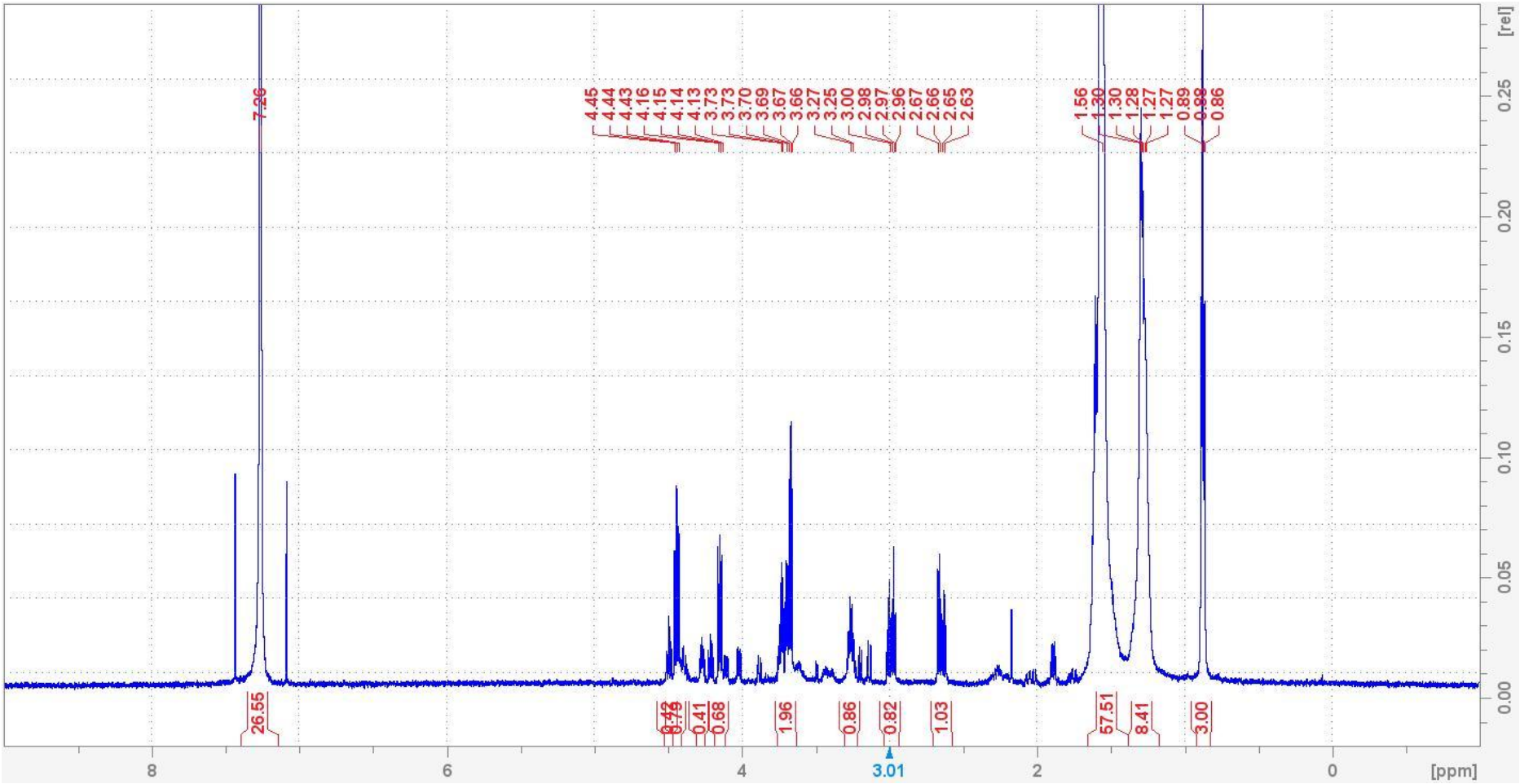

Figure S101. ^{1}H NMR (600 MHz, $CDCl_3$) spectrum of synthesized *n*-C-7 GBL (**10f**).

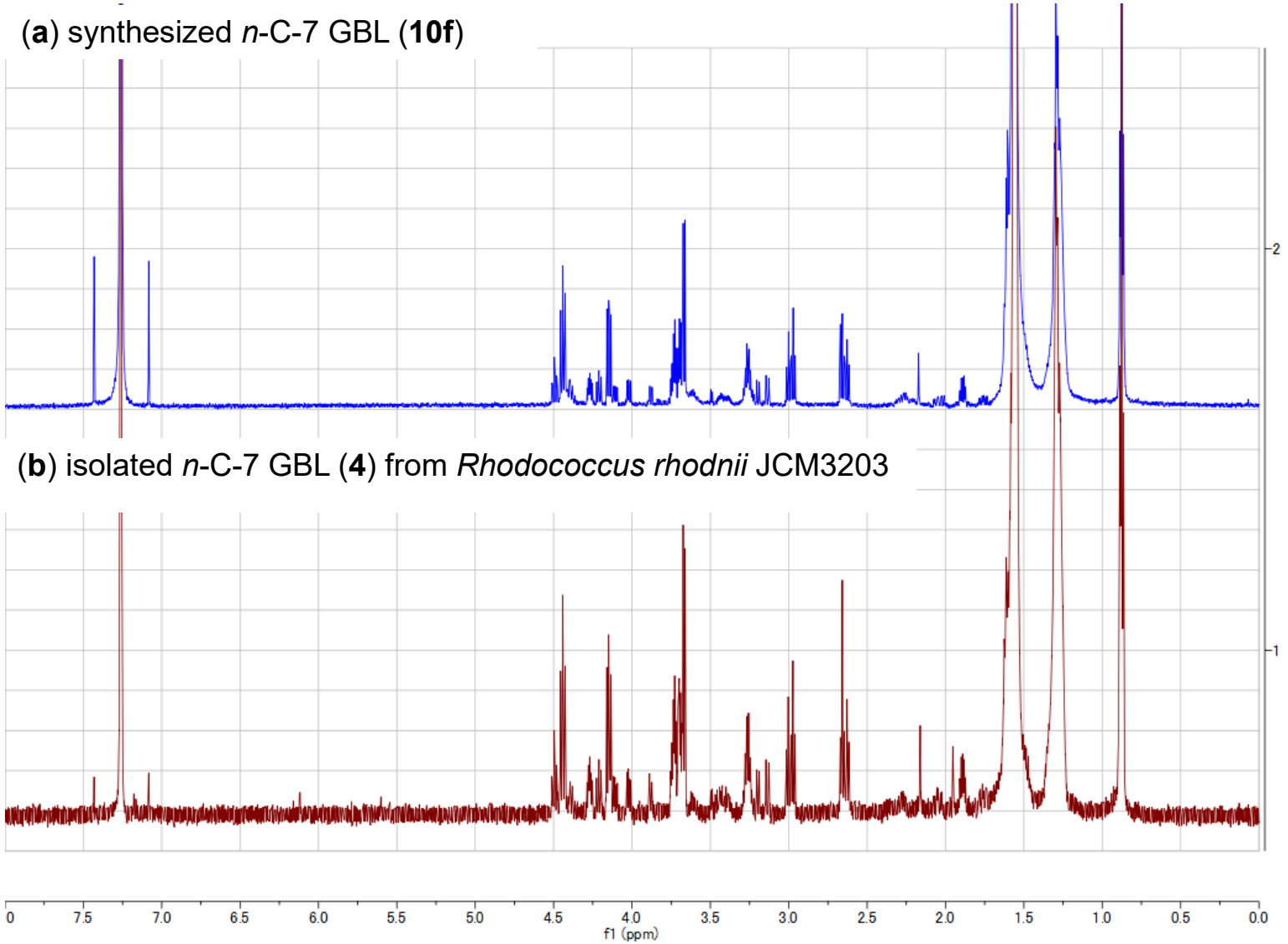

Figure S102. Comparison of ^{1}H NMR (600 MHz, $CDCl_3$) spectra of synthesized *n*-C-7 GBL (**10f**) and isolated natural *n*-C-7 GBL (**4**).

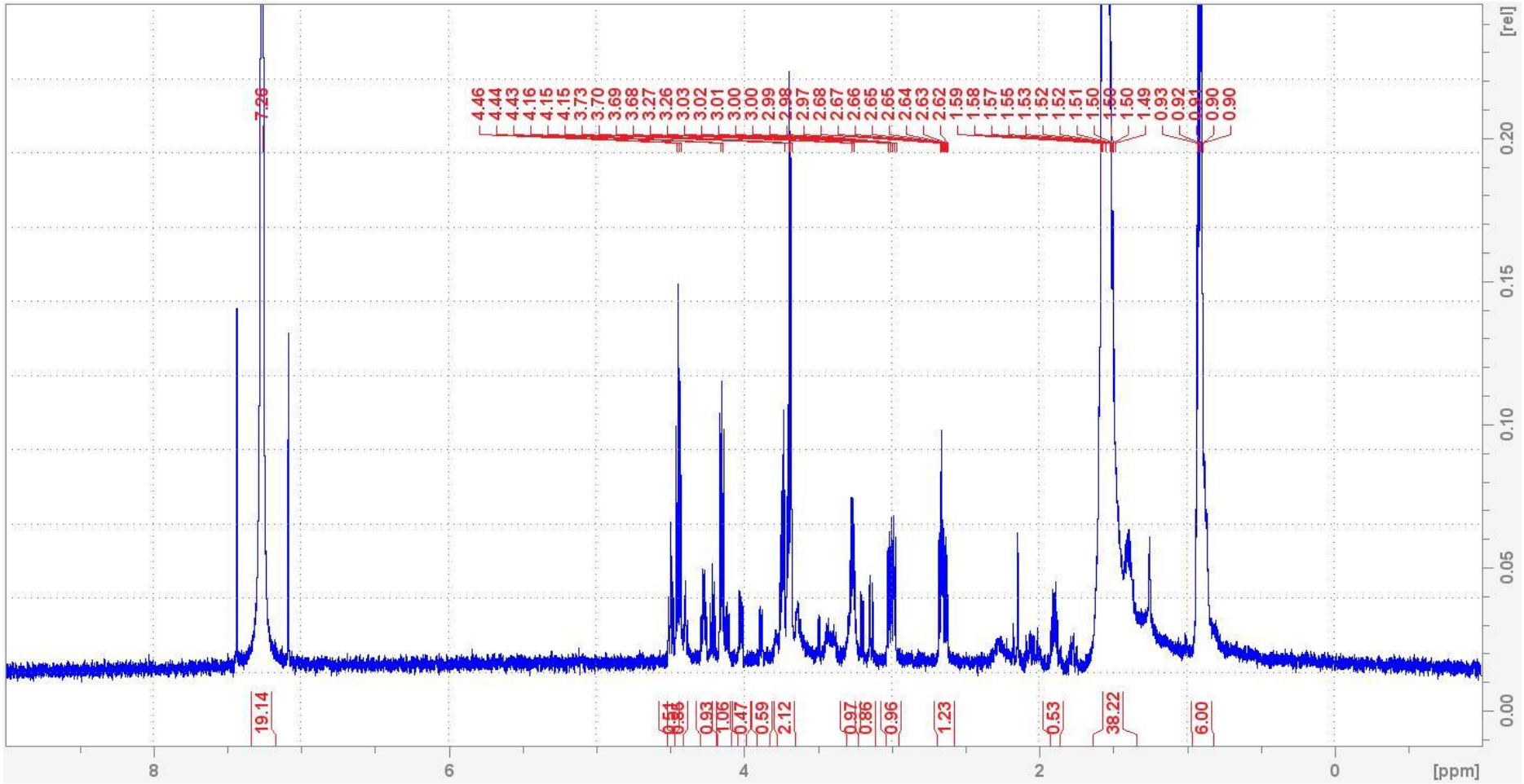

Figure S103. ^{1}H NMR (600 MHz, $CDCl_3$) spectrum of synthesized *iso*-C-5 GBL (**10k**).

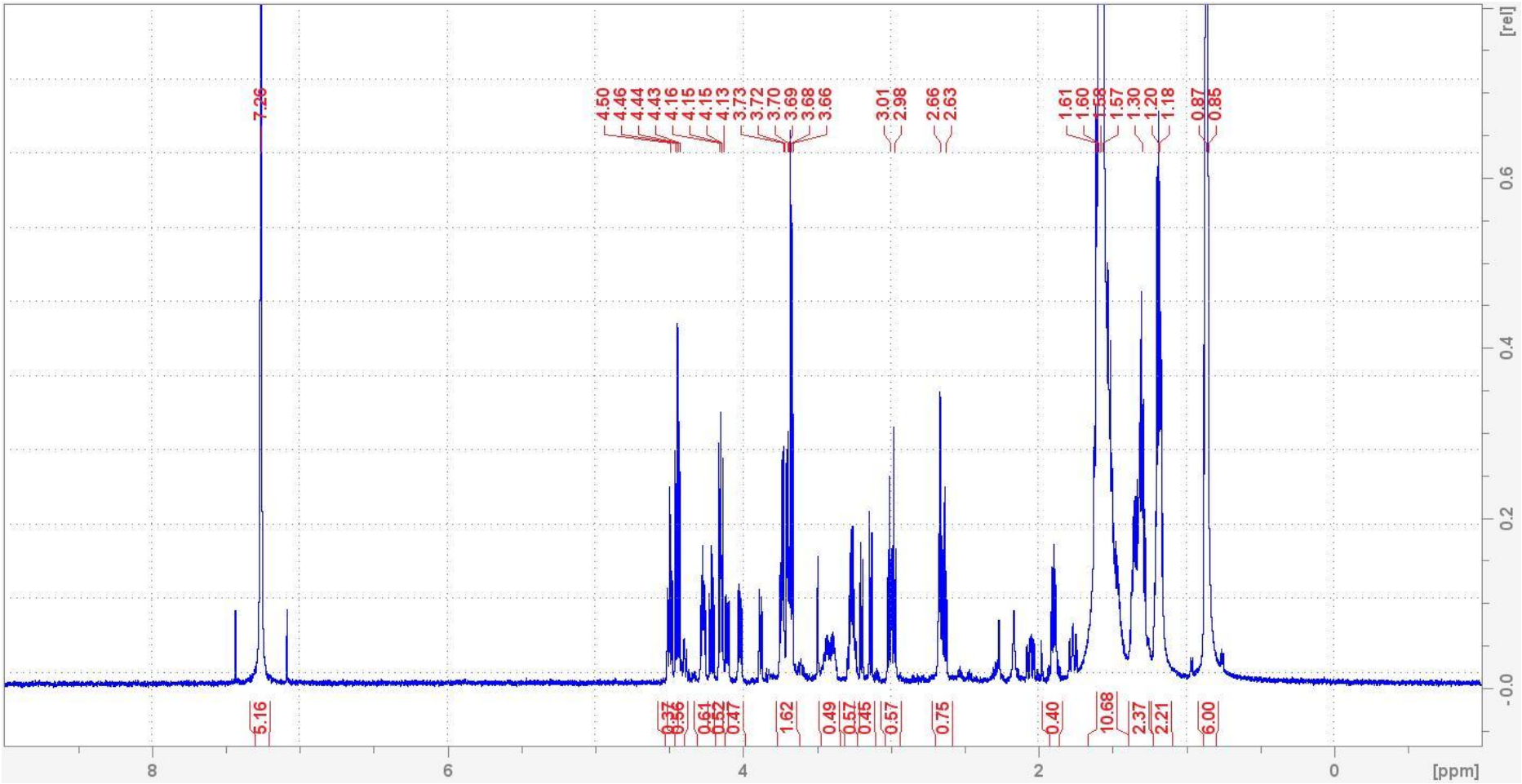

Figure S104. ^{1}H NMR (600 MHz, $CDCl_3$) spectrum of synthesized *iso*-C-7 GBL (**10l**).

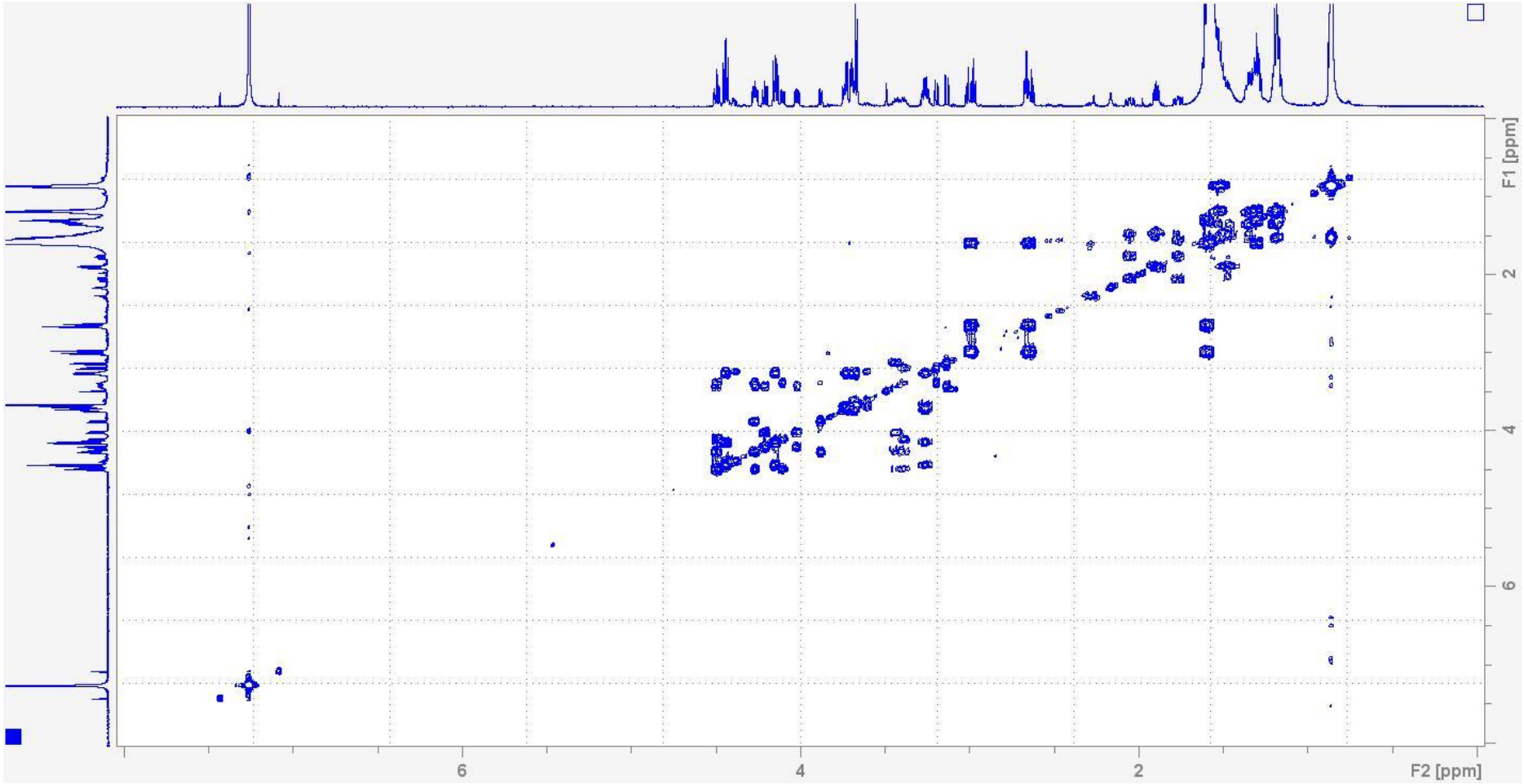

Figure S105. The gradient COSY (600 MHz, $CDCl_3$) spectrum of synthesized *iso*-C-7 GBL (**10l**).

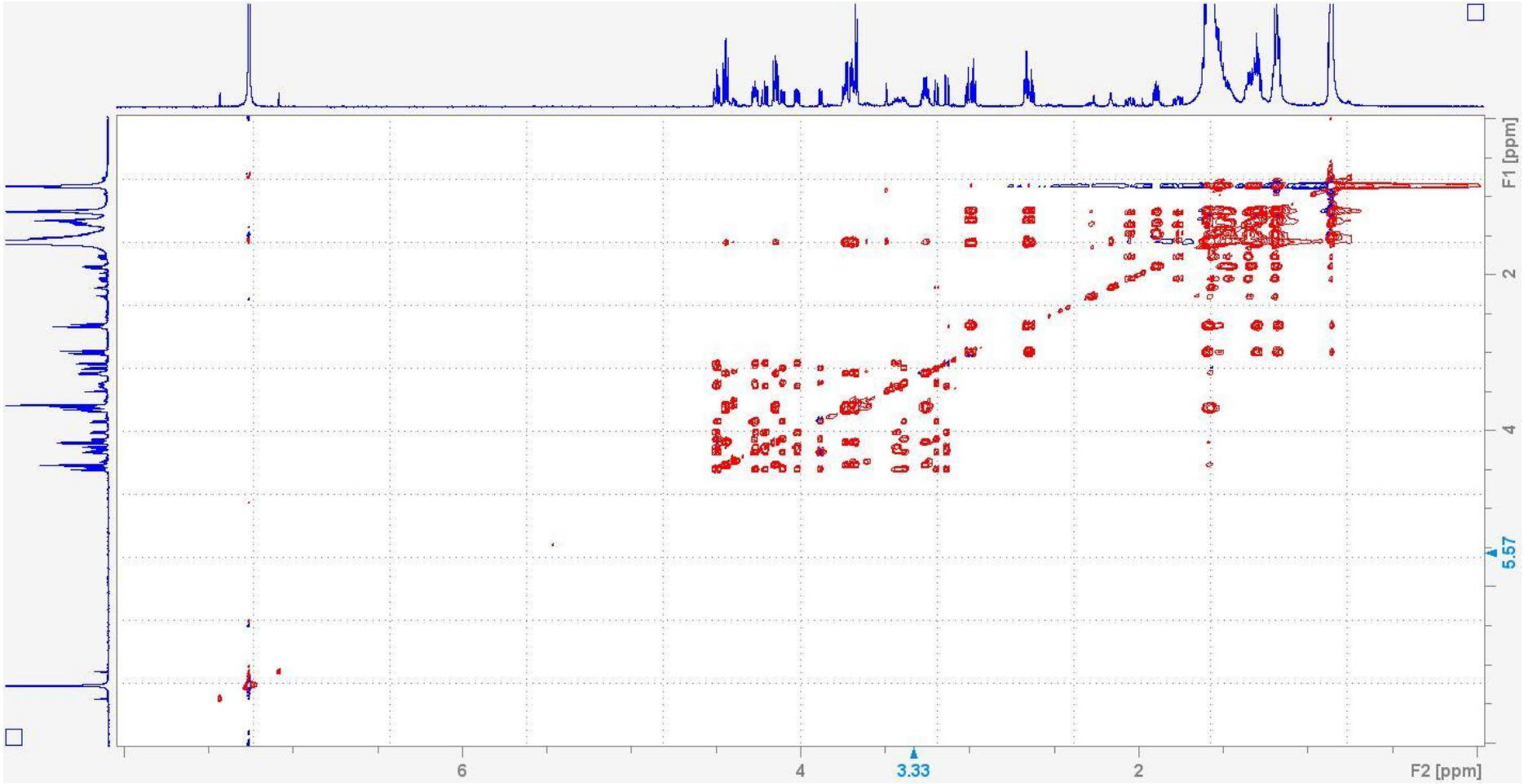

Figure S106. The TOCSY (600 MHz, $CDCl_3$) spectrum of synthesized *iso*-C-7 GBL (**10l**).

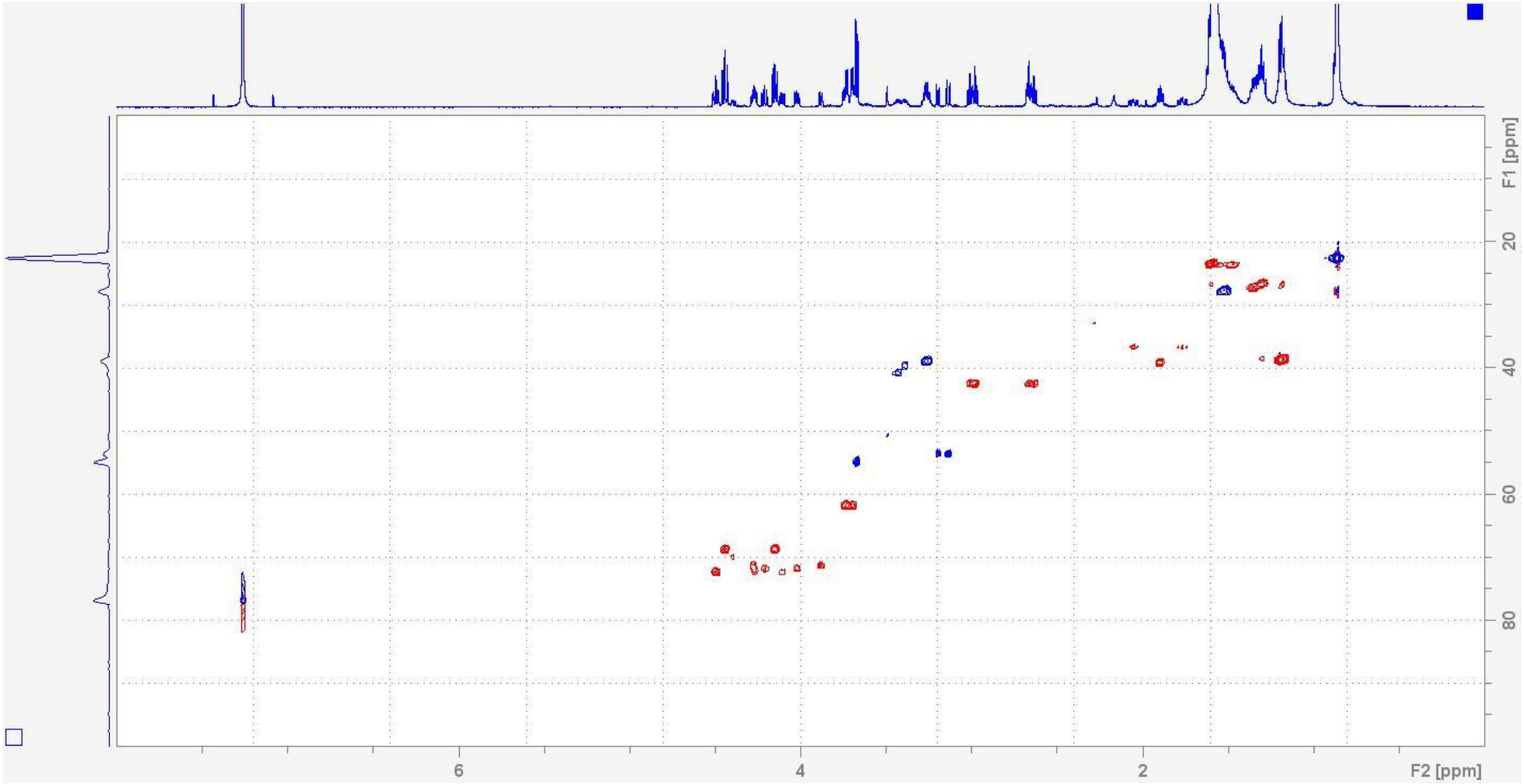

Figure S107. The gradient HSQC (600 MHz, $CDCl_3$) spectrum of synthesized *iso*-C-7 GBL (**10l**).

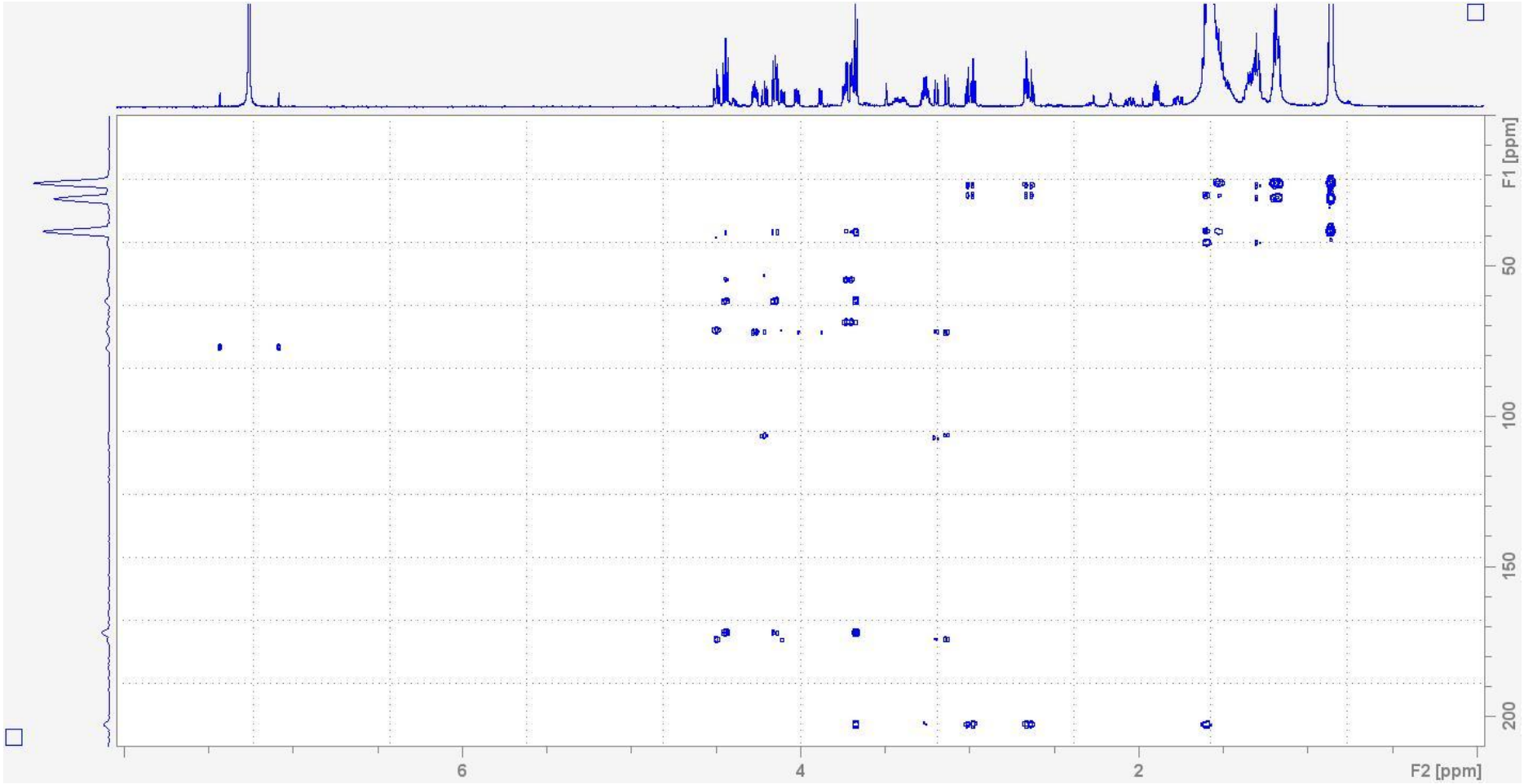

Figure S108. The gradient HMBC (600 MHz, $CDCl_3$) spectrum of synthesized *iso*-C-7 GBL (**10l**).

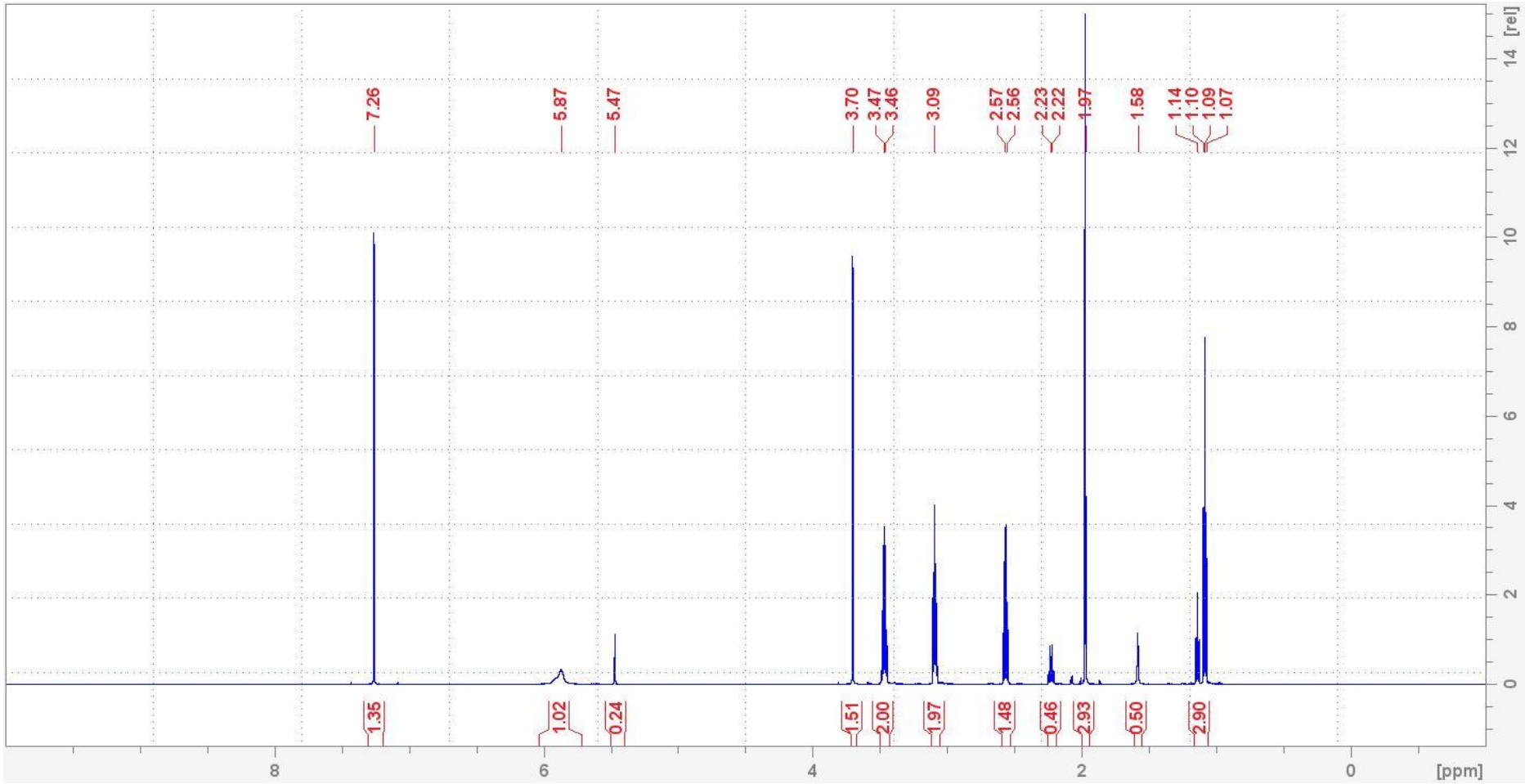

Figure S109. ^{1}H NMR (600 MHz, $CDCl_3$) spectrum of synthesized β-keto pentanoyl SNAC (*n*-C-2 β-ketoacyl SNAC, **6a**).

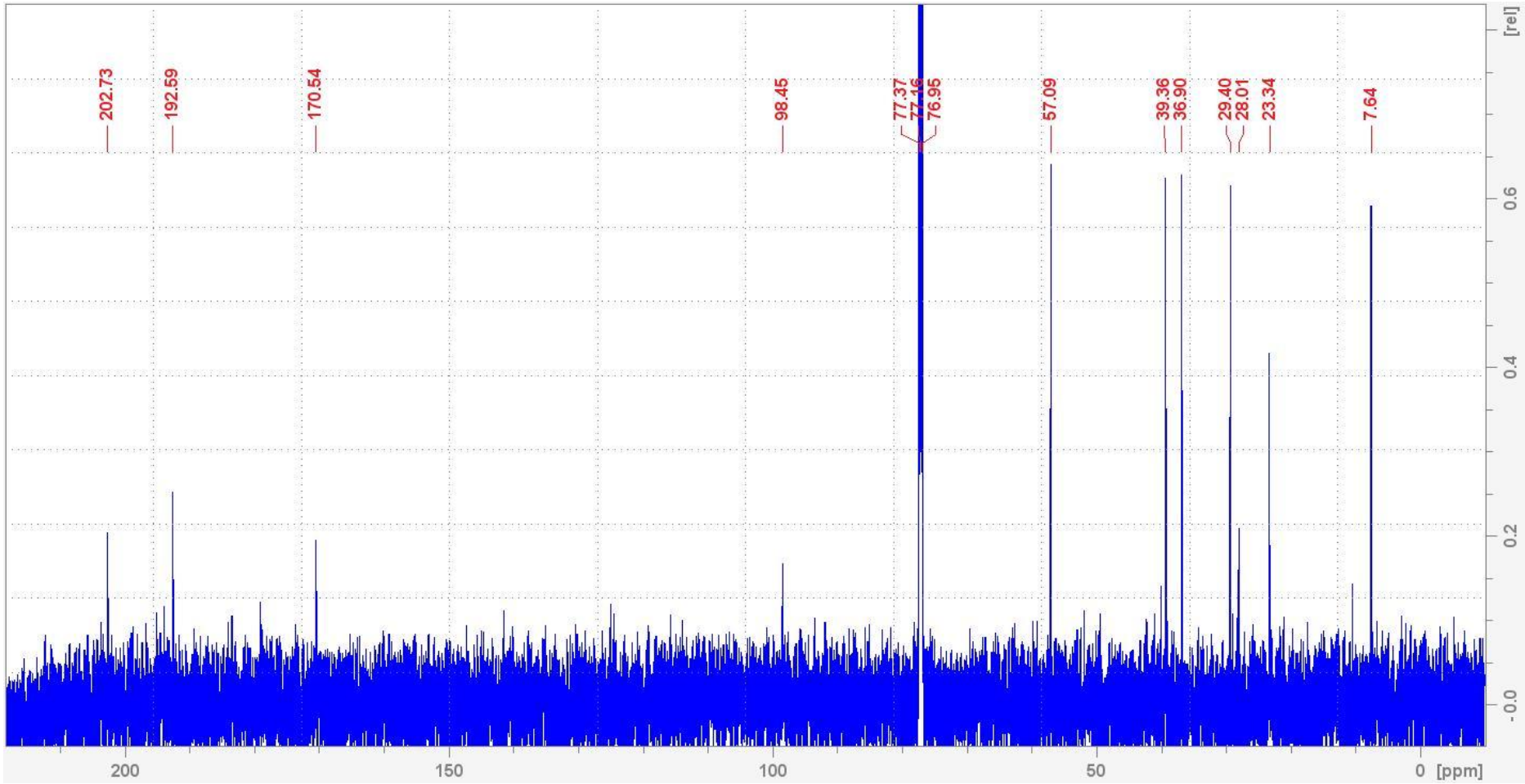

Figure S110. ^{13}C NMR (151 MHz, $CDCl_3$) spectrum of synthesized β-keto pentanoyl SNAC (*n*-C-2 β-ketoacyl SNAC, **6a**).

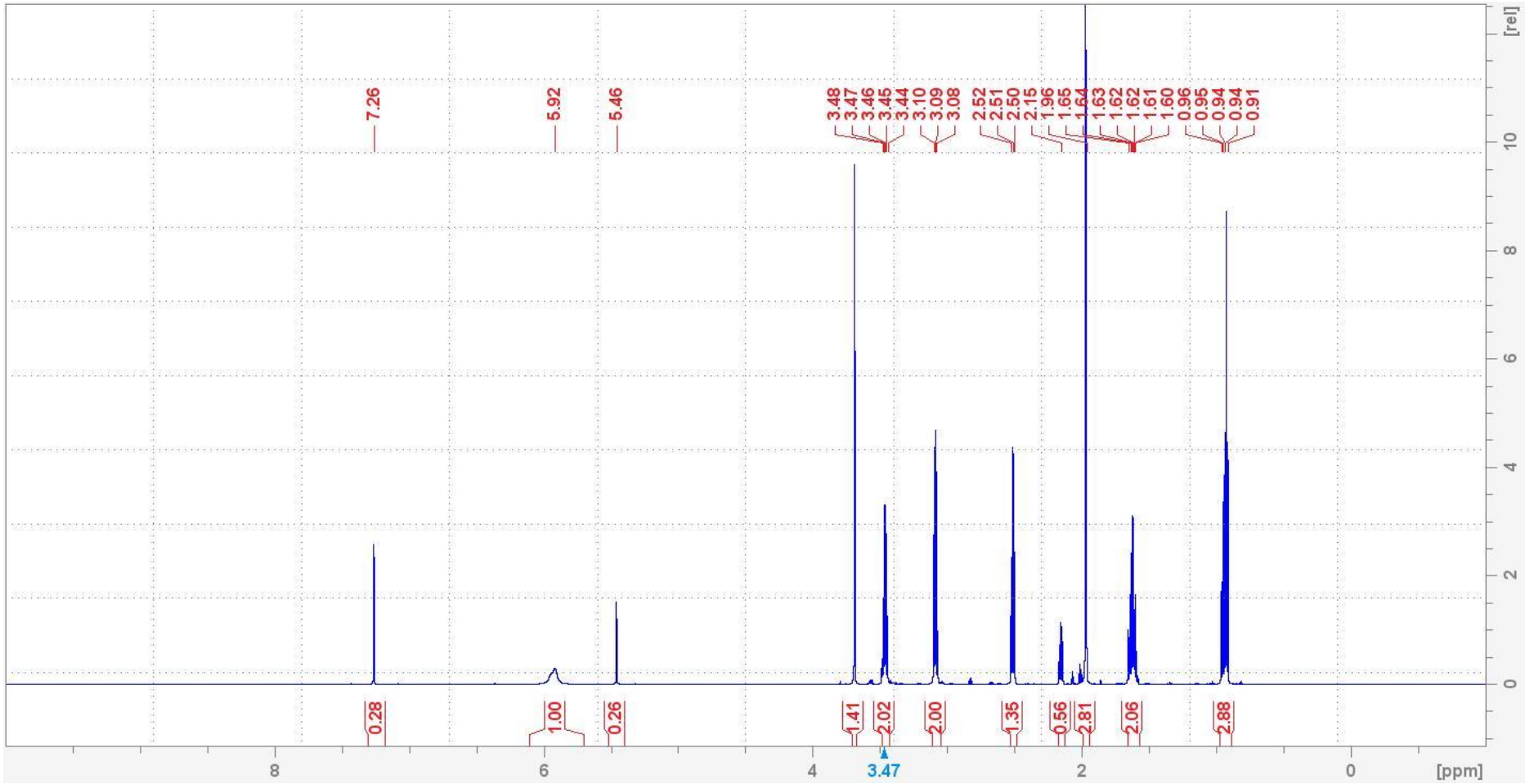

Figure S111. ^{1}H NMR (600 MHz, $CDCl_3$) spectrum of synthesized β-keto hexanoyl SNAC (*n*-C-3 β-ketoacyl SNAC, **6b**).

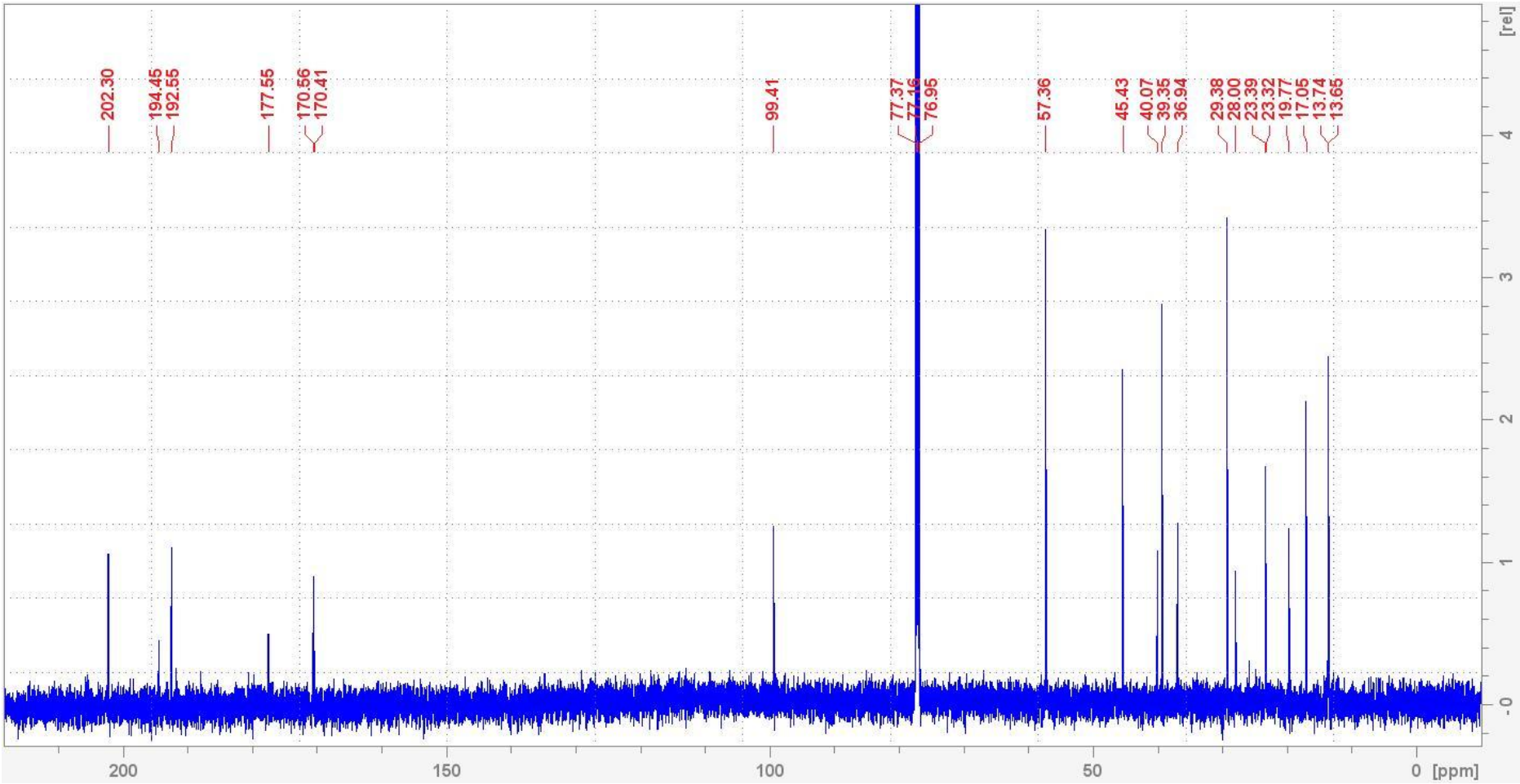

Figure S112. ^{13}C NMR (151 MHz, $CDCl_3$) spectrum of synthesized β-keto hexanoyl SNAC (*n*-C-3 β-ketoacyl SNAC, **6b**).

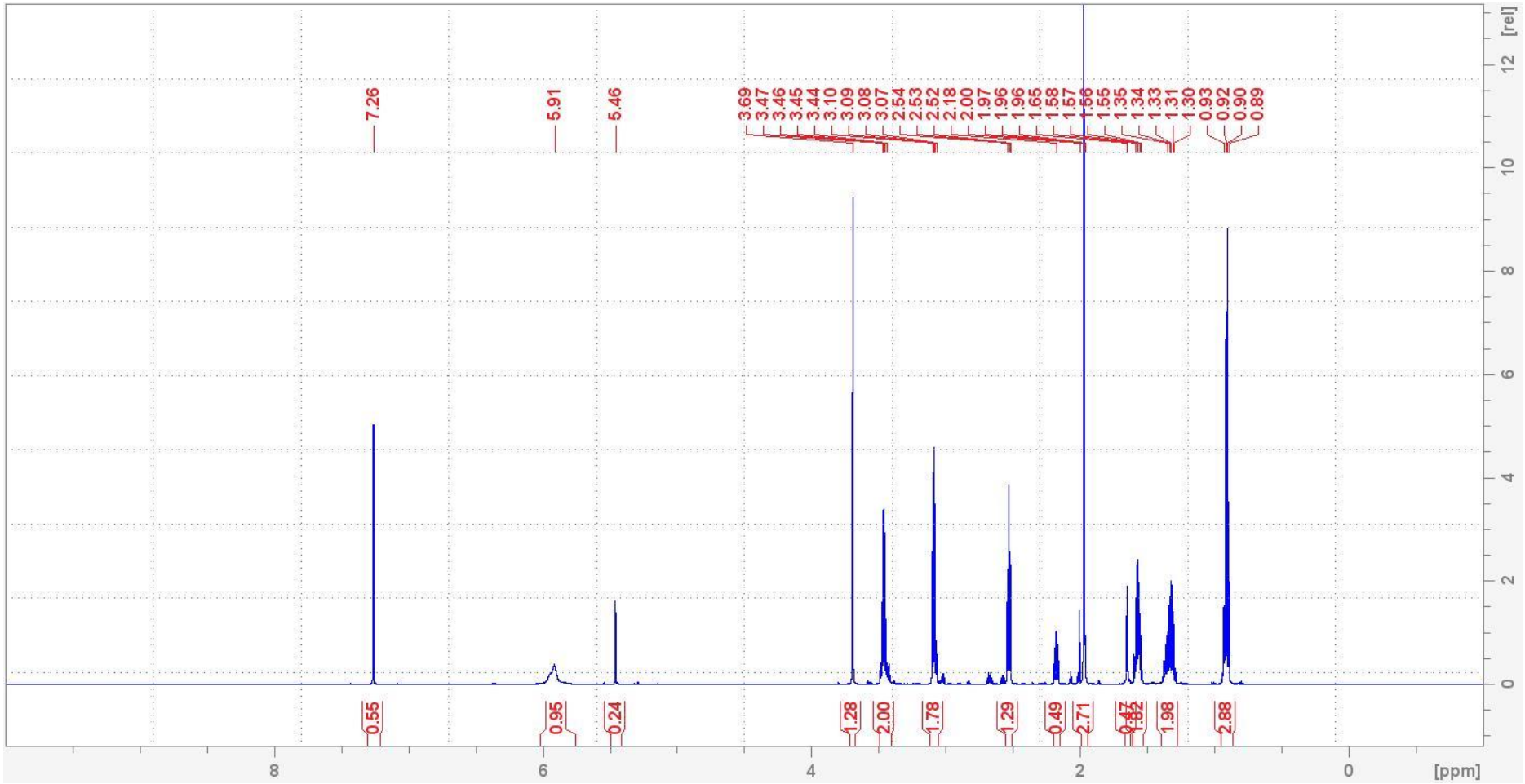

Figure S113. ^{1}H NMR (600 MHz, $CDCl_3$) spectrum of synthesized β-keto heptanoyl SNAC (*n*-C-4 β-ketoacyl SNAC, **6c**).

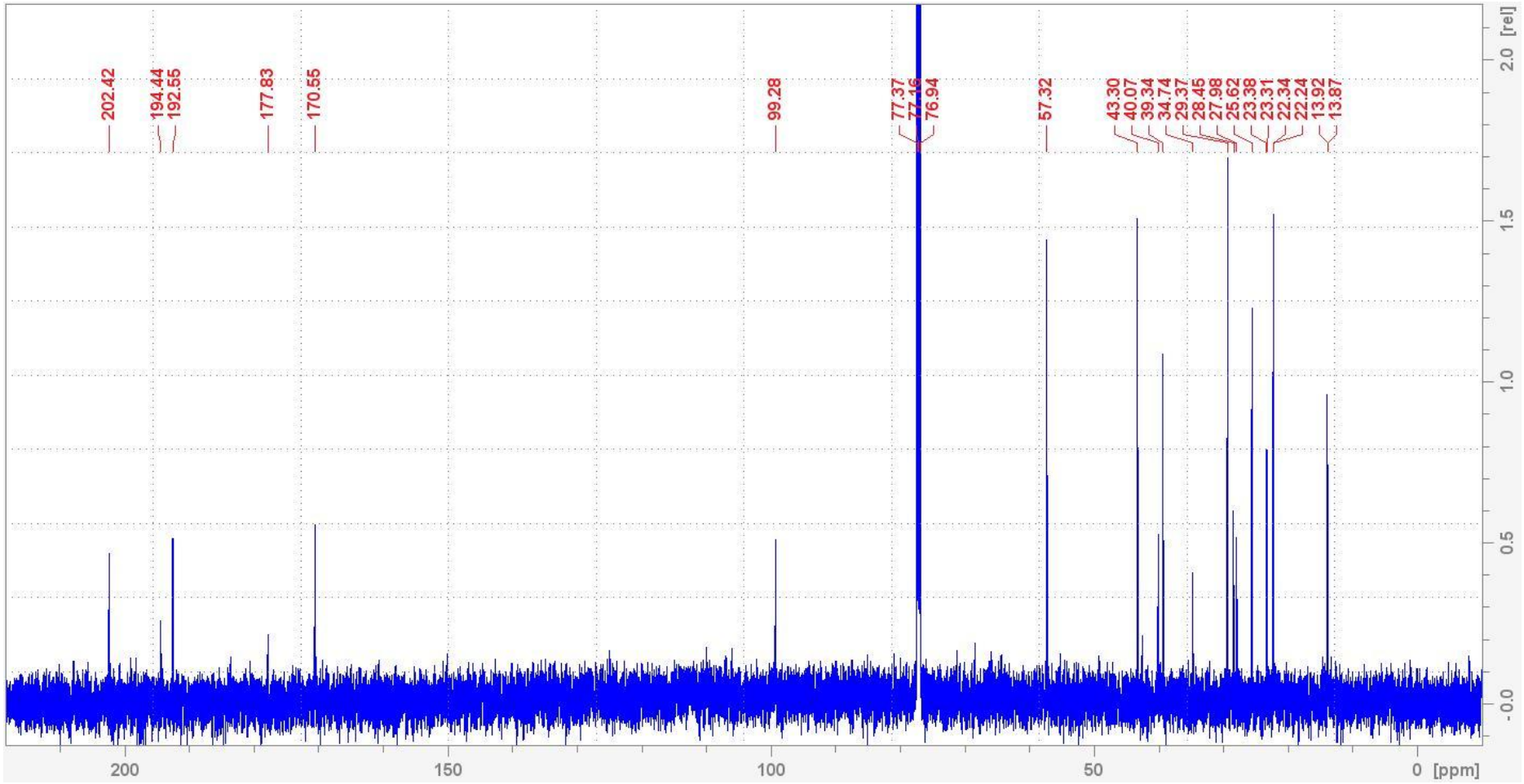

Figure S114. ^{13}C NMR (151 MHz, $CDCl_3$) spectrum of synthesized β-keto heptanoyl SNAC (*n*-C-4 β-ketoacyl SNAC, **6c**).

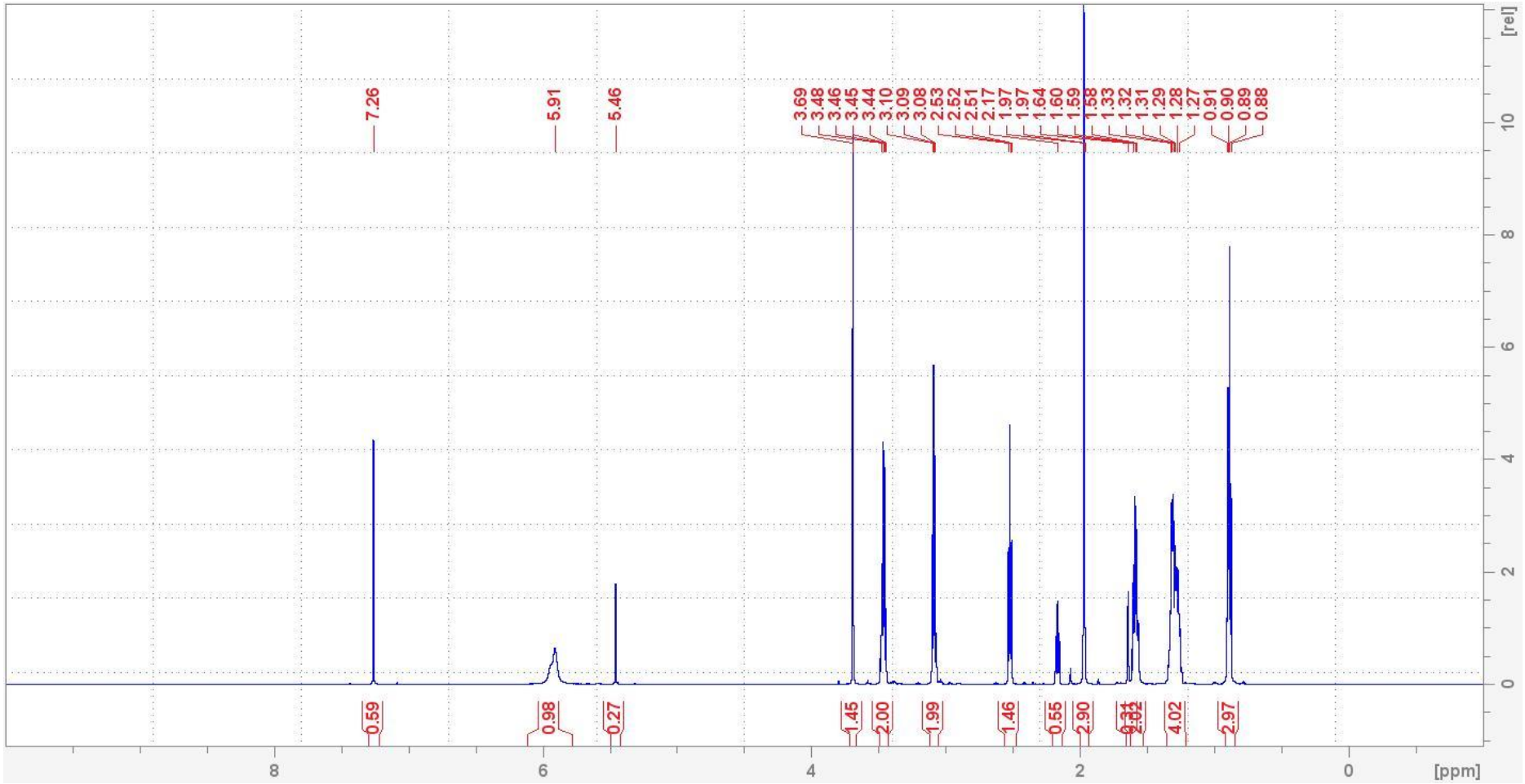

Figure S115. ^{1}H NMR (600 MHz, $CDCl_3$) spectrum of synthesized β-keto octanoyl SNAC (*n*-C-5 β-ketoacyl SNAC, **6d**).

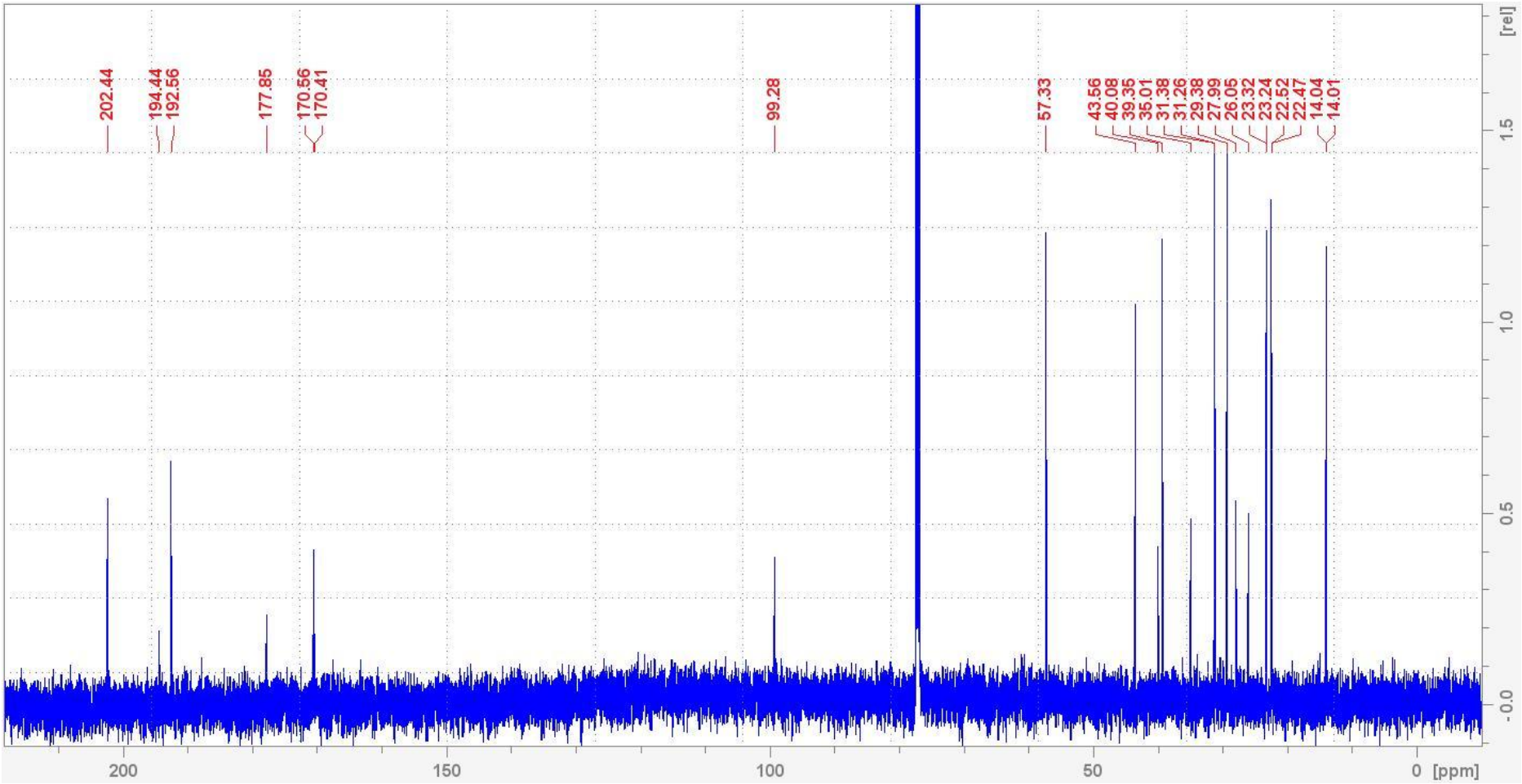

Figure S116. ^{13}C NMR (151 MHz, $CDCl_3$) spectrum of synthesized β-keto octanoyl SNAC (*n*-C-5 β-ketoacyl SNAC, **6d**).

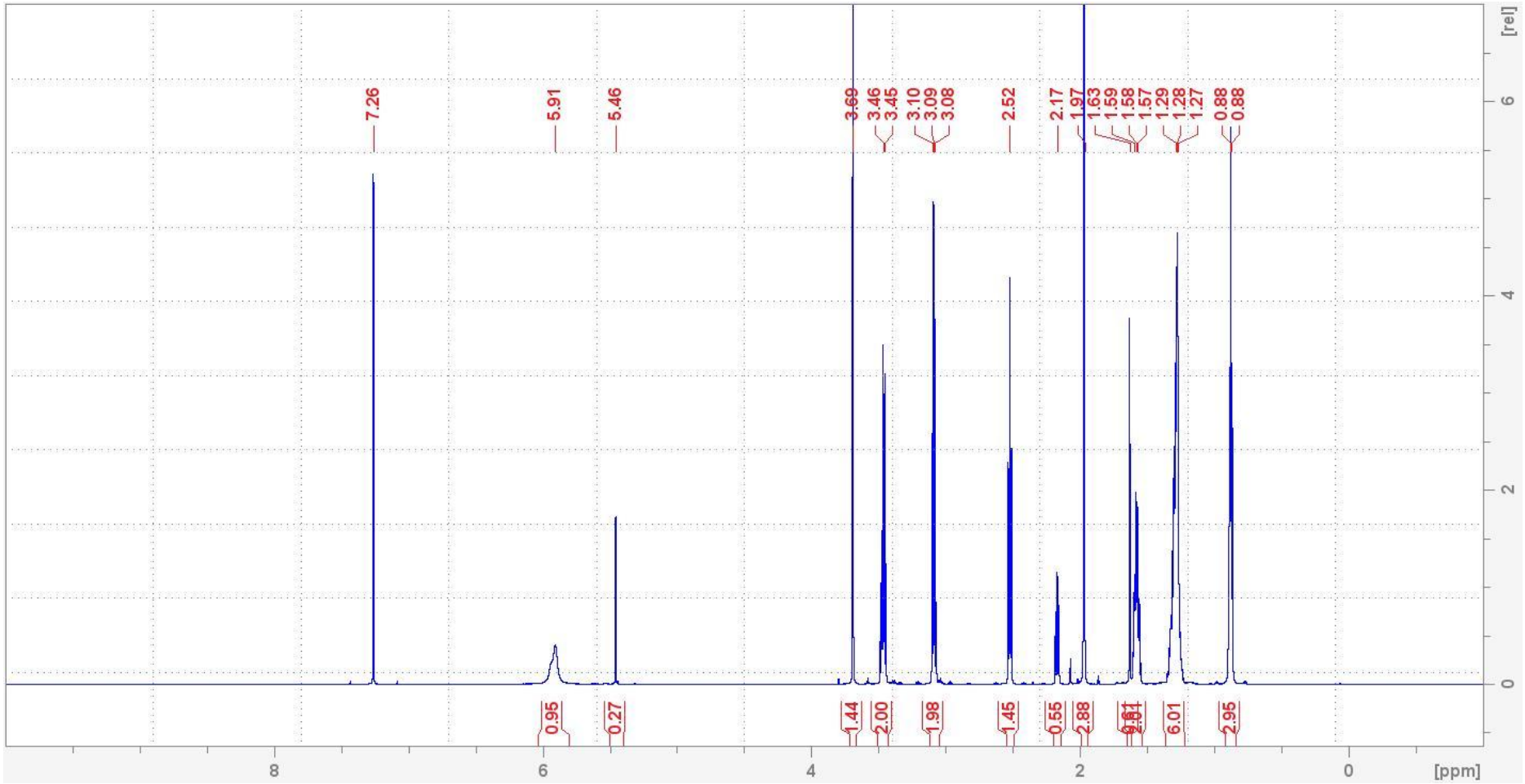

Figure S117. ^{1}H NMR (600 MHz, $CDCl_3$) spectrum of synthesized β-keto nonanoyl SNAC (*n*-C-6 β-ketoacyl SNAC, **6e**).

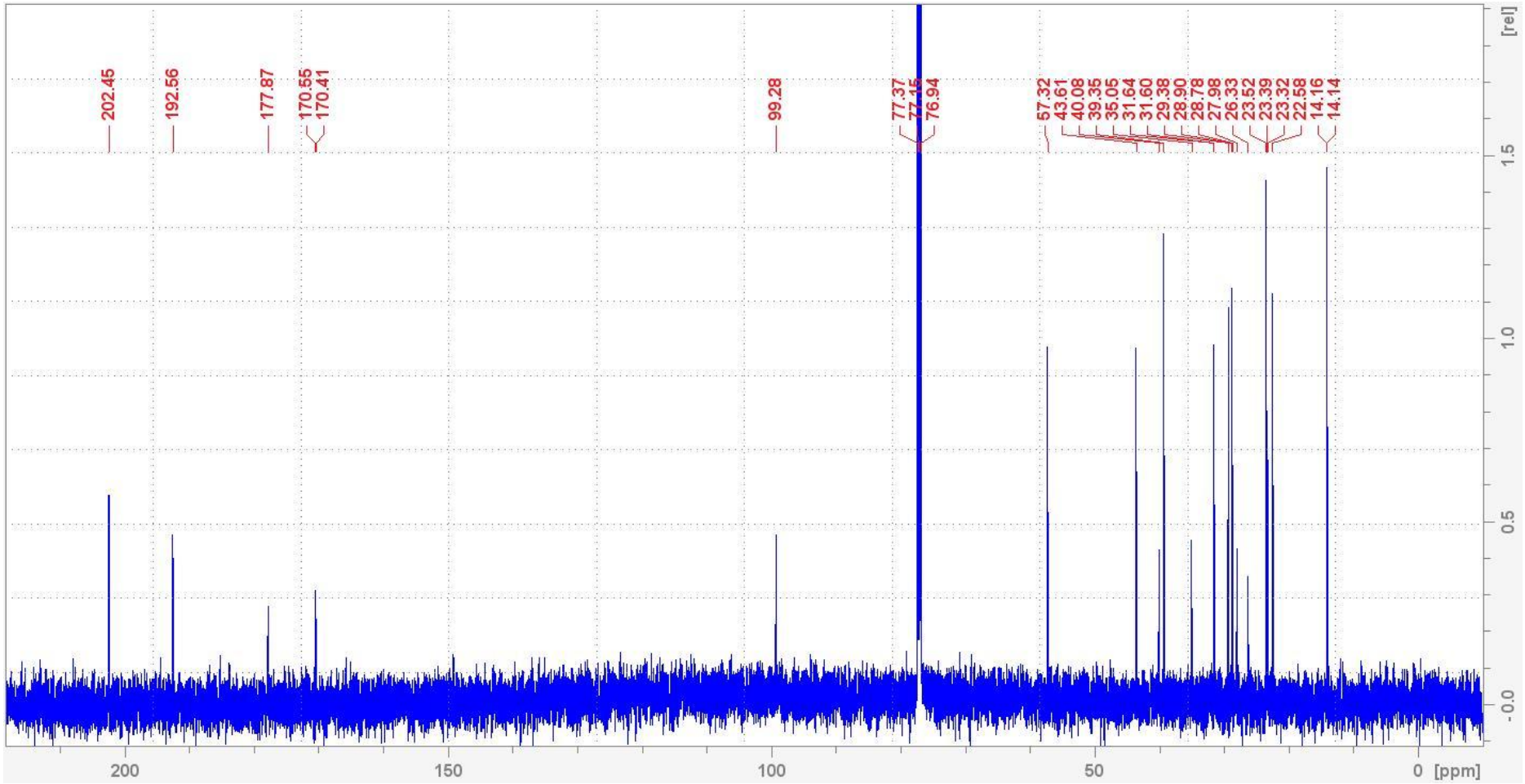

Figure S118. ^{13}C NMR (151 MHz, $CDCl_3$) spectrum of synthesized β-keto nonanoyl SNAC (*n*-C-6 β-ketoacyl SNAC, **6e**).

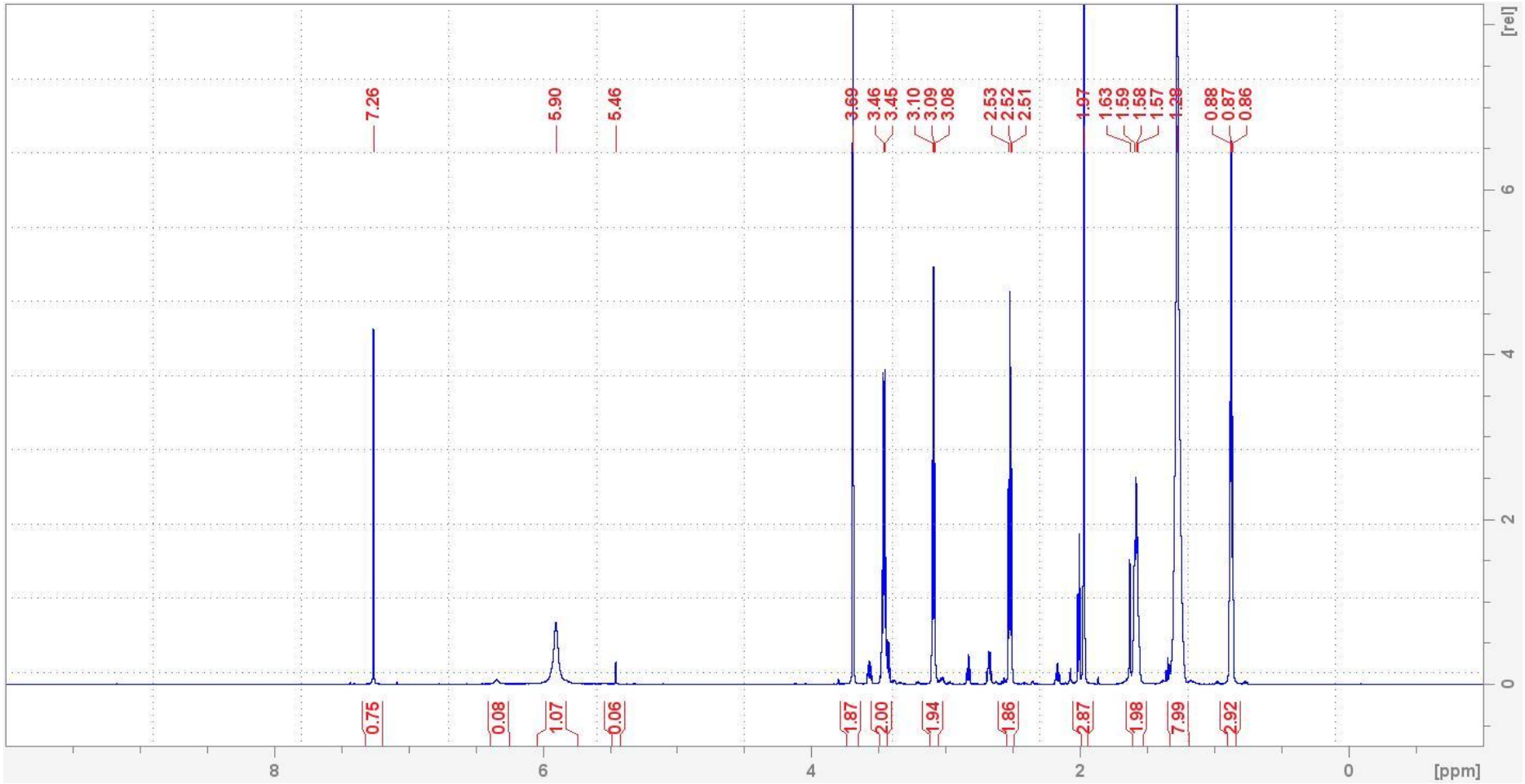

Figure S119. ^{1}H NMR (600 MHz, $CDCl_3$) spectrum of synthesized β-keto decanoyl SNAC (*n*-C-7 β-ketoacyl SNAC, **6f**).

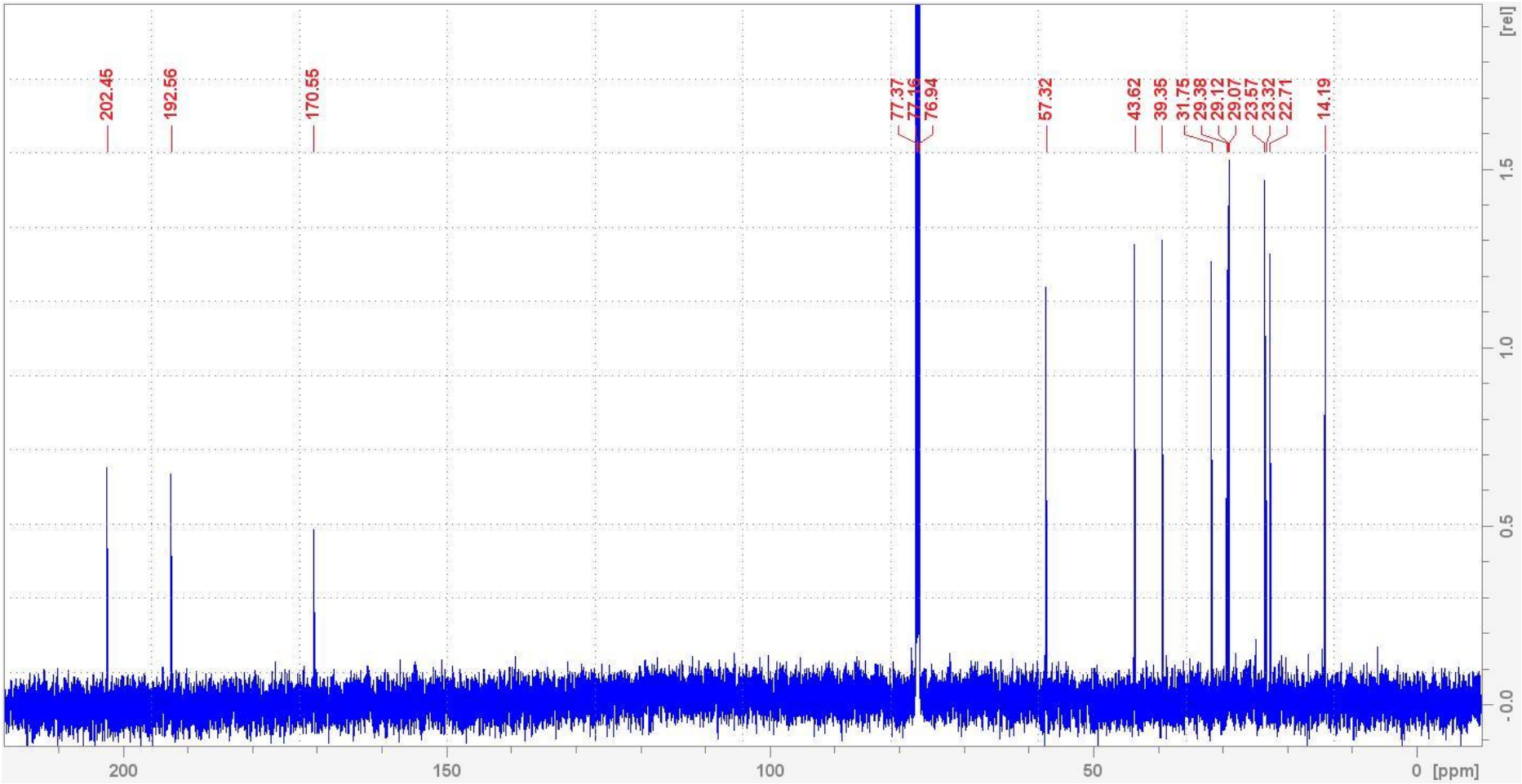

Figure S120. ^{13}C NMR (151 MHz, $CDCl_3$) spectrum of synthesized β-keto decanoyl SNAC (*n*-C-7 β-ketoacyl SNAC, **6f**).

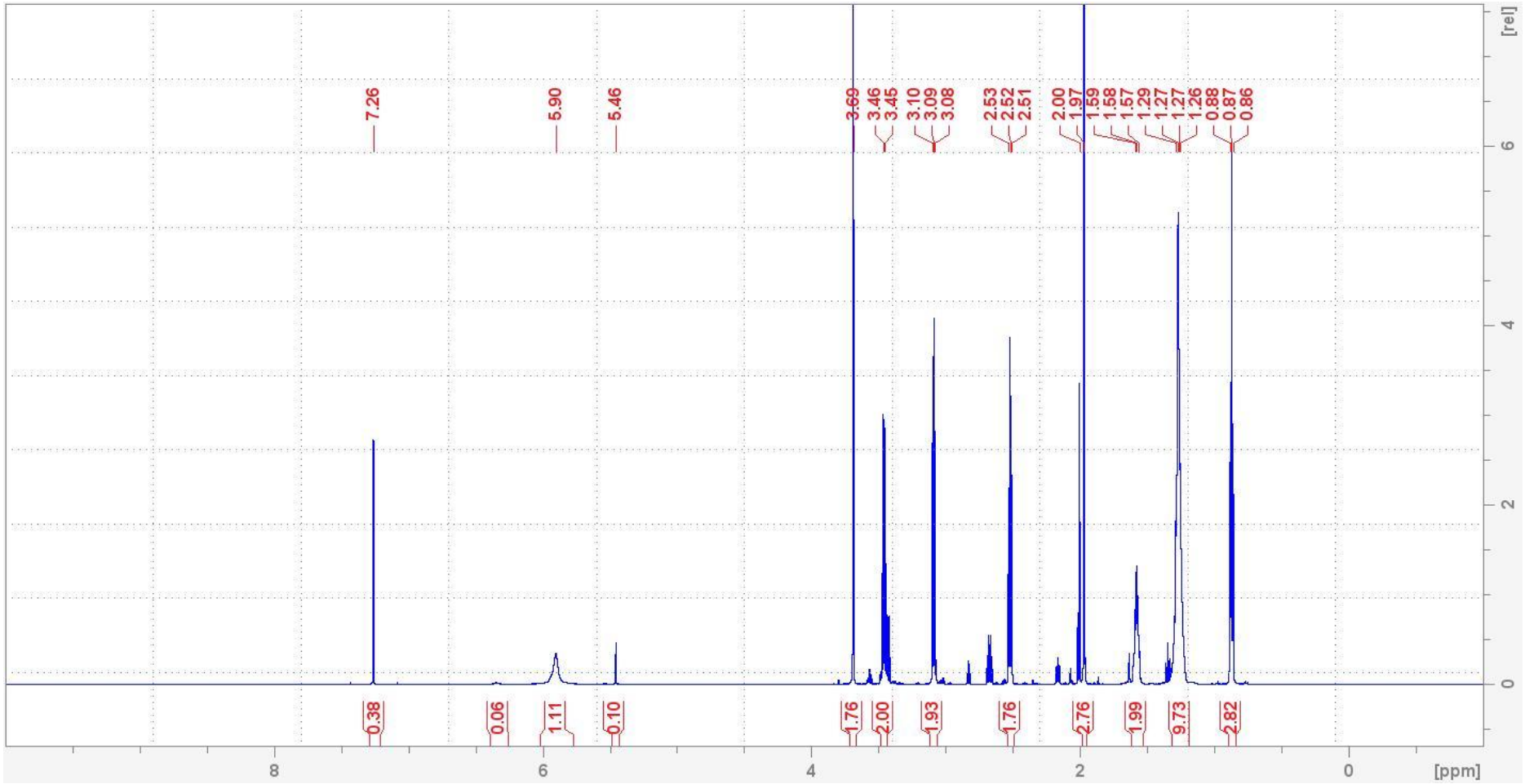

Figure S121. ^{1}H NMR (600 MHz, $CDCl_3$) spectrum of synthesized β-keto undecanoyl SNAC (*n*-C-8 β-ketoacyl SNAC, **6g**).

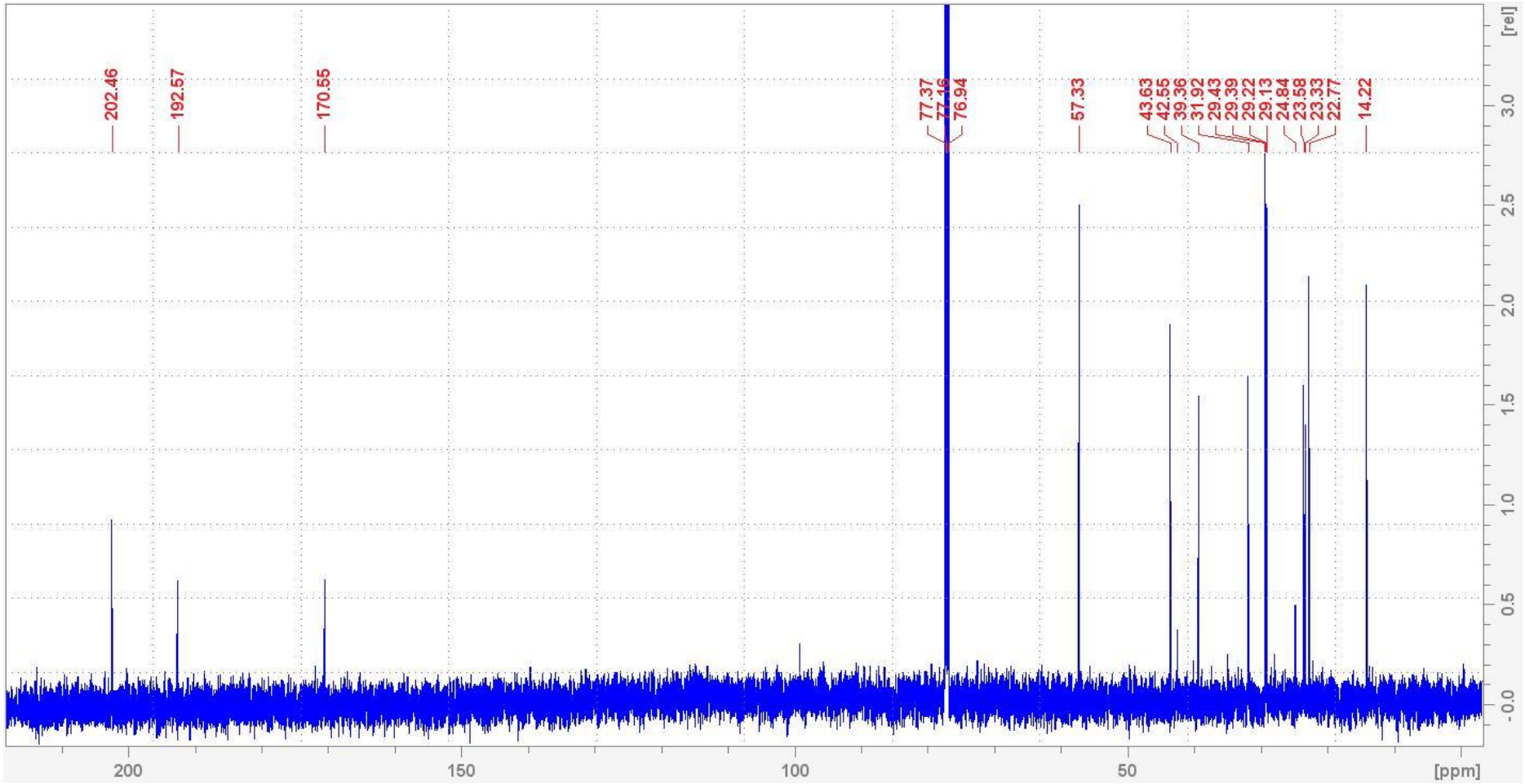

Figure S122. ^{13}C NMR (151 MHz, $CDCl_3$) spectrum of synthesized β-keto undecanoyl SNAC (*n*-C-8 β-ketoacyl SNAC, **6g**).

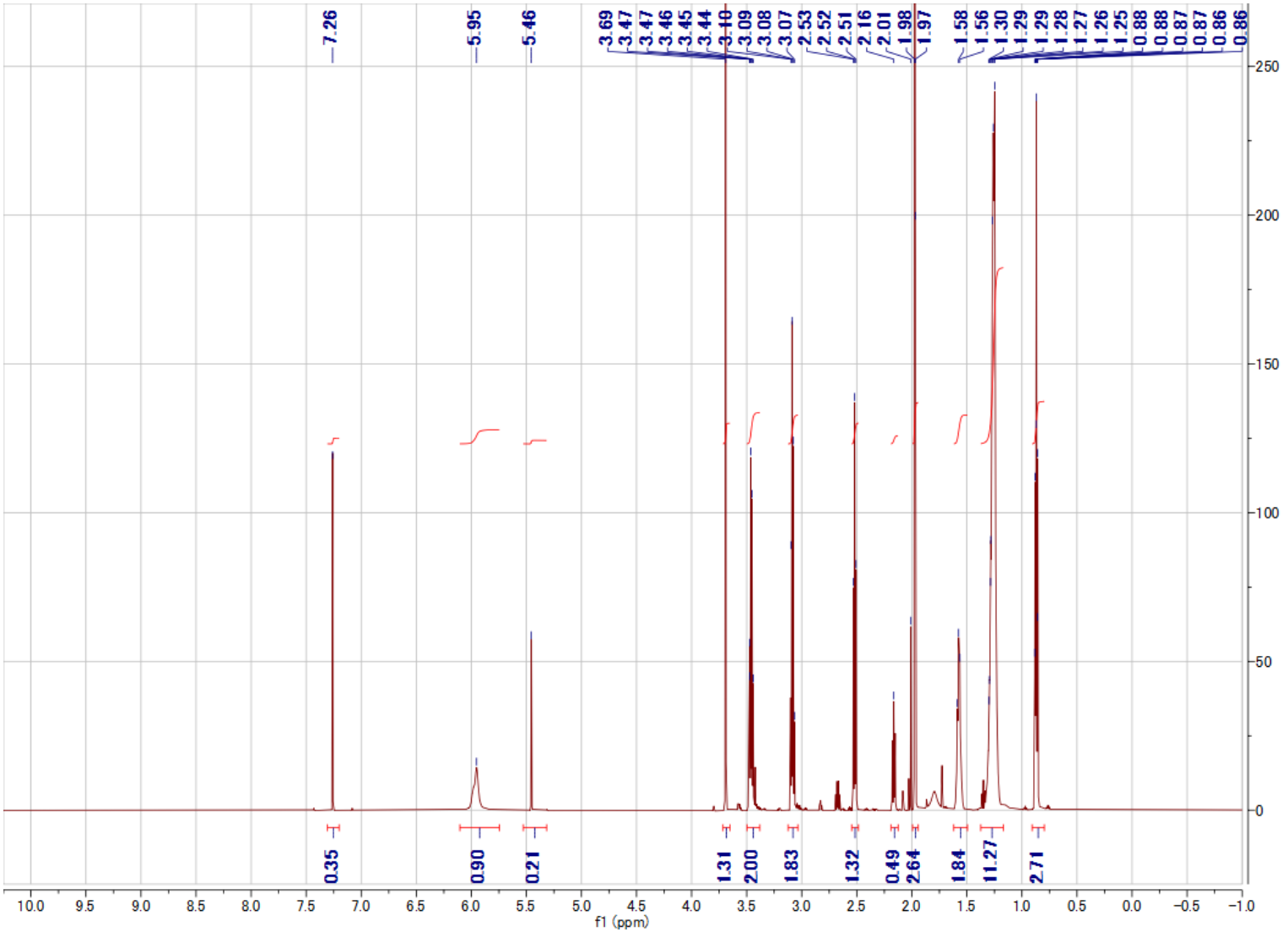

Figure S123. ^{1}H NMR (600 MHz, $CDCl_3$) spectrum of synthesized β-keto dodecanoyl SNAC (*n*-C-9 β-ketoacyl SNAC, **6h**).

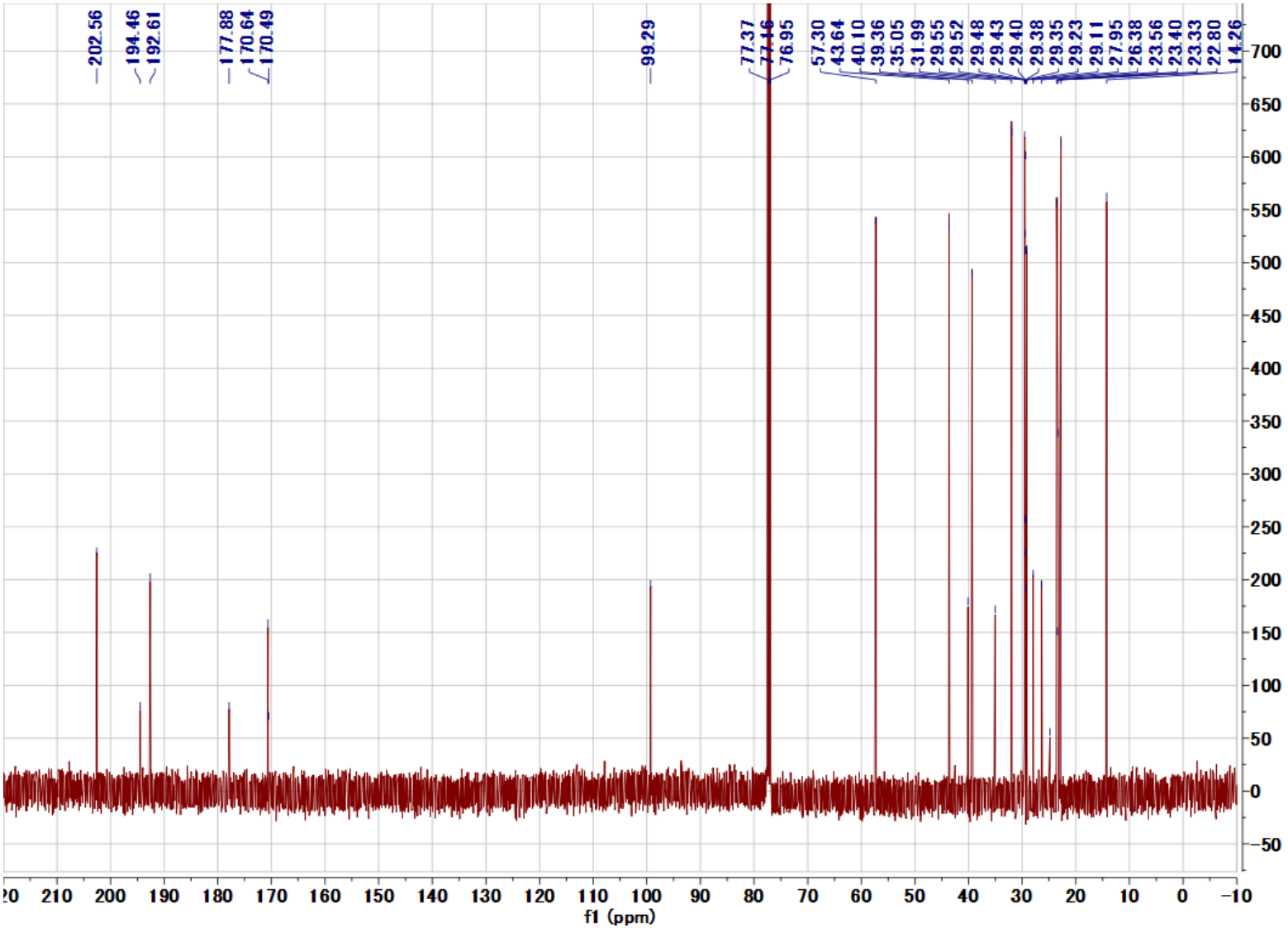

Figure S124. ^{13}C NMR (151 MHz, $CDCl_3$) spectrum of synthesized β-keto dodecanoyl SNAC (*n*-C-9 β-ketoacyl SNAC, **6h**).

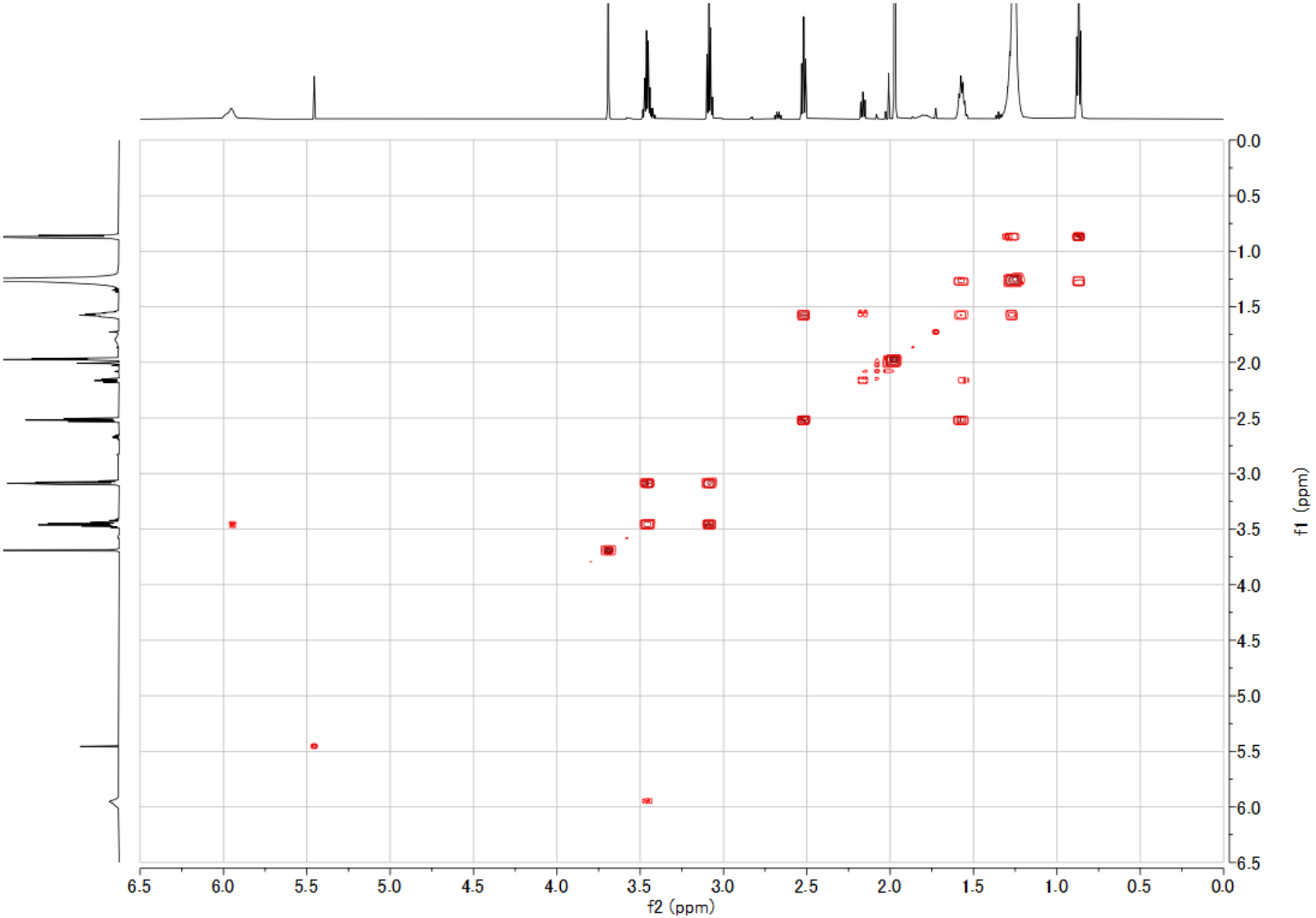

Figure S125. The gradient COSY (600 MHz, $CDCl_3$) spectrum of synthesized β-keto dodecanoyl SNAC (*n*-C-9 β-ketoacyl SNAC, **6h**).

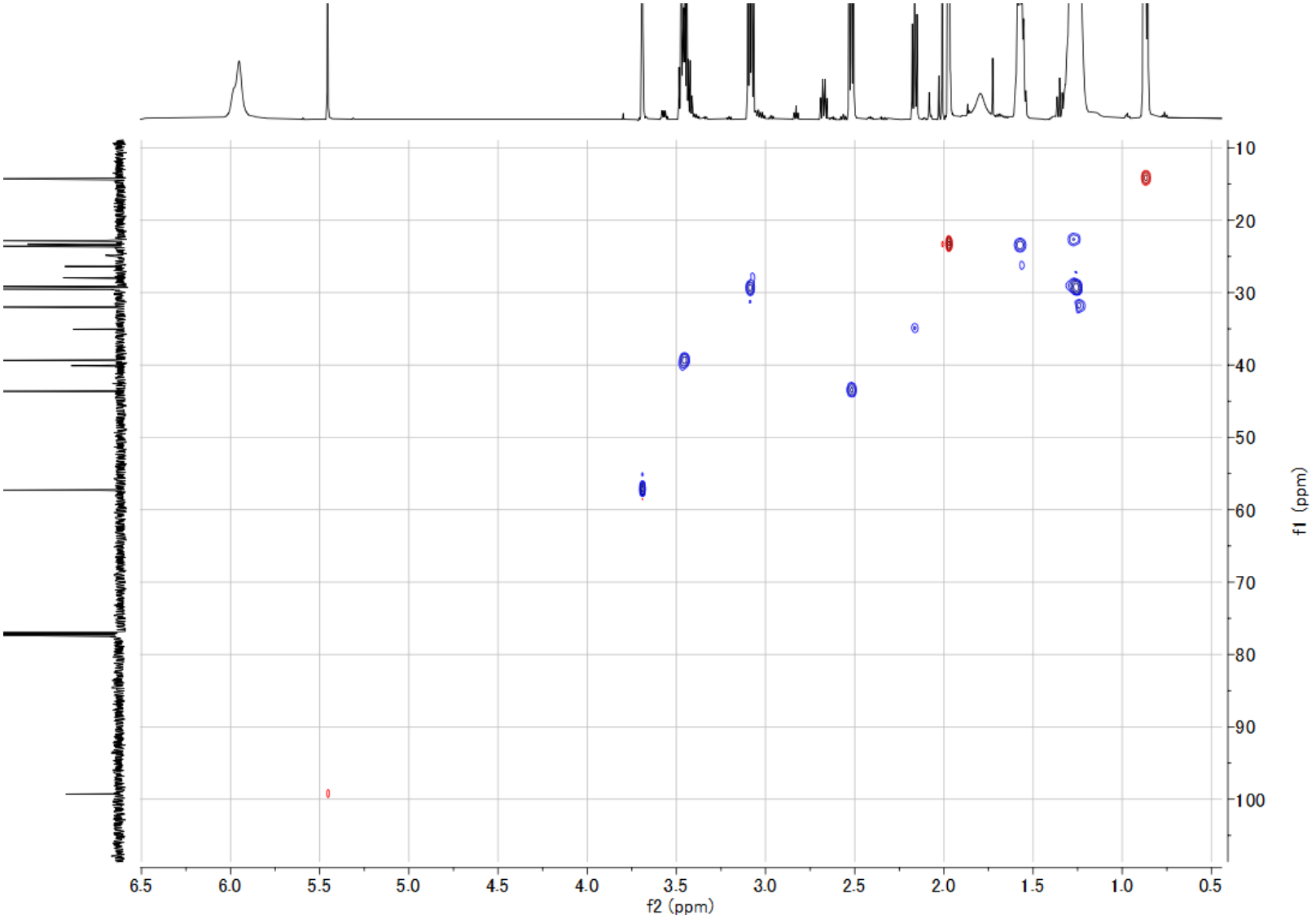

Figure S126. The gradient HSQC (600 MHz, $CDCl_3$) spectrum of synthesized β-keto dodecanoyl SNAC (*n*-C-9 β-ketoacyl SNAC, **6h**).

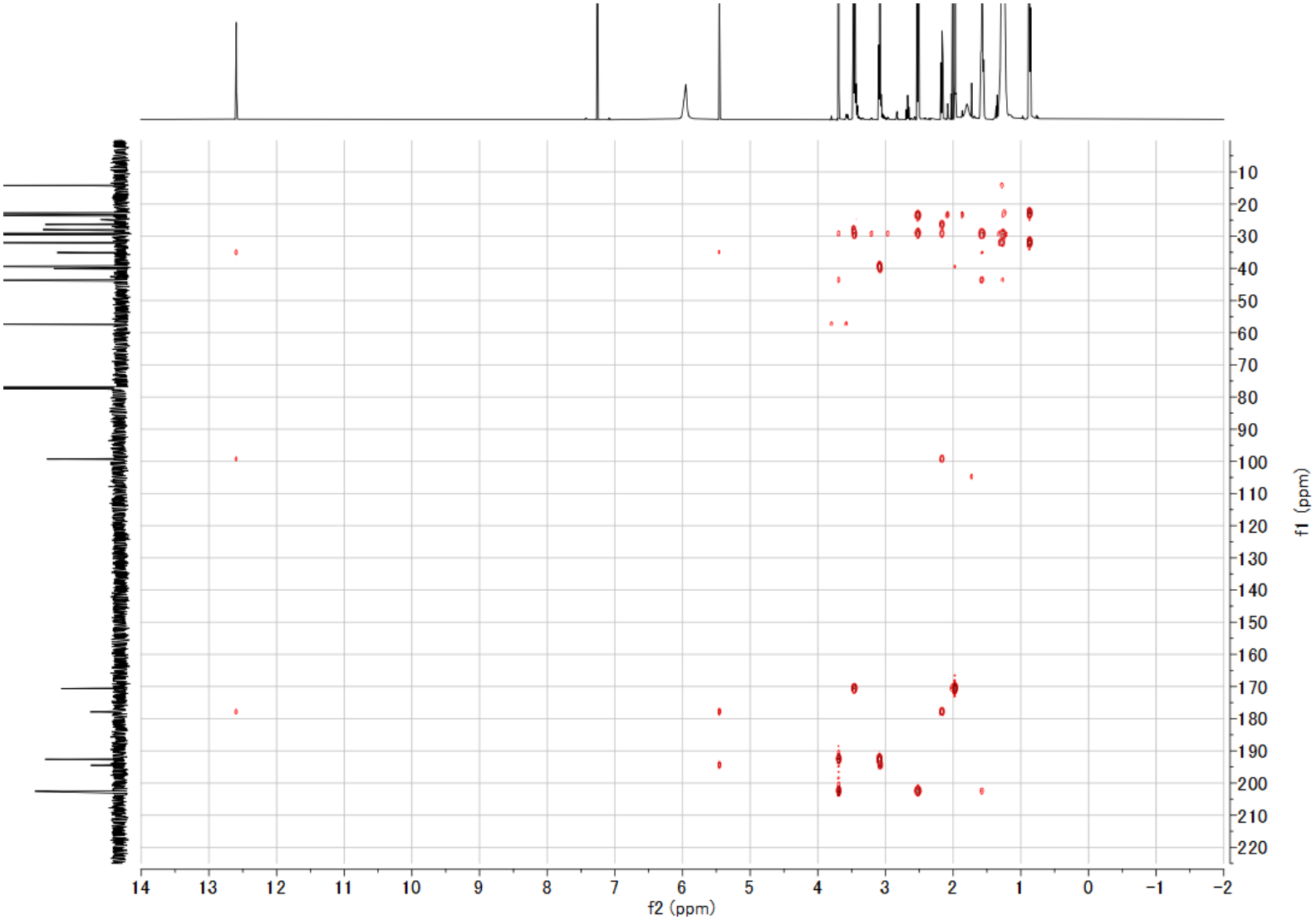

Figure S127. The gradient HMBC (600 MHz, $CDCl_3$) spectrum of synthesized β-keto dodecanoyl SNAC (*n*-C-9 β-ketoacyl SNAC, **6h**).

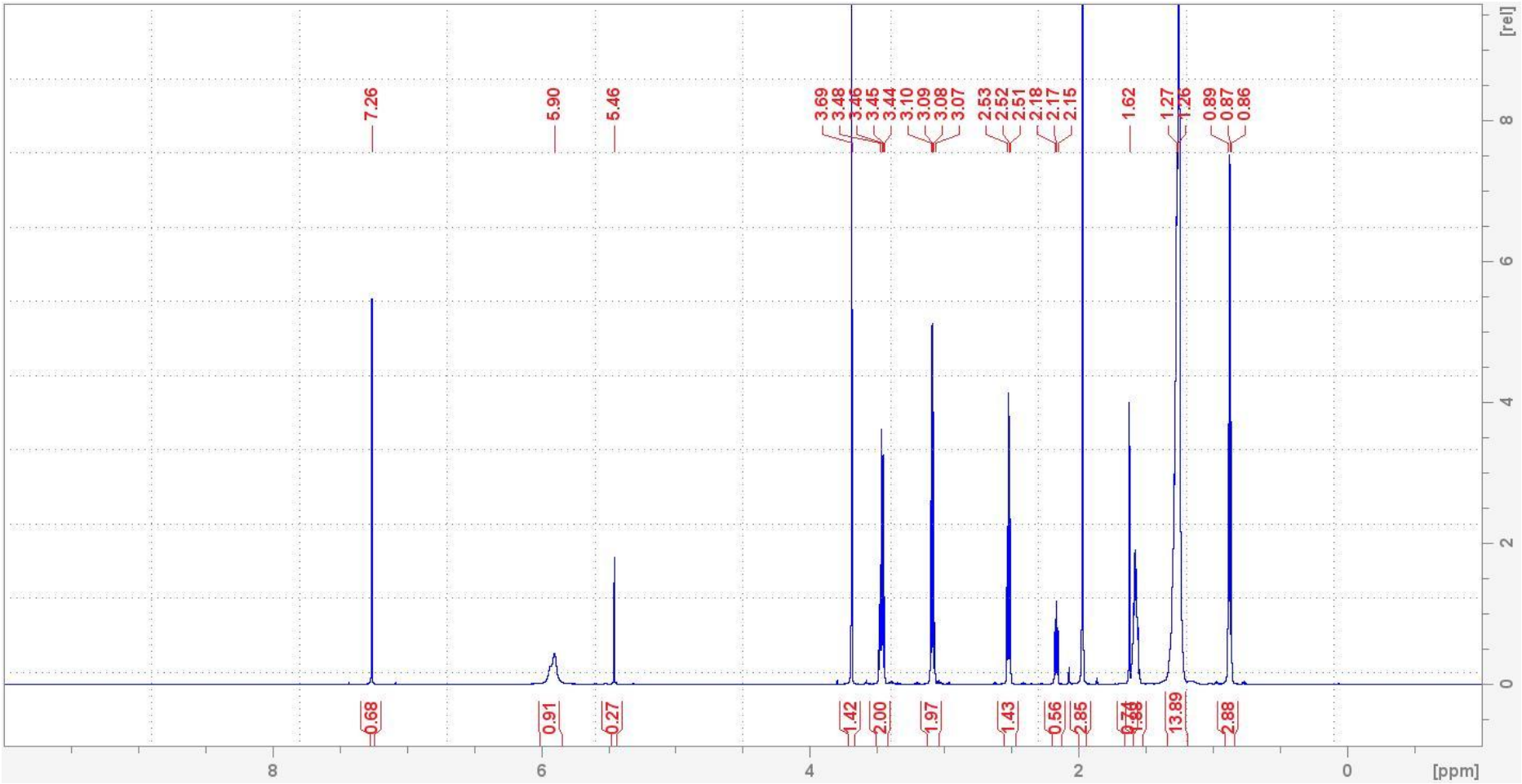

Figure S128. ^{1}H NMR (600 MHz, $CDCl_3$) spectrum of synthesized β-keto tridecanoyl SNAC (*n*-C-10 β-ketoacyl SNAC, **6i**).

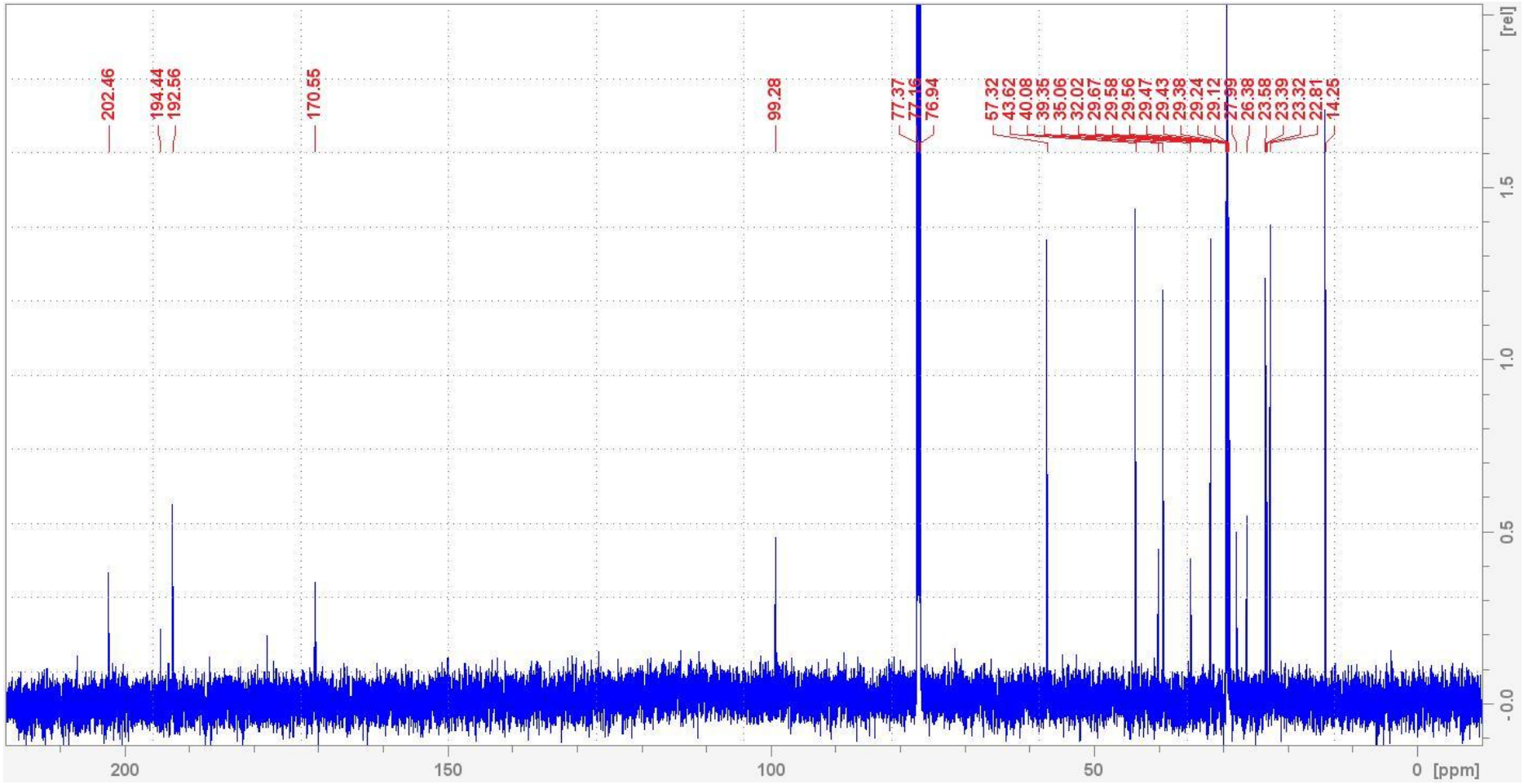

Figure S129. ^{13}C NMR (151 MHz, $CDCl_3$) spectrum of synthesized β-keto tridecanoyl SNAC (*n*-C-10 β-ketoacyl SNAC, **6i**).

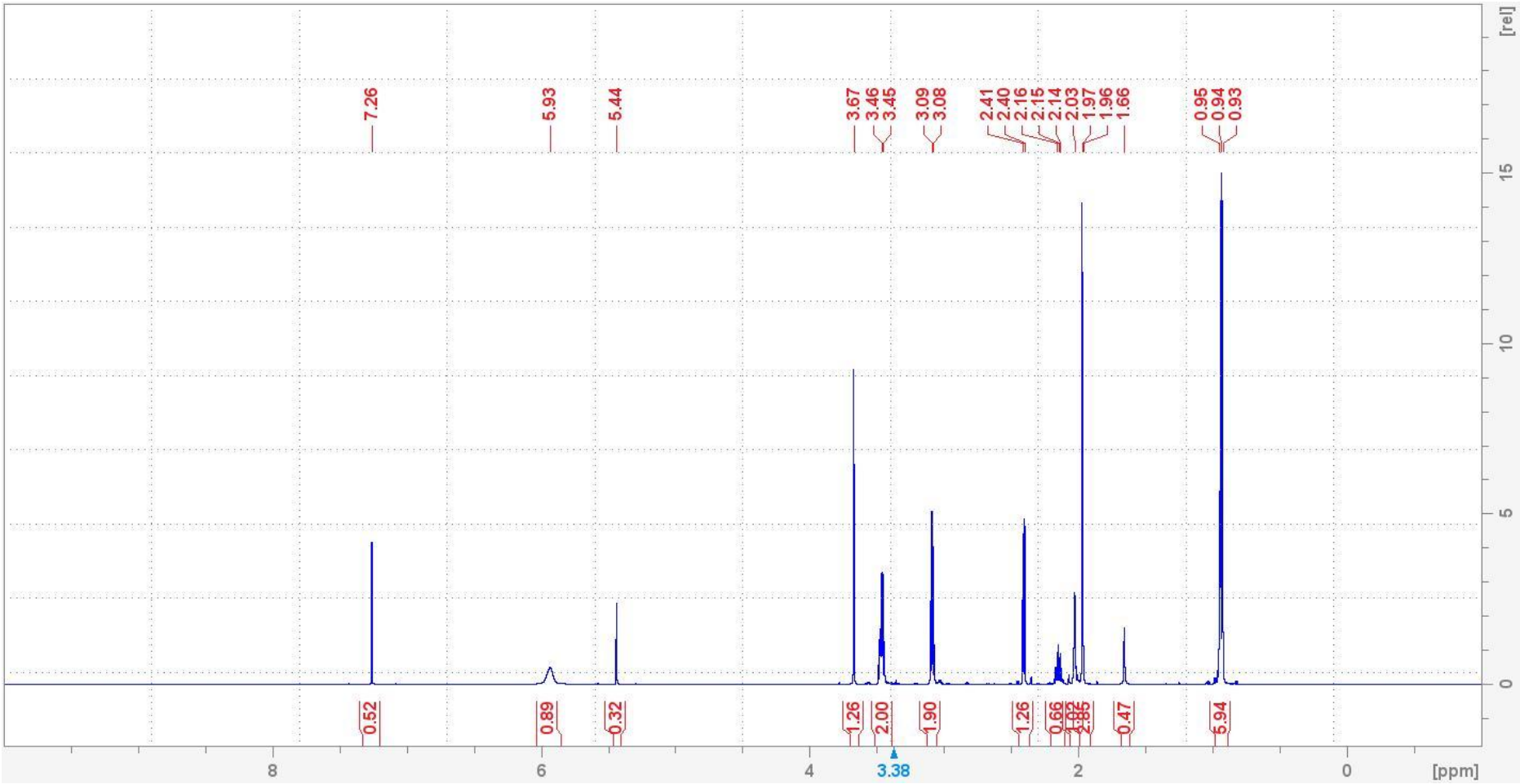

Figure S130. ^{1}H NMR (600 MHz, $CDCl_3$) spectrum of synthesized β-keto *iso*-heptanoyl SNAC (*iso*-C-4 β-ketoacyl SNAC, **6j**).

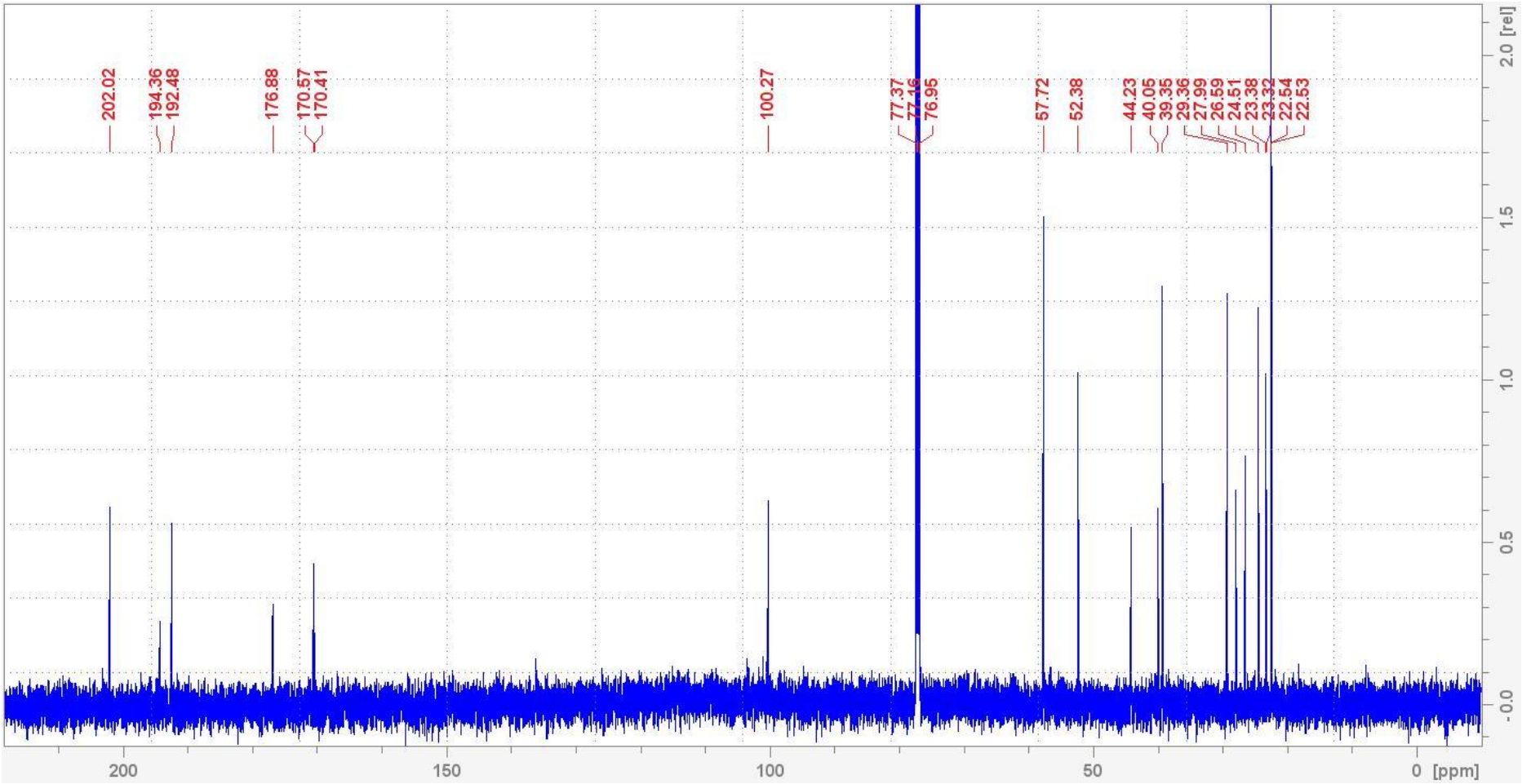

Figure S131. ^{13}C NMR (151 MHz, $CDCl_3$) spectrum of synthesized β-keto *iso*-heptanoyl SNAC (*iso*-C-4 β-ketoacyl SNAC, **6j**).

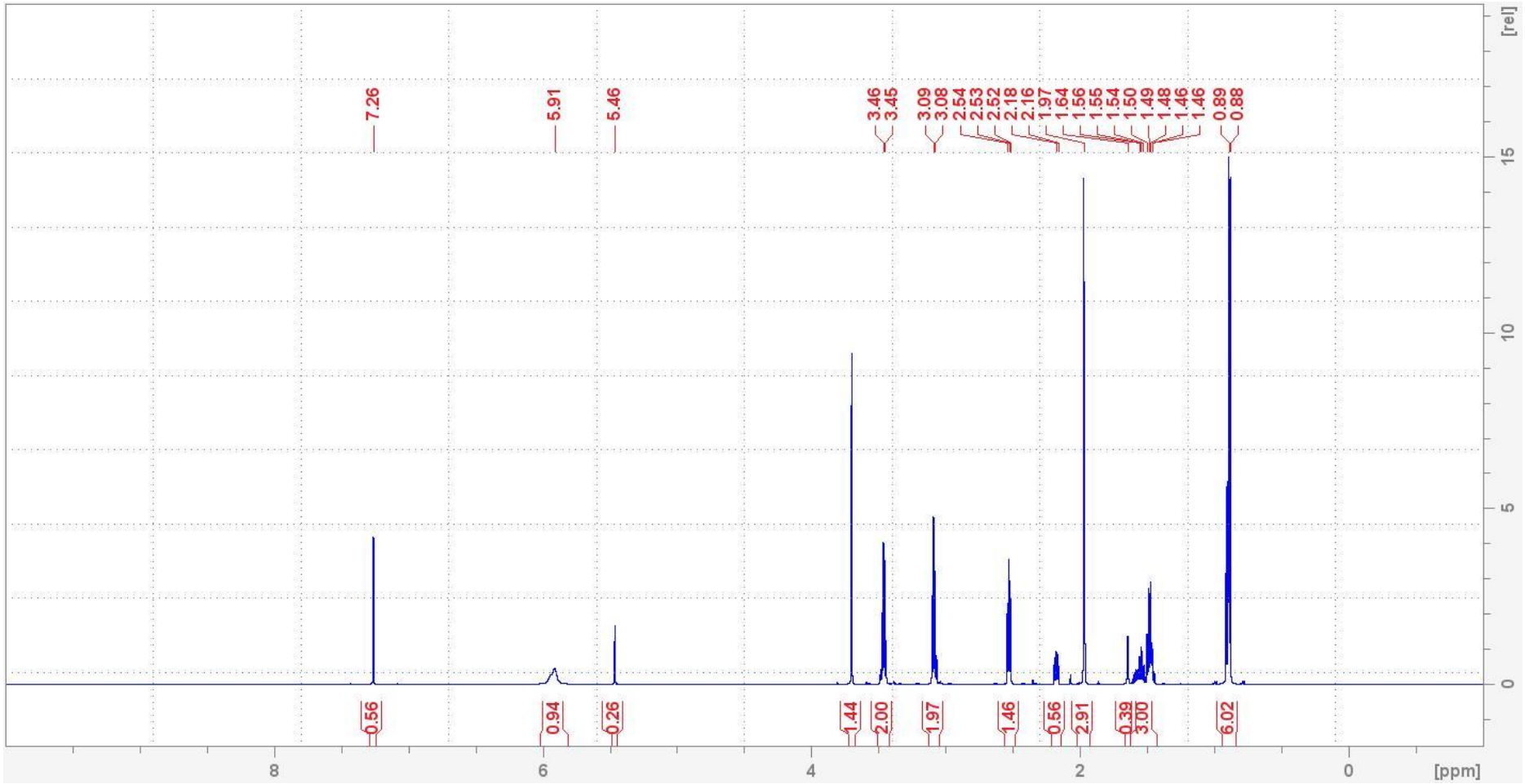

Figure S132. ^{1}H NMR (600 MHz, $CDCl_3$) spectrum of synthesized β-keto *iso*-octanoyl SNAC (*iso*-C-5 β-ketoacyl SNAC, **6k**).

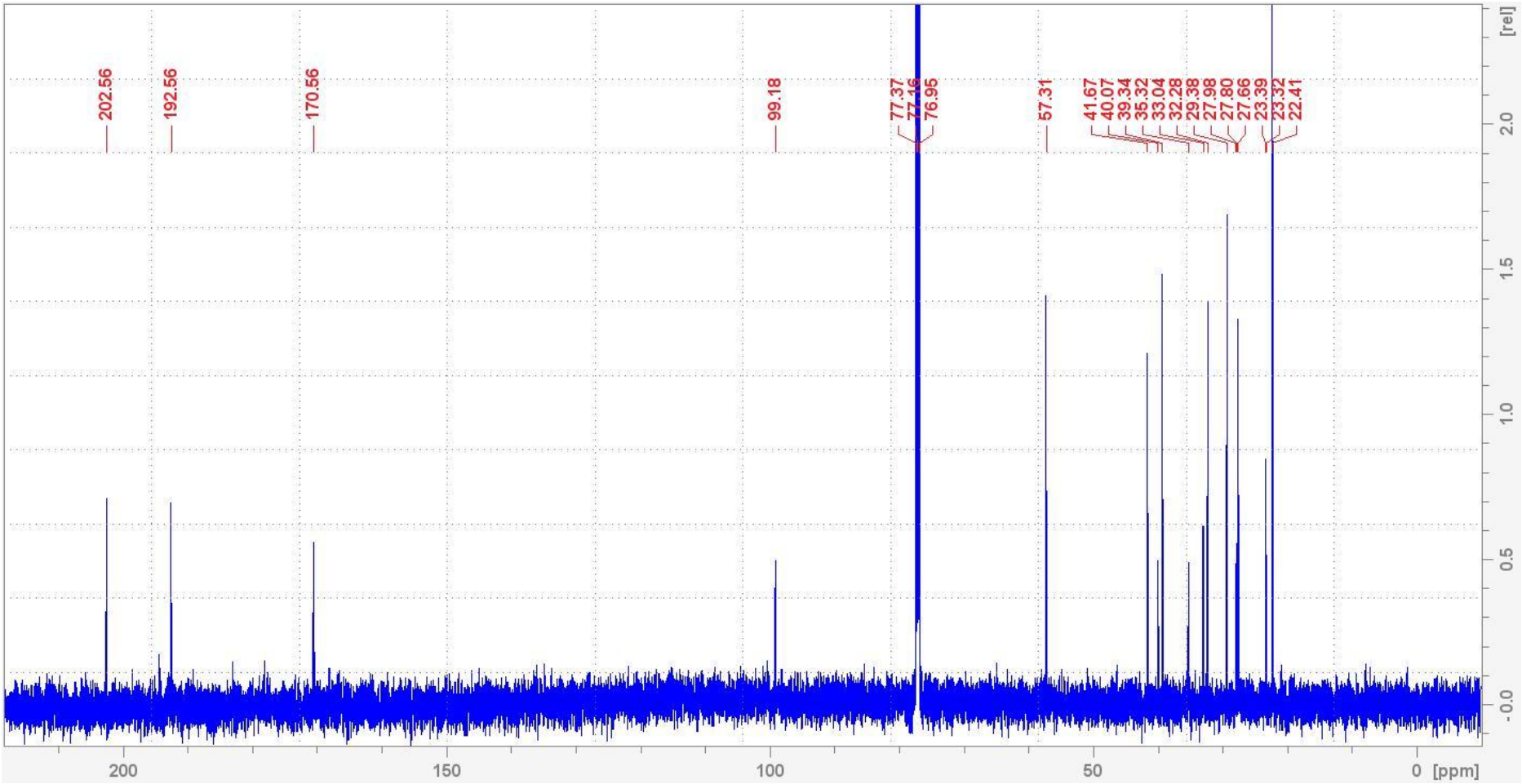

Figure S133. ^{13}C NMR (151 MHz, $CDCl_3$) spectrum of synthesized β-keto *iso*-octanoyl SNAC (*iso*-C-5 β-ketoacyl SNAC, **6k**).

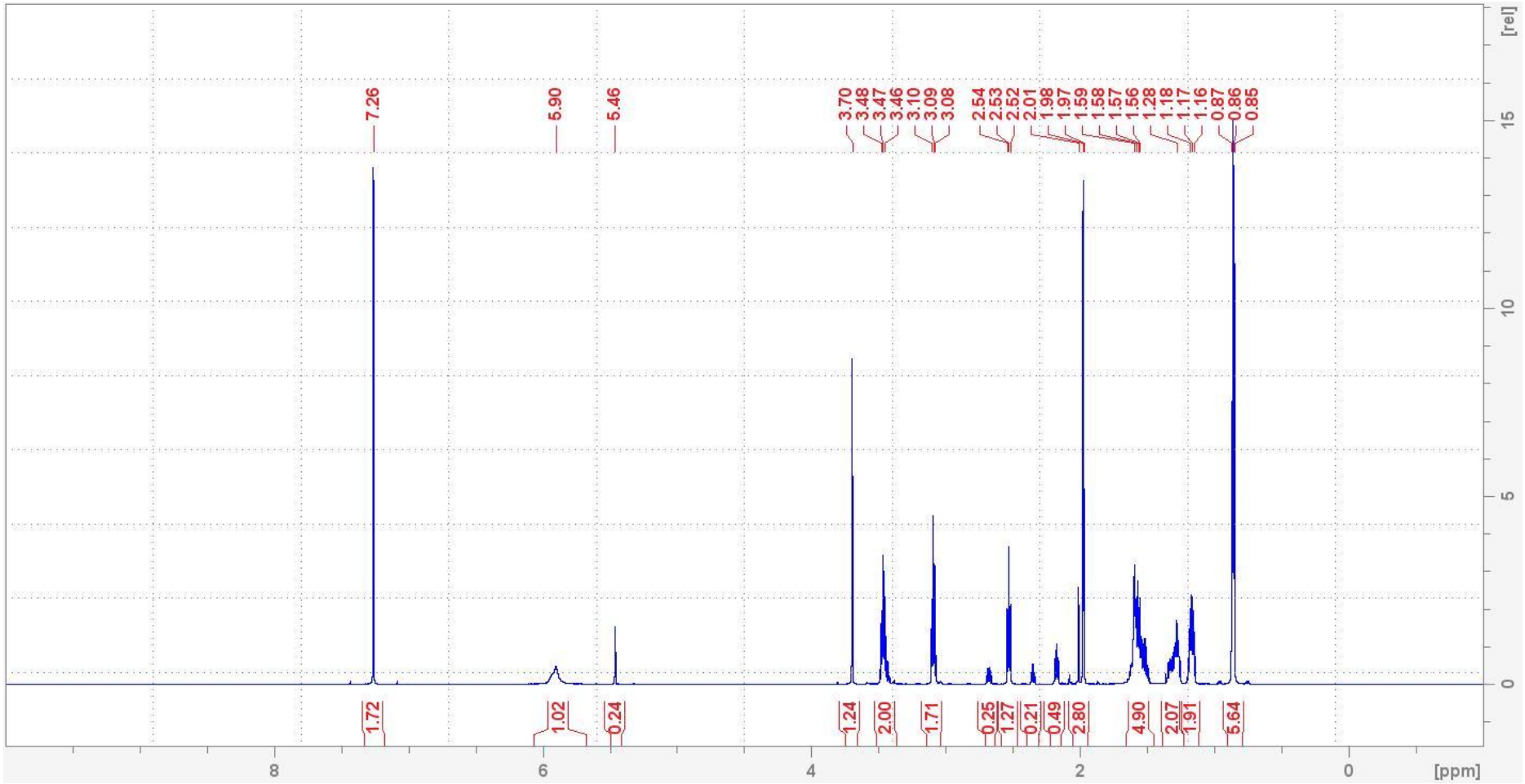

Figure S134. ^{1}H NMR (600 MHz, $CDCl_3$) spectrum of synthesized β-keto *iso*-decanoyl SNAC (*iso*-C-7 β-ketoacyl SNAC, **6l**).

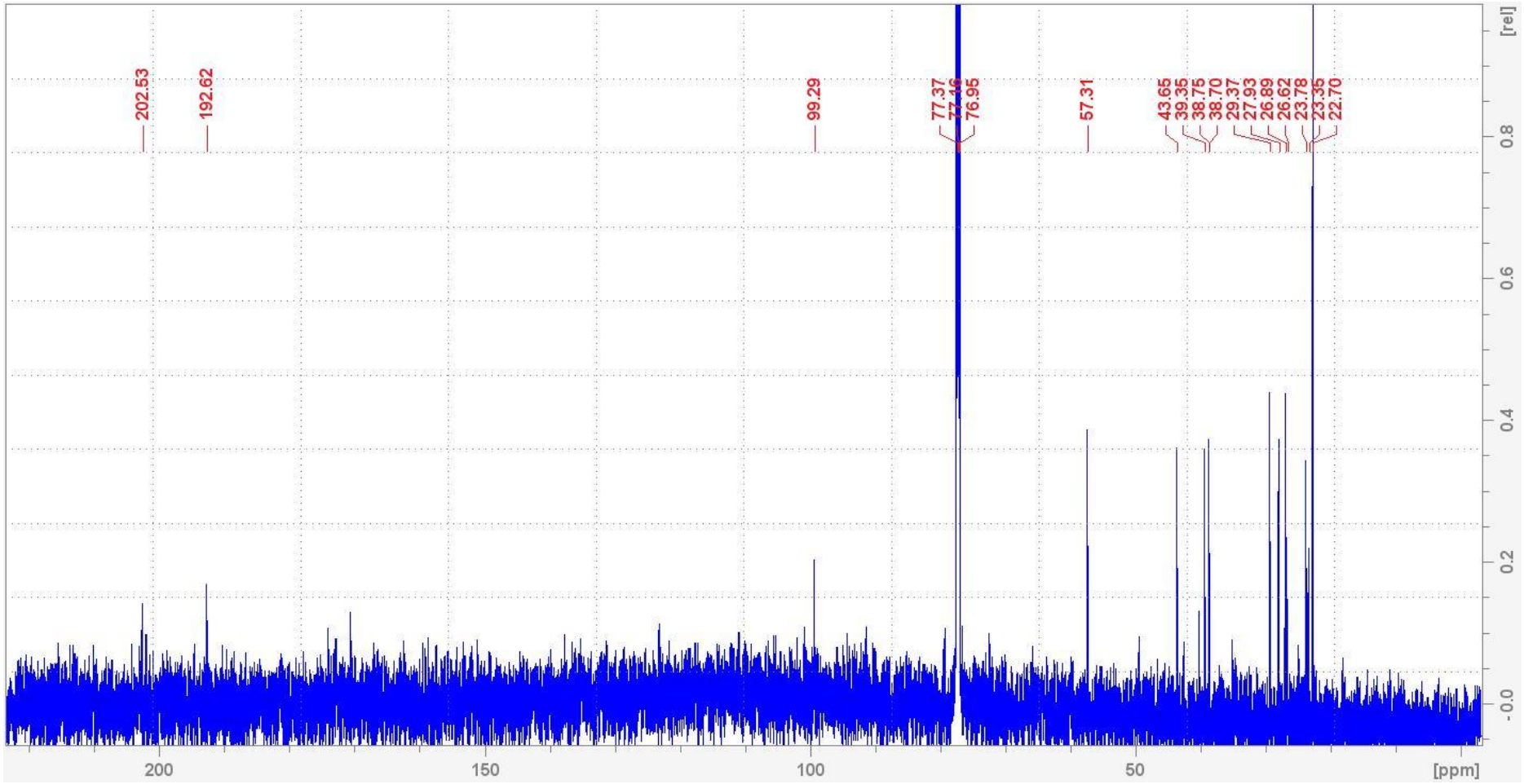

Figure S135. ^{13}C NMR (151 MHz, $CDCl_3$) spectrum of synthesized β-keto *iso*-decanoyl SNAC (*iso*-C-7 β-ketoacyl SNAC, **6l**).